A CRITICAL ANALYSIS OF MITOCHONDRIAL FUNCTIONING AND ASSOCIATED PROTEINS IN OBESITY-RELATED CARDIOMYOPATHY

by

Siddiqah George

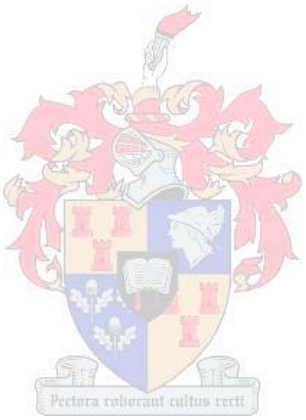

Thesis presented in fulfilment of the requirements for the degree of

Master of Science in Medical Sciences in the

Faculty of Medicine and Health Sciences at Stellenbosch University

Supervisor: Prof. Barbara Huisamen

March 2013

Declaration

By submitting this thesis electronically, I declare that the entirety of the work contained therein is my own, original work, that I am the sole author thereof (save to the extent explicitly otherwise stated), that reproduction and publication thereof by Stellenbosch University will not infringe any third party rights and that I have not previously in its entirety or in part submitted it for obtaining any qualification.

Date: 27 February 2013

Abstract

INTRODUCTION: The mechanism behind obesity-related cardiomyopathies is at present not completely known, however, cardiac insulin resistance has been implicated as one of the main arbitrators of obesity-related cardiovascular disease. A few studies have associated perturbations in the insulin-mediated PI3K/PKB/Akt pathway in mediating this insulin resistance. Moreover, this pathway has been shown to regulate myocardial apoptosis, which in turn has been implicated in a number of cardiovascular diseases. Currently, few studies have compared the early onset and advanced effects of obesity on the heart.

AIMS: To compare the early and advanced stages of obesity in terms of myocardial (i) PI3K/PKB/Akt signalling, (ii) apoptotic signalling and (iii) mitochondrial integrity. Furthermore, we aim to assess the cardiac mitochondrial (i) PI3K/PKB/Akt signalling, (ii) apoptotic signalling and (iii) integrity during the advanced stages of obesity.

METHODS: Male Wistar rats were randomly assigned to either a control or diet-induced obesity (DIO) group. Controls were fed a standard rat chow diet and the DIO group fed a high caloric diet (standard rat chow supplemented with sucrose and condensed milk). The diets were implemented for either 8 or 20 weeks and thereafter, the body weight, intra-peritoneal fat mass, and fasting blood glucose and insulin levels (including intra-peritoneal glucose tolerance tests (IPGTTs)) were determined. Freeze-clamped hearts from both groups were subjected to cytosolic western blot analysis for PI3K p85 subunit, PKB/Akt, GSK-3α/β, Bad, Bax and Bcl-2. A fraction of each heart was also subjected to WB analysis

of the mitochondrial electron transport chain (ETC) complexes (I-V). Thereafter, the above mentioned proteins were also probed for in mitochondria isolated from the 20 weeks group after administering insulin and exposing the hearts to ischemia. Oxidative phosphorylation (OXPHOS) capacity analysis was then conducted on mitochondria isolated from 20 weeks DIO and control groups and thereafter a citrate synthase (CS) activity assay was performed on these mitochondria.

RESULTS: After the 8 and 20 weeks diet, the DIOs had significantly increased intra-peritoneal fat mass, fasting plasma glucose and insulin levels, compared to their controls. *Cytosolic WB analysis*: The tp85, pp85 and pPKB/Akt levels were significantly higher in the DIOs in comparison to the controls after 8 weeks of diet. Furthermore, pBad and Bax expression were significantly elevated in these animals. After 20 weeks of diet, the DIOs had significantly decreased pp85, tPKB/Akt and pPKB/Akt levels. The tBad was significantly elevated, while the Bad phosphorylated over total expression (P/T) ratio was significantly decreased, in these animals. *CS activity assay:* CS activity was significantly decreased in the DIOs, versus the controls, at 20 weeks. *Mitochondrial ETC WB analysis*: The subunit expression in complexes I-III and V did not differ significantly after 8 weeks however, the expression was significantly lower in complexes I and II after 20 weeks. Interestingly, the complexes III and V expression was significantly elevated. *Mitochondrial OXPHOS analysis*: The ADP/O ratio with (1) glutamate or (2) palmitoyl-L- carnitine as substrate, showed a significant decrease in the DIOs at 20 weeks. *Mitochondrial WB analysis*: The pp85 subunit was significantly elevated in the control and DIO groups, exposed to insulin and ischemia, in comparison to the untreated controls. The Bcl-2 levels were significantly decreased in the insulin and ischemia DIOs, when matched against the untreated DIOs. The tBad expression did not differ significantly between the insulin and

untreated controls, while the tBad was significantly augmented in the ischemia controls versus untreated controls. All significant differences were taken as $p<0.05$.

CONCLUSION: The results indicate that the initial stage of diet-induced obesity is associated with cardioprotection as there is augmented PI3K/PKB/Akt pathway signalling and a decrease in apoptotic markers. In contrast, during the advanced stages of obesity a decreased activity in PI3K/PKB/Akt pathway is associated with myocardial apoptosis and decreased mitochondrial function and integrity.

Abstrak

INLEIDING: Die meganisme verantwoordelik vir vetsug-verwante kardiomiopatieë is huidiglik nie bekend nie maar kardiale insulienweerstandigheid word geïmpliseer as een van die hoof bemiddelaars van vetsug-verwante hartsiektes. Verskeie studies het versteurings in die insulien-gemediëerde PI3K/PKB/Akt pad geassosieer met die bevordering van hierdie insulienweerstandigheid. Daarbenewens is dit getoon dat hierdie pad betrokke is in die regulering van miokardiale apoptose, wat op sy beurt geïmpliseer is in 'n aantal kardiovaskulêre siektes. Daar is tans min studies beskikbaar wat die vroeë en laat gevolge van obesiteit op die hart vergelyk.

DOELWITTE: Om die vroeë en gevorderde stadiums van vetsug te vergelyk in terme van miokardiale (i) PI3K/PKB/Akt seintransduksie, (ii) apoptotiese seintransduksie en (iii) mitokondriale integriteit. Verder, het die studie ten doel om die kardiale mitokondriale (i) PI3K/PKB/Akt en (ii) apoptotiese seintransduksie en (iii) integriteit in die gevorderde stadiums van vetsug te bepaal.

METODES: Manlike Wistar rotte is ewekansig toegewys aan óf 'n kontrole of dieet-geïnduseerde vetsug (DIO) groep. Kontroles is met 'n normale rotkos dieet en die DIO groep met 'n hoë kalorie dieet (normale rotkos aangevul met sukrose en kondensmelk) gevoed. Die dieet is vir 8 of 20 weke volgehou en daarna was die liggaamsgewig, intra-peritoneale vet massa, en vastende bloed glukose en insulien vlakke (insluitende intra-peritoneale glukose toleransie toets (IPGTT`s)) bepaal. Gevriesklampte harte van beide groepe is onderwerp aan sitosoliese WB-analise vir die PI3K p85 subeenheid, PKB / Akt, GSK-3α/β, Bad, Bax en Bcl-2. `n Fraksie van hierdie harte is ook onderwerp aan westerse klad analise (WK-analise) van die mitokondriale elektron vervoer ketting (EVK) komplekse

(I-V). Daarna is bogenoemde proteïene ondersoek in mitokondrieë geïsoleer uit die 20 weke groep ná die toediening van insulien en die blootstelling van die harte aan iskemie. Die oksigraaf mitokondriale oksidatiewe fosforilering (OXPHOS) kapasiteit analise is dan op mitokondrieë van 20 weke DIO en kontrole groepe uitgevoer en daarna is 'n sitraatsintase (SS) aktiwiteitstoets gedoen.

RESULTATE: Na die 8 en 20 weke dieet, het die intra-peritoneale vet massa, vastende plasma glukose en insulien vlakke in die DIOs aansienlik toegeneem, in vergelyking met hul kontroles. *Sitosoliese WK-analise*: Die tp85, pp85 en pPKB/Akt vlakke was beduidend hoër in die DIOs in vergelyking met die kontroles, na 8 weke van die dieet. Verder is die pBad en Bax vlakke beduidend verhoog in hierdie diere. Na 20 weke van die dieet, het die pp85, tPKB/Akt en pPKB/Akt vlakke beduidend afgeneem in die DIOs, in vergelyking met die kontroles. Die tBad was beduidend verhoog, terwyl die Bad verhouding van gefosforileerde oor die totale proteïen uitdrukking (P/T)-verhouding) beduidend verminder het in hierdie diere. *SS aktiwiteitstoets*: SS aktiwiteit is beduidend verminder in die DIOs, teenoor die kontroles, op 20 weke. *Mitokondriale EVK WK-analise*: Die subeenheid uitdrukking in komplekse I-III en V was nie beduidend verskillend na 8 weke nie. Na 20 weke egter, was die uitdrukking aansienlik laer in komplekse I en II. Interessant genoeg, is die uitdrukking aansienlik verhoog in komplekse III en V. *Mitokondriale OXPHOS analise*: Die ADP/O verhouding met (1) glutamaat of (2) palmitiel-L-karnitien as substraat, het beduidend afgeneem in die DIOs teen 20 weke. *Mitokondriale WK-analise*: Die pp85 subeenheid was beduidend verhoog in die kontrole en DIO groepe, blootgestel aan insulien en iskemie, in vergelyking met die onbehandelde kontroles. Die Bcl-2 vlakke was beduidend verminder in die insulien en isgemie DIOs, in vergelyking met onbehandelde DIOs. Die tBad uitdrukking het nie beduidend verskil tussen die insulien en onbehandelde

kontroles nie, terwyl die tBad beduidend verhoog was in die isgemie kontroles versus onbehandelde kontroles. Alle beduidende verskille is geneem as $p<0.05$.

GEVOLGTREKKING: Die resultate dui daarop dat die eerste fase van dieet-geïnduseerde obesiteit geassosieer is met kardiale beskerming want `n toename in PI3K/PKB/Akt seintransduksie en 'n afname in apoptotiese merkers is waargeneem. In teenstelling, in die gevorderde stadium van vetsug is daar 'n afname in aktiwiteit in die PI3K/PKB/Akt pad wat verband hou met verhoogde miokardiale apoptose en verminderde mitokondriale funksie en integriteit.

Acknowledgements

I wish to acknowledge the University of Stellenbosch, Ernst and Ethel Eriksen Trust, SANZAF, the Medical Research Council of Southern Africa and the Division of Medical Physiology for their financial assistance. The opinions expressed and conclusions arrived at in this thesis are strictly mine and do not necessarily reflect those of the above mentioned institutions.

My acknowledgement of the following people are by no means in order of importance and each contributed to the successful completion of this thesis in their own unique way.

I wish to express my sincere gratitude to my supervisor Professor Barbara Huisamen as well as Professor Amanda Lochner for their invaluable guidance and patience throughout my Master`s studies.

To Professor Martin Kidd, Doctor`s James Fan, Erna Marais, Ingrid Webster and Shantal Windvogel as well as Nicole Bezuidenhout, Natalie Collop, Arina Cronje, Brian Flepisi, Derick van Vuuren, Corli Wescott, thank you all for your assistance and contributions, it is greatly appreciated.

Monica Piek, Sonja Alberts, Margot Flint, Cindy George, Suzel Hattingh, Thandekile Hafver, Dr. John Lopes, Eva Mudau, Frederick Nduhirabandi, Dr. Ruduwaan Salie; thank you for not only coming to my aid when I really needed it but also for the quick chats and the words of encouragement. I am grateful as it certainly made dull days a little brighter.

To the rest of the staff and students of the Division of Medical Physiology, thank you for being such a wonderful team to work with.

Michelle, Samantha, Berenice and Rabia, I am lucky to call you friends. Thank you for your continued support.

To my father Omar and my sister Aisha, who laughed when I laughed and cried when I cried throughout my studies, know you are very dear to me. Thank you for your continued support and encouragement, I am truly blessed.

Table of Content

List of Illustrations

I : LIST OF TABLES

CHAPTER 2: LITERATURE REVIEW

Chapter 3: Material and Methods

Chapter 4: Results

II: LIST OF FIGURES

CHAPTER 2: LITERATURE REVIEW

CHAPTER 3: MATERIALS AND METHODS

CHAPTER 4: RESULTS

CHAPTER 6: CONCLUSION

List of Abbreviations

I: Units of measurement

%:	percentage
°C:	degrees Celsius
AU:	arbitrary units
Ci:	curie
g:	grams
g:	gravity
IU:	international units
kDa:	kilodalton
kg/m^2:	kilograms per square meter
kJ:	kilojoule

M: molar

mg: milligrams

mg/kg: milligrams per kilogram

mg/ml: milligrams per millilitre

min: minutes

ml: millilitre

mA: milliampere

mM: millimolar

mm^2: cubic millimetres

N: normal

nm: nanometer

P/T: phosphorylated over total

rpm: revolutions per minute

sec:	seconds
µg:	microgram
µl:	microlitre
µg/ml:	micrograms per millilitre
mg/ml:	milligrams per millilitre
µM:	micromolar
µm:	micrometer
V:	volts
v/v:	volume per volume
w/v:	weight per volume

II: Molecular and chemical compounds

ACBP: Acyl-CoA binding protein

ACC: Acetyl-CoA carboxylase

ADP: Adenosine diphosphate

ADP/O: Adenosine diphosphate/oxygen

AIF: Apoptosis-inducing factor

AMP: Adenosine monophosphate

ANT: Adenine nucleotide translocase

Apaf-1: Apoptotic protease-activating factor-1

APS: Ammonium persulfate

ATP: Adenosine triphosphate

ATPase: Adenosine triphosphatase

AVPI: Ala-Val-Pro-Ile

Bad: Bcl-2 associated death protein

Bak: Bcl-2 homologous antagonist killer protein

Bcl-2: B-cell lymphoma-2 protein

Bax: B-cell lymphoma-associated X protein

Bcl-X_L: B-cell lymphoma-extra-large protein

Bid: BH3 interacting domain protein

BH: Bcl-2 homology

BIR: Baculovirus IAP repeat

Bnip3: Bcl-2/adenovirus E1B 19kDa protein-interacting protein3

BSA: Bovine serum albumin

Ca^{2+}: Calcium

$CaCl_2$: Calcium chloride

CACT: Carnitine/acyl-carnitine transferase

CARD: Caspase recruitement

CCCP: Carbonyl cyanide 3-chlorophenylhydrazone

CD36: Cluster determinant 36

CO^2 : Carbon dioxide

Cob: Cytochrome b

CPT-I: Carnitine palmitoyl transferase-I

CPT-II: Carnitine palmitoyl transferase-II

CrP: Creatine phosphate

CS: Citrate synthase

$CuSO_4$: Copper sulphate

CytC1: Cytochrome c1

DAG: Diacylglycerol

DED: Death effector domain

dH_20: Distilled water

DISC: Death-inducing signalling complex

DNA: Deoxyribonucleic acid

DNTB: 5,5-Dithiobis-(2-nitrobenzoic acid)

e^-: Electron

ECL: Enhanced chemiluminescence

EDTA: Ethylene diamine tetra-acetic acid

EFG: Epidermal growth factor

EGTA: Ethylene glycol tetra-acetic acid

EndoG: Endonuclease G

ERK1/2: Extracellular signal-regulated kinases 1 and 2

FABPpm: Fatty acid binding protein

FACS: Fatty acyl-CoA synthetase

FADD: Fas associated death domain

$FADH_2$: 5,10-methylenetetrahydrofolatereductase

FAT: Fatty acid translocase

FATP: Fatty acid translocase protein

FFA: Free fatty acids

FOX: Forkhead box

FOXO1: Forkhead box protein 1

FOXO3a: Forkhead box protein 3a

FOXO4: Forkhead box protein 4

G-1-P: Glucose-1-phosphate

G-6-P: Glucose-6-phosphate

GLUT: Glucose transporter

GLUT1/4: Glucose transporter 1/4

GS: Glycogen synthase

GSK-3: Glycogen synthase kinase-3

GTP: Guanosine 5'-triphosphate

H^+: Proton

H_2O: Water

H_3PO_4: Phosphoric acid

HCl: Hydrochloric acid

HDM2: Human double minute 2

H-FABPc: Heart-type cytoplasmic fatty acid-binding protein

HPLC: High performance liquid chromatography

HRP: Horseradish peroxidase

IAPs: Inhibitor of apoptosis proteins

IKK: I-κb kinase

IL-6: Interleukin-6

ILK: Integrin-linked kinase

IMM: Inner mitochondrial membrane

IR: Insulin receptor

IRS: Insulin receptor substrate

ISP: Rieske [2Fe-2S] protein

KCl: Potassium chloride

K_2HPO_4: Dipotassium phosphate

KH_2PO_4: Monopotassium phosphate

LCFA: Long chain fatty acid

LPL: Lipoprotein lipase

MAPK: Mitogen activated protein kinase

MAPKAP-K1/RSK: MAPK-activated protein kinase-1

Mcl-1: Myeloid cell leukemia-1

MDM2: Murine double minute 2

$MgSO_4$: Magnesium sulphate

MitoK_{ATP}: Mitochondrial K_{ATP}

MPTP: Mitochondrial permeability transition pore

Na^+: Sodium

NaK-tartrate: Sodium potassium tartrate

Na_2CO_3: Sodium carbonate

Na_2HPO_4: Disodium phosphate

$Na_2S_2O_4$: Sodium dithionite

NaOH: Sodium hydroxide

Na_2SO_4: Sodium sulphate

Na_3VO_4: Sodium orthovanadate

NaCl: Sodium Chloride

NAD^+: Nicotinamide adenine dinucleotide

NADH: Reduced nicotinamide adenine dinucleotide

NADH ASHI: NADH-ubiquinone oxidoreductase ASHI

NF-κB: Nuclear factor-κB

$NaHCO_3$: Sodium bicarbonate

Nix/Bnip3L: Bcl-2/adenovirus E1B 19kDa protein-interacting protein 3-like

O_2: Oxygen

OMM: Outer mitochondrial membrane

p85: Protein 85

p110: Protein 110

pp85: Phosphorylated protein 85

PARP: Poly (ADP-ribose) polymerase

pBad: Phosphorylated Bcl-2 associated death

PCA: Perchloric acid

PDH: Pyruvate dehydrogenase

PDK-1: 3-phosphoinositide-dependent kinase-1

PDK-2: 3-phosphoinositide-dependent kinase-2

PGC-1α: PPARγ coactivator-1α

pGSK-3: Phosphorylated glycogen synthase kinase-3

pH: Potential of hydrogen

PH: Pleckstrin homology

PI: Phosphatidylinositol

Pi: Inorganic phosphate

PI3K: Phosphatidylinositol 3 kinase

pPI3K: Phosphorylated phosphatidylinositol 3 kinase

PiC: Inorganic phosphate carrier

PIP3: Phosphatidylinositol (3,4,5) trisphosphate

PKA: Protein kinase A

PKB/Akt: Protein kinase B

pPKB/Akt: Phosphorylated protein kinase B

PKC-*θ*: Protein kinase C-*θ*

PMSF: Phenyl methane sulfonyl fluoride

PPAR-α: Peroxisome proliferator activated receptor-alpha

RISK: Reperfuson injury salvage kinase

RCI: Respiratory control index

ROS: Reactive oxygen species

SDH: Succinate dehydrogenase [ubiquinone] iron-sulfur

SDS: Sodium dodecyl sulphatepolyacrylamide

SDS-PAGE: Sodium dodecyl sulphatepolyacrylamide gel electrophoresis

SH-2: Sarc homology-2

S6K-1: p70 ribosomal S6 kinase-1

Smac/DIABLO: Second mitochondria-derived activator of caspases

SOD: Superoxide dismutase

tp85: Total protein 85

TAG: Triacylglycerol

tBad: Total Bcl-2 associated death

TBAP: Tetrabuthylammonium perchlorate

TBS: Tris buffered saline

TBS-Tween: Tris buffered saline with Tween

TCA: Tricarboxylic acid

TEMED: N,N,N,N-tetramethylethylenediamine

tGSK-3: Total glycogen synthase kinase-3

TNF: Tumour necrosis factor

TNF-α: Tumour necrosis factor-alpha

tPI3K: Total phosphatidylinositol 3 kinase

tPKB/Akt: Total protein kinase B

TRADD: Tumor necrosis factor receptor-associated death domain

Tris: 2-Amino-2-hydroxymethyl-propane-1,3-diol

UDP: Uridine 5'-diphosphate

VDAC: Voltage dependent anion channel

VLDL: Very low density lipoprotein

III: Others

ANOVA: Analysis of variance

MI: Myocardial infarction

BMI: Body mass index

BW: Body weight

CVD: Cardiovascular disease

DIO: Diet-induced obesity

ETC: Electron transport chain

HOMA: Homeostasis model assessment

HPLC: High performance liquid chromatography

I/R: Ischaemia and reperfusion injury

IPGTT: Intra-peritoneal glucose tolerance test

IPC: Ischaemic preconditioning

IPOC: Ischaemic postconditioning

OAA: Oxaloacetate

OD: Optical density

OXPHOS: Oxidative phosphorylation

PVDF: Polyvinylidene fluoride

SABS: South African Bureau of Standards

SEM:	Standard error of the mean
T1DM:	Type 1 diabetes mellitus
T2DM:	Type 2 diabetes mellitus
TUNEL:	Deoxynucleotidyl transferase dUTP nick ending labelling
WB:	Western blot
WHO:	World Health Organization
WT:	Wild-type

Chapter 1: Introduction

1.1 The Obesity Pandemic

1.1.1 Global Statistics for Obesity

Obesity is termed as a surplus amount of body fat in relation to lean mass (body mass index (BMI) >30 kg/m^2), such that the obese individual's health is compromised, whereas overweight (BMI between 25 and 30 kg/m^2) is defined as an elevation in body weight in relation to height [Lopaschuk et al. 2007, Nguyen et al. 2010].

Historically thought of as being restricted to wealthy individuals of developed nations, the incidence of obesity has currently reached epidemic proportions right across the world, for both adults and children alike. With the present global economic crises and the increasing urbanization of developing countries, the number of obese individuals' are only expected to surge. In 2005, around 1.6 billion people were overweight and at least 400 million people were obese across the globe, as indicated by World Health Organization (WHO) estimates. This organization predicts that by the year 2015, 2.3 billion individuals will be overweight and 700 million will be obese worldwide. [Nguyen et al. 2010]

1.1.2 Repercussions of Obesity

The effects of obesity are far reaching as it not only affects the individual but also have implications for the rest of society.

1.1.2.1 The Economic Impacts of Obesity

In terms of the societal impact, an immense financial burden is placed on the global economy on an annual basis as billions are spent on the treatment of obesity-related

physical disabilities and secondary diseases, the so called direct costs of obesity. The indirect economic cost to the global community is estimated to perhaps be more costly than the obesity-related conditions themselves. These indirect costs can be manifested in various ways, for example, additional financial strain is placed on the welfare system as a result of early retirement and unemployment due to obesity-related morbidities. [Yach et al. 2006]

1.1.2.2 The Health Impacts of Obesity

From an individualistic point of view, obesity can severely affect an individual's quality of life as this disease can give rise to an array of other chronic diseases such as cancer, type 2 diabetes mellitus (T2DM) and cardiovascular disease.

In fact, cardiovascular disease is viewed as one of the leading co morbidities of obesity, owing to the large variety of cardiovascular dysfunctions excess weight gain can induce. Obese individuals are at significantly higher risk of developing cardiomyopathies such as congestive heart failure, ischemic heart disease, myocardial infarction and sudden cardiac death, than their leaner counterparts. These disorders are initiated by obesity, and are independent of cardiovascular risk factors or syndromes such as hypertension, dyslipidemia, atherosclerosis and type 2 diabetes mellitus. [Hall et al. 2002, Van Gaal et al. 2006]

Cardiovascular disease-related deaths, a leading mode of death in obese and T2DM individuals across the globe [Coort et al. 2007], has increased from less than 10%, at the start of the 20th century, to 50% at the end of the 20th century [Trivedi et al. 2008]. The existence of a strong correlation between obesity, insulin resistance and myocardial

disease has been duly noted. However, the precise relationship between these three diseases has not been completely elucidated [Bergman et al. 2007]. Thus, the ensuing chapter serves to review this association between obesity, insulin resistance and cardiovascular disease in order to improve our understanding of their complex relationships.

Chapter 2: Literature Review

2.1 Insulin Signalling and the Heart

2.1.1 Overview of the polypeptide hormone insulin

The beta cells of the pancreas are responsible for insulin production, which plays a pivotal role in regulating carbohydrate and fat metabolism by mediating the translocation of transporter proteins to the myocardial sarcolemma. In doing so it facilitates the uptake of glucose and free fatty acids from the blood, which are subsequently stored as energy reserves [Waselle et al. 2005, Bertrand et al. 2008]. The liver, skeletal muscle, adipocytes and the heart are all target organs of insulin action; and in the adipose tissue glucose is metabolized to and stored as triglycerides. On the other hand, glycogen is metabolized from the pre-cursor glucose and stored in the liver and skeletal muscle [Luiken et al. 2004].

The release of insulin from the pancreas is dependent on the concentration of glucose, amino acids as well as fatty acids in the blood [Waselle et al. 2005]. Furthermore, the measure of insulin released by the beta cells will differ depending on the type and intensity of the stimulus, as well as its means of administration [Kahn et al. 2006].

In addition to its role in carbohydrate and fat metabolism, insulin also plays a significant part in ribosomal biogenesis and protein synthesis [Kemi et al. 2008], nuclear factor translation and cardiomyocyte growth [Walsh 2006, O'Neill et al. 2005] as well as the regulation of cell death or survival [Duronio 2008].

The sections to follow, first review substrate utilization and metabolism in the heart during normal physiological conditions and the changes that occur in these during obesity.

Thereafter, the transport proteins involved in the myocardial uptake of these substrates, as well as the role that insulin plays in this process, are discussed.

2.1.2 Myocardial substrate utilization under normal physiological conditions and the transport proteins involved in substrate uptake

The myocardium is one of the biggest consumers of adenosine triphosphate (ATP) in the body and just like any other metabolic tissue it is dependent on various metabolic processes to provide this energy. In order to satisfy this large energy demand, for optimal myocardial functioning, the heart mainly utilizes long-chain fatty acids (LCFA) (60–70%) as it yields the largest amount of ATP of all the metabolic substrates [Bertrand et al. 2008]. Glucose, lactate and ketone bodies further contribute to the heart`s energy requirements [Coort et al. 2007, Bertrand et al. 2008]. However, in order for these metabolic substrates to be metabolised, they have to first gain entry into the cardiomyocyte and this is achieved by the use of various transport proteins.

2.1.2.1 Glucose transporters

There are two forms of glucose transporter (GLUT) proteins present in the myocardium namely GLUT1, which can be found in all tissues, and GLUT4, which is mainly restricted to insulin sensitive tissues [Coort et al. 2007, Bertrand et al. 2008]. Despite the heart expressing a relatively large amount of GLUT1, in comparison to other tissues, GLUT4 expression is still predominant. In terms of cellular location for basal conditions, GLUT1 is mainly located in the sarcolemma and believed to be more involved in mediating basal glucose uptake. GLUT4, on the other hand, is predominantly found in endosomes in the

intracellular compartment of cardiac myocytes. However, there are indications that myocardial intracellular stores of GLUT1 exist which can be recruited to the sarcolemma by insulin, just like GLUT4, as well as by myocyte contraction [Luiken et al. 2004].

2.1.2.2 Fatty acid transporters

Previously, it was thought that LCFAs only entered cells by means of simple diffusion, however in recent years, a number of LCFA membrane associated transport proteins have been identified that are believed to mediate the uptake of LCFA`s.

The latter mechanism is believed to be predominant [Luiken et al. 2004] and despite not being wholly understood, it is known that their translocation to the sarcolemma is arbitrated by insulin. Like GLUT, LCFA transport proteins are located in intracellular endosomes and are thought to work together to facilitate the transport of LCFA`s into the heart [Coort et al. 2007, Luiken et al. 2002].

The first of these transport proteins is a fatty acid translocase (FAT), the rodent homologue of the human homologue cluster determinant 36 (CD36), which is an 88kDa fatty acid translocase protein found at both the sarcolemma as well as in intracellular storage compartments [Coort et al. 2007, Luiken et al. 2002].

2.1.2.2.1 FAT/CD36

This translocase is thought to resemble GLUT1, more so than GLUT4, since its translocation to the sarcolemma increases 1.5 fold when stimulated by insulin, as opposed to GLUT4 which more than doubles at the sarcolemma. Additionally, FAT/CD36 is less concentrated in cytoplasmic endosomes and more prevalent at the sarcolemma under

basal, non-stimulated conditions; much like GLUT1 and in contrast to GLUT4, which is mainly localized in cytoplasmic endosomes under these conditions [Luiken et al. 2002].

Cardiac myocyte contraction serves as another stimulus for the translocation of FAT/CD36 to the sarcolemma and is mediated by the adenosine monophosphate (AMP) kinase signalling pathway (AMPK signalling pathway), which will not be discussed in further detail in this literature review [Coort et al. 2004].

2.1.2.2.2 FABPpm

The 43kDa fatty acid binding protein (FABPpm) is a second type of LCFA transport protein, which is present on the outermost surface of the sarcolemma and which is believed to act together with FAT/CD36 in the LCFA uptake process.

This is supported by data which showed that inhibition of FABPpm, with an anti-FABPpm antibody, decreases LCFA transport across the sarcolemmal membrane. Additionally, when both FAT/CD36 and FABPpm were inhibited the effects were non-additive, suggesting that they act in a similar fashion [Glatz et al. 2001, Luiken et al. 2002, Coort et al. 2004].

2.1.2.2.3 FATP

In cardiac myocytes two isoforms of the fatty acid transport protein (FATP) family, the third type of LCFA transport protein, is found namely, FATP1 and FATP6. FATP6 expression is not only restricted to the heart but is also more abundant than FATP1. These two FATP`s are believed to act together, as well as in conjunction with FAT/CD36, during the LCFA

transport process as they are not only associated with the sarcolemma but also co-localizes with FAT/CD36 [Coort et al. 2007, Luiken et al. 2002].

It is evident from the above that there are quite a number of different transport proteins involved in transporting various substrates into the myocyte, ensuring that that the energy demands of the heart are met.

2.1.3 The role of insulin-mediated PI3K/PKB/Akt signalling in GLUT and FAT/CD36 translocation to the myocardial sarcolemma under normal physiological conditions

Insulin governs myocardial substrate usage and substrate transport protein localization and therefore is involved in the maintenance of normal plasma glucose and lipid concentrations. Insulin is known to activate the PI3K/PKB/Akt pathway, which in turn, mediates the uptake of glucose as well as LCFAs into the myocardium, when standard physiological conditions prevail [Bertrand et al. 2008, Van Gaal et al. 2006, Coort et al. 2004]. The precise insulin-mediated PI3K/PKB/Akt signalling mechanism, which promotes GLUT and FAT/CD36 translocation to the sarcolemma, has not been completely elucidated thus far. However, several studies have been able to shed some light on the signalling mechanism [Luiken et al. 2002, Chabowski et al. 2005].

The insulin-mediated PI3K/PKB/Akt signalling pathway (see figure 2.1) commences when (1) insulin molecules bind to the extracellular segment of the sarcolemmal bound insulin receptor (IR), activating the intrinsic intracellular tyrosine kinase activity of the β-subunits within the receptor. The receptor then undergoes autophosphorylation and activation. (2) Once the IR is activated, it induces the cytoplasmic binding of the adaptor insulin receptor substrate-1 (IRS-1) protein to these receptors, catalyzing the phosphorylation of multiple tyrosine residues within IRS-1. IRS-1 is not the only insulin receptor substrate protein

involved in the insulin receptor cascade, insulin receptor substrate-2 (IRS-2) has also been identified to play an important role in insulin-mediated glucose transport. IRS-1 is the dominant isoform involved in the metabolic effects of insulin in skeletal muscle, adipose tissue and the heart; whereas IRS-2 complements these effects in the liver. Insulin receptor substrate-3 (IRS-3) has been identified in rodent adipocytes but is thought most likely not to be expressed in humans [Sciacchitano et al. 1997]. On the other hand, insulin receptor substrate-4 (IRS-4) is expressed in human embryonic kidney cell lines but has been reported not to be involved in insulin signalling and glucose homeostasis [Fantin et al. 2000].

(3) Once activated, IRS-1 proceeds to recruit the p85 regulatory subunit of phosphatidylinositol 3 kinase (PI3K) and in doing so allows binding of this subunit to the p110 catalytic subunit of the kinase, resulting in activation. This is mediated by the binding of the sarc homology -2 (SH2) domain, which is located in PI3K`s regulatory subunit p85, to the phosphotyrosine residues of IRS-1. Insulin-mediated PI3K activation has been said to mediate GLUT and FAT/CD36 sarcolemmal translocation [Koonen et al. 2005, Schwenk et al. 2010]. (4) PI3K is then able to generate phosphatidylinositol (3,4,5)-triphosphate (PIP3) molecules, by phosphorylating the phosphatidylinositol (PI) phosphates at the third carbon. PIP3 acts like a second messenger to (5) recruit the downstream serine/threonine kinases 3-phosphoinositide-dependent protein kinase-1 (PDK-1) and protein kinase B (PKB/Akt) to the plasma membrane, mainly from the cytosol [Hajduch et al. 2001]. These kinases bind to PIP3 by means of their pleckstrin homology (PH) domains. Subsequently, PDK-1 phosphorylates the T-loop of PKB/Akt at its Thr^{308} residue, while integrin-linked kinase (ILK) is thought to phosphorylate the protein at its Ser^{473} residue, thereby fully activating it [Mora et al. 2004, Bertrand et al. 2008, Coort et al. 2007, Kalra et al. 2010].

PI3K/PKB/Akt signalling has been shown to be involved in GLUT translocation, and it is speculated that this signalling is also involved in the translocation of FAT/CD36 to the membrane [Schwenk et al. 2010]. It has been speculated that the PI3K/PKB/Akt signalling pathway for GLUT and FAT/CD36 insulin-mediated sarcolemmal translocation might disperse at some point as they have different intracellular locations [Holloway et al. 2008]. In support of this speculation, Jain et al. (2012) found that GLUT translocation to skeletal muscle sarcolemma, as well as glucose uptake, was blighted in Munc18c (-/+) mice, upon insulin stimulation. On the other hand, when insulin served as stimulus the elevation in fatty acid transporter translocation to the sarcolemma and fatty acid transport, was unaffected in these mice. Munc18c plays an essential role in the fusion of GLUT4 and other insulin-mediated amino peptidase storage vesicles to the plasma membrane [Thurmond et al. 2000]. (6) Nevertheless, it would seem once PKB/Akt is activated, it stimulates the translocation of (i) GLUT receptors as well as (ii) LCFA transport proteins to the myocardial sarcolemma.

Thus, we see that insulin plays a pivotal role in the translocation of glucose and fatty acid transporters to the myocardial membrane, via the PI3K/PKB/Akt pathway, thereby mediating substrate uptake and metabolism in the heart.

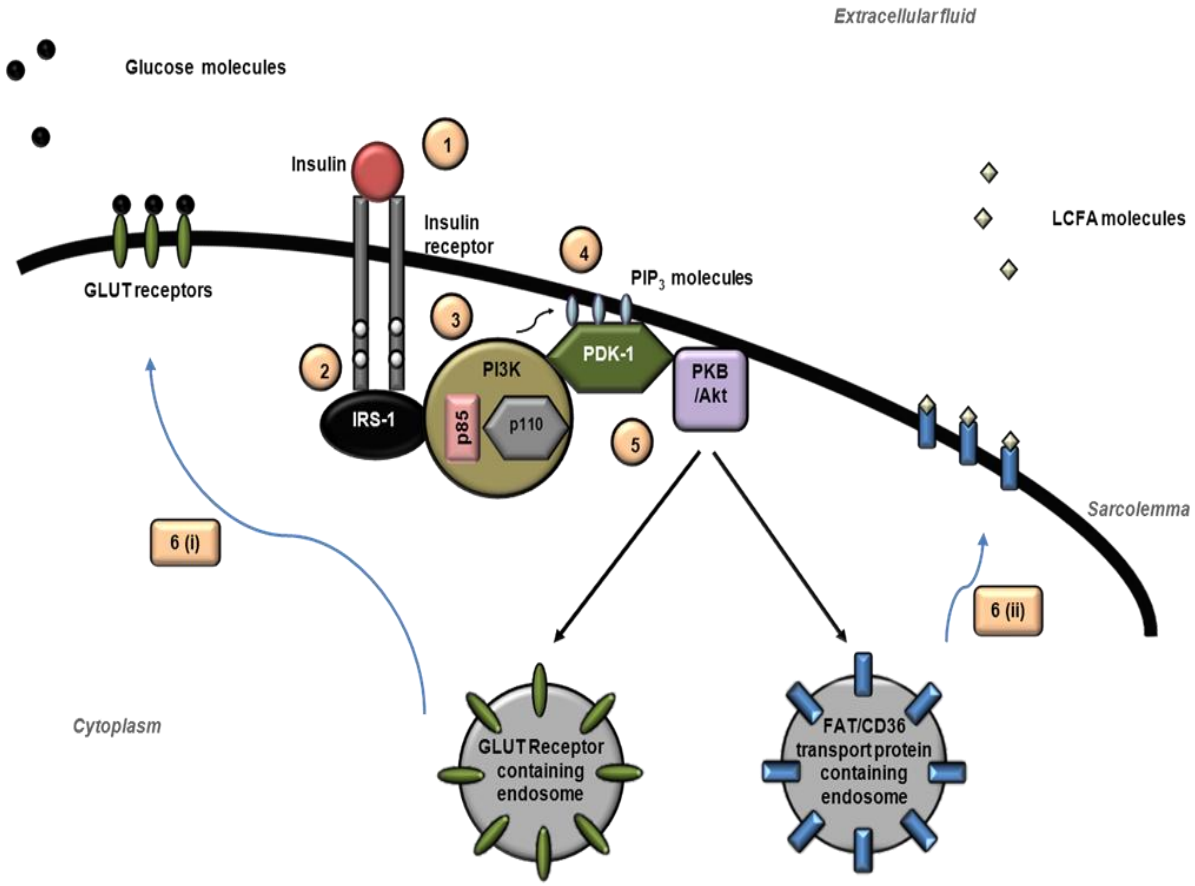

Figure 2.1. Insulin mediated activation of the PI3K/PKB/Akt pathway and its role in translocation of GLUT receptors and FAT/CD36 transport proteins to the myocardial sarcolemma, when normal physiological conditions prevail. Taken and adapted from Coort et al. 2007.

2.1.4 Glucose uptake and metabolism under normal physiological conditions

Once GLUT receptors have translocated to the myocardial sarcolemma, it allows for glucose uptake to ensue. Upon reaching the cytoplasm, glucose is rapidly phosphorylated by the enzyme hexokinase to form glucose-6-phosphate (G-6-P) [Coort et al. 2007, Petersen et al. 2002].

A portion of the G-6-P is metabolised further, in a number of steps as shown in figure 2.2, to provide the heart with ATP for its immediate energy requirements. The first step is the entry of glucose-6-phosphate into the aerobic glycolytic pathway, where one molecule is eventually converted to two molecules of pyruvate with the breakdown of two molecules of ATP to ADP and the release of one molecule of reduced nicotinamide adenine dinucleotide (NADH).

The next major step is the oxidative decarboxylation of pyruvate to acetyl coenzyme-A (acetyl-CoA) by the multienzyme complex pyruvate dehydrogenase (PDH), with the release of more NADH and some carbon dioxide. PDH is situated on the inner mitochondrial membrane.

Acetyl-CoA is therefore formed in the mitochondria where it enters the tricarboxylic acid (TCA) cycle, the third key step, and is converted to oxaloacetate in a series of steps (see figure 2.2). This four carbon molecule proceeds to react with the next incoming acetyl-CoA, forming citrate and thus allowing the TCA cycle to continue. During the oxidation of one molecule acetyl-CoA to one molecule of oxaloacetate, the TCA cycle additionally yields one guanosine 5'-triphosphate (GTP), three NADH and one 5,10-methylenetetrahydrofolate reductase ($FADH_2$) molecules.

The final step of glucose metabolism encompasses oxidative phosphorylation (OXPHOS) whereby the energy rich molecules (GTP, NADH and $FADH_2$) generated during glycolysis, pyruvate decarboxylation and the TCA cycle, donate their electrons to electron carriers.

This donation eventually drives ATP synthesis by the electron transport chain (ETC), located within the mitochondrial membrane. Please refer to figure 2.2. The OXPHOS process will be discussed in greater detail in section 2.1.5.1.

As mentioned, only a portion of myocardial G-6-P is metabolized to produce ATP, the other subset is converted to glycogen for glucose storage [Tirone et al. 2001]. Initially, G-6-P undergoes isomerization to glucose-1-phosphate (G-1-P) and is subsequently converted to uridine 5'-diphosphate glucose (UDP-glucose), which is ultimately polymerized into glycogen by the enzyme glycogen synthase (GS) [Petersen et al. 2002].

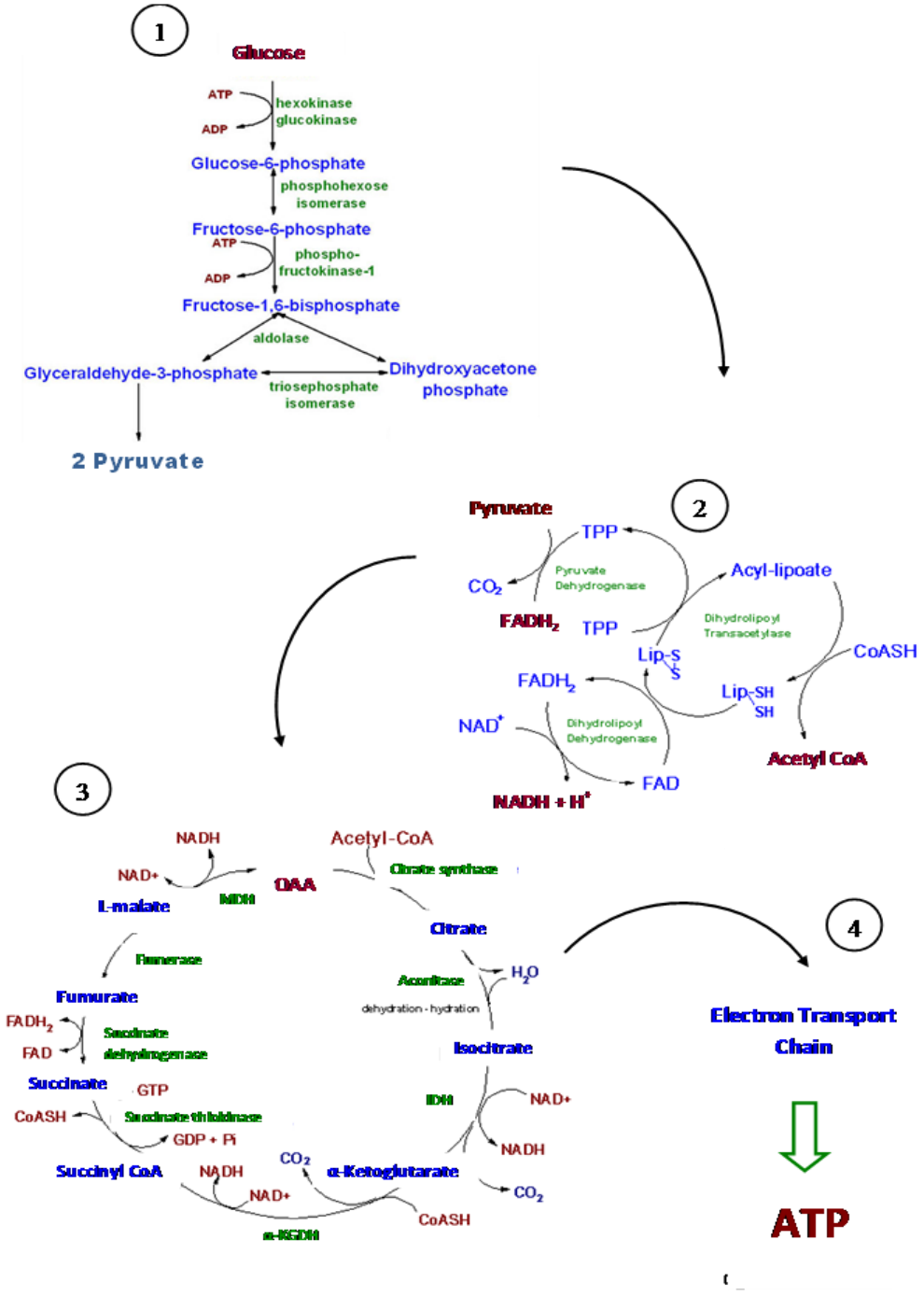

Figure 2.2. Summary of the events during glycolysis and the Kreb`s cycle. (1) Illustrate the oxidation of glucose to pyruvate (2) which is subsequently converted to Acetyl CoA, with the release of energy intermediates. (3) Acetyl Co-A thereafter enters the TCA cycle to release even more energy intermediates, (4) which is eventually reduced by the mitochondrial ETC chain to produce ATP.

Obtained and edited from:

(1) [http://rosswiki2009.pbworks.com/w/page/11977900/Glycolysis]

(2) [http://www.coenzyme-a.com/tca.htm]

(3) [http://thealchemistkitten.files.wordpress.com/2009/11/blaze_tca_cycle.jpg]

2.1.5 Long chain fatty acid uptake and metabolism under normal physiological conditions

LCFAs can be found in the circulation either in complex with albumin or esterified in the lipid core of very-low density lipoproteins (VLDLs) and chylomicrons [Spector 1984, Van der Vusse et al. 2000].

LCFAs which are bound to albumin are able to detach themselves rather easily from this plasma protein whereas esterified LCFAs are only released after being hydrolyzed at the luminal surface of the myocardial endothelium by lipoprotein lipase (LPL). Via an indistinct mechanism, the free LCFAs are transported across the endothelium and are once again bound to albumin, thus serving as the LCFAs “transport vehicle”, when in the extracellular fluid surrounding the cardiac myocytes. Once the LCFAs arrive at the sarcolemma, they once again separate from albumin and are transported across the sarcolemma by means of the various LCFA transport proteins discussed previously [Coort et al. 2007].

Upon entering the cytoplasm of the cardiomyocyte, the LCFAs bind to fatty acid binding proteins, namely heart-type cytoplasmic fatty acid-binding protein (H-FABPc), which act as vehicles for transporting the fatty acids through the aqueous cytoplasm [Coort et al. 2007]. Consequently, these fatty acids are activated by conversion to fatty acyl coenzyme-A molecules (fatty acyl-CoAs), by the enzyme fatty acyl-CoA synthetase (FACS) [Gargiulo et al. 1999], which subsequently binds to the cytoplasmic acyl-CoA binding protein (ACBP)

[Knudsen et al. 2000, Faergeman 2002]. This binding protein serves as another molecular vehicle, which is responsible for transporting the fatty acyl-CoAs to their site of metabolic conversion or breakdown [Schaap et al. 1999, Glatz et al. 2001].

When fatty acyl-CoAs are bound to ACBP they can be transported to: (1) the mitochondria for β-oxidation, (2) a site in the cytoplasm where it will undergo esterification into triacylglycerol (TAG) and phospholipids, and (3) the cytoplasm for entry into signal transduction pathways. The destiny of the fatty acyl-CoAs is determined by the needs of the myocytes at a given point in time. If the plasma content of LCFAs are elevated then insulin will predominantly direct it to TAG and phospholipid esterification, consequently sequestering it as part of the intracellular “lipid pool”. However, if the myocardial ATP demand is high then myocyte contractions will shunt the LCFAs to mitochondrial β-oxidation for energy production [Coort et al. 2007, Coort et al. 2004].

Fatty acyl-CoAs destined for mitochondrial β-oxidation reaches the mitochondria with the assistance of three specific carnitine-dependent enzymes. The first key regulatory enzyme is carnitine palmitoyl transferase I (CPT-I), which acts at the outer mitochondrial membrane to catalyze the formation of acyl-carnitine. Thereafter, acyl-carnitine gets transported into the mitochondria by the second enzyme carnitine/acyl-carnitine transferase (CACT). The third enzyme, carnitine palmitoyl transferase II (CPT-II), generates fatty acyl-CoA at the inner mitochondrial membrane by transferring an acyl group to CoA molecule from the mitochondrial pool [Coort et al. 2007].

Fatty acyl-CoAs are eventually converted to acetyl-CoA, via the process of *β*-oxidation, once it enters the mitochondria and the latter is subsequently metabolized in the citric acid cycle to yield high energy molecules such as GTP, $FADH_2$ and NADH [Schulz 1994, Ghisla 2004]. These molecules are eventually converted to ATP by means of oxidative phosphorylation in the mitochondrial electron transport chain. An overview of (a)

cytoplasmic fatty acid uptake, activation as well as (b) mitochondrial *β*-oxidation is given in figure 2.3 [Coort et al. 2007, Lopuschuk et al. 2010].

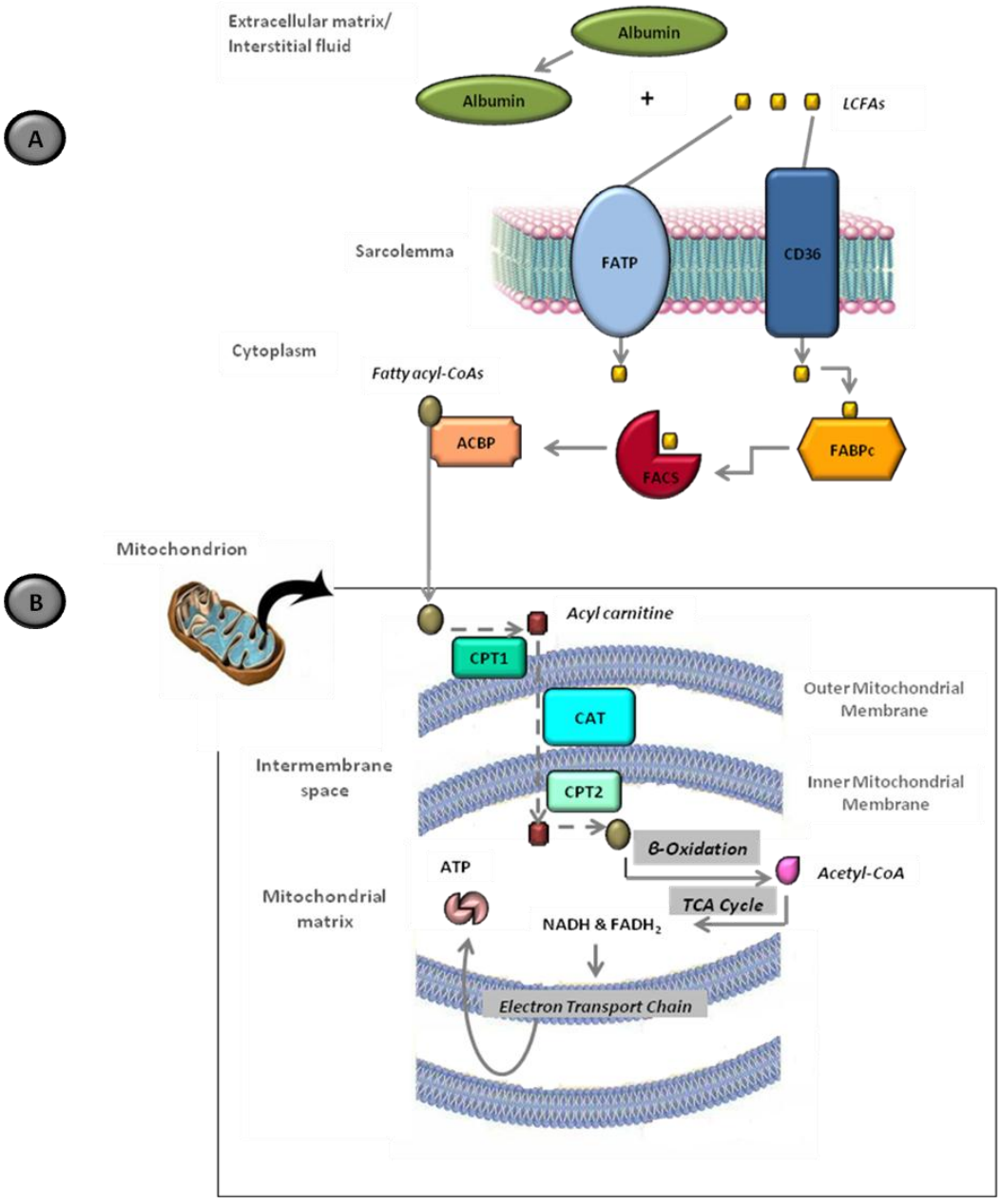

Figure 2.3. Overview of long-chain fatty acid (LCFA) utilization in cardiac myocytes under normal physiological conditions. (a) Initially the LCFAs undergo cytoplasmic uptake and activation in cardiac myocytes. (b) Thereafter, these LCFAs are transported into the mitochondria and undergo *β*-oxidation. Taken and adapted from Coort et al. 2007.

2.1.5.1 A closer look at the oxidative phosphorylation (OXPHOS) process and the mitochondrial electron transport chain (ETC)

Oxidative phosphorylation encompasses two major steps that is, the production of an electrochemical gradient via electron transfer and the synthesis of ATP. An overview of mitochondrial electron transport and ATP synthesis is given in figure 2.4.

2.1.5.1.1 Electron transfer

The most significant function of the mitochondria is to furnish the cell with energy in the form of ATP, which is derived from sources such as fats, proteins and carbohydrates [Leonard et al. 2000]. As mentioned in sections 2.1.4 and 2.1.5, the reducing equivalents i.e. energy rich molecules (GTP, NADH and $FADH_2$) released during the metabolism of these substrates, are what drives ATP synthesis via the process of oxidative phosphorylation in the mitochondrial ETC [Leonard et al. 2000]. The electron transport chain consists of five complexes, namely NADH dehydrogenase, succinate dehydrogenase, cytochrome bc_1 complex, cytochrome *c* oxidase and ATP synthase, otherwise referred to as complexes I to V. There are two components of the ETC which do not form part of the five complexes, but are nonetheless essential for electron (e^-) transfer. These would be cytochrome *c* which interacts with complex IV, and “floats” on the outside of the inner mitochondrial membrane, and ubiquinone (coenzyme Q) which is able to diffuse within the mitochondrial membrane [Pedersen et al. 1999, DiMauro et al. 2009]. Complex I structure has been said to vary according to tissue type, whereas the configuration of complexes II and IV remain more consistent [Rustin et al. 1994].

The oxidative phosphorylation process commences when complex I oxidises NADH to nicotinamide adenine dinucleotide (NAD^+) and transfers two electrons to ubiquinone

(coenzyme Q). During this process four protons (H^+) are pumped across the mitochondrial inner membrane to the intermembrane space, initiating the ETC proton gradient [Pedersen et al. 1999, Garrett et al. 1999]. Ubiquinone passes the electrons from complexes I and II through complex III, cytochrome c, and complex IV, while it pumps protons from the matrix to the intermembrane space in parallel. In complex IV, cytochrome c is reduced and its electrons donated to oxygen (O_2), which generates two water (H_2O) molecules. The protons in the intermembrane space all contribute to the 150mV electrochemical proton gradient that will drive ATP synthesis [Pedersen et al. 1999, Leonard et al. 2000]. The reducing equivalents generated during the metabolism of glutamate, pyruvate, and 3-hydroxybutyrate gain entry into the ETC via complex I. Whereas the electron transfer protein which is attached to coenzyme Q as well as complex I, are points of entry for the reducing equivalents produced from fatty acid β-oxidation. Succinate on the other hand undergoes reduction at complex II [Leonard et al. 2000].

2.1.5.1.2 ATP synthesis

The electrochemical gradient results in the proton concentration in the intermembrane space being much higher than that it the mitochondrial matrix. This unequal distribution of protons causes complex V (ATP synthase) to transfer some of these protons back into the mitochondrial matrix, thus commencing the ATP synthesis step.

ATP synthase contains two key components F_0 and F_1, where F_0 is found in the inner mitochondrial membrane (IMM) and has a rotational capacity, while F_1 extends into the matrix and is unable to rotate. Furthermore, F_0 is responsible for translocating the protons while F_1 synthesizes the ATP.

The F_0 unit seizes a proton and attaches it to the protein rotor, which binds F_0 and F_1 together, causing it to rotate and unload the proton on the inside of the membrane. During this process the rotor spins inside the stationary F_1 subunit changing the chemical energy of the electrochemical gradient to mechanical energy, which in turn brings adenosine diphosphate (ADP) and inorganic phosphate (P_i) into correct alignment for phosphorylation and ATP production. One molecule of ATP is produced from 2 or 3 protons while one molecule of glucose yields about 31.5 molecules of ATP, whereas the saturated fatty acid palmitate yields 106 molecules of ATP [Vo et al. 2004].

2.1.5.1.3 Mitochondrial respiration coupling and uncoupling

As mentioned in the previous section, during the transfer of electrons between the ETC complexes protons are pumped across the inner mitochondrial membrane to the intermembrane space, which creates an electrochemical gradient. This gradient exists because the protons are unable to diffuse back into the matrix, to reach equilibrium, across the IMM. The protons are only able to gain access to the matrix via ATP synthase because the F_0 subunitof this synthase grabs hold of the proton, while the F_1 subunit uses the free energy involved to phosphorylate ADP and produce ATP (as explained in section 2.1.5.1.2). Thus, it is easy to see that the oxidation-reduction reactions and ATP production in the mitochondria are coupled; coining the entire process coupled oxidative phosphorylation [Pendersen et al. 1999, Nicholls et al. 2001, Ricquier 2005].

Uncoupled oxidative phosphorylation occurs when there is a “leak” in the IMM, thus allowing protons to diffuse across it into the matrix that is, without having passed though ATP synthase and without producing ATP. The free energy involved is given off as heat instead [Nicholls et al. 2001, Ricquier 2005].

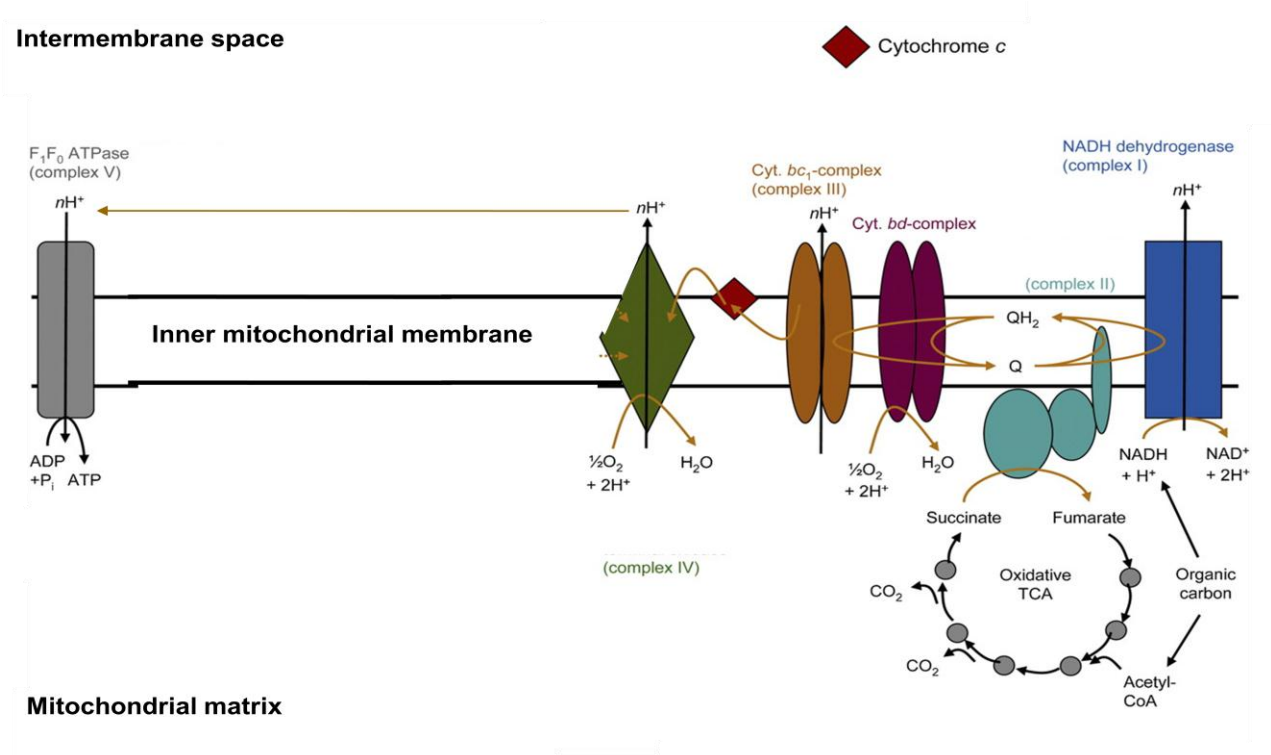

Figure 2.4: Overview of the electron transport process by complexes I to IV and electrochemical proton gradient production in the ETC, and its role in ATP synthesis via ATP synthase (complex V). Taken and edited from Lücker et al. 2010.

2.1.5.1.4 ETC complexes and their subunits

There is mounting evidence that the complexes of the electron transport chain are actually supercomplexes as they consist of multiple dimmers [Schägger et al. 2001]. The mitochondrial ETC complexes of bovine heart, bacteria and other eukaryotes have been characterized more extensively to date, as obtaining sufficient mitochondria from human tissue has proven difficult [Murray et al. 2003]. Therefore, the complex composition of these animals will be discussed in further detail.

Complexes I to V have been reported to contain 42, 4, 11, 13 and 14 polypeptide subunits, respectively [Pedersen et al. 1999, Leonard et al. 2000]; each of which contribute to complex assembly and integrity in their own way.

2.1.5.1.4.1 Complex I

This complex consists of multiple subunits, for example 46 in bovine heart mitochondria with a total molecular weight of 980kDa, whereas human myocardial tissue has 42 subunits with a molecular mass of about 1000kDa. It has been shown, in bovine heart mitochondria, that 7 of the subunits are encoded by mitochondrial DNA, whereas the genes for the other 35 subunits are encoded in the nucleus [Carrol et al. 2003, Murray et al. 2003].

Studies on bovine heart mitochondria have resolved complex I and discovered that it is L-shaped, with one arm located in the mitochondrial membrane and orientated vertically to the plane of the membrane. The other arm is orientated horizontally to the mitochondrial matrix. Furthermore, complex I was found to consist of 3 subcomplexes, namely Iλ (extrinsic arm), Iα (first part of the membrane arm) and Iβ (second part of the membrane

arm). Please refer to table 1 for the subunit composition of subcomplexes Iα, Iλ and Iβ [Carrol et al. 2003].

2.1.5.1.4.2 Complex II

Regardless of species, complex II of the mitochondrial ETC is the simplest in that it contains the least number of subunits. This complex consists of 4 subunits in animals, fungi and bacteria, while the complex consists of 8 subunits in plants [Millar et al. 2004, Morales et al. 2009, Gawryluk et al. 2009]. In the amoeba *Acanthamoeba castellanii (A. castellanii)* as well as other eukaryotes, the molecular weight of this complex was found to be about 130kDa in its active form [Gawryluk et al. 2012]. Please refer to table II for the subunit composition of complex II in *A. castellanii*.

2.1.5.1.4.3 Complex III

This complex, regardless of species, has three common subunits which all have active redox centers, namely cytochrome b (Cob), cytochrome c1 (CytC1) and the “Rieske” [2Fe-2S] protein (ISP). The 280kDa eukaryotic complex III is more complex in that it contains supplementary subunits, whereas bacterial complex III only contain these three subunits [Iwata et al. 1998, Gawryluk et al. 2012]. In bovine heart complex III is composed of 11 subunits [Pedersen et al. 1999, Leonard et al. 2000]. Refer to table III for the subunit composition of complex III in *A. castellanii*.

2.1.5.1.4.4 Complex IV

This 360kDa complex has been reported to contain more than 10 subunits in *A. castellanii* and about 13 subunits in bovine heart [Pedersen et al. 1999, Leonard et al. 2000, Gawryluk et al. 2012]. In addition to the subunits that make up complex IV, there are also additional proteins which assist with the assembly of this complex, as seen in table IV [Gawryluk et al. 2012].

2.1.5.1.4.5 Complex V

In bacteria complex V (ATP synthase) consists of 8 subunits while bovine heart contains 16 subunits [Müller et al. 2003]. As previously mentioned, this complex consists of two major components namely F_1 and F_0, where each component is composed of 5 subunits in *A. castellanii*. The remainder of the subunits are thought to be associated with the F_0 base of ATP synthase. Similar to complex IV, there are also additional proteins that play a role in the assembly of complex V as listed in table V [Gawryluk et al. 2012].

Table I. The subunit composition of subcomplexes Iα, Iλ and Iβ in complex I of bovine mitochondrial ETC. Taken from Carroll et al. 2003.

Subcomplex		
Iα	Iλ	Iβ
75 kDa	75 kDa	AGGG[a]
51 kDa	51 kDa	ASHI
49 kDa	49 kDa	ESSS[a]
30 kDa	30 kDa	MNLL
24 kDa	24 kDa	PDSW
PSST	PSST	SDAP[a,b]
TYKY	TYKY	SGDH
18 kDa	18 kDa	B22
13 kDa	13 kDa	B18
10 kDa	10 kDa	B17
B17.2	B17.2	(B15)
B16.6	B16.6	(B14.5b[c])
B14.7[d]	(B14.7[c,d])	B12
B14.5a	B14.5a	ND4[a,d]
B13	B13	ND5[a,d]
B8	B8	
(42 kDa[d])		
39 kDa		
15 kDa[c]		
MWFE		
PGIV		
SDAP[a,b,d]		
(B15)		
B14		
B9		
ND6[e]		

Table II. The subunit composition of complex II, as well as the assembly proteins which assist in the assembly of this complex, in *A. castellanii* mitochondrial ETC. Taken and edited from Gawryluk et al. 2012.

.

Protein	*Genome*	*Eukaryotes*	*Bacteria*	*Amoebozoa*
SdhA	N	+	+	+
SdhB-1	N	+	+	+
SdhB-2	N	+	+	+
SdhC	N	+	+	+
SdhD	N	+	+	+

N = Nuclear genome

Table III. The subunit composition of complex III in *A. castellanii* mitochondrial ETC. Taken and edited from Gawryluk et al. 2012.

.

Protein	*Genome*	*Eukaryotes*	*Bacteria*	*Amoebozoa*
CIII subunits				
Core1	N	+	+[a]	+
Core2	N	+	+[a]	+
Cob	M	+	+	+
Isp	N	+	+	+
Cytc1	N	+	+	+
Qrc6	N	+	–	+
Qcr7	N	+	–	+
Qcr8	N	+	–	+
Qcr9	N	+	–	+
Qcr10	N	+	–	+
CIII assembly proteins				
Bcs1	N	+	+[b]	+
Cbp3	N	+	+	+

N = Nuclear genome

M = Mitochondrial genome

[a] The Core protein 1 and 2 have bacterial homologs (M16 proteases), but are not components of bacterial CIII.

Table IV. The subunit composition of complex IV, as well as the associated proteins of this complex, in *A. castellanii* mitochondrial ETC. Taken and edited from Gawryluk et al. 2012.

Protein	*Genome*	*Eukaryotes*	*Bacteria*	*Amoebozoa*
CIV subunits				
Cox1/2	M	+	+	+
Cox3	M	+	+	+
Cox1-c	N	+	+[a]	+[a]
Cox4	N	+	–	+
Cox5b	N	+	–	+
Cox6a	N	+	–	+
Cox6b-1	N	+	–	+
Cox6b-2	N	+	–	+
Cox6c[b]	N	+	–	+
Cox7a[b]	N	+	–	-
Cox7c-1	N	+	–	+
Cox7c-2	N	+	–	+
CIV-associated proteins				
Cox11	N	+	+	+
Cox17	N	+	–	+
Cox19	N	+	–	+
Cox23	N	+	–	+
Cmc1	N	+	–	+
Sco1	N	+	+	+
Pet100	N	+	–	+
Cox10	N	+	+	+
Cox15	N	+	+	+
Shy1	N	+	+	+
Pet191	N	+	–	+

N = Nuclear genome

M = Mitochondrial genome

Table V. The subunit composition of complex V (ATP synthase), as well as the associated proteins of this complex, in *A. castellanii* mitochondrial ETC. Taken and edited from Gawryluk et al. 2012.

Protein	*Genome*	*Eukaryotes*	*Bacteria*	*Amoebozoa*
CV proteins				
$F_1\alpha$ (Atp1)	M	+	+	+
$F_1\beta$ (Atp2)	N	+	+	+
$F_1\gamma$ (Atp3)	N	+	+	+
$F_1\varepsilon$ (Atp15)	N	+	-	+
$F_1\delta$ (Atp16)	N	+	+	+
F_oa (Atp6)	M	+	+	+
F_ob (Orf25; Atp4)	M	+	+	+
F_oc (Atp9)	M	+	+	+
F_oOSCP (Atp5)	N	+	+	+
F_oA6L (OrfB; Atp8)	M	+	+[a]	+
Atpd[b] (Atp7)	N	+	-	+
Atpg[b] (Atp20)	N	+	-	+
Atpi/j[b] (Atp18)	N	+	-	+
Atpf (Atp17)	N	+	-	+
15510[c]	N	-	-	-
31[c]	N	-	-	-
24711[c]	N	-	-	-
MDH[d]	N	+	+	+
CV-associated proteins				
INH1	N	+	-	+
Atp10	N	+	-	+
Atp11	N	+	-	+
Atp12	N	+	+	+
Atp23	N	+	-	+
NCA2	N	+	-	+

N = Nuclear genome

M = Mitochondrial genome

2.2 Obesity and Insulin signalling

2.2.1 What is Insulin Resistance?

A common pathology of obesity is insulin resistance [Reaven 2008] which is classified as the inability of normal physiological levels of insulin to prompt a sufficient response in target tissues such as skeletal muscle, liver, adipose tissue and of course, the heart [Mlinar et al. 2007, Schwenk et al. 2008].

2.2.2 Changes in substrate utilization by the heart during obesity

2.2.2.1 Reduced glucose metabolism

A number of studies have been published regarding myocardial substrate utilization during a pathophysiological state such as obesity. Many of these studies involve analyzing expression, subcellular localization and functional regulation of GLUT4 and FAT/CD36 as these are imperative factors that ascertain the rate of substrate utilization [Coort et al. 2004].

Studies showed that insulin stimulated activity of the PI3K/PKB/Akt pathway was reduced in cardiac myocytes isolated from rats that were exposed to a high fat diet and later developed T2DM [Ouwens et al. 2005], as well as in cardiac myocytes isolated from insulin resistant obese Zucker rats [Coort et al. 2007].

Additionally, it was found that insulin-stimulated (physiological concentrations) GLUT4 translocation and glucose uptake were reduced in cardiomyocytes and cardiac muscle isolated from insulin resistant obese rats [Coort et al. 2007].

2.2.2.2 Increased fatty acid β-oxidation

In insulin resistant obese Zucker rats, it was found that myocardial LCFA uptake was increased in the hearts of these animals, which coincided with an elevation in the quantity of FAT/CD36 at the sarcolemma and a decrease in the FAT/CD36 intracellular content. The total FAT/CD36 content in the heart from the obese animals remained unchanged, indicating that there is a permanent relocation of FAT/CD36 from its intracellular compartment to the sarcolemma and this is most likely the reason for the increased LCFA uptake. Additionally, the rate of cardiac LCFA oxidation was unaffected while the content of TAG in myocardium as well as the rate at which LCFAs were converted to TAG, were augmented in these obese rats [Coort et al. 2004, Luiken et al. 2002].

Most studies conducted on humans are restricted to skeletal muscle. Nevertheless, the findings of these studies can be extrapolated to the myocardium, as it too is a muscle and regulates its substrate utilization similar to skeletal muscle [Coort et al. 2007]. Analysis of skeletal muscle, in obese and T2DM human subjects and compared to lean controls, indicated a similar increase in intracellular TAG content and an increase in the amount of FAT/CD36 protein at the sarcolemma as in the hearts of obese Zucker rats. Additionally, the rate of palmitate (a saturated fatty acid) transport was elevated in these obese and T2DM human subjects [Bonen et al. 2002].

As these studies have indicated, there is a strong correlation between obesity and cardiac insulin resistance and it would seem that the pivotal factor connecting these two conditions might be metabolic disturbances, such as increased LCFA and decreased glucose uptake, within the myocardium [Coort et al. 2007].

2.2.3 Changes in substrate utilization by the heart during cardiomyopathies

During myocardial pathophysiological conditions such as ischemia-reperfusion injury, hypertrophy, atrophy and advanced heart failure, it has been reported that substrate utilization in the heart and its subsequent ATP production, were altered. During these cardiomyopathies there is a reduction in fatty acid β-oxidation and elevated glucose metabolism, as indicated by a number of studies in humans, canines and rodents [Rosano et al. 2008, Hajri et al. 2001, Huss et al. 2005, Stanley et al. 2005]. Several of these cardiomyopathies have been shown to lead to heart failure [Taha et al. 2007] and thus, the changes in substrate utilization during heart failure will be discussed in further detail.

There are conflicting studies but the general consensus, recently achieved, is that during the initial stages of heart failure, substrate utilization is still relatively normal in that fatty acids still serve as the main and glucose as the secondary energy source. It is during the late stages of the disease that fatty acid metabolism is blunted and glucose oxidation is upregulated [Stanley et al. 2005, Lopuschuk et al. 2010].

It is thought that the heart perceives these pathologies as stressors and responds to it by changing its substrate metabolism, depending on whether or not the “stress” is acute or sustained. When the “stress” is acute the changes in substrate utilization manifest itself on the cytosolic level and can be considered transient. On the other hand, during chronic myocardial stress the initial metabolic changes become permanent as it becomes regulated on the nuclear level [Rajabi et al. 2007].

The precise mechanism is currently not known whereby the substrate switch on the cytosolic level leads to the changes seen on the nuclear level. It is speculated that the transcriptional level of a number of enzymes and transporters that play significant roles in myocardial substrate uptake and metabolism are elevated in the normal adult human

heart, in comparison to the foetal heart [Razeghi et al. 2001, Sack et al. 1997, Rajabi et al. 2007]. While the transcriptional levels of these genes in the adult heart are thought to decline to the level found in the foetal heart during heart failure [Razeghi et al. 2001, Rajabi et al. 2007]. Please refer to table 1.

Other changes seen during advanced heart failure include a reduction in peroxisome proliferator-activated receptor-α (PPAR-α) expression and activity [Barger et al. 2000] as well as PPARγ coactivator-1α (PGC-1α) [Heusch et al. 2005, Gottlieb 1999, Downward 2003, Depre et al. 2005, Lazar 1997], both of which are essential in regulating mitochondrial metabolism and biogenesis [Huss et al. 2005, Rajabi et al. 2007]. The attenuation in the activity of the electron transport chain activity as well as a reduction in the flux of mitochondrial oxidative phosphorylation has also been noted during this stage of heart failure [Rajabi et al. 2007]. In addition, a few studies in humans and rodents have shown that the activity of several of the ETC complexes were downregulated [Jaretta et al. 2000, Casademont et al. 2002, Scheubel et al. 2002, Stanley et al. 2005].

2.2.3.1 Could similar changes in myocardial substrate utilization occur in advanced obesity-related cardiomyopathies?

Transgenic (TG) mice, overexpressing of GLUT1 were used to augment intracellular glucose in the heart, while these animals were also fed a high fat diet for 20 weeks to elevate fatty acid levels. The wild-type (WT) and TG mice fed high fat diets developed diet-induced obesity and insulin resistance. The WT mice displayed elevated myocardial fatty acid oxidation and reduced glucose in response to the high fat diet. On the other hand, this diet did not increase the fatty acid oxidation in the TG mice however they showed significantly higher levels of glucose oxidation in the heart. Furthermore, the study found

that metabolic gene expression favoured glucose utilization as the elevated glucose levels induced decreased PPAR-α and 3-oxoacid CoA transferase expression, while the expression of acetyl-CoA carboxylase was enhanced in these mice. Lastly, when TG mice were fed a high fat diet they displayed elevated myocardial oxidative stress and contractile dysfunction [Yan et al. 2009].

This study suggests that despite the presence of elevated fats in the diet, the transgenic diet-induced obese mice favour glucose over fatty acid utilization after 20 weeks. The decreased myocardial fatty acid and increased glucose oxidation seen in these mice could be associated with the decreased PPAR-α and 3-oxoacid CoA transferase and elevated acetyl-CoA carboxylase expression.

Belfiore et al. (1998) stated that increased plasma free fatty acids, glucose and insulin levels are associated with obesity. Furthermore, the increased free fatty acids induced inhibition of pyruvate dehydrogenase (PDH), by increasing acetyl-CoA levels, thereby blunting glucose metabolism. Whereas, increased plasma glucose and insulin levels inhibit CPT-I, via enhanced malonyl-CoA production, thus inhibiting fatty acid oxidation. These mechanisms are thought to occur through the short-term as well as the long term effects of obesity.

On the other hand, as discussed in section 2.2.2 obesity is associated with increased fatty acid β-oxidation and decreased glucose oxidation. Perhaps these metabolic substrate changes seen are associated with the initial stages of obesity and the start of myocardial insulin resistance. Whereas those observed by Yan et al. (2009) could represent the changes in substrate utilization during advanced obesity and when insulin resistance is in a progressive stage.

Currently, little research has been done that compares the substrate utilization during the early onset and the advanced stages of obesity, thus it would be difficult to say whether the difference in substrate utilization seen by Yan et al. and those discussed in section 2.2.2 are due to the stage of obesity.

Table VI. Differences in the protein level of enzymes and transporters that play significant roles in myocardial substrate uptake and metabolism as well as myocardial structure, in the adult, foetal, hypertrophic and atrophied rodent heart. Taken from Rajabi et al. 2007.

MHC-α*	↑	↓	↓	↓
MHC-β*	↓	↑	↑	↑
Cardiac α-actin	↑	↓	↓	↓
Skeletal α-actin	↓	↑	↑	↑
GLUT1	=	=	=	=
GLUT4	↑	↓	↓	↓
mCPT-I	↑	↓	↓	↓
lCPT-I	=	=	=	=
mCK	↑	↓	↓	↓
PPAR-α	↑	↓	↓	↓
PDK2	↑	↓	↓	↓
PDK4	↑	↓	↓	↓
mGS	↑	↓	↓	↓
MCD	↑	↓	↓	↓
UCP2	↑	(↓)	↓	(↓)
UCP3	↑	(↓)	(↓)	(↓)

Relative changes are expressed by either increase ↑ or decrease ↓ compared to a hypothetical baseline. Arrows in parenthesis (↑) (↓) indicate trends, but not significant changes of data in the literature cited.

* The ratio of MHC-α/MHC-β is different in human heart

2.3 Obesity and Cardiac Insulin Resistance

The precise mechanism by which cardiac insulin resistance is mediated during obesity is at present not completely understood and thought to be complicated and attributable to multiple factors. Furthermore, research aimed at elucidating the mechanism of insulin resistance has mainly focused on skeletal muscle. This has nonetheless provided valuable insight into how myocardial insulin resistance could be mediated. One thought is that myocardial metabolic anomalies such as excess intracellular lipid accumulation could be one of the main culprits in initiating the pathophysiology. The change in myocardial substrate preference during obesity, discussed in section 2.2.2, is thus thought to be an arbitrator of obesity-related myocardial insulin resistance [Coort et al. 2007, Goodpastor et al. 2004, Petersen et al. 2002].

2.3.1 Alluding to the mechanism of obesity-related cardiac insulin resistance

Obese individuals consume more calories than they burn, in comparison to lean counterparts, resulting in a greater availability of metabolic energy that needs to be stored in the adipose tissue. This surplus adiposity, particularly intra-abdominal fat accumulation, hinders the ability of insulin to suppress hormone-sensitive lipase (HSL) and in turn, lipolysis in the adipose tissue. The rest of the proposed mechanism will be explained in figure 2.5.

The elevated lipolysis in the adipocytes (1) subsequently increase plasma free fatty acid levels (2) which activate insulin secretion. (3) Thus stimulating permanent FAT/CD36 translocation to the myocardial sarcolemma during obesity, as mentioned in 2.2.2.2, (4) which allows for the uptake of these excess extracellular free fatty acids (LCFAs) into the

myocardium. Additionally, there is a greater conversion of LCFAs into TAG which is also subsequently oxidised, increasing the intracellular content of TAG metabolites (ceramide, diacylglycerol (DAG) and acetyl-CoA). It is thought that by increasing the myocardial uptake of excess extracellular LCFAs, the heart has shifted its substrate metabolism to increased fatty acid utilization, as discussed in 2.2.2. (5) The intracellular TAG metabolites proceeds to activate protein kinase C -*θ* (PKC-*θ*), (6) diminishing tyrosine and enhancing serine phosphorylation of IRS-1. (7) This reduces the ability of IRS-1 to recruit and activate PI3K, which sequentially hinders the activation of protein kinase B (PKB/Akt) [Petersen et al. 2002]. When PKB/Akt activation is diminished then (8) GLUT translocation to the sarcolemma and glucose uptake is reduced. This reduction in glucose uptake is thought to be the second shift in substrate utilization seen during obesity, as discussed in section 2.2.2. The decrease in glucose uptake is thought to reduce glycogen synthesis and (9) elevate blood glucose levels, rendering the cardiomyocyte insulin resistant as the high glucose blood levels stimulate the secretion of even more insulin, while the cells' ability to take up the extracellular glucose is severely blunted.

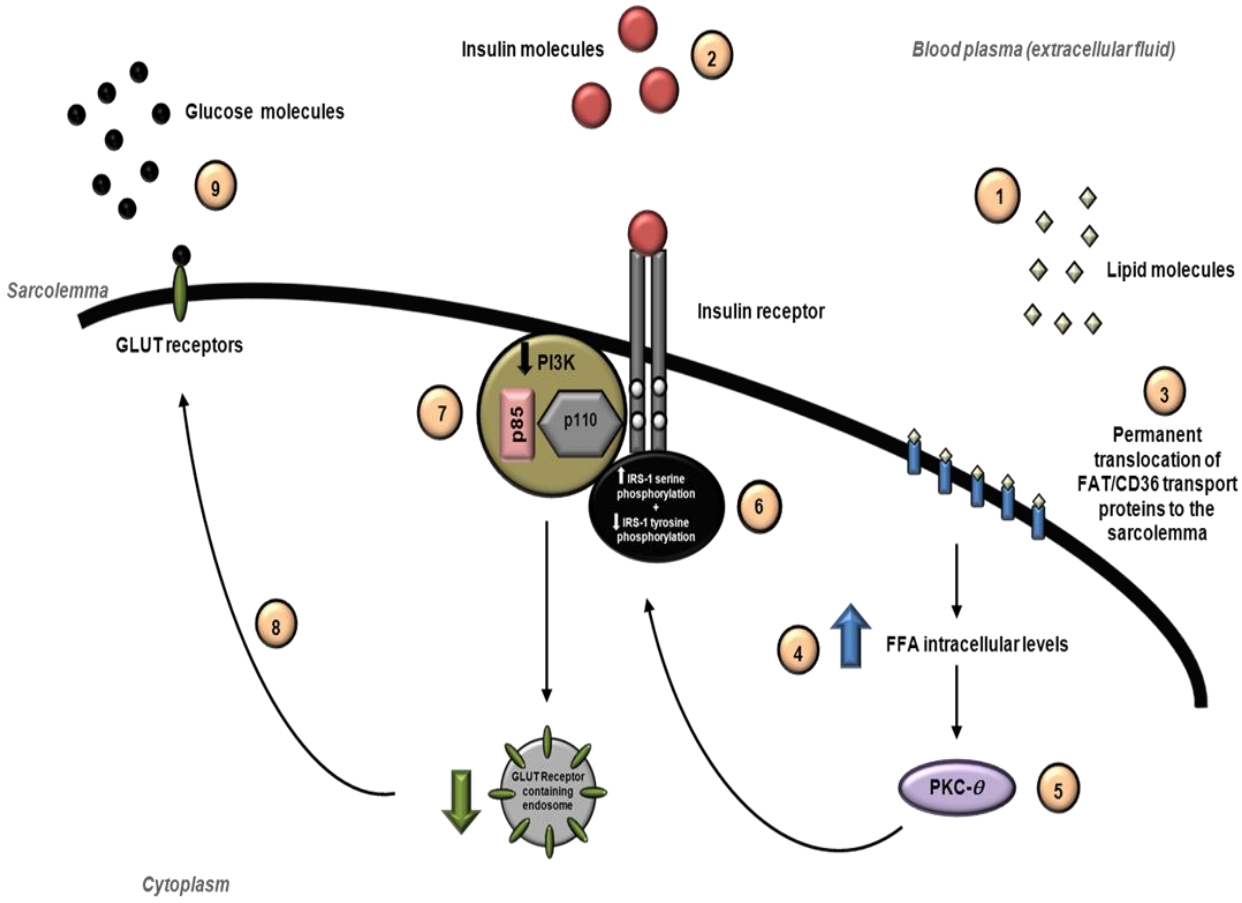

Figure 2.5. Metabolic abberations involving the insulin mediated PI3K/PKB/Akt pathway in the obese individual, in pathophysiological conditions. Taken and adapted from Coort et al. 2007.

2.3.1.1 How does the excess free fatty acids in the plasma, accumulate in ectopic organs during obesity?

A bone of contention for researchers is the mechanism by which the excess intracellular lipids accumulate in ectopic organs such as skeletal muscle, liver, pancreas and the heart during obesity, resulting in insulin resistance. There are currently four hypotheses or theories available, which attempt to explain this metabolic aberration.

2.3.1.1.1 The portal/visceral hypothesis

This hypothesis proposes that obese individuals are characterized by elevated adipocyte lipolysis and accordingly, there is an increased secretion of fatty acids into the plasma and as a result the flux of fatty acids into the liver, via the portal vein, is augmented. Additionally, these fatty acids are also able to infiltrate skeletal muscle, the heart and pancreas. Hepatic TAG production and assembly into VLDLs are thus enhanced, consequently elevating the secretion of VLDLs into the plasma. The high lipid plasma levels stimulate the secretion of insulin which in turn activates the translocation of LCFA transport proteins to the myocardial sarcolemma. This translocation to the sarcolemma is permanent as the plasma lipid levels are chronically elevated in the obese individual. This is in contrast to the non-obese individual where the translocation is transient due to normal lipid handling by the adipose tissue and liver [Van Gaal et al. 2006, Bergman et al. 2007, Kahn et al. 2006].

This theory then latches onto the Randle cycle by suggesting that insulin resistance in these target organs, including the heart, is achieved by increased intracellular concentrations of acetyl-CoA, as a result of increased LCFA oxidation. The increased acetyl-CoA then augments the concentration of G-6-P and decreases hexokinase activity,

ultimately causing a reduction in glucose uptake and oxidation [Bergman et al. 2007, Rasvussin et al. 2002, Coort et al. 2007].

2.3.1.1.2 Ectopic fat storage syndrome hypothesis

This hypothesis proposes that the adipocyte stem cell precursors, from which the mature adipocyte is derived, lack their full proliferative and differentiation ability. Thus, the existing peripheral adipocytes undergo hypertrophy when there is excess energy or fat available, as is the case in obesity. The subcutaneous fat depots soon become saturated and the fatty acids filter into the ectopic organs such as the liver, skeletal muscle and heart, causing insulin resistance in the target organ [Ravussin et al. 2002].

2.3.1.1.3 Impaired fat oxidation hypothesis

In this hypothesis it is suggested that whole body LCFA oxidation is blighted in the obese person, increasing plasma LCFA content and elevating ectopic lipid accretion; culminating in insulin resistance of the ectopic organ [Ravussin et al. 2002, Bergman et al. 2007].

2.3.1.1.4 Endocrine paradigm hypothesis

This theory puts forward the idea that because adipocytes are also endocrine cells they are able to secrete cytokines and hormones [Bergman et al. 2007, Aguilera et al. 2008]. It is thought that these hormones or endocrine factors are able to influence the metabolism and biology of peripheral tissues such as the liver, muscle and heart and cause insulin resistance [Kahn et al. 2006, Ravussin et al. 2002, Bergman et al. 2007].

It would seem that the majority of the literature favours the portal/visceral hypothesis. However, it should be noted that there is mounting evidence supporting the other three hypotheses. It could then be suggested, that the key to understanding the mechanism behind obesity induced ectopic intracellular lipid accumulation, might not lie in only one theory but rather a combination of all four theories.

2.4 Obesity and the insulin-mediated PI3K/PKB/Akt pathway

As seen in the previous sections, the insulin-mediated PI3K/PKB/Akt pathway plays a significant role in regulating glucose and fatty acid metabolism in the heart, while any aberrations in this pathway can mediate myocardial insulin resistance. The following sections will review the role that key components of the PI3K/PKB/Akt pathway plays in myocardial glycogen synthesis, during the normal physiological state and during obesity.

2.4.1 The role of the insulin-mediated PI3K/PKB/Akt pathway in glycogen synthesis

2.4.1.1 The PKB/Akt protein

PKB/Akt is a 57kDa protein which possesses three isoforms, namely PKBα (Akt1), PKBβ (Akt2) and PKBγ (Akt3), and regardless of the isoform, contains an amino-terminal pleckstrin homology (PH), a carboxy-terminal regulatory and a kinase domain [Hajduch et al. 2001, Lawlor et al. 2001].

Growth factors, insulin, and DNA damage all serve as stimuli for the activation of cytoplasmic PKB/Akt under normal physiological conditions and once it is activated, PKB/Akt can migrate to an array of subcellular compartments [Parcellier et al. 2008]. In these subcellular compartments, such as the Golgi apparatus, endoplasmic reticulum,

mitochondria and nucleus [Hajduch et al. 2001], PKB/Akt phosphorylates substrates and regulates target molecules and genes [Hajduch et al. 2001, Parcellier et al. 2008].

Insulin stimulates the activation of tissue specific PKB/Akt isoforms. In the heart all isoforms of PKB/Akt are expressed however, that of PKBα/Akt1 and PKBβ/Akt2 was found to be the most expansive [Matsui et al. 2001].

The main isoform found in skeletal muscle and hepatocytes is PKBα/Akt1, whereas PKBβ/Akt2 is mainly expressed in adipocytes. The insulin-mediated activation of PKBγ/Akt3 did not occur in these two tissue types but has been detected in other cell lines [Walker et al. 1998].

Studies indicate that PKBα/Akt1 is most likely plays an important role in growth and PKBβ/Akt2 in metabolism whereas, PKBγ/Akt3 is thought to not be essential for either growth or metabolism [Chen et al. 2001, Cho et al. 2001]. Instead PKBγ/Akt3 is thought to play a role in myocardial hypertrophy and neurological phenotype [Taniyama et al. 2005, Sussman et al. 2010].

Phosphorylation of PKB/Akt at two specific residues is required for full activation, these residues being Thr^{308} and Ser^{473} for PKBα/Akt1, Thr^{309} and Ser^{474} for PKBβ/Akt2 and Thr^{305} and Ser^{472} for PKBγ/Akt3. These residues are located in the kinase and carboxy-terminal regulatory domains, respectively [Delcommenne et al. 1998, Taniyama et al. 2005].

PDK-1 was found to be responsible for the phosphorylation of Thr^{308} while the kinase enzyme responsible for Ser^{473} phosphorylation has not yet been completely characterized, it is believed to be PDK-2 (3-phosphoinositide-dependent protein kinase-2) [Hajduch et al. 2001, Kobayashi et al. 1999, Lawlor et al. 2001].

2.4.1.2 PBK/Akt and glycogen synthesis

Glycogen synthesis is the body`s mechanism of disposing of excess glucose and when this process is impaired in any way, as is the case in obesity, it paves the way for tissue specific insulin resistance [Pearce et al. 2004]. PKB/Akt is able to exert its control over this metabolic process via the phosphorylation and thus inhibition of the serine/threonine protein kinase glycogen synthase kinase-3 (GSK-3) [Rao et al. 2007]. This subsequently stimulates the activation of the enzyme glycogen synthase, and glycogen synthesis [Parcellier et al. 2008], all of which will be reviewed in the sections that follow.

2.4.1.2.1 Glycogen synthase kinase-3 (GSK-3) protein

A significant role has been established for GSK-3 in a wide selection of biological processes, such as cellular proliferation and differentiation, protein synthesis, embryonic development and apoptosis. GSK-3 has been found to regulate these processes by phosphorylating a number of proteins, thereby activating a variety of pathways [Frame et al. 2001, Xu et al. 2009]. One of the first roles assigned to GSK-3, was in the regulation of the glycogen synthesis process [Xu et al. 2009], the mechanism of which is discussed in more detail in the sections that follow.

GSK-3 is found in two isoforms namely, GSK-3α and GSK-3β [Pearce et al. 2004], is constitutively active when the cells do not receive a stimulus [Hajduch et al. 2001] and is expressed in all cells and tissues [Ciaraldi et al. 2006].

Furthermore, this kinase has an N-terminal residue, Ser^{21} for GSK-3α and Ser^{9} for GSK-3β, that is regulated at all times by PKB/Akt (for the purpose of glucose metabolism), determining whether or not the kinase will remain activated or if its activation will be

downregulated [Rao et al. 2007, Lawlor et al. 2001, Hajduch et al. 2001]. However upon insulin stimulation, activated PKB/Akt phosphorylates these isoforms at their N-terminal residues, Ser^{21} (GSK-3α) and Ser^{9} (GSK-3β), subsequently leading to GSK-3 inhibition [Rao et al. 2007, Lawlor et al. 2001, Hajduch et al. 2001].

GSK-3 is also regulated, via phosphorylation, by a number of other substrates, each having their own biological significance (which is reviewed elsewhere), such as MAPK-activated protein kinase-1 (MAPKAP-K1/RSK), epidermal growth factors (EGF) and p70 ribosomal S6 kinase-1 (S6K1) [Frame et al. 2001, Doble et al. 2003, Xu et al. 2009].

2.4.1.2.2 GSK-3 during normal physiological conditions

When insulin sensitive cells are not stimulated by insulin (during periods of rest or fasting for example) in a normal, healthy individual, then PKB/Akt activation is inhibited and prevents the phosphorylation and inactivation of GSK-3 at their respective serine residues [Rao et al. 2007, Lawlor et al. 2001, Hajduch et al. 2001]. This in turn ensures that GSK-3 remains active and thus, capable of phosphorylating and inhibiting the enzyme glycogen synthase and the glycogen synthesis process [Pearce et al. 2004].

Active GSK-3 also has the ability to phosphorylate IRS-1 at its serine and threonine residues thus mediating a diminished interaction between IRS-1 and the insulin receptor by advancing the disintegration of IRS-1 [MacAulay et al. 2007, Boura-Halfon et al. 2009]. As a result the insulin signalling cascade is downregulated, reducing the translocation of GLUT receptors to the sarcolemma. Glucose uptake as a consequence is downregulated, thus maintaining normal blood glucose levels [Pearce et al. 2004].

In contrast, when cells are stimulated by insulin (postprandial for example), PKB/Akt is able to phosphorylate and inactivate GSK-3. In this subsequent repressed state, GSK-3 cannot phosphorylate and block glycogen synthase; thus losing its inhibitory control over

the glycogen synthesis process. Furthermore, inactive GSK-3 is unable to phosphorylate and thereby disintegrate IRS-1, promoting GLUT receptor translocation to the sarcolemma and glucose uptake. This not only further promotes glycogen synthesis but also reduces the elevated blood glucose levels [Pearce et al. 2004].

2.4.1.2.3 GSK-3 during obesity

Section 2.4.1.2.2 emphasizes the significant role that GSK-3 plays in insulin mediated glucose and glycogen metabolism as well as the influence the protein has on blood glucose levels. More importantly, it highlights the potential role of GSK-3 in mediating insulin resistance, a major hallmark of obesity.

Indeed, GSK-3 expression or activity has been found to be significantly augmented in the skeletal muscle of animal models of insulin resistance [Ferrannini 1998, Eldar-Finkelman et al. 1997] as well as in insulin resistant T2DM patients [Nikoulina et al. 2000] Additionally, GSK-3 levels were not only found to be elevated in obese and insulin resistant high-fat fed mice [Eldar-Finkelman et al. 1999] and obese Zucker rats [Dokken et al. 2005] but in the skeletal muscle of obese humans as well [Henriksen et al. 2006].

The actions of activated GSK-3 in the normal, healthy individual give rise to the inhibition of glucose uptake and glycogen synthesis when the cells are not stimulated by insulin, as seen in section 2.4.1.2.2. Thus, the hypothesis is that glucose uptake and glycogen synthesis would be significantly downregulated during periods of rest in the obese individual. Furthermore, this is seen as a key contributing factor in mediating obesity-related insulin resistance.

A study conducted by Pearce et al. (2004) utilizing genetically engineered mice, which had excessively augmented GSK-3 expression specifically in their skeletal muscle, displayed

diminished muscle glycogen content despite increased plasma insulin levels at rest [Rao et al. 2007]. This study thus supports the role of GSK-3 as a potential mediator of insulin resistance.

GSK-3 is suspected to intensify obesity, by increasing body weight and intra-peritoneal fat mass. Eldar-Finkelman et al. (1997) found, when comparing two different strains of genetically engineered mice subsequent to being fed a high fat diet for 15 weeks, that the obesity and diabetes prone strain (C57BL/6J) had an increased body weight of 30%. The A/J strain, which is resistant to diet-induced obesity and diabetes, on the other hand only had a fairly small increase in body weight, about 4 grams per animal on average. In addition, the GSK-3 activity in the epididymal fat tissue of the C57BL/6J mice displayed a two-fold increase in comparison to the control animals, while there was no significant difference in the skeletal muscle enzyme activity between the C57BL/6J and control mice. These findings thus indicate that GSK-3 might play an important role in mediating increased adiposity during the obese state.

2.5 Obesity and Myocardial Cell Death

2.5.1. Modes of cell death

Apoptosis is a rigorously controlled biological, energy dependent, process crucial for the removal of unwanted or damaged cells [Gupta 2001]. This type of cell death encompasses cell shrinkage and the formation of small apoptotic bodies, plasma membrane blebbing, chromatin condensation and DNA fragmentation [Bennet 2002, Clerk et al. 2003, Dragovich et al. 1998, Strasser et al. 2000]. Apoptosis is also marked by alterations in

mitochondrial membrane permeability and the release of proteins from the mitochondrial intermembrane space [Krysko et al. 2008].

Autophagy was previously thought of as a second type of cell death but has recently been defined as a “housekeeping” process as it destroys damaged and dysfunctional organelles and protein aggregates in cells by means of degradation, under normal and aberrant physiological conditions [Dong et al. 2010]. This strictly regulated process is characterized by autophagic vacuoles which is composed of double membranes and is also activated when a cell is deprived of essential nutrients or growth factors [Krysko et al. 2008].

The third type of cell death, necrosis, or sometimes referred to as oncosis, is associated with swift cytoplasmic swelling which causes the intracellular organelles to swell as well, furthermore resulting in plasma membrane blebbing (reversible process). Eventually, the plasma membrane and organelles rupture, releasing (amongst others) lysosomal enzymes which cause inflammation in the adjacent cells and tissue [Dive et al. 1992, Krysko et al. 2008].

As a result of these features necrosis has long been thought of as an uncontrolled and “accidental” process [Krysko et al. 2008]. However, it has recently been shown that the necrotic process is regulated via the interaction of several biochemical and molecular activities at various cellular levels.

Necrosis is elicited by stressors such as ATP depletion, ischemia, when a cell is unable to maintain ionic homeostasis, heat, high concentrations of reactive oxygen species (ROS) such as hydrogen peroxide, osmotic shock as well as mechanical stress; and is often characterized by unwanted cell loss in pathophysiological states [Festjens et al. 2006, Vanden Berghe et al. 2007].

Apoptotic cell death will be discussed in greater detail in the sections to follow, for the purpose of this review, whereas autophagic and necrotic cell death are reviewed elsewhere [Dong et al. 2010, Festjens et al. 2006].

2.5.2 The role of the insulin-mediated PI3K/PKB/Akt pathway in myocardial apoptosis.

The PI3K/PKB/Akt pathway is known to be cardioprotective [Rubio et al. 2009] and mediates its protection by activating PKB/Akt which in turn, promotes survival and prevents death of the cardiomyocytes [Hill et al. 2002] by moderating the process of apoptosis either directly or indirectly [Franke et al. 1997, Hemmings 1997]. Myocardial apoptosis is mediated by two pathways; (1) the extrinsic pathway, otherwise known as the death receptor pathway, and (2) the intrinsic pathway, also viewed as the mitochondrial dependent pathway [Bishopric et al. 2001].

2.5.2.1 The death receptor apoptotic (extrinsic) pathway

In terms of the extrinsic pathway, there are actually a number of pathways that fall into this category. The receptors of the Fas and tumour necrosis factor receptor-I (TNFR-I) death receptor pathways, are active in cardiomyocytes and have been associated with the development of cardiovascular disease [Lee et al. 2009a]. These pathways are the most well-known of the death receptor apoptotic pathways and as the name suggests, are mediated by their respective receptors (Fas and TNF receptors) [Peter et al. 2003, Wang et al. 2003]. An overview of the signalling cascade of the Fas and TNFR death receptor apoptotic (extrinsic) pathways are given in figure 2.6.

Fas and TNFR-I are two of the death receptors which contain death domains that are able to undergo trimerization or aggregation once Fas ligands and tumour necrosis factor-α (TNF-α) bind to their respective receptors [Gupta 2001, Baines et al. 2005]. This in turn allows for the recruitment of adaptor molecules, Fas-associated death domain (FADD) and tumour necrosis factor receptor-associated death domain (TRADD) (for Fas and TNFR-I receptors, respectively) which are localized in the cytoplasm and contain their own death domains [Peter et al. 2003, Wang et al. 2003]. For the TNFR-I death pathway, TRADD first has to recruit FADD in order to mediate the activation of apoptosis, whereas FADD is directly recruited in the Fas death pathway [Gupta 2001]. Once recruited, FADD is able to bind to cytoplasmic procaspase-8 via the interaction of their homologous death effector domains (DED). The binding of the death domain (located in the ligand), FADD and procaspase-8 forms a complex known as the death-inducing signalling complex (DISC) [Gupta 2001, Yang et al. 1998]. While in the complex, procaspase-8 is activated to active or mature caspase-8, by means of autoproteolysis, which in turn activates caspase-3 (also called “effector” or “executioner” caspase) [Gupta 2001, Baines et al. 2005, Yang et al. 1998]. Activated caspase-3 subsequently cleaves many “death” substrates (cytoplasmic as well as nuclear), leading to DNA fragmentation and the morphological modifications coupled to apoptosis [Gupta 2001].

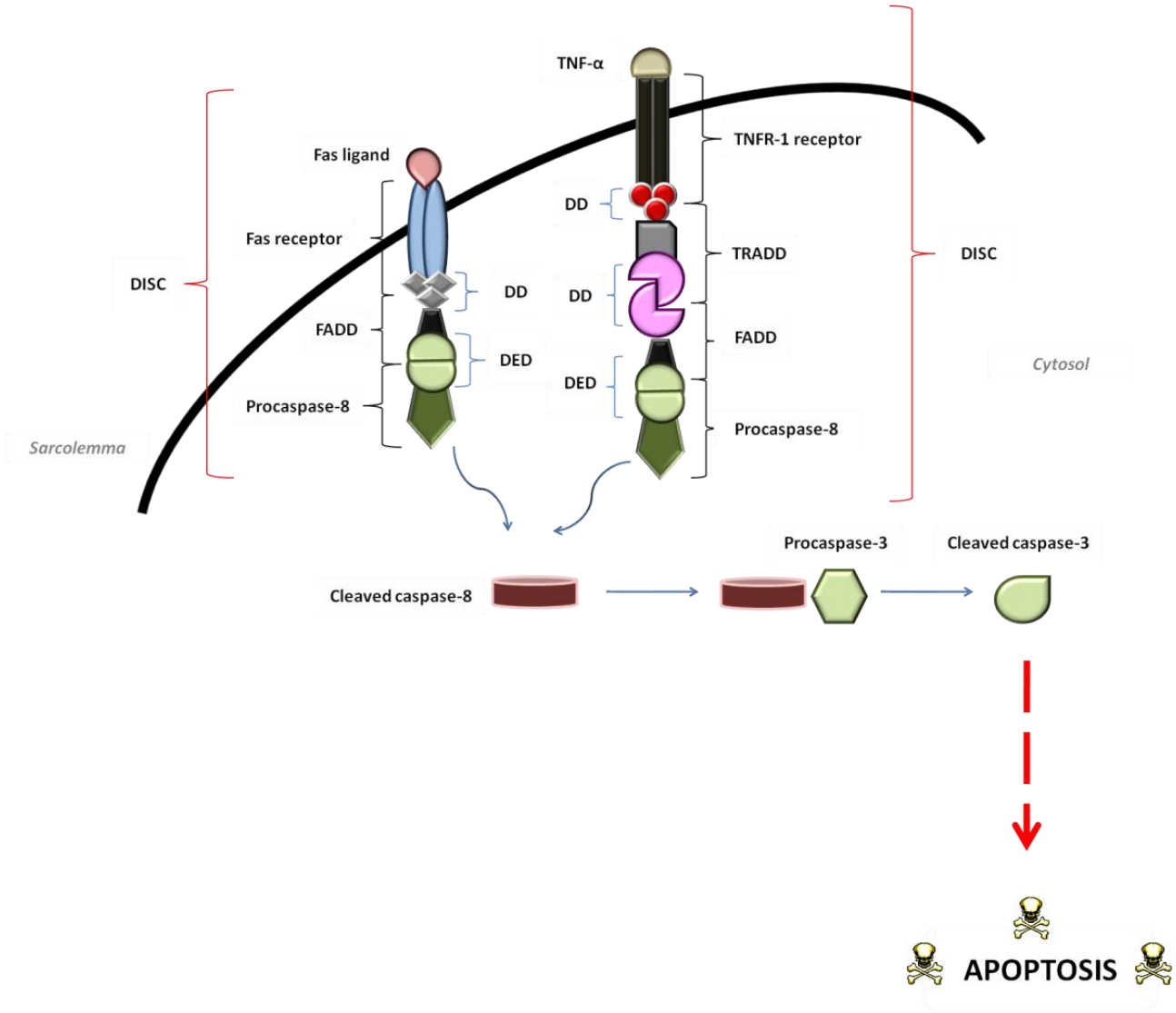

Figure 2.6. The signalling cascade of the Fas and TNFR death receptor apoptotic (extrinsic) pathways. Taken and adapted from Tumane et al. 2010.

2.5.2.2 PKB/Akt indirectly moderates apoptosis: The role of PKB/Akt in the extrinsic apoptotic pathway

When health prevails the insulin-mediated activation of PKB/Akt is unhampered, as reviewed in section 2.1.3. Activated PKB/Akt is known to phosphorylate and activate I-κB kinase (IKK) at its Thr^{23} residue [Parcellier et al. 2008]. In turn, activated IKK is responsible for the phosphorylation of I-κBα on its Ser^{32} and Ser^{36} residues, subsequently leading to its rapid degradation via an ubiquitin/proteasome system [Kane et al. 1999, Ozes et al.1999]. I-κBα is a member of the I-κB family, a family of regulatory proteins which are able to inhibit nuclear factor-κB (NF-κB) [Hayden et al. 2004]. I-κB inhibits NF-κB by forming a complex with it and thus sequestering it in the cytoplasm [Huang et al. 2009] NF-κB is expressed in all cell types and is involved in the cellular response to a variety of stimuli such as stress, bacterial or viral antigens, free radicals, , cytokines and ultraviolet irradiation [Patel et al. 2009]. Degradation of I-κBα liberates NF-κB from its hold, thereby promoting its activation [Ozes et al. 1999] and migration to the nucleus [Huang et al 2009]. This subsequently enables NF-κB to activate a wide variety of genes, one group being the genes which encode for caspase inhibitors [Barket et al. 1999] while another group consists of the anti-apoptotic genes, which includes those that code for B-cell lymphoma-extra large (Bcl-X_L) [Parcellier et al. 2008]. The PKB/Akt-mediated activation of these genes, via NF-κB, highlights the pro-survival or protective function of PKB/Akt as well as NF-κB [Ozes et al. 1999].

NF-κB is increased during obesity [Huang et al. 2009] but it is still undecided whether it is the PI3K/PKB/Akt pathway or tumour necrosis factor-α (TNF-α), which is also upregulated during obesity, which causes this increase [Ruan et al. 2002]. Two separate studies have implicated PKB/Akt in the activation of NF-kB via TNF-α in embryonic kidney cells and human cervical carcinoma cells [Ozes et al. 1999] as well as in breast cancer cells [Burow

et al. 2000]. In contrast, Bieler et al. (2007) showed that simultaneous activation of PKB/Akt and NF-kB was required for the survival of human umbilical vein endothelial cells exposed to TNF (the isoform was not stipulated in this study) thereby implicating that these pathways were activated separately by TNF.

There is mounting experimental evidence that supports the possibility of NF-κB as a key mediator in the genesis of insulin resistance [Patel et al. 2009] when a high fat diet is followed and during obesity, as indicated by studies using hepatic IKK-β knockout mice [Arkan et al 2005] or transgenic mice which overexpress IKK-β in the liver [Cai et al. 2005]. These studies support NF-κB as being the main contributor to insulin resistance as opposed to IKK, as previously suggested [Arkan et al. 2005].

TNF-α is thought to induce insulin resistance primarily via the serine phosphorylation of IRS-1. One of the multiple functions of NF-κB is to regulate the actions of TNF-α, which in turn is also a powerful activator of NF-κB (as indicated above); suggesting regulatory interplay between these two molecules [Patel et al. 2009].

In addition to IKK, PKB/Akt is also known to phosphorylate forkhead box protein O1 (FOXO1) on Thr^{24}, Ser^{256} and Ser^{319}, as well as forkhead box protein O3a (FOXO3a) and O4 (FOXO4) on three comparable sites in the nucleus (reviewed in Burgering et al. 2003). Forkhead box (FOX) proteins are a family of transcription factors that play a variety of significant roles in gene expression regulation, genes which are involved in apoptosis, cell growth, proliferation, differentiation, development and metabolism [Tuteja et al. 2007, Manning et al. 2007]. PKB/Akt mediated phosphorylation of FOXO allows 14-3-3 proteins to bind the transcription factors via their Thr^{24} and Ser^{256} residues, dislodging FOXO from their target genes and mediating their translocation to the cytoplasm, thus inhibiting the transcription factors [Manning et al. 2007].

Bcl-2 interacting mediator of cell death (BIM) protein as well as Fas ligand are pro-apoptotic and are both targets of unphosphorylated (active) FOXO transcription factors, thus sequestering FOXO in the cytoplasm (therefore inhibiting it) which promotes cell survival [Dijkers et al. 2002, Brunet et al. 1999].

Furthermore, PKB/Akt is able to phosphorylate murine double minute 2 (MDM2) (or human double minute 2 (HDM2) in humans) on its Ser^{166} and Ser^{186} residues, which in turn activates MDM2/HDM2 and promotes the translocation of this protein from the cytoplasm to the nucleus. MDM2/HDM2 acts like an E3 ubiquitin ligase in that it binds ubiquitin to p53, thereby arbitrating ubiquitination on numerous p53 lysine residues. This subsequently prepares p53 for proteosomal degradation [Mayo et al. 2001, Iwakuma et al. 2003].

Puma and Noxa are two pro-apoptotic members of the Bcl-2 family which are transcriptional targets of p53-mediated apoptosis. Thus, degradation of p53 would reduce Puma and Noxa levels and promote cell survival. Although, the significance of decreased Puma and Noxa levels to PKB/Akt mediated cell survival still has to be investigated [Villunger et al. 2003].

As discussed, the PI3K/PKB/Akt pathway plays an important role in promoting cell survival via mediators such as NF-κB, FOXO and MDM2/HDM2. Furthermore, NF-κB is highlighted as possibly playing a role in the arbitration of obesity-induced insulin resistance.

2.5.2.3 The mitochondrial-dependent apoptotic (intrinsic) pathway

The mitochondrial-dependent apoptotic pathway is activated on the receipt of various apoptotic stimuli, including ischemia-reperfusion, hypoxia, oxidative stress and loss of

growth factors [Regula et al. 2003, Weiss et al. 2003, Gustafsson et al. 2007], all of which fuel mitochondrial permeability transition. Augmented permeability of both the inner and the outer mitochondrial membranes are hallmark features of mitochondrial permeability transition [Weiss et al. 2003, Zamzami et al. 2001, Crompton et al. 2002]. An overview of the mitochondrial-dependent apoptotic (intrinsic) pathway signalling cascade is given in figure 2.7.

A protein complex that bridges the inner and outer mitochondrial membranes, the mitochondrial permeability transition pore (MPTP), have been identified as the determinant of mitochondrial permeability [Baines et al. 2005]. It was previously thought that the transition pore consisted of the voltage dependent anion channel (VDAC), adenine nucleotide translocase (ANT) and cyclophilin-D. These pore constituents were thought to be located in the outer membrane, inner membrane and matrix of the mitochondrion respectively [Zamzami et al. 2001, Crompton et al. 2002].

The latest research however, utilizing genetic knockouts, rules out VDAC as one of the main structural components of the MPTP. On the other hand, the structural role of cyclophilin-D in the pore has been confirmed, while the role of ANT is still controversial and thought to possibly play more of a regulatory than a structural function. Furthermore, these studies suggest a structural substitute for ANT in the MPTP namely, mitochondrial inorganic phosphate carrier (PiC) [Juhaszova et al. 2008, Leung et al. 2008].

Nevertheless, once the mitochondria are permeabilized, the intermembrane space releases a number of different proteins that are mediators of the apoptotic process, including cytochrome *c*, second mitochondria-derived activator of caspases

(Smac/DIABLO), endonuclease G (EndoG), and apoptosis-inducing factor (AIF) [Baines et al. 2005].

2.5.2.3.1 Cytochrome *c*

Cytochrome *c* is a component of the mitochondrial ETC [Liu et al. 1996] that is responsible for ferrying electrons from complex III to complex IV of the chain [Lee et al. 2009]. When cytochrome *c* is released, upon apoptotic stimuli, it is able to bind to apoptotic protease-activating factor-1 (Apaf-1) in the cytosol [Lee et al. 2009], increasing its affinity for dATP or ATP [Jiang et al. 2000]. The bond between Apaf-1 and dATP or ATP, independent of cytochrome *c,* is rather weak and thus cytochrome *c* plays a significant role in that it either opens up the nucleotide binding site or stabilizes the bound nucleotide to Apaf-1 [Jiang et al. 2000]. Once dATP or ATP attaches itself to the Apaf-1/cytochrome *c* complex, it facilitates the oligomerization of the complex, to form a multimeric apoptosome [Zou et al. 1999, Adrain et al. 2001].

Once complexed in the apoptosome, the caspase recruitment (CARD) domain of Apaf-1 becomes exposed, enabling it to recruit numerous procaspase-9 molecules to the complex and subsequently arbitrate their autoactivation [Wang 2001]. The activated caspase-9 can now cleave and activate downstream executioner caspases such as caspase-3 and -7, just as caspase-8 cleaves and activates caspase-3 in the death receptor apoptotic pathway (section 2.5.2.3) [Rodriguez et al. 1999, Robertson et al. 2000]. The condensation of nuclear chromatin, fragmentation of DNA and the disintegration of the nuclear membrane as well as the formation of apoptotic bodies, soon occur as a result of the cleavage of vital intracellular compounds by the activated executioner caspases [Wang 2001].

2.5.2.3.2 Smac/DIABLO

Mature Smac/DIABLO proteins can be found in the mitochondrial intermembrane space in healthy cells and is discharged into the cytosol, upon the reception of apoptotic stimuli [Wang 2001, Verhagen et al. 2000]. Prior to mature Smac/DIABLO becoming a mitochondrial protein, its precursor is produced in the cytosol and then carried to the mitochondria. Once there, the precursor undergoes cleavage which serves to expose the four amino acid residues Ala-Val-Pro-Ile (AVPI), on the now mature Smac/DIABLO protein. Through AVPI, Smac/DIABLO will be able to bind to the baculovirus IAP repeat (BIR) domain of inhibitor of apoptosis proteins (IAPs) at a later stage, after it has been triggered by apoptotic stimuli. IAPs are bound to pro-apoptotic procaspases-3 and -9 when there is a lack of apoptotic stimuli, thus inhibiting apoptosis [Wang 2001]. Once the cell receives apoptotic signals, Smac/DIABLO is released into the cytosol [Du et al. 2000, Verhagen et al. 2000] and impounds the IAPs, thereby indirectly freeing procaspases-3 and -9 which in turn promotes apoptosis [Wang 2001, Verhagen et al. 2002].

2.5.2.3.3 Endonuclease G (EndoG)

EndoG, as the name suggests, is a nuclease that is encoded by a nuclear gene and translated in the cytosol, and eventually transported to the mitochondria [Côté et al. 1993]. It is believed that a significant portion of these nucleases proceed to reside in the intermembrane space of the mitochondrion and is released into the cytosol upon apoptotic signals, similar to cytochrome *c*. The ultimate function of EndoG, once it reaches the cytosol, is to stimulate nucleosomal DNA fragmentation [Wang 2001].

The activity of EndoG has been identified to be independent of caspase activation [Liu et al. 1997, Enari et al. 1998] indicating that it initiates an analogous apoptotic pathway to that of the caspase-dependent apoptotic pathway [Wang 2001].

2.5.2.3.4 Apoptosis inducing factor (AIF)

AIF is a flavoprotein that is located in the mitochondrial intermembrane space [Susin et al.1999] and is essential for the assembly and/or the stabilization of the respiratory complex I as well as oxidative phosphorylation [Lee et al. 2009]. This flavoprotein is released into the cytosol once apoptosis is induced [Candé et al. 2002]. This flavoprotein, just like EndoG, acts independently of caspases [Miramar et al. 2001] and once it reaches the cytosol it stimulates the condensation of nuclear chromatin and the fragmentation of high-molecular-weight (50kb) DNA [Yu et al. 2002].

2.5.2.4 The Bcl-2 family and its regulation of the intrinsic apoptotic pathway

The Bcl-2 family regulates the intrinsic pathway of apoptosis and consists of pro-apoptotic as well as anti-apoptotic protein members, all of which share at least four conserved regions known as Bcl-2 homology (BH) domains [Lee et al. 2009]. The anti-apoptotic members, which include B-cell lymphoma-2 (Bcl-2) and Bcl-X_L, contain all four subtypes of BH domains and obstruct the function of the pro-apoptotic Bcl-2 proteins by promoting cell survival [Gustafsson et al. 2007]. The anti-apoptotic Bcl-2 proteins are crucial for cell survival and have been shown to defend cells against a wide variety of apoptotic stimuli or cellular stressors [Lee et al. 2009].

The pro-apoptotic Bcl-2 proteins are divided into two distinctive subfamilies according to which domains they contain. The multidomain proteins, which include B-cell lymphoma-

associated X (Bax) and Bcl-2 homologous antagonist killer (Bak), all share three BH domains (BH domains 1 to 3); whereas the BH3-only domain proteins, for instance Bcl-2/adenovirus E1B 19kDa protein-interacting protein 3 (Bnip3), Bcl-2/adenovirus E1B 19kDa protein-interacting protein 3-like (Nix/Bnip3L), Bcl-2 associated death (Bad), BH3 interacting domain (Bid), Noxa, and Puma, only contain one domain (BH domain 3) as the name suggests [Danial et al. 2004, Huang et al. 2000].

The precise mechanism of how the Bcl-2 family proteins moderate apoptosis is at present not completely clear. Three different models of apoptotic regulation have been suggested by Gustafsson et al. (2007), based on evidence from the literature.

The first model indicates that pro-apoptotic Bax and Bak directly interact with one or two different anti-apoptotic Bcl-2 proteins and are thus retained in an inactive conformation. Pro-apoptotic BH3-only proteins are thought to bind and defuse the anti-apoptotic Bcl-2 proteins and in doing so, release Bax and Bak upon an apoptotic signal. [Gustafsson et al. 2007] The studies by Willis et al. (2005) and Chen et al. (2005b) provide evidence for this model.

An alternative model suggests that certain pro-apoptotic BH3-only proteins, such as tBid and Bim, directly bind to Bax and Bak and thereby initiates apoptosis [Gustafsson et al. 2007]; as proposed by a number of studies [Cartron et al. 2004, Harada et al. 2004, Kuwana et al. 2005, Kuwana et al. 2002, Wang et al. 1996].

The third model implies that anti-apoptotic Bcl-2 family members prevent the activation of pro-apoptotic Bax and Bak by impounding pro-apoptotic BH3-only proteins to the cytosol. When the activated BH3-only proteins overcome the anti-apoptotic Bcl-2 proteins (that is, upon an apoptotic stimulus), they either directly activate Bax or Bak or they activate an unknown factor in the cytosol or mitochondria that is needed for Bax or Bak activation. In

doing so, the apoptotic process is triggered [Gustafsson et al. 2007], as suggested by several studies [Cheng et al. 2001, Clohessy et al. 2006, Gomez-Bougie at al. 2004, Han et al. 2004].

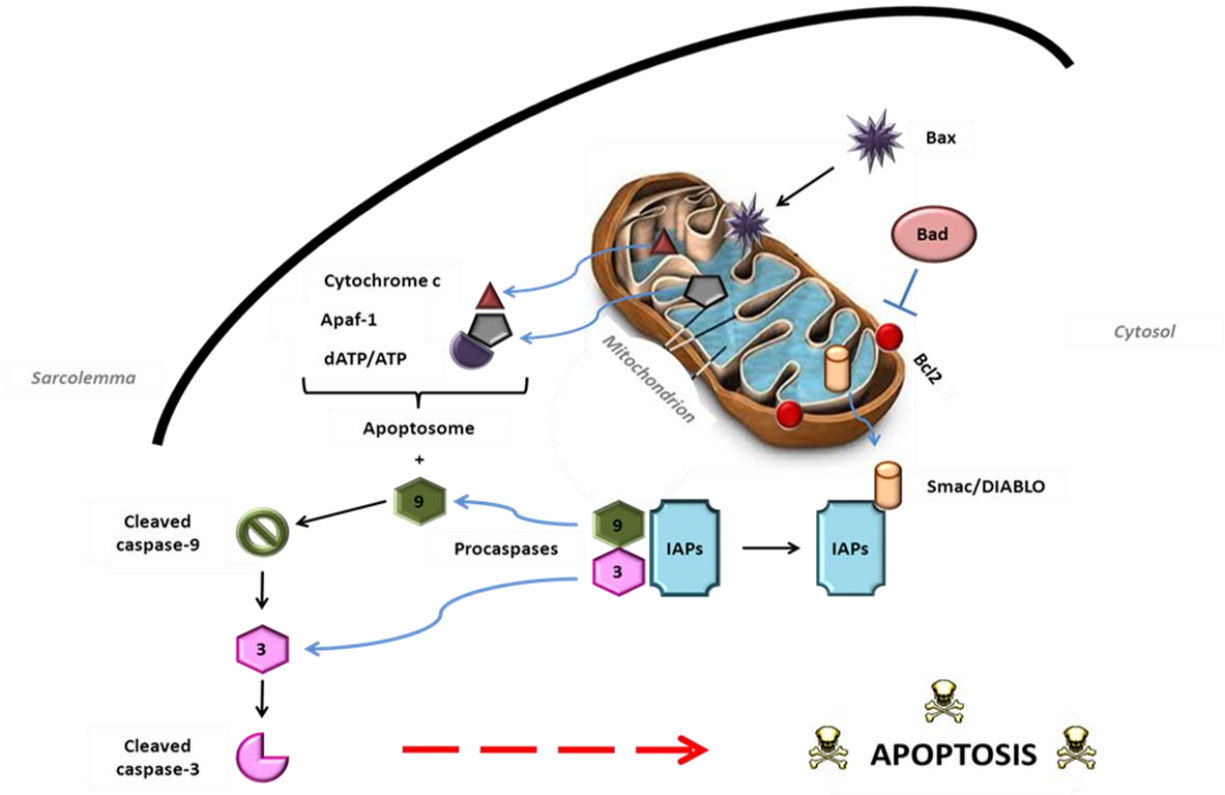

Figure 2.7. The signalling cascade of the mitochondrial-dependent apoptotic (intrinsic) pathway. Taken and adapted from Crow et al. 2004.

2.5.2.5 PKB/Akt directly moderates apoptosis: The role of PKB/Akt in the intrinsic apoptotic pathway

2.5.2.5.1 PKB/Akt and Bad protein

Under normal physiological conditions, once myocardial PKB/Akt is activated it is able to phosphorylate the pro-apoptotic Bad protein in some cell types [Kharas et al. 2005, Sussman et al. 2011], at its Ser^{136} residue [Sale et al. 2008] and in doing so, promotes cell survival [Datta et al. 1999]. The phosphorylation of Bad ensures that it is released from its complex with anti-apoptotic Bcl-2 or Bcl-X_L [Sale et al. 2008], which are located on the mitochondrial membrane, and binds to cytosolic 14-3-3 proteins [Parcellier et al. 2008]. This sufficiently sequesters Bad in the cytosol, thus blocking its pro-apoptotic function and prevents it from initiating mitochondrial-dependent apoptosis [Sale et al. 2008]. In turn, Bcl-2 and Bcl-X_L are free to promote cell survival [Parcellier et al. 2008].

The pro-apoptotic protein Bad has been shown to be elevated in the myocardium of obese rats [Lee at al. 2008].This protein is known to stimulate apoptosis by forming a heterodimer with the anti-apoptotic proteins, Bcl-2 or Bcl-X_L, thus blocking their cardioprotective effects [Sussman et al. 2011], as previously explained.

2.5.2.5.2 PKB/Akt and Bax protein

Another member of the Bcl-2 family is the pro-apoptotic protein Bax [Gogvadze et al. 2006], which is predominantly located in the cytosol of healthy cells. One of the many functions of activated PKB/Akt in the myocardium [Sussman et al. 2011] is to phosphorylate Bax, at its Ser^{184} residue [Gardai et al. 2004], thus sequestering it in the cytosol and away from mitochondrial membranes and thereby blocking its pro-apoptotic

functions [Gardai et al. 2004]. This containment of Bax in the cytosol is achieved by its heterodimerization with Bcl-X_L or myeloid cell leukemia differentiation protein-1 (Mcl-1) [Gardai et al. 2004, Gross et al. 1999, Cory et al. 2003].

Another central role of activated PKB/Akt may very well be to suppress conformational changes in Bax and inhibit its migration to the mitochondria, thereby averting loss of mitochondrial membrane potential and the activation of caspase-3 [Yamaguchi et al. 2001]. Activated PKB/Akt is thought to mediate the suppression of Bax conformational changes by directly impeding the interaction between Bax and Bid or Bax-interacting factor-1 (Bif-1), both of which participate in conformational changes in Bax and are pro-apoptotic members of the Bcl-2 family [Majewski et al. 2004a, Majewski et al. 2004b, Sussman et al. 2011].

A number of studies have highlighted the relationship between PKB/Akt activation, Bcl-2 family member regulation, and inhibition of cardiomyopathic damage [Johnassen et al. 2001, Kato et al. 2003, Kuwahara et al. 2000, Negoro et al. 2001, Pastukh et al. 2005, Uchiyama et al. 2004]. The inhibition of Bax translocation to the mitochondria, specifically via phosphorylation by PKB/Akt, has not been shown in the heart. However, mice which are homozygous for the deleted Bax gene have been shown to be protected against ischemia-reperfusion injury [Hochhauser et al. 2003].

Upon apoptotic stimuli, Bax undergoes a conformational change that exposes its N- and C-terminals [Nechushtan et al. 1999], allowing it to insert itself in the outer mitochondrial membrane and oligomerize with the membrane [Mattson et al. 2003]. Subsequently, a “protein-permanent” pore is formed within the mitochondrial membrane which allows the release of cytochrome *c* into the cytosol, thus initiating apoptosis [Nechushtan et al. 1999].

There are a number of other protein members of the Bcl-2 family which are activated by a variety of different stimuli, which have been shown to play significant roles in determining myocardial cell death or survival. A few of these proteins exerted their pro-apoptotic functions and promoted apoptosis in the heart [Gustafsson et al. 2007, Kubli et al. 2008, Capano et al. 2006, Hamacher-Brady et al. 2006, Wei et al. 2001, Zong et al. 2001], while the anti-apoptotic proteins exerted their cardioprotective functions [Imahashi et al. 2004, Brocheriou et al. 2000, Chen et al. 2001, Gustafsson et al. 2007]. However, these will not be reviewed here.

2.5.2.6. PKB/Akt directly moderates the intrinsic apoptotic pathway independently of the Bcl-2 family

Hexokinase I (HKI) and hexokinase II (HKII) are two isoforms of the hexokinase protein, essential in the first step of glucose metabolism [Robey et al. 2006], which have been shown to distinctively bind to the outer mitochondrial membrane (OMM) [Parcellier et al. 2008]. Several studies have highlighted hexokinases as the downstream effectors of growth factor and PKB/Akt arbitrated cell survival [Majewski et al. 2004a, Gottlob et al. 2001, Robey et al. 2006, Majewski et al. 2004b, Brunet et al. 1999, Robey et al. 2005]. PKB/Akt is believed to inhibit the hexokinase disengagement, the detachment being initiated by apoptosis, from the mitochondria [Gottlob et al. 2001]. This interrelation between PKB/Akt and hexokinase is believed to prevent the release of cytochrome *c* from the mitochondria to preserve their integrity, much like Bcl-2 [Kennedy et al. 1999]. PKB/Akt differs from Bcl-2 in that it has been found to be dependent on glucose to exert its protective function [Gottlob et al. 2001, Rathmell et al. 2003].

2.5.2.7 PKB/Akt regulation of GSK-3 and its role in apoptosis

GSK-3, when inhibited, has been found to be cardioprotective [Gomez et al. 2008], where inhibition of GSK-3 is achieved by the phosphorylation of Ser^{21} for GSK-3α and Ser^{9} for GSK-3β via activated PKB/Akt, as discussed in section 2.4.1.2.2 It was shown by Maurer et al. (2006) that, activated GSK-3 induces apoptosis, upon the removal of the growth factor interleukin-3 (IL-6). Active GSK-3 stimulates the Ser^{159} phosphorylation of anti-apoptotic Mcl-1, which in turn encourages ubiquitination and results in Mcl-1 degradation by the proteasome. This in turn, provokes the release of cytochrome *c* from the mitochondria thereby initiating apoptosis. These observations emphasize the central role of PKB/Akt in the regulation of cell survival, via the inhibition of GSK-3 and in turn, the stability of Mcl-1 [Maurer et al. 2006, Parcellier et al. 2008].

2.6 Apoptosis and Obesity-induced Cardiovascular Disease

Apoptosis has been linked to cardiac myocyte death, which is characteristic of heart failure [Bernecker at al. 2003, Singal et al. 2000, Abbate et al 2006], atherosclerosis [Clarke et al. 2008], cardiac hypertrophy [Aharinejad et al. 2008], myocardial infarction [Abbate et al. 2006] and ischemia/reperfusion injury [Gao et al. 2008, Sodha et al. 2008]. This cluster of cardiovascular diseases, are examples of cardiomyopathies which are defined as diseases of the cardiac muscle which can be implicated in the dysfunction of the heart. A cardiomyopathy can be classified either by the dominant physiological feature of the pathology or by the disease that is causing the pathology [Davies 2000]. Obesity cardiomyopathy is defined as a myocardial disease which occurs during obesity and is mediated by the obese state as it cannot be explained by other causes such as diabetes mellitus, hypertension, or coronary artery disease [Wong et al. 2007]. Indeed, heart failure

[Barouch et al. 2006] and myocardial ischemia/reperfusion injury [Yue et al. 2005, Shibata et al. 2005] have been characterized by myocardial apoptosis that has been linked to obesity in animal models.

2.6.1 Obesity Cardiomyopathy: Apoptosis and Heart Failure

Congestive heart failure manifests itself during the late stages of a plethora of cardiovascular diseases and is defined by a cardiac output that is ultimately well below the threshold required for an organism to function [Neuss et al. 2001]. Characteristic features of this cardiomyopathy include changes in the expression pattern of intracellular and extracellular matrix proteins, progressive loss of cardiomyocytes, and dilation or enlargement of the heart chambers [Narula et al. 2000, Neuss et al. 2001, Wencker et al. 2003].

During the initial stages of heart failure the decline in cardiac output is compensated for by myocardial hypertrophy and dilation, ensuring that there is adequate, though not optimal, cardiac output [Narula et al. 2000]. However, these compensatory mechanical adaptations soon become inadequate to maintain a sufficient cardiac output [Katz 1994], culminating in cardiac dysfunction. The mechanism by which cardiac hypertrophy, which is activated by heart failure, concludes in myocardial dysfunction is not that apparent. [Narula et al. 2000, Wencker et al. 2003].

It has been hypothesized that apoptosis might be the key mediator in the progression of myocardial hypertrophy to cardiac dysfunction in congestive heart failure [Neuss et al. 2001, Eichhorn et al. 1996, Beltrami et al. 1995, Narula et al. 1996, Narula et al. 1999, Olivetti et al. 1997, Reed et al. 1999]. The basis for this hypothesis is that since adult cardiomyocytes are terminally differentiated and cannot divide, growth stimulation (via

neurohumoral alterations and cytokine expression) of the cardiomyocytes of the failing heart, therefore results in the initiation of apoptosis instead [Narula et al. 2000]. At the outset, the stimulation of growth leads to cardiac hypertrophy but as the cardiac output declines, the chronic growth stimulation results in apoptosis [Narula et al. 1999].

Diverse experimental species and models of heart failure have been used to test the hypothesis that apoptosis may be responsible for cardiac dysfunction in heart failure. Much controversy still surrounds the role of apoptosis in this regard, despite the considerable amount of studies done on this topic. What remains unclear is whether apoptosis is just a coincidence, a protective mechanism, or whether it is a key participant in the development of the cardiomyopathy [Neuss et al. 2001, Wencker et al. 2003].

2.6.2 Obesity Cardiomyopathy: Apoptosis and Ischemia/Reperfusion

While short periods of ischemia allow the heart to recover quite well despite an initial degree of impairment, prolonged periods of ischemia are associated with irreversible myocardial damage. The aforementioned will prevail provided that reperfusion, defined as the reinstatement of normal blood flow, rapidly succeeds the ischemia [Halestrap et al. 2007].

2.6.2.1 What is Ischemia/Reperfusion Injury?

This type of injury is categorized by myocardial damage that occurs during reperfusion that aggravates the damage incurred during the ischemic period by having an additive effect [Halestrap et al. 2007]. During ischemia/reperfusion injury there is a release of various enzymes and cardiomyocyte changes which are associated with necrosis [Halestrap et al.

1998, Suleiman et al. 2001, Halestrap et al. 2004], where the necrotic area in the heart is defined as the infarct [Halestrap et al. 2007]. Apoptosis has also been implicated in ischemia/reperfusion injury as some cardiomyocytes at the borders of the infarct has been found to undergo this type of cell death [Fliss et al. 1996, Anversa et al. 1998].

2.6.2.2 Causes of Ischemia/Reperfusion Injury

There is an escalating body of evidence that underlines disrupted mitochondrial functioning as the determinant of both myocardial necrosis and apoptosis that are associated with ischemia/reperfusion injury [Halestrap et al. 1998, Halestrap et al. 2004, Shanmuganathan et al. 2005, DiLisa et al. 2006].

In particular, it is the elevated intracellular concentration of calcium [Ca^{2+}] as well as reactive oxygen species (ROS), that commences during ischemia and intensifies during reperfusion (due to a second torrent of ROS production and increased intracellular [Ca^{2+}] [Kevin et al. 2003]), that is believed to mediate the damaging effects on the mitochondria [Halestrap 2006, Solaini et al. 2005].

During ischemia, the switch to increased anaerobic glucose metabolism causes lactic acid levels to increase and the cell`s pH (pHi) to swiftly decline, which in turn activates the $Na^+/H^+$ antiporter in an attempt to restore the intracellular pHi. However, glycolysis yields fewer ATP molecules than fatty acid β-oxidation which causes the cell`s ATP concentrations to rapidly plunge. In turn, this results in Na/K ATPase inhibition and an increase in myocellular sodium concentration [Na^+], which sequentially blunts pHi restoration. Furthermore, the Na^+/Ca^{2+} antiporter, which is responsible for pumping Ca^{2+} out of the cell, is either repressed or reversed which augments intracellular [Ca^{2+}] [Halestrap et al. 1998, Halestrap et al. 2004, Solaini et al. 2005].

There is a radical escalation in ROS cellular content [Kevin et al. 2003] that is not only the cause of myocardial damage during ischemia but is believed to make the heart more susceptible to damage during reperfusion [Halestrap et al. 2007]. Inhibition of repair processes, which are dependent on ATP, and loss of cardiomyocyte integrity are two of the aberrations that occur as a result of increased intracellular ROS and [Ca^{2+}] as well as ATP diminution, during ischemia [Halestrap et al. 1998, Halestrap et al. 2004, Solaini et al. 2005].

. Mitochondria are not only a source of ROS production but have been identified as targets of ROS and calcium damage as well, as indicated by the disruption of electron transport chain activity in the mitochondria of ischemic hearts [Solaini et al. 2005, Chen et al. 2006].

On the whole, the rise in intracellular ROS and [Ca^{2+}] content has been shown to be the trigger for the opening of the mitochondrial permeability transition pore (MPTP) during ischemia/reperfusion injury [Halestrap et al. 1998, Halestrap et al. 2004, DiLisa et al. 2006, Solaini et al. 2005, Garcia Dorado et al. 2006].

2.7 The role of the PI3K/PKB/Akt pathway in heart failure and ischemia/reperfusion injury

When the PI3K/PKB/Akt pathway mediator GSK-3 is inhibited, it has been found to reduce ischemia/reperfusion injury in the heart [Das et al. 2008, Gomez et al. 2008] and to be cardioprotective during heart failure [Hirotani et al. 2007]. GSK-3-mediated myocardial protection is mediated via the mitochondria but the precise mechanism is not entirely known [Das et al. 2008].

GSK-3 has been proposed to play a major role in the cardioprotection associated with ischemic preconditioning [Tong et al. 2002, Murphy et al. 2005]. Ischemic preconditioning entails the exposure of the heart to two or three cycles of short periods of ischemia,

interspersed by brief periods of reperfusion [Edwards et al. 2000]. If this preconditioning takes place within 1-3 hours of a prolonged period of ischemia then the heart has been found to be protected against ischemia/reperfusion injury in both humans and experimental animals [Edwards et al. 2000, Yellon et al. 2003, Kloner et al. 2006].

During ischemic preconditioning, adenosine, bradykinin endogenous opioids and catecholemines are released and interact with their respective G-protein coupled receptors [Juhasova et al. 2004, Downey et al. 2007]. Consequently, PI3K is activated and in turn phosphorylates and activates PKB/Akt [Hausenloy et al. 2006, Hausenloy et al. 2005], amongst other kinase enzymes (discussed in Tong et al. 2004, Hausenloy et al. 2007, Liem et al. 2007).

PKB/Akt is known to phosphorylate and inhibit GSK-3, as mentioned in section 2.4.1.2, and in doing so, its pro-apoptotic properties are blocked and cell survival is promoted [Jope et al. 2004]. The exact cardioprotective effect of GSK-3 on the mitochondria is not completely understood but it is thought that GSK-3 inhibition allows its migration to the mitochondria [Juhaszova et al. 2004]. It is at present undecided whether the phosphorylation of VDAC by GSK-3 (either directly or indirectly), could play a role in sensitizing the cell to MPTP opening as VDAC has recently been ruled out as an essential constituent of the MPTP (as discussed in section 2.5.2.3) [Juhaszova et al. 2004, Pastorino et al. 2005, Das et al. 2008].

In addition to GSK-3, PKB/Akt (once activated by PI3K) has also been found to phosphorylate Bad and Bax during ischemia/reperfusion injury, inhibiting their pro-apoptotic effects by preventing them from migrating to the mitochondria, as discussed in sections 2.5.2.5.1 and 2.5.2.5.2 [Rácz et al. 2008].

2.8 A Closer Look at the of Mitochondrial Permeability Transition Pore (MPTP) during Apoptosis

Only a few essential metabolites and ions can gain access to the mitochondria through its inner membrane under normal physiological conditions, ensuring that the cell`s membrane potential and pH gradient is maintained and oxidative phosphorylation is able to proceed [Halestrap et al. 2007].

In contrast, during unhealthy conditions where there are high intracellular calcium levels, oxidative stress, elevated phosphate and low adenine nucleotide concentrations, the MPTP opens (a non-specific pore). In the open state, the MPTP allows just about any molecule smaller than 1.5kDa into the mitochondria and in doing so, disintegrates the “permeability barrier” of the inner membrane [Halestrap et al. 2007].

One consequence of MPTP opening is the unobstructed movement of protons over the inner mitochondrial membrane, which results in uncoupling of oxidative phosphorylation. ATP synthesis is not only inhibited but the ATPase pump shunts the existing ATP back into the cell and in doing this, hydrolyses the ATP [Halestrap et al. 2007]. This brisk deterioration in ATP leads to not only the activation of phospholipases, proteases and nucleases, all degradative enzymes, but an impairment of cellular homeostasis (ionic and metabolic) [Halestrap et al. 2004, Halestrap et al. 2006, Solaini et al. 2005].

A second outcome of MPTP opening is the depolarization of the mitochondrial membrane which results in additional pore opening in that particular mitochondrion [Scorrano et al. 1997] and once the mitochondrion is completely open it begins to expand at length [Bernardi et al. 1999]. Ultimately, the outer membrane ruptures and cytochrome *c* and other vital pro-apoptotic factors are discharged from the mitochondria, allowing them to mediate cell death [Doran et al. 2000, Halestrap et al. 2007].

2.9 Motivation for objectives and hypothesis of our study

2.9.1 Motivation

A review of the literature has shown that obesity-related cardiomyopathies are complex and mediated by multiple factors. What has come to light is that cardiac insulin resistance is implicated as one of the main causes of obesity-related CVD. A few studies have implicated perturbations in the insulin-mediated PI3K/PKB/Akt pathway in mediating this insulin resistance. Moreover, the PI3K/PKB/Akt pathway has been shown to regulate myocardial apoptosis, indicating that this pathway not only regulates metabolism but also plays a significant role in determining cell fate.

Despite the large number of studies conducted, the mechanism of obesity-related cardiovascular diseases has not been completely elucidated. Of great interest, but for which few studies can be found, is the role of the PI3K/PKB/Akt and apoptotic pathway in the early versus advanced stages of obesity.

2.9.2 Objectives

The first objective of the study was to compare the early and advanced stages of obesity in terms of cardiac:

(i) Cytosolic PI3K/PKB/Akt signalling

(ii) Cytosolic apoptotic signalling

(iii) Mitochondrial integrity

The second objective was to assess the following in the myocardium during the advanced stages of obesity:

(i) Mitochondrial PI3K/PKB/Akt signalling

(ii) Mitochondrial apoptotic signalling

(iii) Mitochondrial function

(iv) Mitochondrial integrity

2.9.3 Hypothesis

We hypothesize that obesity will have different effects on the myocardium during the initial and advanced stages of obesity. We propose that elevated PI3K/PKB/Akt and attenuated intrinsic apoptotic signalling will take place in the cytosol during the initial stages of obesity. During the advanced stages of obesity we hypothesize that signalling via the PI3K/PKB/Akt pathway will be downregulated in the cytosol, while that of apoptotic signalling will be augmented. Furthermore, we theorize that the signalling via these two pathways will be associated with increased cardioprotection during the initial stages, while this protection will be lost during the advanced stages of obesity.

It terms of mitochondrial PI3K/PKB/Akt and apoptotic signalling, we hypothesize this will be downregulated and upregulated in the heart, respectively, in the advanced stages of obesity. Additionally, we anticipate that mitochondrial integrity and function will be negatively affected.

Chapter 3: Materials and Methods

3.1 Materials

The reagents utilized in this study, for the various experiments, were purchased at a number of different companies such as:

Bayer-Bayer

Eutha-naze (sodium pentobarbital).

BDH Laboratory

$Na_2S_2O_4$, trichloroacetic acid (TCA) and perchloric acid (PCA).

Cell Signalling technology

Antibodies against total and phosphorylated: PI3K (p85 subunit), PKB/Akt Ser^{473}, GSK-3α/β Ser^{9} and Bad.

Antibodies against total: Bax, Bcl-2 and β-Tubulin.

Clover S.A. (Pty) Ltd.

Elite fat free instant milk powder.

Eli Lilly (S.A.) (Pty) Ltd.

Humulin R (regular biosynthetic human insulin).

GE Healthcare (formerly known as Amersham Biosciences)

ECL™ anti-rabbit Ig, horseradish peroxidase linked whole secondary antibody (from donkey), ECL™ anti-mouse Ig, horseradish peroxidase linked species-specific whole secondary antibody (from sheep).

Merck NT laboratory supplies (Pty. Ltd)

NaCl, KCl, $CaCl_2$, KH_2PO_4, $NaHCO_3$, $MgSO_4$, $NaSO_4$, NaK-Tartrate, $CuSO_4$, Na_2CO_3, HCl, H_3PO_4, Na_2HPO_4, NaOH, Na^+ pyrophosphate, Folin Ciocalteus (Folin C) reagent, sodium dodecyl sulphate (SDS), tris (hydroxylmethyl) aminomethane, acrylamide, D-glucose, glutamate, malate, sucrose, glycine, Tween-20.

MitoSciences

MitoProfile® Total OXPHOS Rodent Western Blot Antibody (Catalogue # MS604).

Roche Diagnostics

Bovine serum albumin (BSA).

Sigma-Aldrich Life Science

Na_2VO_3, ammonium persulfate (APS), mecarpto-ethanol, N,N,N,N,-tetramethylethylenediamine (TEMED), Ponceau S (reversible) staining solution, phenylmethylsulphonyl fluoride (PMSF), EGTA, EDTA, β-glycerophosphate, triton-X-100, aprotonin, leupeptin), 99% pure methanol, palmitoyl-L-carnitine, succinate,rotenone, oligomycin, carbonyl cyanide m-chlorophenylhydrazone (CCCP), ATP, AMP, ADP, CrP, 12.% (v/v) HPLC graded methanol, tetrabuthylammonium perchlorate (TBAP).

3.1.1 Animals

Ethical approval for this study was obtained from the Ethics Committee of Stellenbosch University, Faculty of Medicine and Health Sciences (Ethics number: 08/11/013). To maintain ethical standards, the revised South African National Standard for the care and use of laboratory animals for scientific purposes (South African Bureau of Standards (SABS), SANS 10386, 2008) was consulted throughout the study.

For the purpose of this study, age and weight matched male Wistar rats, which had been weaned at 4 weeks of age, were utilized. The rats were housed in the University of Stellenbosch Central Research Facility and were given free access to food and water. They were subjected to a 12-hour artificial day/night cycle where a constant temperature of 22°C and humidity of 40% were maintained.

3.2 Methods

3.2.1 Study design

Rats weighing ± 200g were randomly assigned to either a control or a diet-induced obesity (DIO) group. Control rats were fed a standard rat chow diet which supplied an average of 380kJ of energy per day. The DIO group were fed an obesity inducing diet that is, a high caloric diet which consisted of standard rat chow (33%), sucrose (7%), sweetened full cream condensed milk (Clover®) (33%) and distilled water (27%), which provided an average of 575kJ energy per day (refer to table 3.1). This method of diet-induced obesity and the average daily kilojoules intake was previously described by Du Toit et al. (2008).

In reference to figure 3.1, the control and DIO groups were further subdivided into two groups according to the time period they were placed on their respective diets, that is the 8

and 20 weeks groups. The 8 weeks group represented the early stages of diet-induced obesity, while the 20 weeks group exemplified the advanced stages thereof. A further subdivision occurred in the 8 weeks group that is, groups 8_A and 8_B. Likewise, the 20 weeks group was subdivided into groups 20_A, 20_B, 20_C and 20_D.

Following their specific diet period, all of the animals in the 8 weeks group and the 20 weeks group were fasted overnight, anaesthetized and then subjected to an intra-peritoneal glucose tolerance test (IPGTT) to evaluate blood glucose homeostasis (refer to part (i) of figure 3.1). All the animals were allowed to recover for at least 1 week before any further experiments were conducted.

Additionally, once the animals were anaesthetized, blood was collected from the jagular vein, prior to glucose administration, and allowed to clot on ice and thereafter centrifuged for 10 minutes at 11 500rpm and 4ºC. The resultant serum was collected and stored at -80ºC for serum insulin level determination at a later stage in order to assess whole-body insulin sensitivity.

Throughout all of the experiments, the animals were anaesthetized and weighed, to determine their total body weight as a measure of obesity, prior to being sacrificed. Once the hearts had been removed, the intra-peritoneal fat was collected (surrounding the kidneys and testes) and weighed to gauge intra-peritoneal adipocity.

Groups 8_A and 20_A were sacrificed and their hearts immediately freeze-clamped in liquid nitrogen and stored at -80^{o}C. These myocardial tissue were later subjected to western blot analysis to determine the early and advanced effects of diet-induced obesity with regard to protein markers of the PI3K/PKB/Akt and apoptotic signalling pathway (listed in figure 3.1(i)), in the cytosolic fraction of the heart. Groups 8_B and 20_B were sacrificed and their hearts freeze-clamped in liquid nitrogen and stored at -80^{o}C which were later used to

prepare mitochondrial lysates. These were then subjected to western blot analysis of various protein subunits (listed in figure 3.1(i)) located in the mitochondrial electron transport chain (ETC) in order to assess mitochondrial integrity.

The animals in group 20_C were further subdivided into groups $20_{C(i)}$ to $20_{C(iii)}$, sacrificed and their fresh hearts used for mitochondrial isolation upon which various respiration analyses were subsequently done (refer to figure 3.1(ii)), in order to moderate mitochondrial function during the advanced stages of obesity.

The control animals in group 20_D were subdivided into an untreated, insulin and ischemia group and administered their various treatments as stipulated in section 3.5.1. This protocol was repeated with the DIO animals in group 20_D. Post sacrifice, the fresh hearts of all the animals in group 20_D were utilized to produce mitochondrial lysates which were stored at -80^{o}C. These were later used to assess the effects of advanced diet-induced obesity on the translocation of protein markers of the PI3K/PKB/Akt and apoptotic signalling pathway (refer to figure 3.1(ii)) from the cytosol to the mitochondria, via western blot analysis.

Table 3.1: Macronutrient composition of control versus DIO diets

	Control group	**DIO group**	**Difference**
Carbohydrates	**60%**	**65%**	**5%**
Protein	**30%**	**19%**	**11%**
Fat	**10%**	**16%**	**6%**
KJ/day	***± 380KJ/day***	***± 575KJ/day***	***± 195KJ/day***

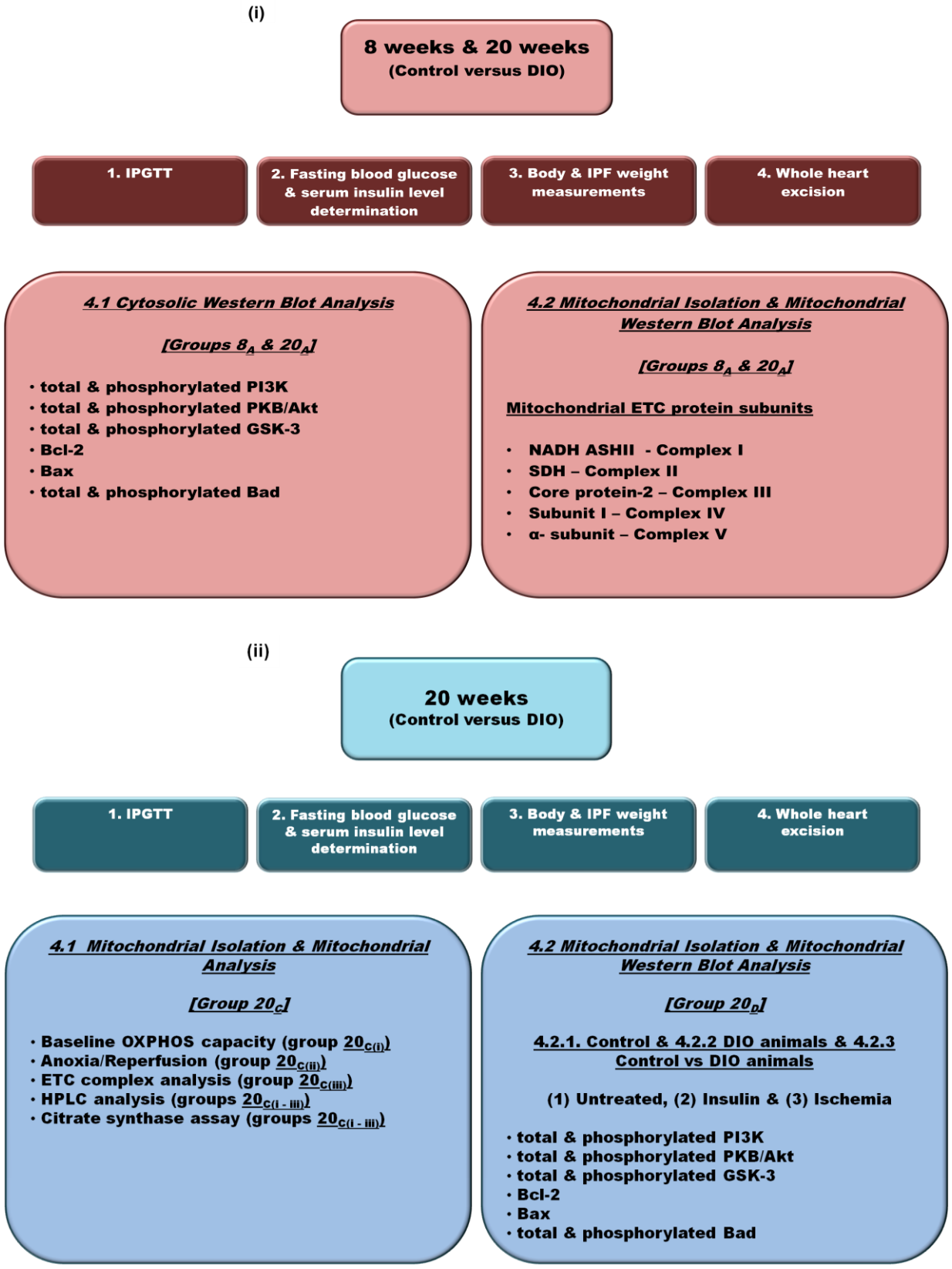

Figure 3.1: (i) and (ii) Study design for the respective groups after 8 and 20 weeks of diet.

3.3 Experimental procedures

3.3.1. Intra-peritoneal glucose tolerance test (IPGTT)

Prior to this specific experiment, the animals were deprived of food for a period of 18 hours but given free access to water. The rats were anaesthetized with sodium pentobarbital (55mg/kg body weight) by intra-peritoneal injection and blood samples were subsequently collected by means of a pin-prick in the tail. These drops of blood were placed on the absorbent film of a disposable test strip (Gluco Plus™, distributed by CIPLA DIBCARE, Bellville, South Africa) which was then inserted into a glucometer (Gluco Plus™, distributed by CIPLA DIBCARE, Bellville, South Africa) to determine the baseline blood glucose level. The animals then received an intra-peritoneal injection of a 50% D-glucose solution, 1g/kg body weight, and the fasting blood glucose level subsequently determined at various time intervals (refer to figure 3.2).

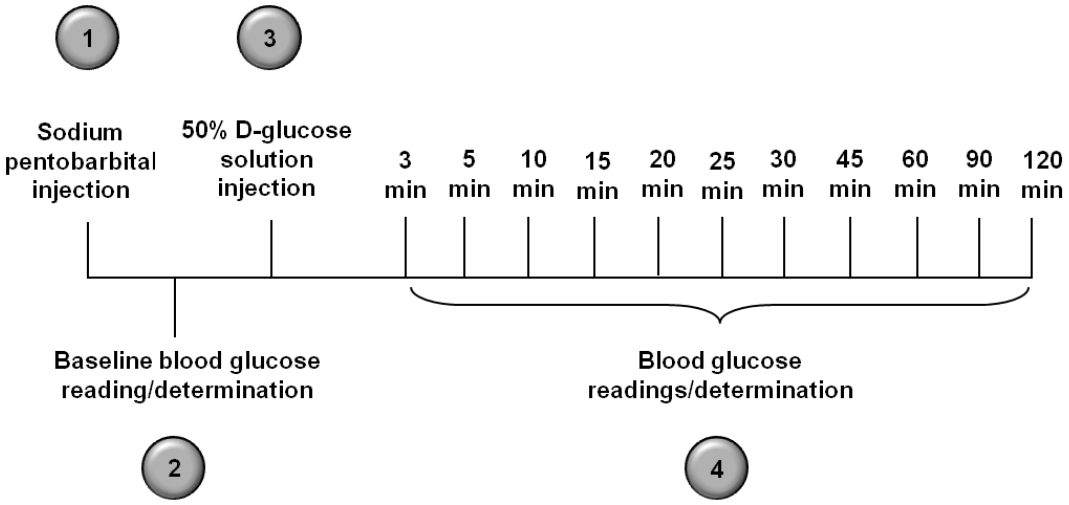

Figure 3.2: Experimental protocol for the intra-peritoneal glucose tolerance test (IPGTT).

3.3.2 Whole heart excision

After the IPGTT's, the animals were allowed to recover for a period of 1 week. Animals were then anaesthetized with sodium pentobarbital (160mg/kg) until a foot-pinch showed a lack of consciousness. Their hearts were removed and washed in ice cold Krebs-Henseleit buffer (pH 7.4) containing 119mM NaCl, 24.9mM $NaHCO_3$, 4.74mM KCl, 1.19mM KH_2PO_4, 0.6mM $MgSO_4$, 0.5mM Na_2SO_4, 1.25mM $CaCl_2$ and 11 mMD-glucose. The hearts were then freeze clamped in liquid nitrogen and stored at -80^oC for western blot analysis.

3.3.3 Fasting serum insulin level determination

The serum from the fasted blood which had been collected from the experimental animals, as stipulated in section 3.2.1, were defrosted at room temperature. The purchased Coat-A-Count® Insulin assay (Diagnostics Products Corporation, LA, USA), used for the quantitative measurement of serum insulin levels, provided all the necessary solutions and materials, all of which were brought to room temperature.

Uncoated polypropylene tubes were labelled for total counts (T_1 – T_2) as well as non-specific binding (N_1 – N_2), while fourteen of the insulin antibody-coated tubes were labelled as such: number 1 = Max_B (representing maximum insulin binding) and numbers 2-14 = $Std_{1\text{-}14}$ (representing the rest of the standards). Furthermore, the rest of the insulin antibody-coated tubes were allocated for the controls ($C_{n+1,2,3...}$) and the samples ($S_{n+1,2,3...}$). 200µl of the zero calibrator A was subsequently pipetted into the non-specific binding and maximum binding tubes. Thereafter, 200µl of each remaining calibrator, control and sample was pipetted into their respective prepared tubes. 1.0ml of ^{125}I insulin was then added to each tube, vortexed and then incubated for 18-24 hours at room temperature. Post incubation, all tubes (except the total count tubes) were placed in a

foam decanting rack and inverted on paper towels, for about 3 minutes, to allow the effluent to drain. Any excess moisture surrounding the top half of the tube was removed with a cotton bud. The radioactivity was then measured in each tube using a gamma scintillation counter (Cobra II Auto Gamma, A.D.P, South Africa).

3.4 Whole heart analysis

3.4.3 Western blot analysis of cytosolic PI3K/PKB/Akt and apoptotic pathway signaling proteins

(i) Lysate preparation

Heart tissue (250mg) from groups 8_A and 20_A, which had been stored at -80^{o}C, were homogenized on ice in 700µl ice-cold lysis buffer with a polytron PT-10 homogenizer (PCU Kinematica, Luzern, Switzerland) for 2 x 4 seconds at setting 4. The lysis buffer, which was used throughout all of the experiments, contained 20mM Tris-HCl (pH 7.5), 1mM EGTA, 1mM EDTA, 150mM NaCl, 1mM Na_2VO_3, 1mM β-glycerophosphate, 2.5mM sodium-pyrophosphate, 0.3mM PMSF, 1% (v/v) Triton X-100, 10µg/ml leupeptin, 10µg/ml aprotonin and 50µg/ml PMSF. The homogenates were then incubated on ice for 15 minutes and thereafter centrifuged (Eppendorf Centrifuge 5413, Hamburg, Germany) at 4^{o}C and 11 500rpm for 10 minutes. The resultant supernatants were then subjected to a Bradford protein determination.

(ii) Bradford protein determination [Bradford 1976]

A series of protein standards were prepared, in duplicate, from a diluted bovine serum albumin (BSA) solution (diluted 1:5 with dH_2O) in order to obtain a standard curve.

Throughout all of the experiments, a BSA stock solution with a known protein concentration of 1.22µg/µl was used. The diluted BSA solution was aliquoted into protein determination tubes such that the protein concentration increased linearly. That is, each tube had the following amount of protein (in µg) in the tube 2.42, 4.83, 9.66, 14.50 and 19.33. The volume pipetted into each tube was (in µl): 10, 20, 40, 60 and 80, thereafter dH_2O was added to each tube to give a final volume of 100µl. The supernatants from the experimental samples, refer to 3.4.3 (i), were diluted 1:10 with dH_2O and 5µl of each of these samples were further diluted with 95µl of dH_2O, in duplicate, with a final volume of 100µl. Subsequently, 900µl of diluted Bradford reagent (1:5 with dH_2O) was added and the samples vortexed and incubated at room temperature for 15-30 minutes. The Bradford reagent stock solution consisted of 0.01% (w/v) Coomassie Brilliant Blue G-250, 4.7% (v/v) ethanol, and 8.5% (v/v) phosphoric acid. The absorbance values were read at 595nm using a spectrophotometer (Spectronic® 20 Genesys™, Spectronic Instruments, USA). The generated standard curve and optical density (OD) values were subsequently used to determine the protein concentration of the experimental samples in milligrams per millilitre (mg/ml).

From the standard curve, the volume of experimental sample, lysis buffer and 3x Laemmli sample buffer, needed to prepare an aliquot of each experimental sample (with a final volume of 180µl), was calculated. The 3x Laemmli sample buffer contained 63mM Tris-HCl (pH 6.8), 10% Glycerol, 2% SDS, 0.002% Bromophenol Blue and 5% 2-mercaptoethanol. Addition of the lysis buffer ensured that all the samples were diluted to an equal protein concentration. Lastly, the samples were boiled for 5 minutes and stored at -80ºC for use during gel electrophoresis.

(iii) Sample loading and gel electrophoresis

The experimental samples, refer to 3.4.3 (ii), were defrosted by boiling it for 5 minutes. The samples were then centrifuged at room temperature and 15 000rpm (Sigma® 101M Centrifuge, distributed by Lasec SA, Cape Town, South Africa) for 5 minutes and the proteins therein separated by means of sodium dodecyl sulphate polyacrylamide gel electrophoresis (SDS-PAGE) using the standard Bio-Rad Mini-Protein III system (Bio-Rad, CA, USA). Throughout the study, a 4% stacking gel was utilized whereas the percentage resolving gel used depended on the molecular weight of the protein in question (refer to table 3.2). The experimental samples and a prestained protein ladder were loaded into the gel and the running buffer, containing 250mM Tris, 192mM glycine and 1% sodium dodecyl sulphate (SDS), subsequently poured into the system. Electrophoresis of the gels followed at 100 volts (V) and 200 milliampere (mA) for 10 minutes initially and thereafter for 65 minutes at 200V and 200mA.

Table 3.2: Acrylamide gel constituents for SDS-PAGE

	Resolving Gel			Stacking Gel
	7.5% Gel	***10% Gel***	***12% Gel***	***4% Gel***
dH_2O	4.65ml	3.85ml	3.35ml	2.7ml
1.5 M Tris-HCl (pH 8.8)	2.50ml	2.50ml	2.50ml	-------
0.5 M Tris-HCl (pH 8.8)	-------	-------	-------	1.25ml
10% SDS	90µl	90µl	90µl	50µl
40% Acrylamide	1.7ml	2.25ml	2.7ml	450µl
10% APS	50µl	50µl	50µl	50µl
99% TEMED	20µl	20µl	20µl	10µl

(iv) Electroblotting and blockage of non-specific binding

Following separation, the proteins were transferred to a polyvinylidene flouride (PVDF) membrane (Immobilon P^{TM}, Millipore, MA, USA) using an electrotransfer system (BioRad Mini Transblot System, BioRad, CA, USA) at 200V and 200mA, while submerged in a transfer buffer containing 25mM Tris-HCl, 192mM glycine and 20% v/v methanol for 1 hour. Post transfer, the PVDF membranes were soaked in 99% pure methanol for 30 seconds and then left to air-dry for 15 minutes. Ponceau S (reversible red) staining solution (0.1% Ponceau S (w/v) and 5.0% acetic acid (w/v)) was subsequently used to ascertain the presence of the proteins and to confirm if the transfer process was successful. To remove the Ponceau red stain from the membranes, it was washed with washing buffer (TBS-Tween) composed of 10% of a 10x Tris-buffered saline (TBS) solution (50mM Tris, 150mM NaCl and 90% dH_20), 90% dH_2O and 0.1% Tween-20. The washing occurred for 3 x 5 minutes at room temperature on a rotator (LAB Rotator: Model DSR 2800V, Digisystem Laboratory Instruments Inc., Taiwan). This washing protocol was followed throughout all of the experiments, unless stipulated otherwise.

The membranes were then blocked, from non-specific protein binding, by incubating them in membrane blocking buffer composed of TBS-Tween and 5% fat free milk powder, for 1.5 to 2 hours. Post incubation, the membranes were washed and incubated in the primary (1°) antibody, all of which were diluted according to the manufacturers' instructions (refer to table 3.3), that specifically recognizes the protein of interest. The incubation took place overnight at 4^{o}C on the LAB Rotator.

Table 3.3: Protein characteristics for western blot analysis

	Molecular weight	Quantity loaded	Resolving gel	1^{o} antibody dilution	2^{o} antibody dilution
tp85	85kDa	80µg	7.5%	1:1000 TBS-Tween	1:4000 TBS Tween
pp85	85kDa	80µg	7.5%	1:1000 5% milk/TBS-Tween	1:4000 5% milk/TBS-Tween
PKB/Akt*	60kDa	40µg	10%	1:1000 TBS-Tween	1:4000 2.5% milk/TBS-Tween
GSK3α/β*	46kDa	60µg	10%	1:1000 5% milk/TBS-Tween	1:4000 5% milk/TBS-Tween
Bcl2	28kDa	40µg	12%	1:1000 5% milk/TBS-Tween	1:4000 5% milk/TBS-Tween
Bax	20kDa	40µg	12%	1:1000 2.5% milk/TBS-Tween	1:4000 2.5% milk/TBS-Tween
tBad	23kDa	120µg	12%	1:1000 TBS-Tween	1:4000 TBS-Tween
pBad	23kDa	120µg	12%	1:1000 5% BSA	1:4000 0.5% milk/TBS-Tween

* The same 1^{o} and 2^{o} antibody dilution factor was used for the total and phosphorylated versions of these proteins.

(v) Secondary (2^{o}) antibody incubation and protein detection

The following day, the PVDF membranes were thoroughly washed and thereafter the membranes were incubated at room temperature on the LAB Rotator in anti-rabbit horseradish peroxidise-labelled secondary antibody. The secondary antibody was diluted according to manufacturers' instructions for each specific protein of interest (refer to table 3.3), for 1 hour at room temperature. After secondary antibody incubation, the membranes were thoroughly washed.

In terms of protein detection, PVDF membranes were coated with enhanced chemiluminescence (ECL) detection reagents for 40 seconds in a dark room.

Subsequently, the membranes were exposed to an autoradiography film (Amersham Hyperfilm ECL (# RPN 2103), GE Healthcare UK Limited, Buckinghamshire, UK) to detect light emission from the protein of interest. The interval of exposure differed for each protein of interest.

(vi) Densitometry

Once the proteins were detected by chemiluminescence, the autoradiography films were scanned (Epson Perfection V700 Photo Scanner, Digital ICE Technologies, Indonesia) and analysed with densitometry (UN-SCAN-IT, Silk Scientific Inc., Orema, Utah, USA). This technique detects the density of each protein band, which is an indication of the amount of protein present, and relays that density in terms of total pixel values or arbitrary densitometry units.

x) Equal loading determination

To verify that unequal loading was not a factor, the PVDF membranes were stripped of all antibodies as well as the ECL detection reagents by washing them with distilled water (dH_2O) for 2 x 5 minutes at room temperature on the LAB Rotator. The membranes were then incubated for 5 minutes in 0.2M NaOH on the belly dancer at room temperature and then again washed with dH_2O, as previously mentioned. Thereafter, steps (iv) to (vi) of the protocol were followed. The β-Tubulin primary antibody was diluted, according to manufacturer`s instructions, 1:1000 (5µl 1º antibody in 5ml TBS-Tween), while the anti-rabbit horseradish peroxidise-labelled secondary antibody was diluted 1:4000 (5µl 2º antibody in 20ml TBS-Tween). Equal protein loading was confirmed, if all of the protein bands on the β-tubulin autoradiography films had an equal density as seen in figure 3.3.

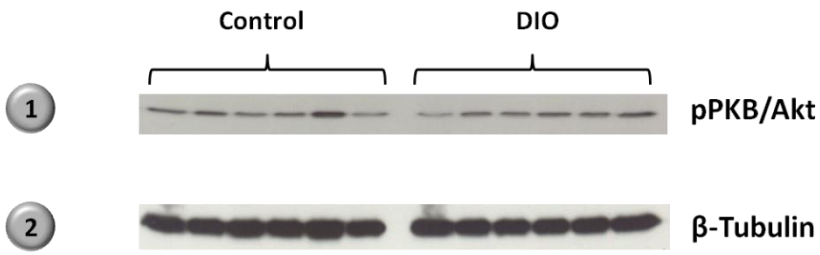

Figure 3.3: The (1) pPKB/Akt and (2) β-Tubulin autoradiography films, as an example confirmed equal loading.

xi) P/T ratio

The P/T ratio is that of the phosphorylated over the unphosphorylated (total) form of a particular protein and was obtained by dividing the arbitrary densitometry units, as described in section 3.4.3 (vi), of the phosphorylated by that of the unphosphorylated protein.

xii) Sample number (n-value)

All the n-values displayed on the graphs in Chapter 4 indicate the number of individual samples (hearts) per group. The images accompanying the graphs in figures 4.4-4.6, 4.11-4.14 and 4.19-4.32 represent the autoradiography films developed during protein exposure, as explained in section 3.4.3 (v). The western blot experiment was duplicated with a different set of samples (i.e. more than one electroblot was run per protein of interest) for the previously mentioned graphs.

3.5 Cardiac mitochondrial analyses

3.5.1 Western blot analysis of mitochondrial PI3K/PKB/Akt and apoptotic pathway signaling proteins

(i) Mitochondrial isolation

Prior to mitochondrial isolation, the control and DIO animals in group 20_D were subdivided into a control, insulin and ischemia group. (1) Control: after anaesthesia of the rats, hearts were excised and arrested in a sorval tube with ice cold KE isolation medium (pH 7.4), which contained 0.18M KCl (13.42g/L) and 0.01M EDTA (3.72g/L), for 1-3 minutes. (2) The insulin group: Animals were injected intra-peritoneally with 20 units of a 100IU/ml insulin solution and given a 10 minute waiting period. Thereafter, they were anaesthetized and their hearts excised as explained in section 3.3.2. (3) Ischemia: the hearts from these animals were arrested in room temperature KE isolation medium and left for 25 minutes at room temperature.

Subsequently, all of the fresh hearts were snipped into small pieces with scissors and the majority of the blood removed by repetitive washing with the ice cold isolation medium. All further procedures were performed on ice. The tissue was homogenized while submerged in the ice cold isolation medium, on ice with the Polytron PT10 homogenizer for 2 x 4 seconds (setting 4). Next the sorval tube was filled to the top with the ice cold isolation medium and the homogenate was centrifuged for 10 min at 2 500rpm (755 x g) and 4°C in a Sorval® RC6 Plus, Thermo Electron Corporation, Osterode, Germany (SS34 rotor)). The resultant supernatants were decanted into a clean sorval tube and centrifuged at 12 500rpm (18 800 x g) to obtain a mitochondrial pellet which was subsequently resuspended in 1ml ice cold lysis buffer, refer to 3.4.3 (i), and homogenized using a glass Teflon Potter Elvehjem homogenizer. The lysates were further homogenized with a polytron (Virsonic

Digital 550, The VirTis Co., USA) for 2 x 3 seconds at setting 3. The lysates were left to undergo additional digestion on ice for 15 minutes and thereafter it was centrifuged for 10 minutes at 11 500rpm at 4ºC. The resultant supernatant was collected and the protein concentration determined by the method of Bradford, as explained in step (ii) of section 3.4.3. Thereafter, the mitochondrial lysates were subjected to western blot analysis, as laid out in steps (iii) to (x) of section 3.4.3.

3.5.2 Western blot analysis of mitochondrial ETC complex protein subunits

(i) Mitochondrial isolation

For the purpose of this experiment, frozen (at -80ºC) myocardial tissue, from groups 8_B and 20_B, were subjected to the same protocol as indicated in section 3.5.1 (i).

(ii) Sample loading and gel electrophoresis

10µg of each mitochondrial lysate sample, and 5µl of the molecular weight marker, were loaded into a commercially available pre-cast acrylamide gradient gel (Mini-Protean® TGX™, BioRad, CA, USA). Electrophoresis then proceeded in the previously mentioned Bio-Rad Mini-Protein III system, which was filled to the top with electrophoresis running buffer containing 25mM Tris, 192mM glycine and 0.1% SDS. The proteins were separated at 150V and 150mA for 2 hours or until the bromophenol blue dye of the Laemmli sample buffer had run out of the bottom of the gel. Thereafter, the gel was soaked in electroblotting transfer buffer, which contained 25mM Tris, 192mM glycine, 10% methanol and 0.1% SDS, for 30 minutes.

(iii) Electroblotting and blockage of non-specific binding

Subsequent to soaking the gel, it was assembled in a standard transfer sandwich, using a PVDF membrane, which was placed in the Bio-Rad Mini Transblot system and fully submerged in electroblotting transfer buffer. Electroblotting was carried out at 150mA and 150V for 2 hours. Post transfer, the proteins were fixed by immersing the PVDF membranes in methanol and the protein transfer confirmed with Ponceau red reversible dye, as explained in section 3.4.3 (iv). Throughout the experiment, the membranes were washed with membrane washing buffer, containing phosphate buffered saline solution (PBS) (1.4mM KH_2PO_4, 8mM Na_2HPO_4, 140mM NaCl and 2.7mM KCl, pH 7.3) and 0.05 % Tween-20, for 3 x 5 minutes.

The membranes were blocked overnight, at 4ºC on the LAB Rotator, in membrane blocking buffer containing PBS and 5% fat free milk powder. Post blocking, the membranes were incubated in a MitoProfile® Total OXPHOS Rodent Western Blot Antibody Cocktail, dilution factor 1:1000 (5µl primary antibody in 5ml 1 % fat free milk powder/PBS), at room temperature for 2 hours on the belly dancer.

(iv) Secondary (2^o) antibody incubation and protein detection

The membranes were incubated in anti-mouse horseradish peroxidase (HRP) conjugated secondary antibody, dilution factor 1:4000 (5µl primary antibody in 20ml 1% fat free milk powder/PBS), at room temperature for 2 hours on the LAB Rotator.

(v) Densitometry

The same protocol was followed as in section 3.4.3 (vi).

(vi) Equal loading determination

The same protocol was followed as in section 3.4.3 (x).

3.5.3 Mitochondrial respiration analyses

Mitochondria were prepared from fresh hearts (from all of the animals in group 20_C) as described in section 3.5.1 The mitochondrial pellet was resuspended in 500µl KE isolation medium and homogenized with the glass Teflon Potter Elvehjem homogenizer. 50µl of each mitochondrial sample was precipitated in 1ml of 10% trichloroacetic acid (TCA) overnight at 4ºC for subsequent Lowry protein determination. Furthermore, 50µl of the resuspension was stored at -80ºC for citrate synthase assay analysis at a later stage.

(ii) Lowry protein determination [Lowry et al. 1951]

The precipitated samples were centrifuged for 15 minutes at 2 500rpm (755 x g) (Heraeus Megafuge 16R Centrifuge, Thermo Fisher Scientific Inc. (NYSE: TMO), USA). Thereafter, the supernatant was discarded while 500µl 1N NaOH was added to the pellet and vortexed. The proteins in the samples were then dissolved by heating it in a water bath at 70°C for 10 minutes or until the solution was lucid. Subsequently, 500µl dH_20 was added to each sample and then vortexed rendering a 0.5N NaOH solution.

Three different albumin stock solutions, of which the protein concentration was known, were pipetted into lucham tubes and used to produce a standard curve. 0.5N NaOH was used as a blank. In duplicate, 50µl of the mitochondrial samples was added to lucham-tubes. Thereafter, 1ml NaK-Tartrate-$CuSO_4$ solution, consisting of 2% NaK-Tartrate, 1% $CuSO_4.5H_2O$ and 2% Na_2CO_3, was added to each tube within a 10-30 second time

interval. The tubes were vortexed after each addition and after 10 minutes, 100µl diluted Folin Ciocalteu's solution (diluted 1:3) was added at the same time interval. The tubes were again vortexed after each addition and subsequently left for 30 minutes to incubate at room temperature. The optical density was read at visible light (750nm). The generated standard curve and OD values were then used to determine the protein concentration of the mitochondrial samples in mg/ml.

(iii) Oxygraph calibration

Respiration of isolated mitochondria was measured at 25°C using an oxygraph containing a Clarke-type electrode disc (Hansatech Oxygraph, distributed by Scientific Associates cc (Tokai, RSA), whereby the O_2 consumption was measured in nmolO_2/ml/min.

One of two incubation media was used to calibrate the oxygraph prior to the actual experiment, depending on its objective of that experiment. To assess respiration when glutamate served as a metabolic substrate, the glutamate incubation medium (pH 7.4) was used, which consisted of 250mM sucrose, 10mM Tris-HCl (pH 7.4), 8.5mM $K_2HPO_4.2H_2O$, 5mM glutamate and 20mM malate. In contrast, 5mM palmitoyl-L-carnitine replaced the 5mM glutamate in the glutamate incubation medium (i.e. palmitoyl-L-carnitine incubation medium) in order to establish respiration in the presence of fatty acids (metabolic substrate).

An aliquot (the volume was dependent on the end reaction volume) of the incubation media was pipetted into the chamber of the oxygraph, subsequently an imprecise but small amount of sodium dithionite ($Na_2S_2O_4$) was added to the chamber to scavenge all oxygen and render the medium anoxic. The chamber was sealed and the oxygraph calibrated to a 0 and 100% oxygen level. After the calibration the chamber was repetitively rinsed with dH_2O to remove all remnants of the $Na_2S_2O_4$.

(iv) Baseline mitochondrial respiration analysis

Referring to figure 3.4, (1) 650µl of the incubation medium was added to the oxygraph chamber and allowed to become saturated with air for about 90 seconds. The first set of experiments used the glutamate medium whereas a separate set of experiments used the palmitoyl-L-carnitine incubation medium. (2) Thereafter, 50µl of the mitochondrial suspension (cardiac mitochondria isolated from group $20_{C(i)}$) was added and its equilibration in the chamber recorded for 90-120 seconds. (3) Hereafter 50µl ADP was added and the stopper rapidly closed, effectively sealing the chamber. (4) The active mitochondrial state 3 respiration was recorded that is, the mitochondria were allowed to use all the ADP to produce ATP. (5) Once the all the ADP was depleted, (6) state 4 respiration was allowed to ensue (the mitochondria were allowed to respire in the absence of a high energy phosphate) (7) until all the oxygen in the chamber was depleted. O_2 consumption was measured in nmolO_2/ml/min at 25ºC. The concentration of the ADP (stock solution diluted 250x) was determined spectrophotometrically by reading the absorbance in a quartz cuvette at a UV wavelength of 259nm. The molar extinction coefficient of ADP is 15.4×10^6.

State 3 and 4 respiration was computed as the natoms oxygen consumed (during their respective respiration states) per milligram mitochondrial protein per minute (natoms O_2/mg mitochondrial protein/min).

The respiratory control index (RCI) was calculated as the ratio of state 3 to state 4 respiration, whereas the ADP/O ratio was established as the amount of ADP phosphorylated (to ATP) over the amount of oxygen consumed during state 3 respiration.

The oxidative phosphorylation rate was calculated as the state 3 respiration rate multiplied by the ADP/O ratio.

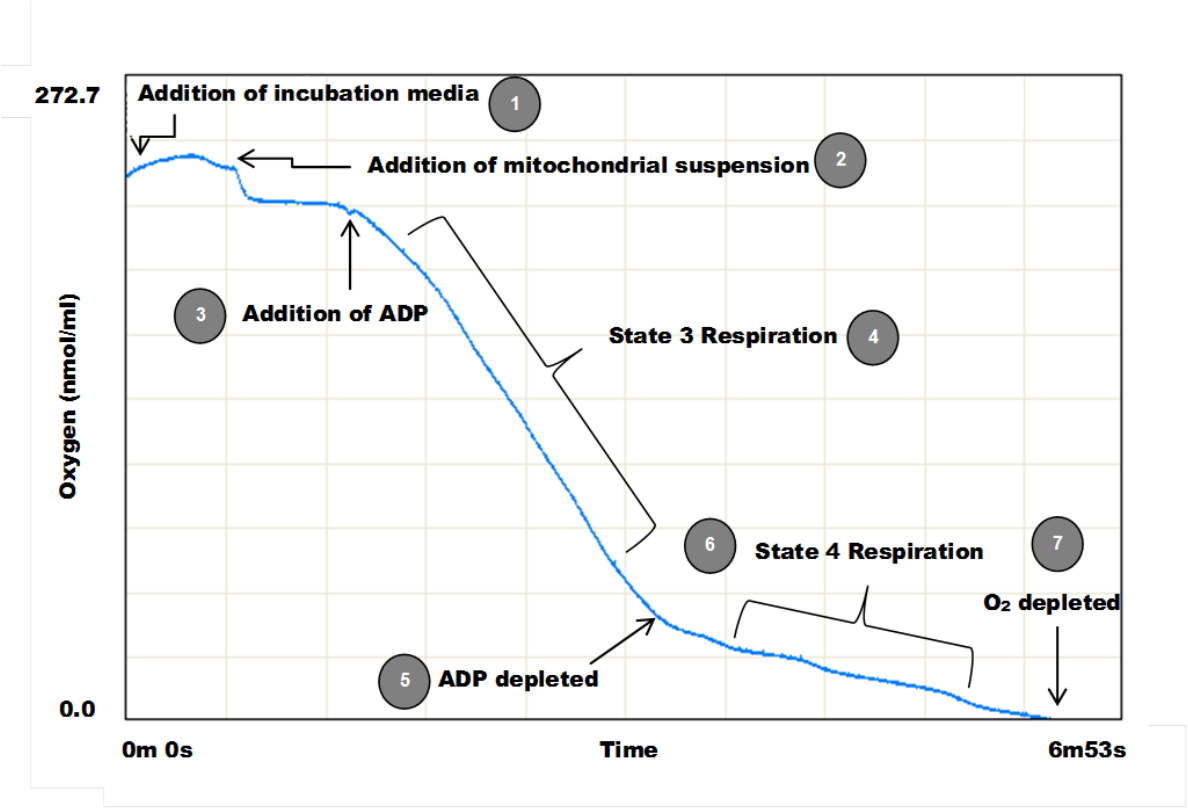

Figure 3.4: A standard respiration graph produced by an oxygraph

(v) Anoxia/Reperfusion analysis

During this analysis 600µl incubation medium was added to the chamber and after 90 seconds 100µl of the mitochondrial suspension added. Following a 90 seconds equilibration period, 50µl ADP was added and the chamber sealed. The mitochondria were allowed to reach state 3 and state 4 respiration and thereafter 100µl of a 17.7mM ADP solution was added and the chamber rapidly sealed again, allowing for maximum stimulated respiration. Consequently, the oxygen levels within the chamber became completely depleted, making the chamber anoxic. This was allowed to proceed for 20 minutes after which the mitochondria were re-oxygenated by removing the stopper and bubbling air through the reaction mixture with a plastic Pasteur pipette. The mitochondria were then allowed to regain state 3 respiration for 2 minutes. A recording of mitochondrial oxygen consumption was taken throughout the experiment. This protocol was followed for two separate sets of experiments, the first using glutamate and the second using palmitoyl-L-carnitine incubation medium.

Subsequent to the anoxia/reperfusion analysis, the state 3 percentage recovery was computed as indicated below:

$$State\ 3\ \%\ Recovery\ = \left(\frac{State\ 3\ respiration\ after\ reperfusion}{State\ 3\ respiration\ before\ reperfusion}\right) \times 100$$

(vi) Mitochondrial electron transport chain complex analysis [Lanza et al. 2009]

Prior to the experiment, the oxygraph was a calibrated (as explained in 3.5.3 (iii)) and a baseline mitochondrial respiration analysis was conducted to measure respiration without substrates (as explained in 3.5.3 (iv)). For this experiment, 680µl incubation medium was pipetted into the oxygraph chamber and after 90 seconds, 20µl of the mitochondrial suspension was added. After another 90 seconds had passed, 50µl ADP was added and the chamber sealed with the stopper. A different pharmaceutical substance, each one inhibiting or uncoupling a specific complex within the ETC, was then injected through the capillary tube in the chamber stopper. After each addition the reaction was allowed to progress for at least 120 seconds with continuous recording. The order of addition was as follows: (1) 45µl of a 80Mm succinate stock solution, (2) 8µl of a 50µM rotenone stock solution, (3) 5µl of a 5mg/1ml oligomycin stock solution and (4) 8µl of a 5mM carbonyl cyanide m-chlorophenylhydrazone (CCCP) stock solution. This protocol was followed for two separate sets of experiments, the first using 5mM glutamate (glutamate incubation medium) and the other using 5mM palmitoyl-L-carnitine (palmitoyl-L-carnitine incubation medium) as substrate.

The protocol used by Lanza et al., indicate the purpose of the various ETC inhibitors and uncouplers, which will briefly be discussed below:

(1) Succinate: Succinate can stimulate respiration above the glutamate and malate stimulated state 3 thresholds by providing additional electron flow through complex II.

(2) Rotenone: Rotenone, in addition to succinate, is used to assess the function of complex II as it also selectively stimulates the flow of electrons through complex II in the presence of succinate. This is achieved by inducing a redox shift that effectively inhibits all of the NADH-linked dehydrogenases in the TCA cycle.

(3) Oligomycin: Induces state 4 respiration by inhibiting the F_o unit of the ATP synthase enzyme, thus blocking the proton channel and effectively eliminating ATP synthesis. Due to the lack of ADP phosphorylation, there is a leakage of protons across the inner mitochondrial membrane and thus, oligomycin is used to indicate the degree of uncoupled respiration or proton leak.

(4) CCCP: This uncoupler dissipates the proton gradient across the inner mitochondrial membrane and thus, uncouples oxidative phosphorylation.

3.5.4 High performance liquid chromatography (HPLC)

Prior to the HPLC analysis, the final reaction mixtures (from the experiments laid out in 3.5.3 (iv), (v) and (vi)) were removed from the oxygraph chamber and added to 1ml of 6% PCA (perchloric acid). This allowed for protein precipitation which took place on ice for a maximum of 30 minutes. Thereafter, the mixture was centrifuged at 4000rpm at 4°C for 10 minutes and 1 ml of the supernatant removed and added to 5µl universal pH indicator, transforming the supernatant from colourless to purple. A neutralization mixture (40% saturated KOH-KCl and 0.2M Tris-HCl in a 2:3 ratio) was progressively (± 5µl at a time) added to the supernatant until it turned green in colour, indicating a neutral pH (pH 7.0 - pH 7). Subsequently, the mixture was centrifuged at 4000rpm at 4°C for 3 minutes. The

resultant supernatants were then filtered through a 0.45µm nitrocellulose filter (Millipore, MA, USA) into Eppendorf tubes and stored at -80°C for subsequent HPLC analysis.

For our experiments, we performed reverse-phase HPLC using a Spectra Physics (SP8440 XR) on-line UV detector (CA, USA) with a wavelength of 210nm. The mobile phase consisted of a buffer containing 257mM KH_2PO_4, 1.18mM tetrabutylammoniumphosphate (TBAP), 12.5 % (v/v) HPLC graded methanol, pH 4.0 with H_3PO_4. The column (distributed by Phenomenex®, UK), which was 250mm in length and had an internal diameter of 4.6mm, was packed with LUNA C18 (2) with a particle size of 5µm and was filtered and de-gassed with helium.

The amount of ATP, ADP, AMP and CrP were all quantified (in µmol/g mitochondrial protein) subsequent to the HPLC analysis, from the peak area ratio which was based on the calibration or standard curve generated from each individual standard. All of the standards used had known concentrations: ATP = 0.4535nmol/10µl, ADP = 0.5853nmol/10µl, AMP = 0.7200nmol/10µl and CrP = 0.7640nmol/10µl.

3.5.6 Citrate synthase assay

Prior to the assay, CellLytic M Cell lysis reagent (Catalogue # C2978, Sigma, St. Louis, USA) (about 200µl per g of mitochondrial tissue) was added to 50µl of each the mitochondrial samples (which had been stored at -80ºC in KE isolation medium). A citrate synthase assay kit (Catalogue # CS0720, Sigma, St. Louis, USA) was then used to determine the level of citrate synthase activity in each mitochondrial sample. The kit consisted of 1x Assay buffer solution, 30mM Acetyl-CoA, 10mM 5,5'-dithiobis-(2-nitrobenzoic acid) (DTNB), 10mM oxaloacetate (OAA) solution and a diluted citrate synthase solution which served as the positive control. Subsequently, two reaction

mixtures were prepared (1 and 2) both containing 10µl Acetyl-CoA and 10µl DTNB solution. In addition, reaction mixture 1 also contained 920µl of the assay buffer, whereas mixture 2 contained 90µl of this buffer. 10µl of the diluted citrate synthase solution was added to reaction mixture 2 which served as the enzyme standard (positive control) from which a standard curve was later generated. Furthermore, 10µl of the mitochondrial samples were added to reaction mixture 1, which was later used to determine the citrate synthase activity these samples.Thereafter, the positive control and mitochondrial samples were heated to 25ºC and transferred to a 1ml absorbance reading cuvette and the OD measurements taken at a wavelength of 412nm every 20 seconds for a total of 1.5 minutes to measure any baseline reaction. 50µl of the oxaloacetate solution was then added to all of the samples, the samples gently mixed and the OD measurements taken again every 20 seconds for a total of 1.5 minutes to measure the total citrate synthase activity. The generated standard curve and OD values were then used to calculate the level of citrate synthase activity in µmol/mg protein/minute.

3.5.6 Statistical analyses

For the purpose of this study, results were statistically compared using Microsoft GraphPad Prism, version 5.0. The unpaired Student t-test was used to compare one variable between two groups while the one-way analysis of variance (1-way ANOVA) test, followed by a Bonferroni post hoc test, was used to compare a single variable amongst more than two groups . On the other hand, a two-way analysis of variance (2-way ANOVA) test was used to compare multiple variables amongst more than two groups. All of the values were expressed as the mean ± standard error of the mean (SEM) and a p-value of less than 0.05 ($p<0.05$) was considered statistically significant.

Chapter 4: Results

4.1 Physiological parameters

4.1.1 8 weeks

Consequent to following their respective diets, there was no significant difference between the control and DIO group with respect to their total body weight. In contrast, the DIO animals presented with significant increases in their intra-peritoneal fat mass ($p<0.05$), fasting blood glucose levels ($p<0.05$) and serum insulin levels ($p<0.05$) when compared to their controls. Please refer to table 4.1.

4.1.2 20 weeks

In comparison to the control animals, the DIO animals showed a significant elevation in both their total body weight ($p<0.0001$) and intra-peritoneal fat mass ($p<0.0001$). Additionally, these animals displayed significantly augmented fasting blood glucose levels ($p<0.001$) as well as serum insulin levels ($p<0.0001$). Please refer to table.4.1.

Table 4.1: The various physiological parameters of the DIO versus control animals subsequent to 8 and 20 weeks on their respective diets.

	8 Weeks		
	Control	*DIO*	*n-value per group*
Body weight (g)	342.50 ± 6.98	338.40 ± 7.06	20
Intra-peritoneal fat weight (g)	11.70 ± 0.57	14.13 ± 0.78 *	20
Fasting blood glucose levels (mmol/L)	4.84 ± 0.19	5.70 ± 0.25 *	8
Fasting serum insulin levels (µlU/ml)	29.09 ± 2.59	41.25 ± 4.01 *	10
	20 Weeks		
	Control	*DIO*	*n-value per group*
Body weight (g)	439.40 ± 11.25	535.90 ± 21.94 ***	10
Intra-peritoneal fat weight (g)	14.25 ± 1.77	29.49 ± 3.16 ***	10
Fasting blood glucose levels (mmol/L)	4.32 ± 0.21	5.28 ± 0.15 **	10
Fasting serum insulin levels (µlU/ml)	52.56 ± 2.17	145.8 ± 6.13 ***	6

*p<0.05, **p<0.001 and ***p<0.0001 present statistically significant differences

4.2 Intra-peritoneal glucose tolerance test (IPGTT) data

4.2.1 8 weeks

Subsequent to following their respective diets for a period of 8 weeks, the DIO animals displayed a significantly bigger area under the curve (AUC) (749.7mg/ml/min, p=0.0034), in comparison to the control animals (604.8mg/ml/min), during a 2 hour IPGTT (figure 4.1). Additionally, the baseline fasting blood glucose levels was significantly elevated in the DIO group (4.55mmol/L ± 0.24, $p<0.01$), in contrast to their controls (3.91mmol/L ± 0.17).

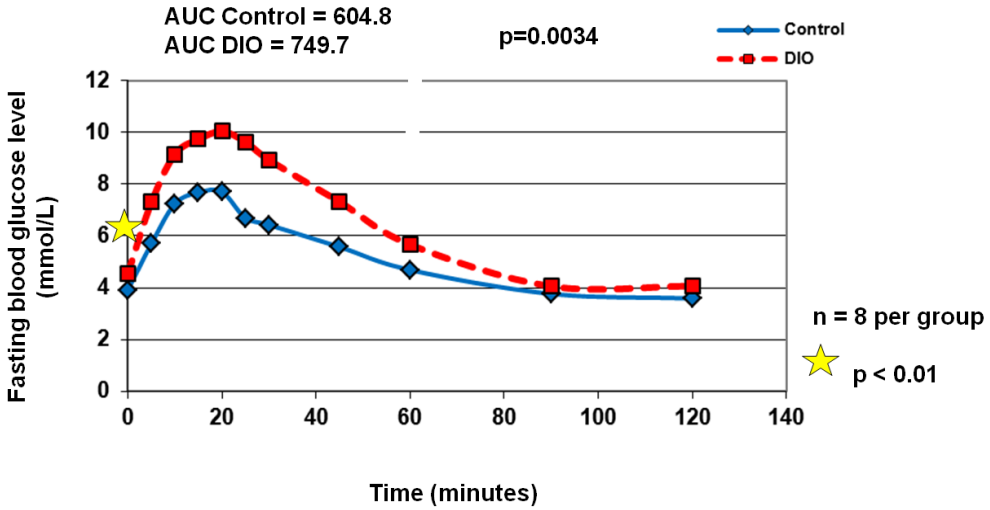

Figure 4.1: The fasting blood glucose levels of control versus DIO animals, following an 8 weeks high caloric diet, during a 2 hour IPGTT.

4.2.2 20 weeks

The DIO animals displayed a significantly greater AUC (568.0mg/ml/min, p=0.0043) in comparison to the control animals (466.8mg/ml/min) during a 2 hour IPGTT, following 20 weeks of diet (figure 4.2). As seen in figure 4.3, the DIO animals showed significantly higher fasting blood glucose levels at the zero (a) (5.28mmol/L ± 0.15, p<0.01) and 2 hour (b) time points (4.15 mmol/L ± 0.15, p<0.01), in comparison to the control animals (4.32 mmol/L ± 0.21 and 3.38 mmol/L ± 0.18, respectively).

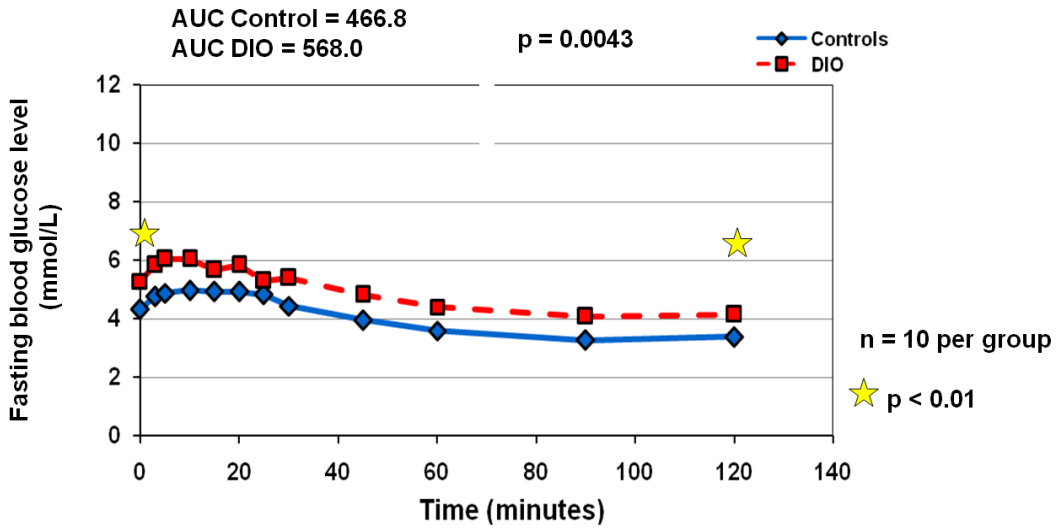

Figure 4.2: The fasting blood glucose levels of control versus DIO animals, following a 20 weeks high caloric diet, during a 2 hour IPGTT.

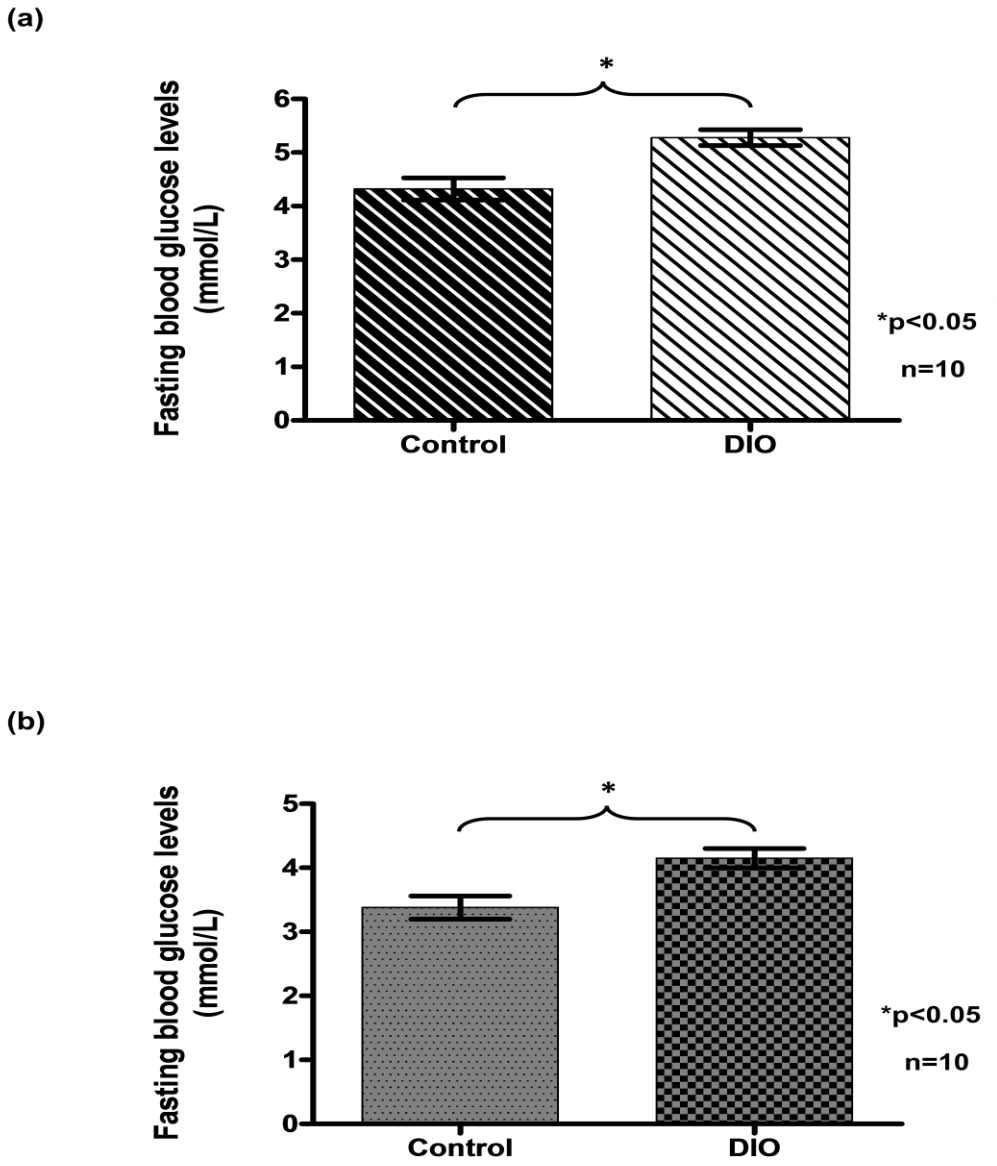

Figure 4.3: The fasting blood glucose levels of control versus DIO animals (n=10 per group), following a 20 weeks high caloric diet, during a 2 hour IPGTT at the zero (a) and 2 hour (b) time points.

4.3 Effects of 8 weeks high caloric diet on myocardial protein signalling

4.3.1 Western blot data (cytosolic PI3K/PKB/Akt and apoptotic signalling analysis)

4.3.1.1 p85 subunit of phosphatidylinositol-3 kinase (p85 PI3K)

Subsequent to following their respective diets for 8 weeks, the total p85 (tp85) as well as the phosphorylated p85 (pp85) subunit levels (of the PI3K protein) were significantly higher in the DIO animals when normalized to their controls, figure 4.4 (a) and (b) respectively. Additionally, the P/T ratio was also found to be significantly elevated in the DIO animals when compared to the control animals (figure 4.4 (c)).

4.3.1.2 Protein kinase B (PKB)

After following their respective diets for a period of 8 weeks, The DIO animals showed no significant differences, in comparison to their controls, when the protein level of total PKB/Akt (tPKB/Akt) was analysed in whole heart lysates (figure 4.5 (a)).

The protein level of phosphorylated PKB/Akt (pPKB/Akt) (figure 4.5 (b)) as well as the P/T ratio (figure 4.5 (c)) were significantly higher in the DIO animals, when matched against their controls.

4.3.1.3 Glycogen synthase kinase-3 α/β (GSK-3 α/β)

Subsequent to following their respective diets for a period of 8 weeks, the DIO animals showed no significant differences, in comparison to their controls, when the protein level of total GSK-3 α/β, (tGSK-3 α/β) was analysed in whole heart lysates (figure 4.6 (a)). When

evaluated, the DIO group had both a significantly higher level of phosphorylated GSK-3 α/β, (pGSK-3 α/β) and P/T ratio in comparison to their controls (figure 4.6 (b) and (c)).

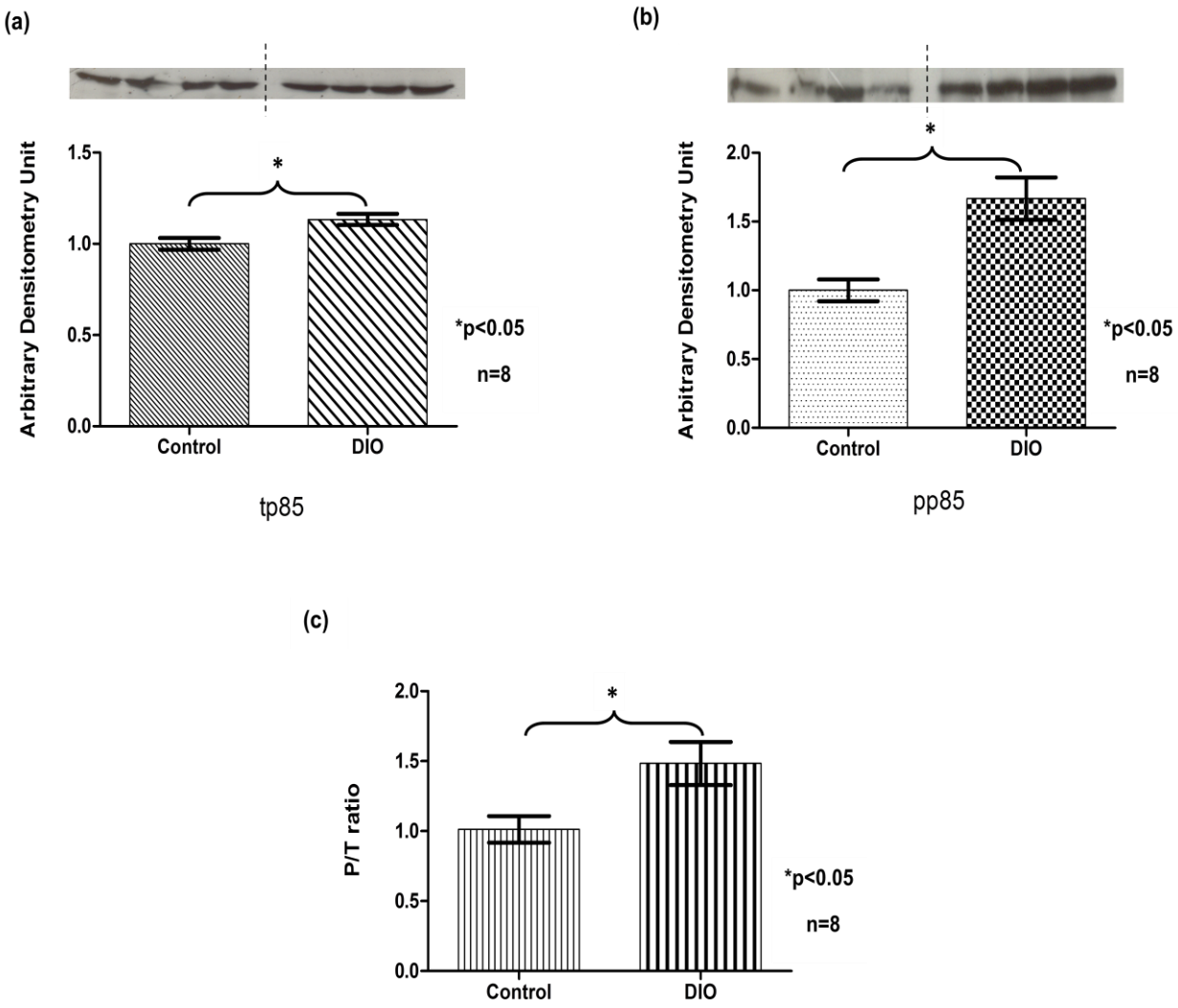

Figure 4.4: The myocardial tp85 (a) and pp85 (b) levels as well as the P/T ratio (c) in control versus DIO animals (n=8 per group), following 8 weeks of their respective diets.

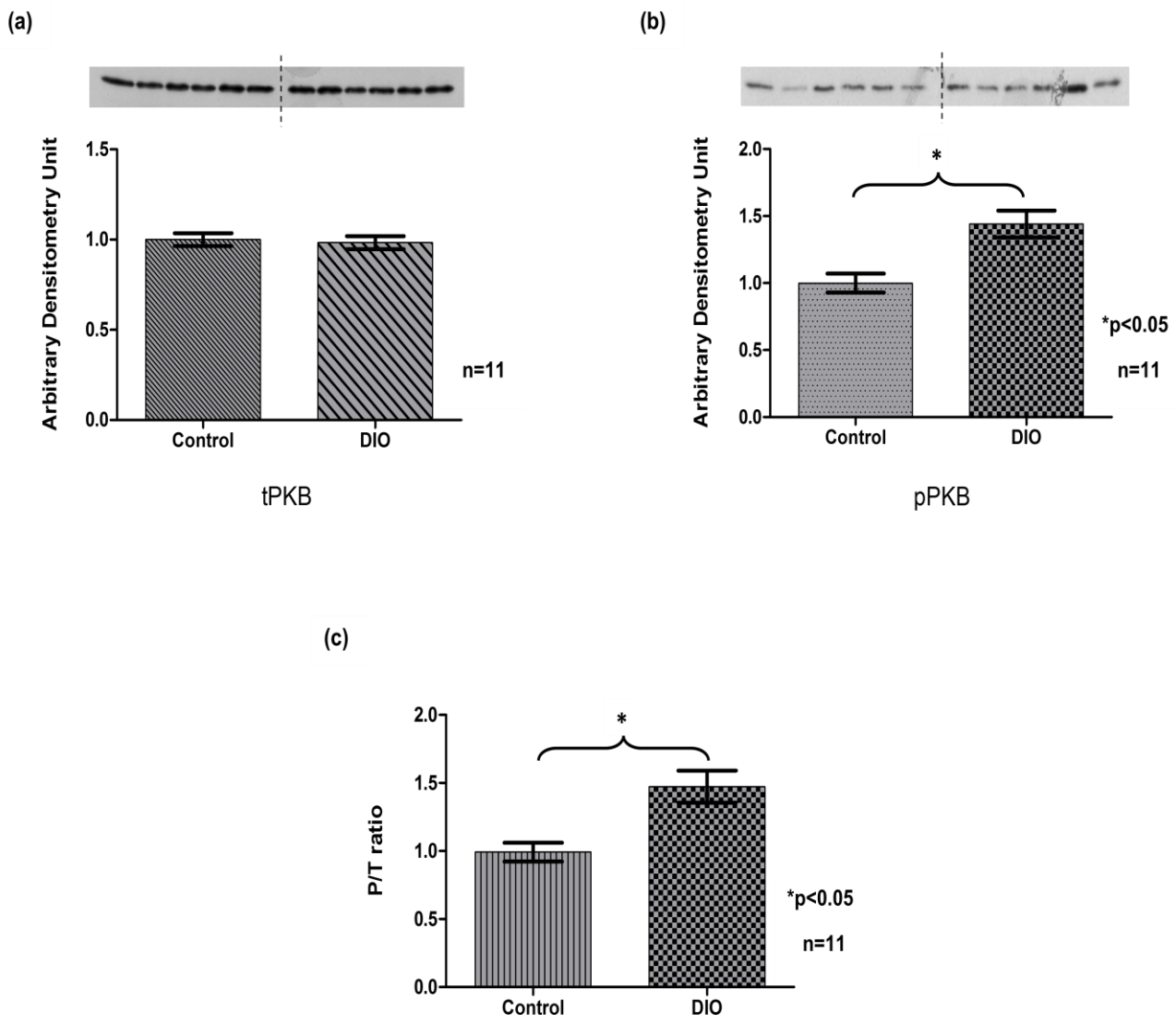

Figure 4.5: The myocardial tPKB/Akt (a) and pPKB/Akt (b) levels as well as the P/T ratio (c) in control versus DIO animals (n=11 per group), following 8 weeks of their respective diets.

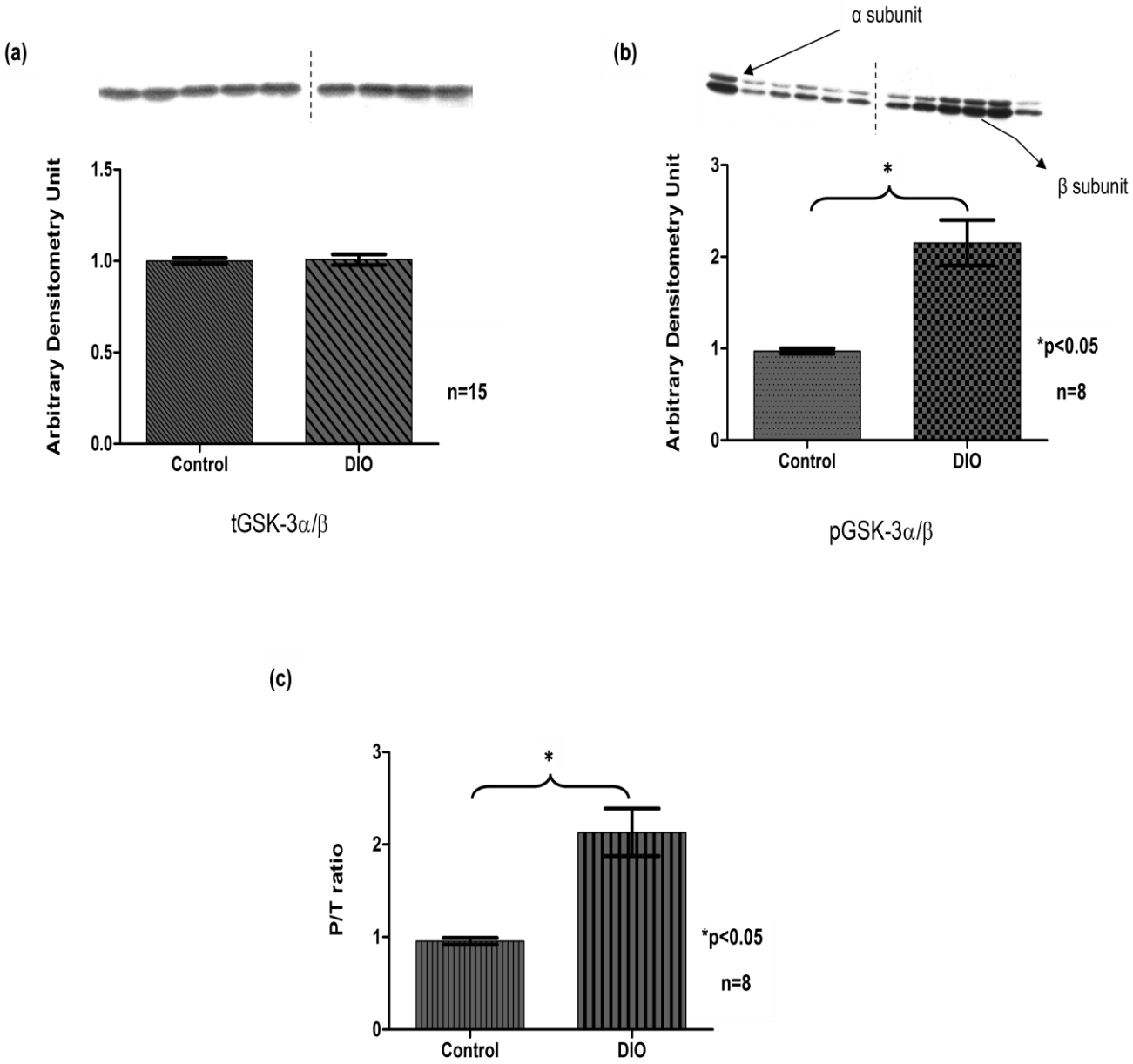

Figure 4.6: The myocardial tGSK-3 α/β (n=15 per group) (a) and pGSK-3 α/β (b) levels as well as the P/T ratio (n=8 per group) (c) in control versus DIO animals, following 8 weeks of their respective diets.

4.3.1.4 Bcl-2 associated death promoter (Bad) protein

The myocardial level of total Bad (tBad) was not significantly different between the control and DIO groups, following 8 weeks of their respective diets (figure 4.7 (a)).

The phosphorylated Bad (pBad) protein level as well as the P/T ratio was significantly higher in the DIO animals, as seen in figure 4.7 (b) and (c).

4.3.1.5 Bcl-2 associated X (Bax) protein

The DIO group exhibited significantly higher levels of myocardial Bax protein (figure 4.8 (a)) and Bcl-2 protein (figure 4.8 (b)), when compared to their control groups, upon the completion of 8 weeks of their respective diets.

4.3.1.6 Bax/Bcl-2 protein ratio

There was no significant difference between the control and DIO animals in terms of their Bax/Bcl-2 protein ratio, after 8 weeks of their respective diets (figure 4.8 (c)).

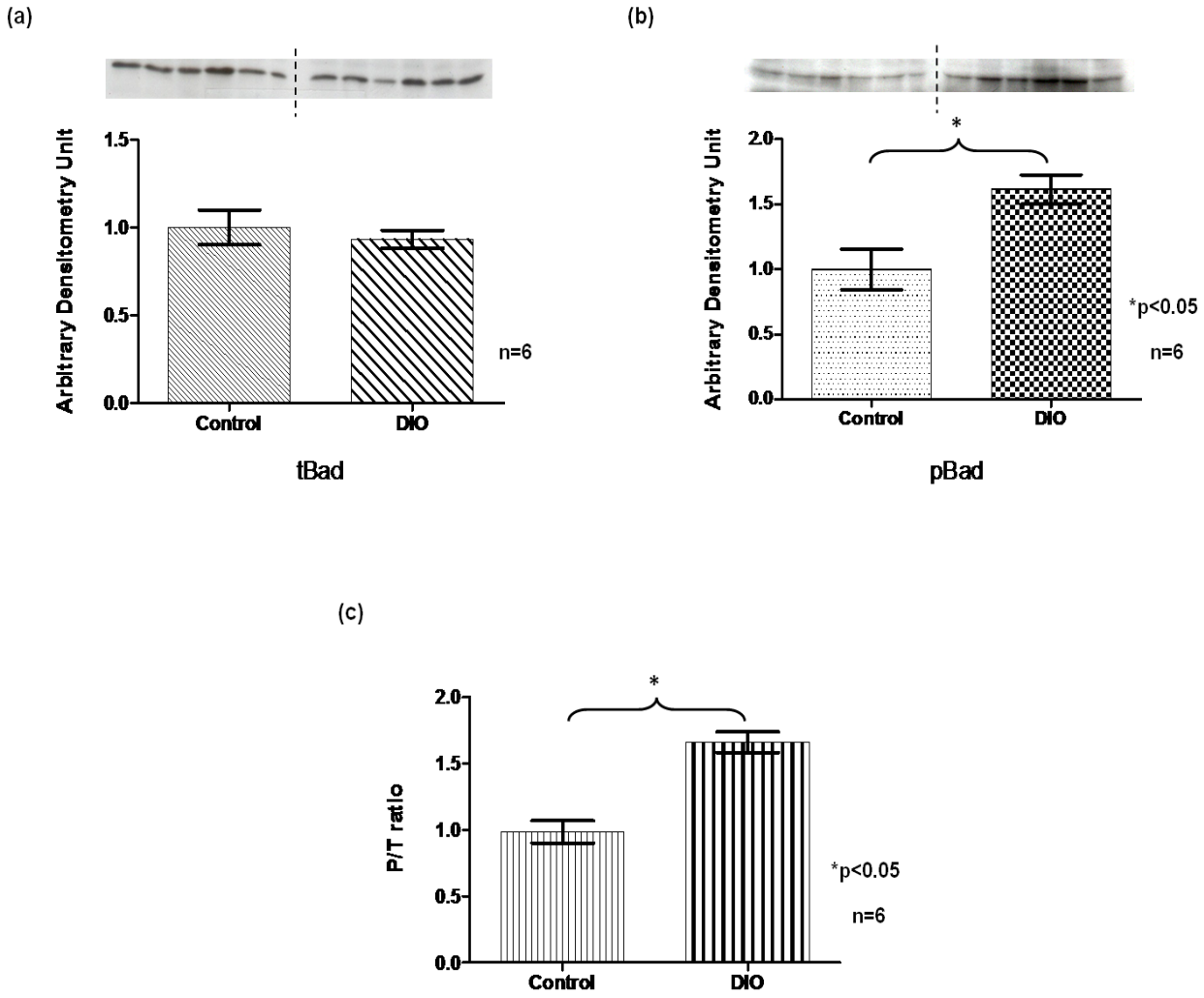

Figure 4.7: The myocardial tBad (a) and pBad (b) levels as well as the P/T ratio (c) in control versus DIO animals (n=6 per group), following 8 weeks of their respective diets.

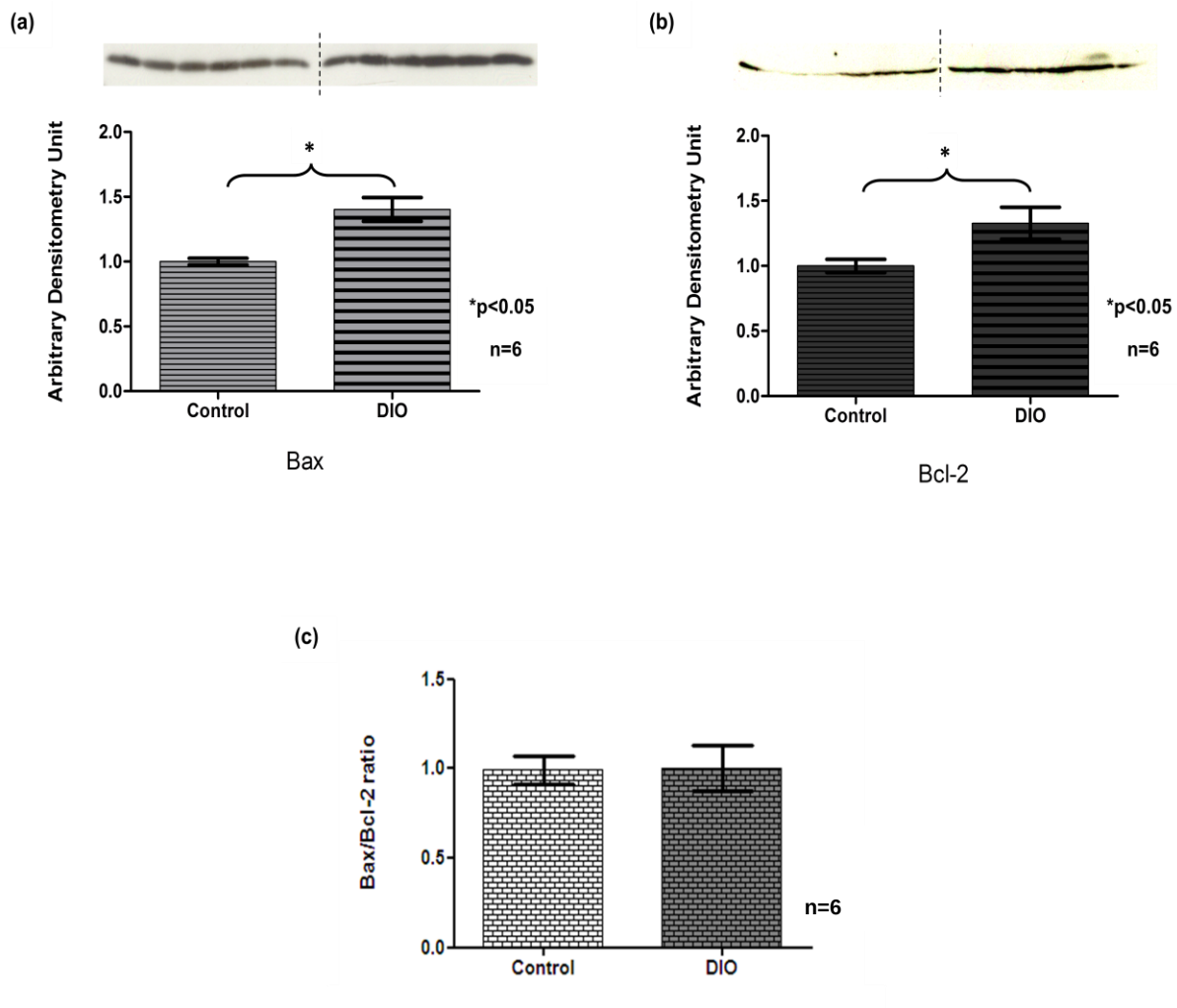

Figure 4.8: The myocardial Bax (a) and Bcl-2 (b) levels as well as the Bax/Bcl-2 ratio (c) in control versus DIO animals (n=6 per group), following 8 weeks of their respective diets.

4.4 Effects of 8 weeks high caloric diet on cardiac mitochondrial integrity

4.4.1 Western blot data (myocardial mitochondrial ETC complex analysis)

4.4.1.1 NADH-ubiquinone oxidoreductase ASHI (NADH ASHI) subunit (of the ETC Complex I)

The DIO group showed no significant difference in their level of NADH ASHI subunit when compared to the control group, subsequent to 8 weeks of their respective diets (figure 4.9 (a)).

4.4.1.2 Succinate dehydrogenase [ubiquinone] iron-sulfur (SDH) subunit (of the ETC Complex II)

No significant difference was found in the level of SDH subunit, in the DIO group when compared to the control group, following 8 weeks of their respective diets (figure 4.9 (b)).

4.4.1.3 Core protein 2 (UQCR2/QCR2) subunit (of the ETC Complex III)

No significant difference was found in the level of Core protein-2 subunit, in the DIO group when compared to the control group, following 8 weeks of their respective diets (figure 4.9 (c)).

4.4.1.4 Subunit I (of the ETC Complex IV)

No protein bands were revealed upon exposure.

4.4.1.5 α-subunit (of the ETC Complex V/ATP synthase)

No significant difference was found in the level of α-subunit, in the DIO group when compared to the control group, following 8 weeks of their respective diets (figure 4.9 (d)).

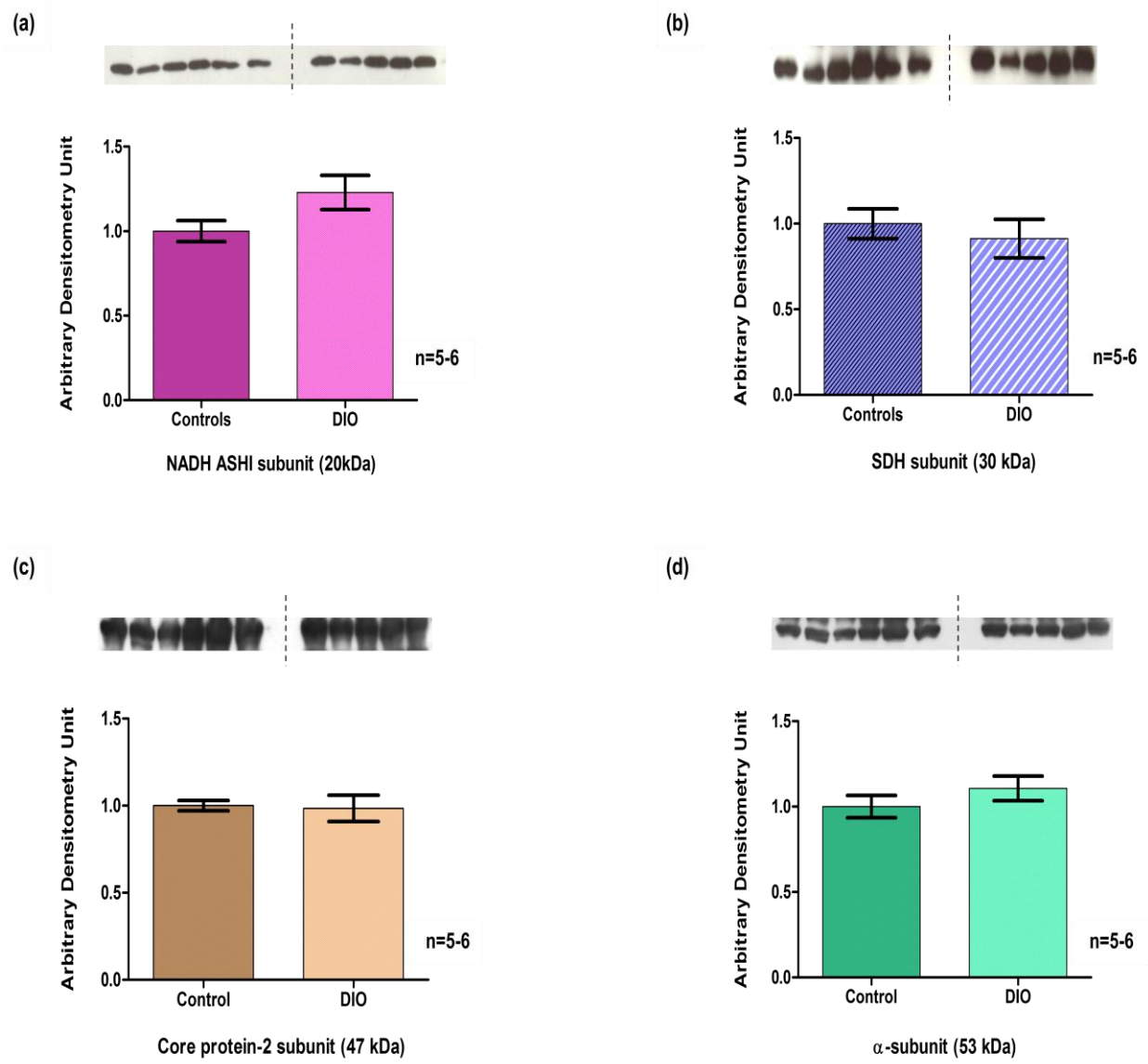

Figure 4.9: The mitochondrial complex NADH ASHI (a), SDH (b), (c) Core protein-2 and (d) α- subunit levels in control (n=5 per group) versus DIO animals (n=6 per group), following 8 weeks of their respective diets.

4.5 Effects of 20 weeks high caloric diet on myocardial protein signalling

4.5.1 Western blot data (Cytosolic PI3K/PKB/Akt and apoptotic signalling analysis)

4.5.1.1 p85 subunit of phosphatidylinositol-3 kinase (p85 PI3K)

The myocardial tp85 subunit level was not significantly different between the DIO and control group, subsequent to following their respective diets for 20 weeks (figure 4.10 (a)).

The level of pp85 subunit as well as the P/T ratio was significantly lower in the DIO animals when assessed against their controls, as seen in figure 4.10 (b) and (c) respectively.

4.5.1.2 Protein kinase B (PKB)

Subsequent to 20 weeks of their respective diets, the DIO animals presented with significantly lower levels of myocardial tPKB/Akt as well as pPKB/Akt, when compared to their control animals (figure 4.11 (a) and (b), respectively). However, no significant difference was found between the DIO and control groups with respect to their P/T ratios, as seen in figure 4.11 (c).

4.5.1.3 Glycogen synthase kinase-3 α/β (GSK-3 α/β)

In comparison to the control group, the DIO group showed no significant difference in their tGSK-3 α/β protein level subsequent to following their respective diets for 20 weeks, as seen in figure 4.12 (a).

The pGSK-3 α/β level and P/T ratio was significantly lower in the DIO group, when matched against their controls. Figure 4.12 (b) and (c) respectively.

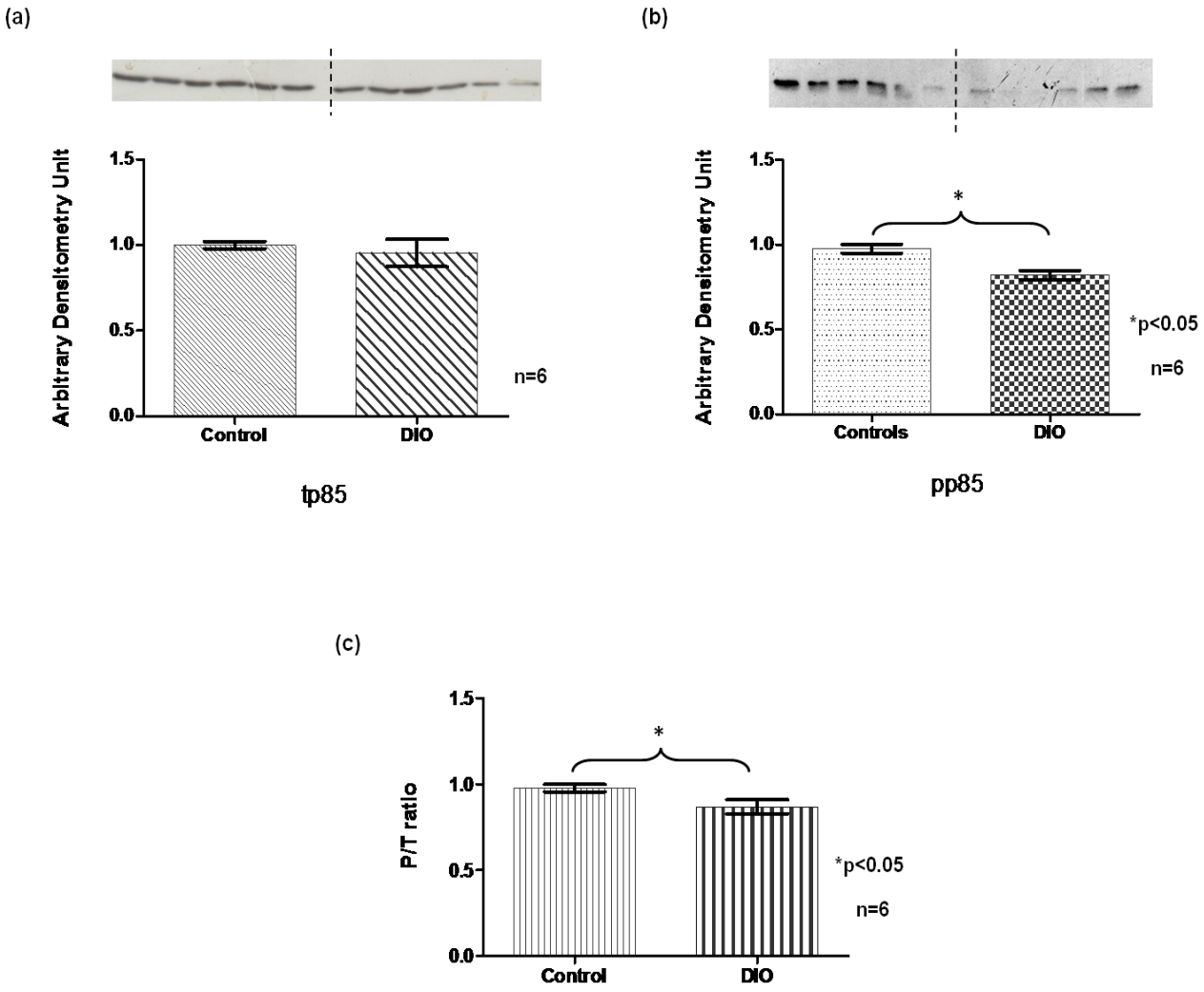

Figure 4.10: The myocardial tp85 (a) and pp85 (b) levels as well as the P/T ratio (c) in control versus DIO animals (n=6 per group), following 20 weeks of their respective diets.

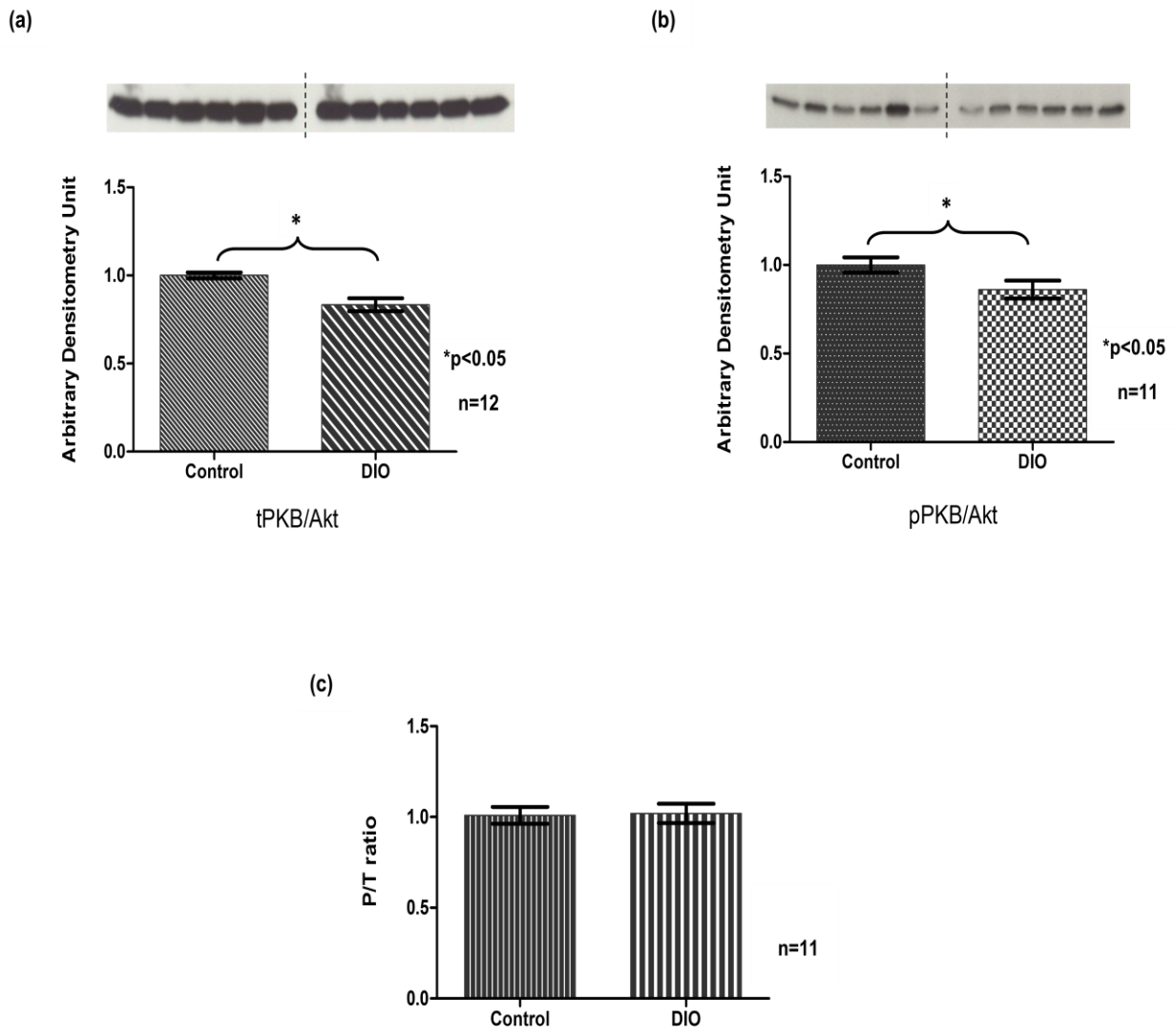

Figure 4.11: The myocardial tPKB/Akt (n=12 per group) (a) and pPKB/Akt (b) levels as well as the P/T ratio (n=11 per group) (c) in control versus DIO animals, following 20 weeks of their respective diets.

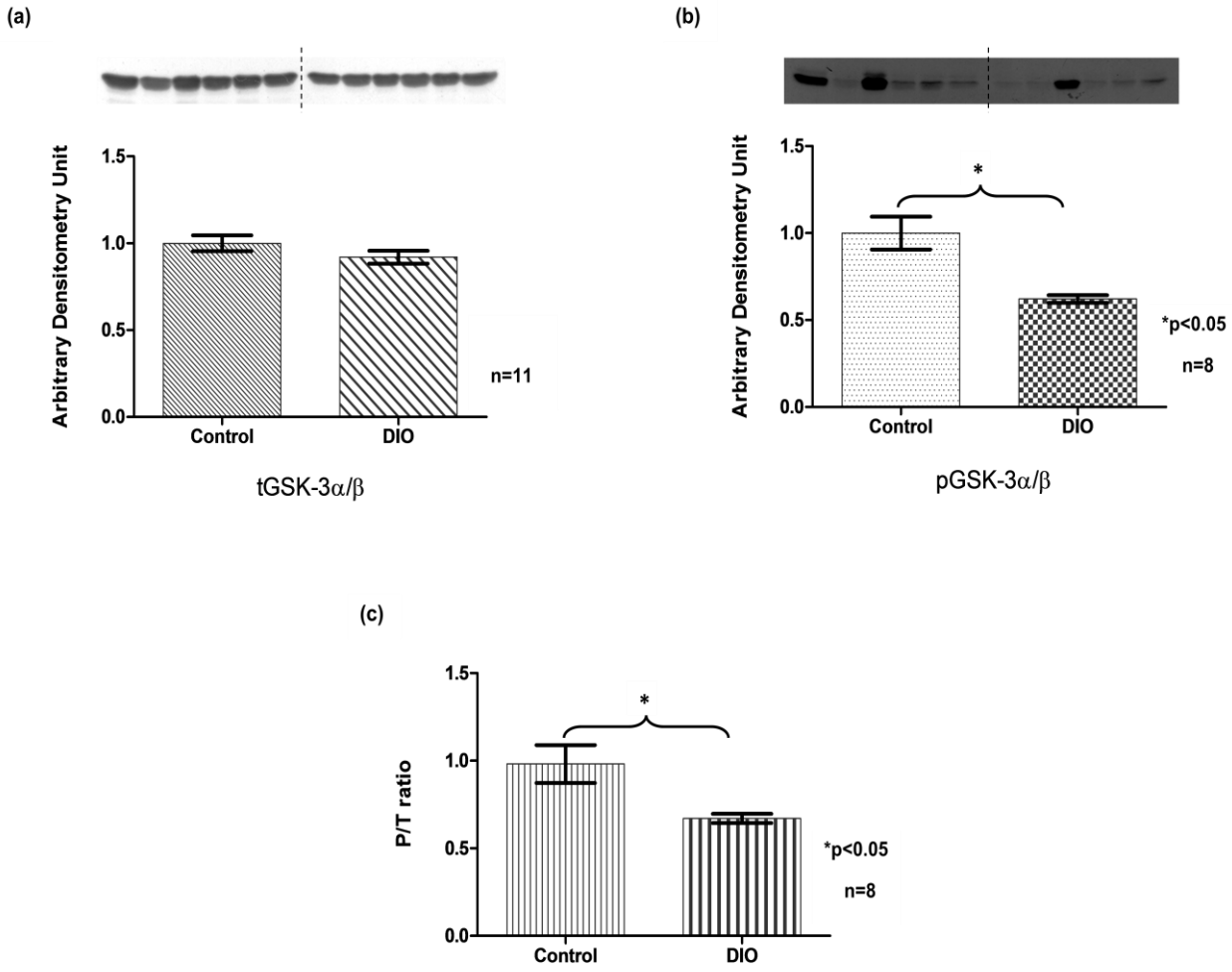

Figure 4.12: The myocardial tGSK-3 α/β (n=11 per group) (a) and pGSK-3 α/β (b) levels as well as the P/T ratio (n=8 per group) (c) in control versus DIO animals, after following their respective diets for a 20 week period.

4.5.1.4 Bcl-2-associated death promoter (Bad) protein

The tBad protein level was significantly elevated in the DIO animals, in comparison to the control animals, following 20 weeks of their respective diets (figure 4.13 (a)).

There was no significant difference between the control and DIO animals in terms of their myocardial pBad protein level (figure 4.13 (b)), while the P/T ratio was significantly decreased in the DIO animals (figure 4.13 (c)).

4.5.1.5. Bcl-2-associated X (Bax) and B-cell lymphoma/leukemia2 (Bcl-2) protein

The Bax as well as the Bcl-2 protein level was not significantly different between the DIO and control groups following 20 weeks of their respective diets, as seen in figure 4.14 (a) and (b) respectively.

4.5.1.6 Bax/Bcl-2 protein ratio

There was no significant difference between the control and DIO animals in terms of their Bax/Bcl-2 protein ratio, after 20 weeks of their respective diets (figure 4.14 (c)).

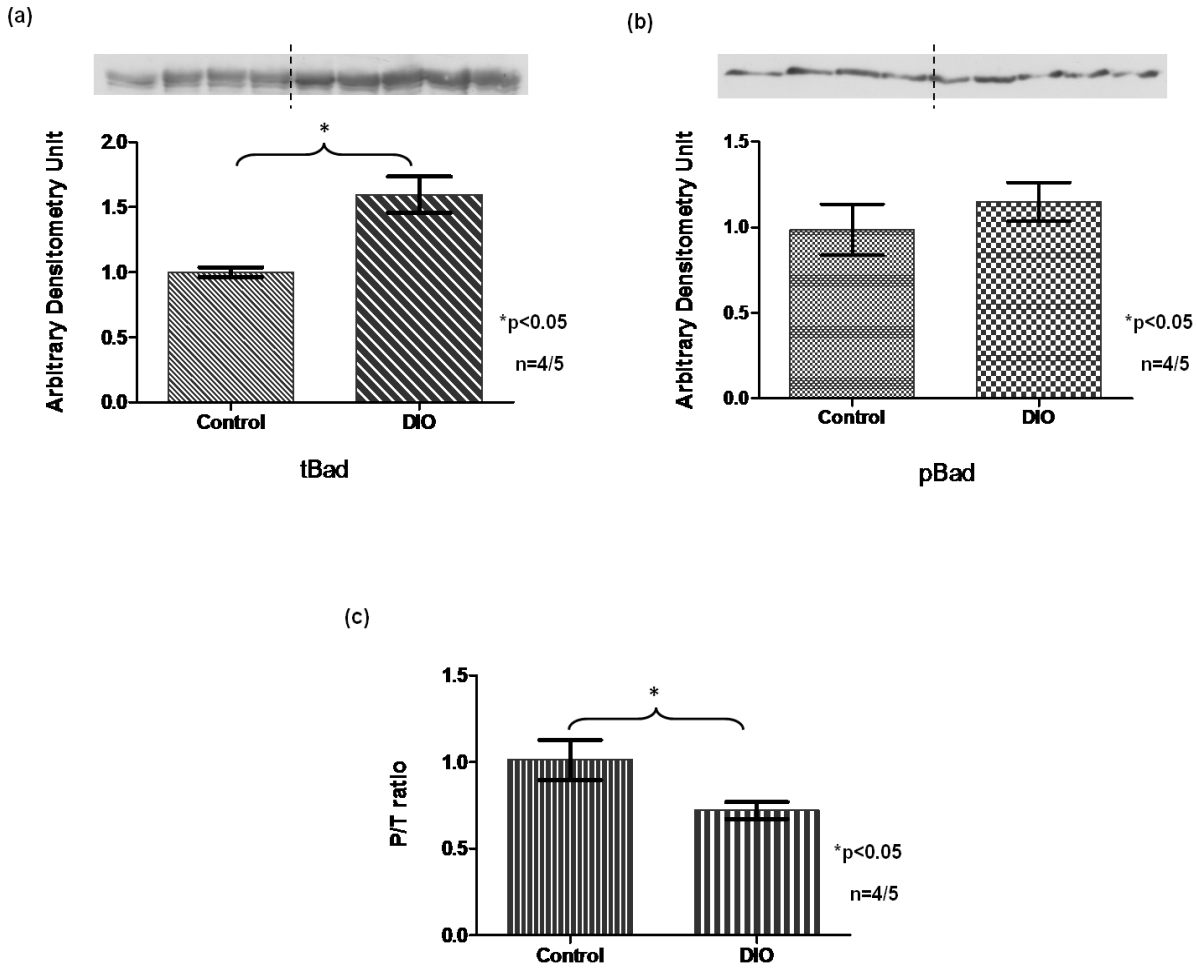

Figure 4.13: The myocardial tBad (a) and pBad (b) levels as well as the P/T ratio (c) in control (n=4 per group) versus DIO animals (n=5 per group), after following their respective diets for a 20 week period.

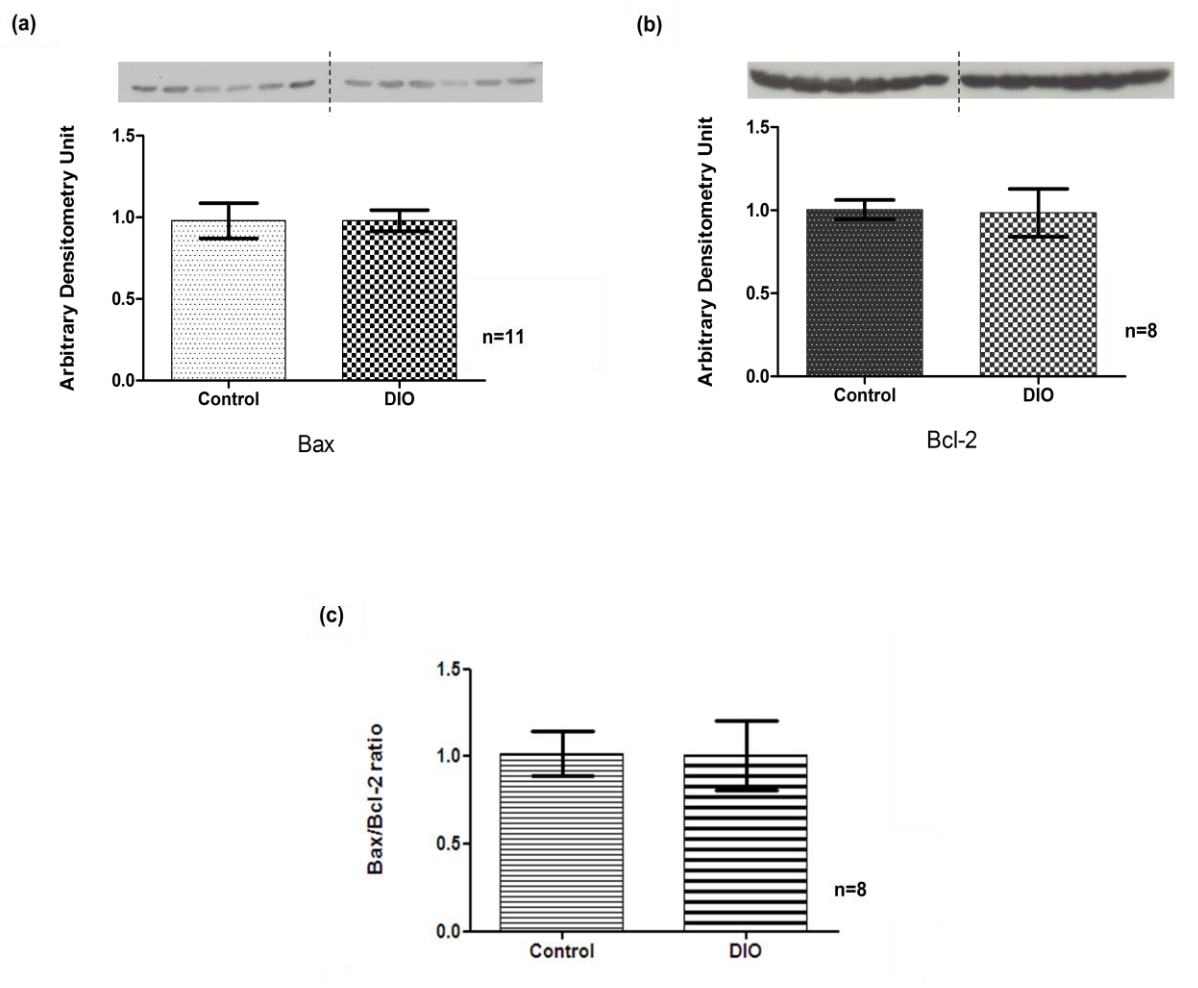

Figure 4.14: The myocardial Bax (n=11 per group) (a) and Bcl-2 (b) levels as well as the Bax/Bcl-2 ratio (n=8 per group) (c) in control versus DIO animals, after following their respective diets for a 20 week period.

4.6 Effects of 20 weeks high caloric diet on cardiac mitochondrial integrity

4.6.1 Western Blot data (Myocardial mitochondrial ETC complex analysis)

4.6.1.1 NADH-ubiquinone oxidoreductase ASHI (NADH ASHI) subunit (of ETC Complex I)

The NADH ASHI subunit level was significantly lower in the DIO animals than in the control animals subsequent to 20 weeks of their respective diets, as depicted in figure 4.15 (a).

4.6.1.2 Succinate dehydrogenase [ubiquinone] iron-sulfur (SDH) subunit

The DIO animals had a significantly lower level of the SDH subunit, when compared to the control animals, after having followed their respective diets for a period of 20 weeks (figure 4.15 (b)).

4.6.1.3 Core protein-2 (UQCR2/QCR2) subunit (of the ETC Complex III)

The DIO animals had a significantly higher level of the Core protein 2 subunit, when compared to the control animals, after having followed their respective diets for a period of 20 weeks (figure 4.15 (c)).

4.6.1.4 Subunit I (of the ETC Complex IV)

No protein bands were revealed upon exposure.

4.6.1.5 α-subunit (of the ETC Complex V/ATP synthase)

A significantly higher level of the α-subunit was found in the DIO animals, in comparison to the control animals, after having followed their respective diets for a period of 20 weeks (figure 4.15 (d)).

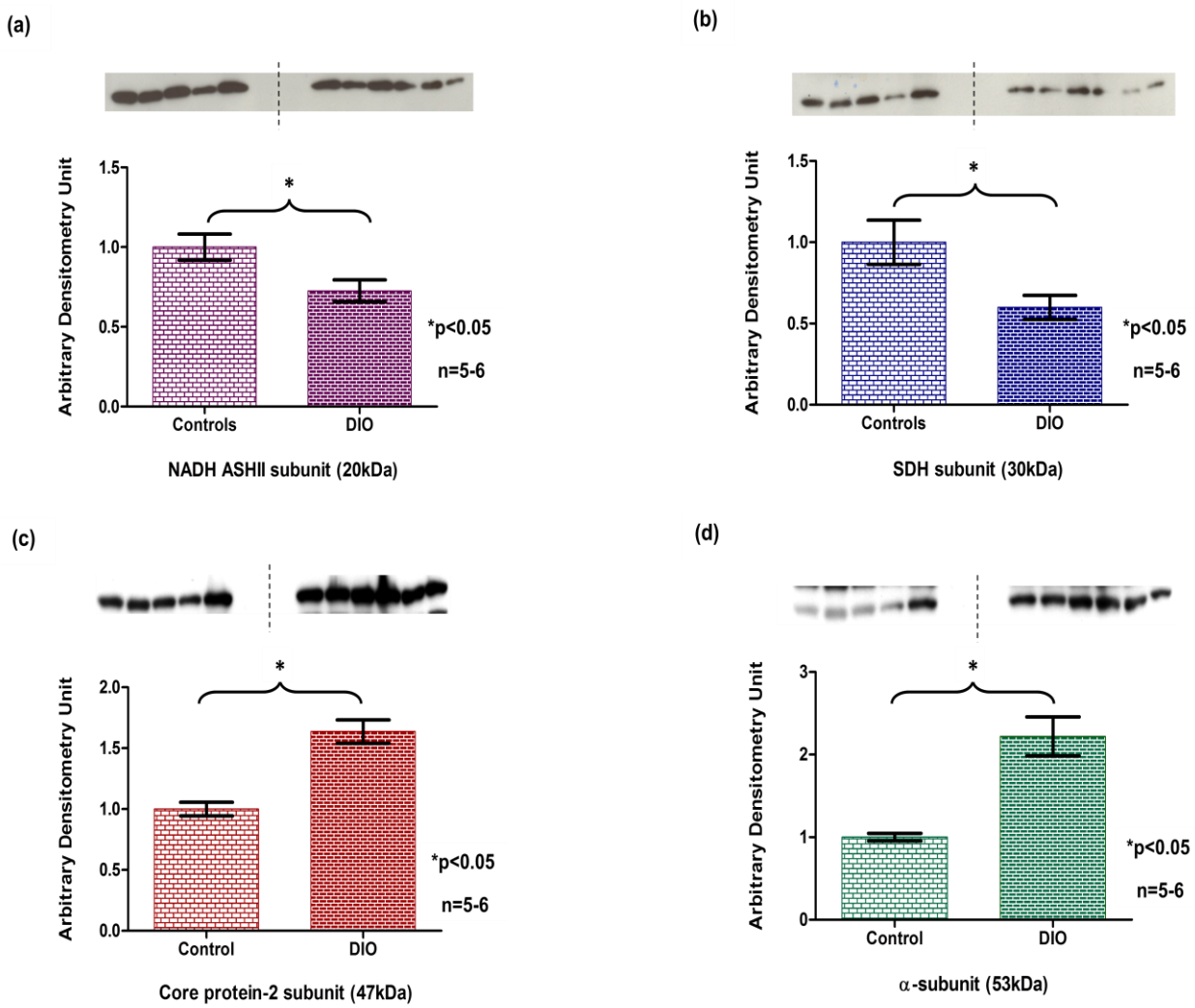

Figure 4.15: The mitochondrial complex NADH ASHI (a), SDH (b), Core protein-2 (c) and α- (d) subunit levels in control (n=5 per group) versus DIO animals (n=6 per group), following 20 weeks of their respective diets.

4.7 Effects of 20 weeks high caloric diet on cardiac mitochondrial function

4.7.1 Cardiac mitochondrial function and anoxia/reperfusion data

Table 4.2 The ADP/O ratio, State 3, State 4, oxidative phosphorylation (OXPHOS) rate, RCI as well as the percentage recovery of the control and DIO groups, using glutamate as a substrate, following 20 weeks of their respective diets.

	ADP/O ratio	State 3 (QO2(3)) natoms O_2/mg prot/min	State 4 (QO2(4)) natoms O_2/mg prot/min
Control	2.77 ± 0.24	434.50 ± 50.56	89.09 ± 25.05
DIO	2.16 ± 0.14	605.30 ± 54.73	161.20 ± 46.61
p-value	0.039*	0.041*	0.203
n-value	6	7	6
	OXPHOS rate QO2 (3) * ADP/O	**RCI** $QO_2(3)$ / $QO_2(4)$	**% State 3 Recovery** (%)
Control	1051 ± 162.60	6.14 ± 1.15	28.27 ± 7.53
DIO	1303 ± 141.40	2.62 ± 0.39	26.98 ± 6.77
p-value	0.271	0.043*	0.901
n-value	6	5	7

* denotes a statistically significant difference of p<0.05.

Table 4.3 The ADP/O ratio, State 3, State 4, oxidative phosphorylation (OXPHOS) rate, RCI as well as the percentage recovery of the control and DIO groups, using palmitoyl-L-carnitine as a substrate, following 20 weeks of their respective diets.

	ADP/O ratio	State 3 (QO2(3)) natoms O_2/mg prot/min	State 4 (QO2(4)) natoms O_2/mg prot/min
Control	2.73 ± 0.24	118.1 ± 7.62	104.00 ± 19.75
DIO	1.88 ± 0.24	217.2 ± 44.43	131.20 ± 10.77
p-value	0.030*	0.059	0.254
n-value	6	5	6
	OXPHOS rate QO2 (3) * ADP/O	**RCI** $QO_2(3)$ / $QO_2(4)$	**% State 3 Recovery** (%)
Control	369.30 ± 60.43	1.98 ± 0.65	20.09 ± 7.84
DIO	332.20 ± 69.68	2.17 ± 0.66	79.04 ± 20.04
p-value	0.696	0.838	0.021*
n-value	6	6	6

* denotes a statistically significant difference of p<0.05.

After following a high caloric diet for a period of 20 weeks, the DIO group showed no significant differences, in comparison to the control group, in terms of the mitochondrial State 4, OXPHOS rate and percentage recovery when glutamate was used as a substrate. However, a significant difference was observed in the DIO animals when the ADP/O ratio, State 3 and RCI were analysed (table 4.2).

When palmitoyl-L-carnitine was used as a substrate, the DIO group displayed significant differences in their ADP/O ratio and percentage recovery, while analyses of their State 3 and 4, RCI and OXPHOS rate yielded no significant differences (table 4.3).

4.7.2 Cardiac mitochondrial complex inhibition data

Table 4.4 The State 3 respiration, in control versus DIO animals following 20 weeks of their respective diets, subsequent to the addition of succinate or the mitochondrial complex inhibitors rotenone, oligomycin and CCCP, using glutamate as a substrate.

	Succinate	Rotenone	Oligomycin	CCCP
Control	**157.60 ± 22.61**	**36.08 ± 4.60**	**30.44 ± 3.17**	**5.40 ± 1.38**
DIO	**163.20 ± 16.19**	**49.70 ± 5.87**	**39.80 ± 4.98**	**9.09 ± 0.59**
p-value	**0.848**	**0.098**	**0.131**	**0.041***
n-value	**6**	**6**	**6**	**6**

*** p<0.05 denotes a statistically significant difference**

Table 4.5 The State 3 respiration, in control versus DIO animals following 20 weeks of their respective diets, subsequent to the addition of succinate or the mitochondrial complex inhibitors rotenone, oligomycin and CCCP, using palmitoyl-L-carnitine as a substrate.

	Succinate	Rotenone	Oligomycin	CCCP
Control	**53.52 ± 7.32**	**33.99 ± 3.41**	**34.99 ± 1.61**	**5.341 ± 0.39**
DIO	**71.50 ± 22.38**	**38.39 ± 7.68**	**28.75 ± 6.34**	**8.697 ± 2.68**
p-value	**0.432**	**0.593**	**0.327**	**0.206**
n-value	**6**	**6**	**6**	**6**

When glutamate was used as a substrate, the DIO group, when compared to the controls, showed no significant difference in terms of their state 3 respiration following the addition of succinate, rotenone and oligomycin. However, the DIO did display a significant difference in the state 3 respiration after the addition of CCCP (refer to table 4.4).

The DIO group showed no significant difference in their state 3 respiration when any of the above mentioned mitochondrial complex inhibitors were utilised and palmitoyl-L-carnitine was used as a substrate, as depicted in table 4.5.

4.7.3 Cardiac mitochondrial citrate synthase activity data

There was a significantly decreased level of citrate synthase activity in the DIO animals, in comparison to the control animals, after following their respective diets for 20 weeks. Refer to figure 4.16.

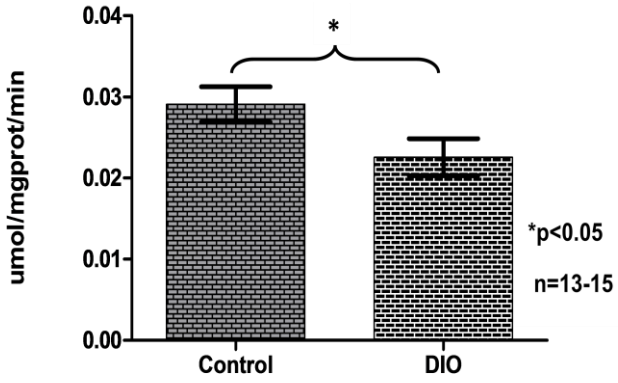

Figure 4.16: The citrate synthase activity level (µmol/mg mitochondrial protein/minute) in control (n=13 per group) versus DIO animals (n=11 per group), subsequent to 20 weeks of diet.

4.7.3 High pressure liquid chromatography (HPLC) analysis data

4.7.3.1 ATP produced

The amount of ATP produced was not significantly different between the DIO and control animals, following 20 weeks of their respective diets, when either glutamate or palimotyl-L-carnitine was used as a substrate as seen in figure 4.17 (a) and (b), respectively.

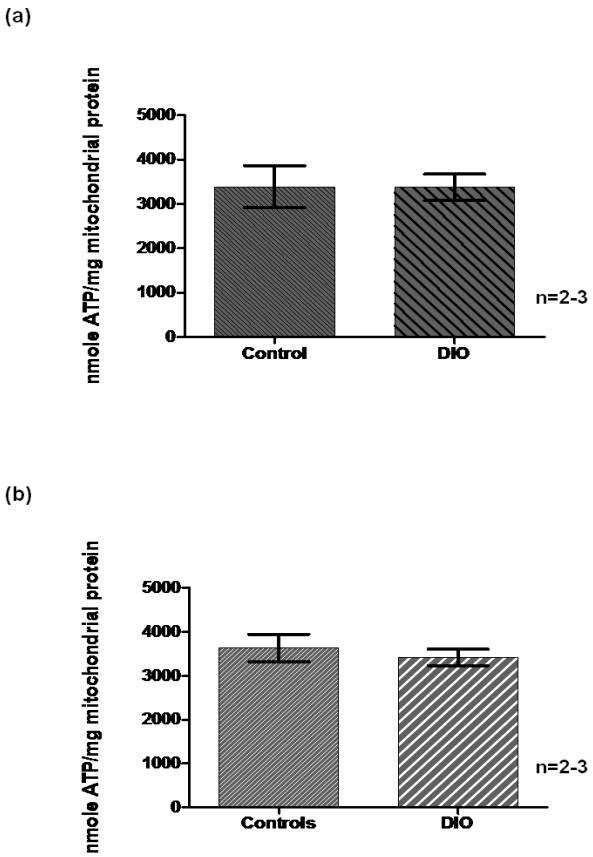

Figure 4.17: The amount of ATP produced in control (n=2 per group) versus DIO animals (n=3 per group), subsequent to a 20 week period of their respective diets, using glutamate (a) and palmitoyl-L-carnitine (b) as a substrate.

4.7.3.2 ATP/O ratio

The ATP/O was significantly decreased in the DIO in comparison to the control animals, following 20 weeks of their respective diets, when glutamate as well as palimotyl-L-carnitine was used as a substrate as seen in figure 4.18 (a) and (b), respectively.

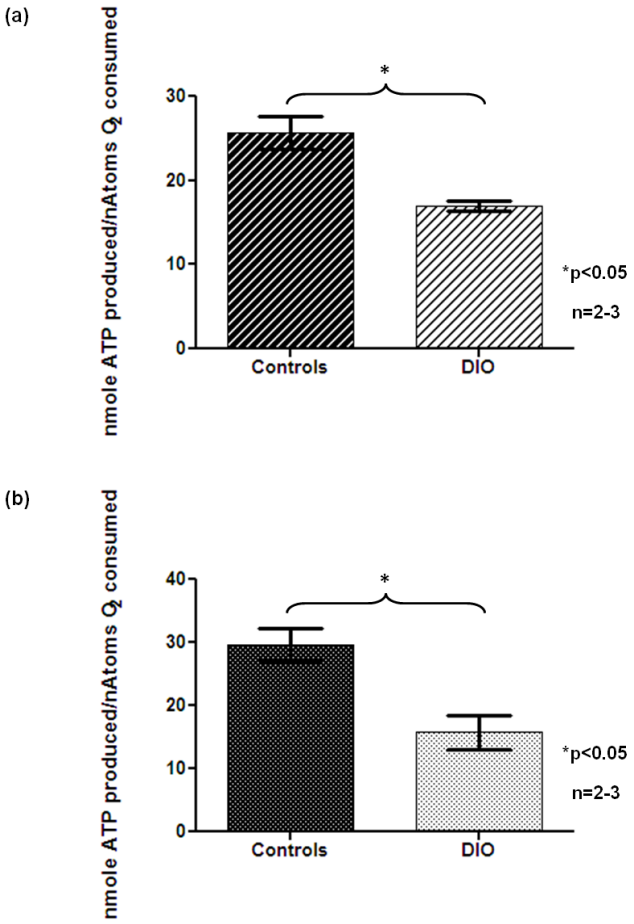

Figure 4.18: The ATP/O ratio in control (n=2 per group) versus DIO animals (n=3 per group), subsequent to a 20 week period of their respective diets, using glutamate (a) and palmitoyl-L-carnitine (b) as a substrate.

4.8 Effects of 20 weeks high caloric diet on cardiac mitochondrial protein signalling

4.8.1 Western blot data (Mitochondrial PI3K/PKB/Akt and apoptotic signalling analysis)

4.8.1.1 p85 subunit of phosphatidylinositol-3 kinase (p85 PI3K)

Control: There were no significant differences between the untreated, insulin treated and ischemia subjected control groups in terms of the tp85 protein subunit levels found at the mitochondria isolated from the hearts of these groups (figure 4.19 (a)). The pp85 level and the P/T ratio were significantly higher in the cardiac mitochondria for both the insulin and ischemia groups, in comparison to the untreated controls. However, no significant difference was found between the insulin and ischemia groups in terms of pp85 level and P/T ratio. Refer to figure 4.19 (b) and (c), respectively.

DIO: The tp85 (a) and pp85 levels (b) were significantly higher in the insulin and the ischemia groups when compared to the untreated group (figure 4.20). Additionally, the pp85 subunit level was significantly higher in the ischemia group in comparison to the insulin group (figure 4.20 (b)).

In comparison to the untreated DIOs, the P/T ratio was significantly higher in the ischemia group but not the insulin group. Furthermore, the P/T ratio was significantly elevated in the ischemia DIO group in comparison to the insulin DIO group. Refer to figure 4.20 (c).

Control versus DIO: When the DIOs were compared to the controls, the pp85 level (b) and the P/T ratio (c) was significantly elevated in the untreated, insulin and ischemia DIO

groups (figure 4.21). There was no significant difference between these groups in terms of tp85 subunit level at their cardiac mitochondria (figure 4.21 (a)).

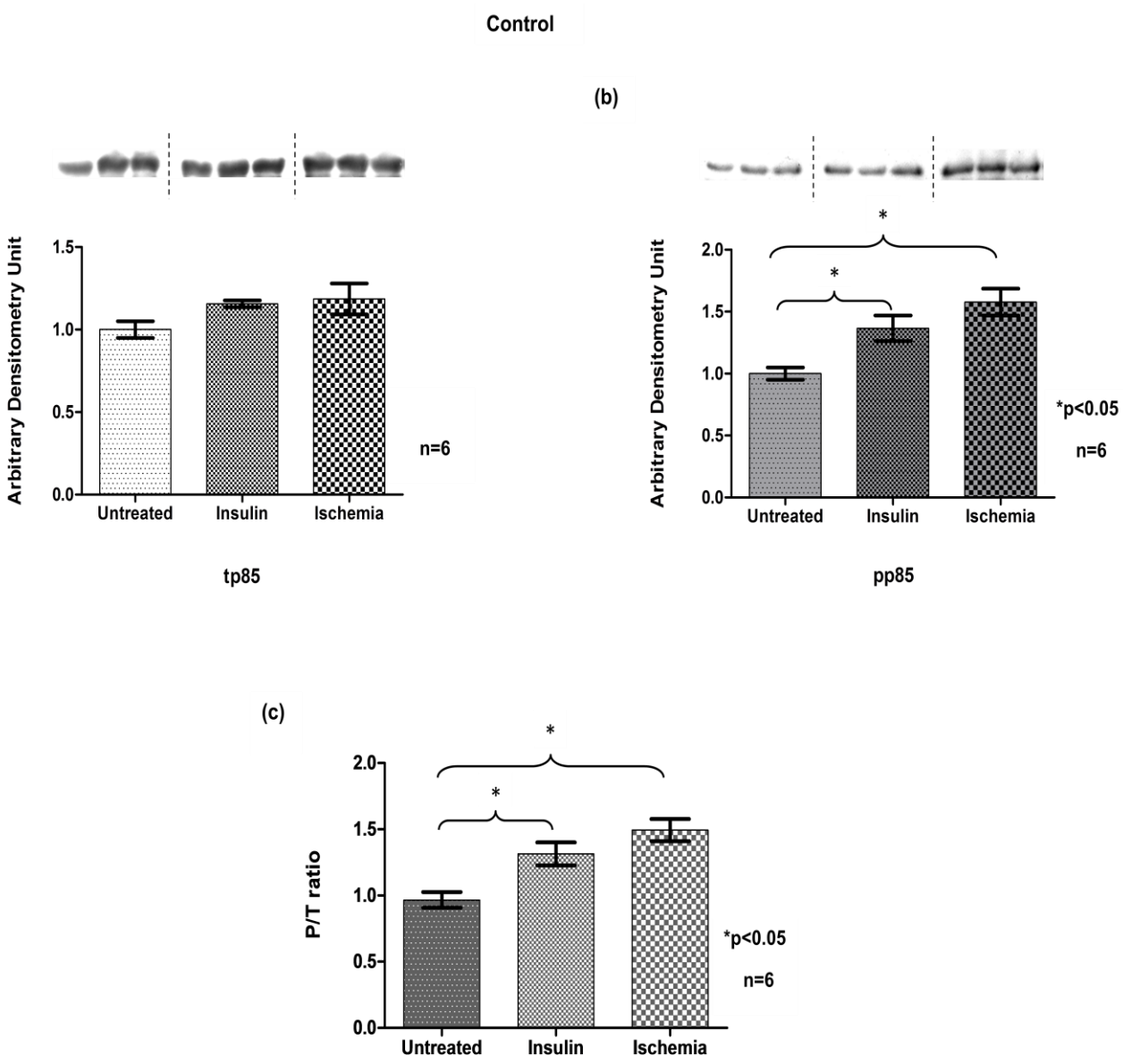

Figure 4.19: The mitochondrial tp85 (a) and pp85 (b) levels as well as the P/T ratio (c) in untreated versus insulin versus ischemia control animals (n=6 per group), following 20 weeks of their respective diets.

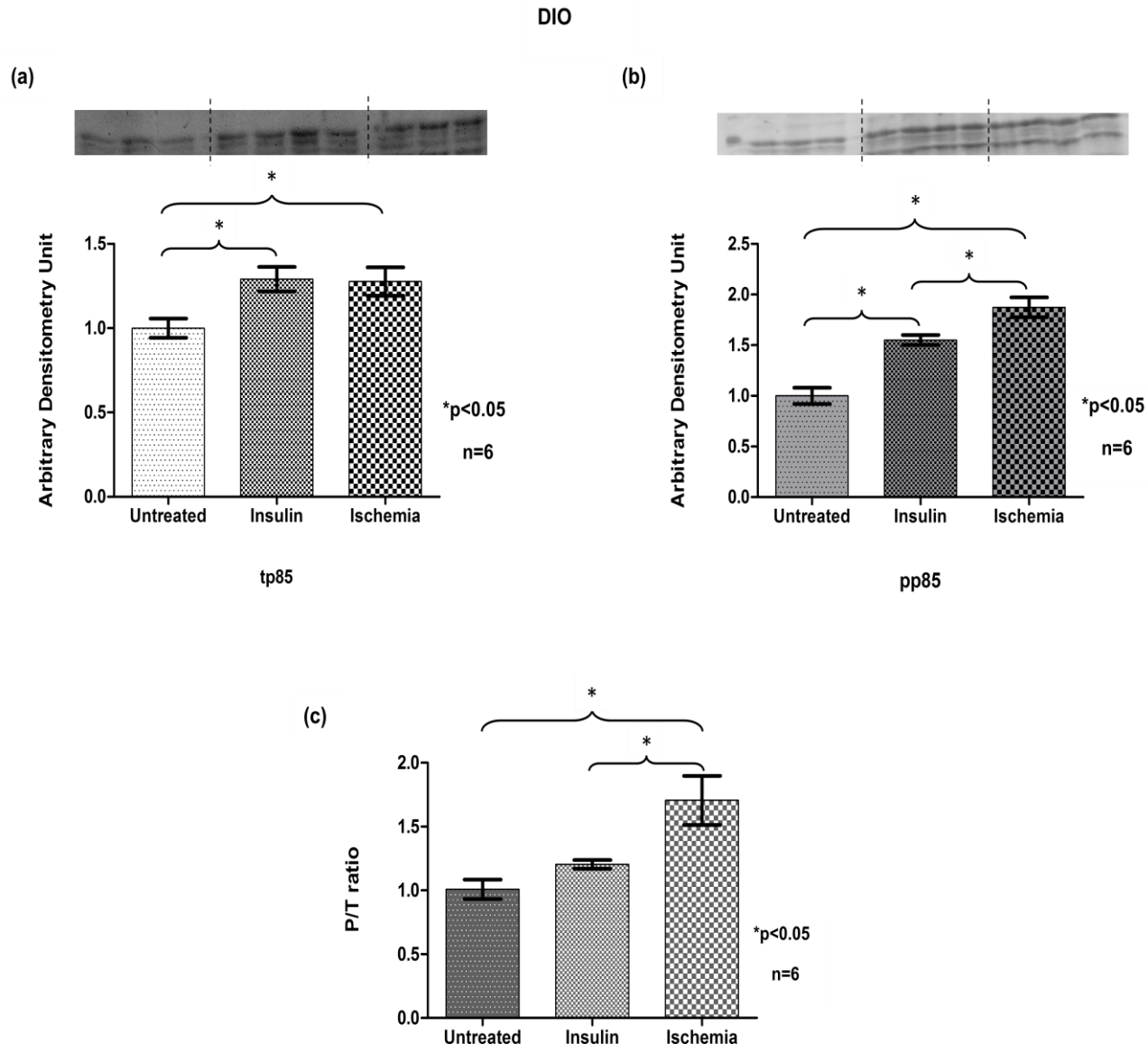

Figure 4.20: The mitochondrial tp85 (a) and pp85 (b) levels as well as the P/T ratio (c) in untreated versus insulin versus ischemia DIO animals (n=6 per group), following 20 weeks of their respective diets.

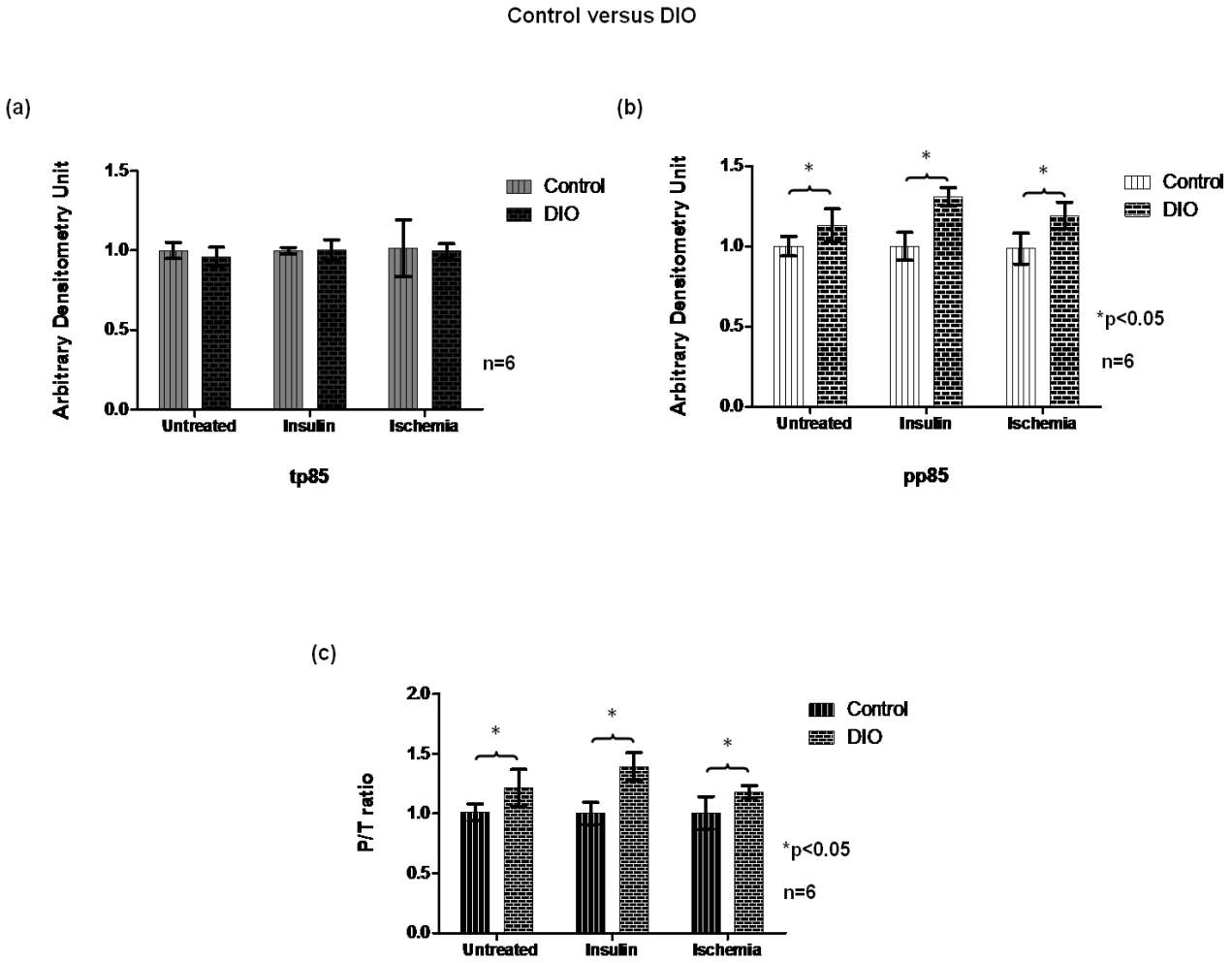

Figure 4.21: The mitochondrial tp85 (a) and pp85 (b) levels as well as the P/T ratio (c) in untreated, insulin and ischemia control versus DIO animals (n=6 per group), following 20 weeks of their respective diets.

4.8.1.2 Protein kinase B (PKB)

Control: The mitochondrial tPKB/Akt subunit level was significantly higher in the insulin group, in comparison to the untreated group, as well the ischemia group when compared to the insulin group. No significant difference was found between the untreated and ischemia groups. Refer to figure 4.22 (a).

The insulin and ischemia groups were significantly higher than the untreated group when the mitochondrial pPKB/Akt level was determined. No significant difference was found when comparing the insulin and ischemia groups with each other. Refer to figure 4.22 (b).

The P/T ratio was significantly higher in the ischemia group when compared to the untreated group, while no significant difference was found between the insulin and untreated group. The P/T ratio was found to be significantly higher in the ischemia group when compared to the insulin group. Refer to figure 4.22 (c).

DIO: No significant differences were found between any of the groups in terms of tPKB/Akt subunit levels. Refer to figure 4.23 (a).

The pPKB/Akt level (a) as well as the P/T ratio (b) were significantly lower in the ischemia group in comparison to the untreated group. Furthermore, the pPKB/Akt level (a) and the P/T ratio (b) were significantly lower in the ischemia group when compared to the insulin group. Refer to figures 4.23 (b) and (c).

Control versus DIO: When comparing the tPKB/Akt subunit level between all possible groups, no significant differences were found (a). The pPKB/Akt level (b) and the P/T ratio

(c) were significantly lower in the untreated, insulin and ischemia DIO groups in comparison to their controls. Refer to figure 4.24.

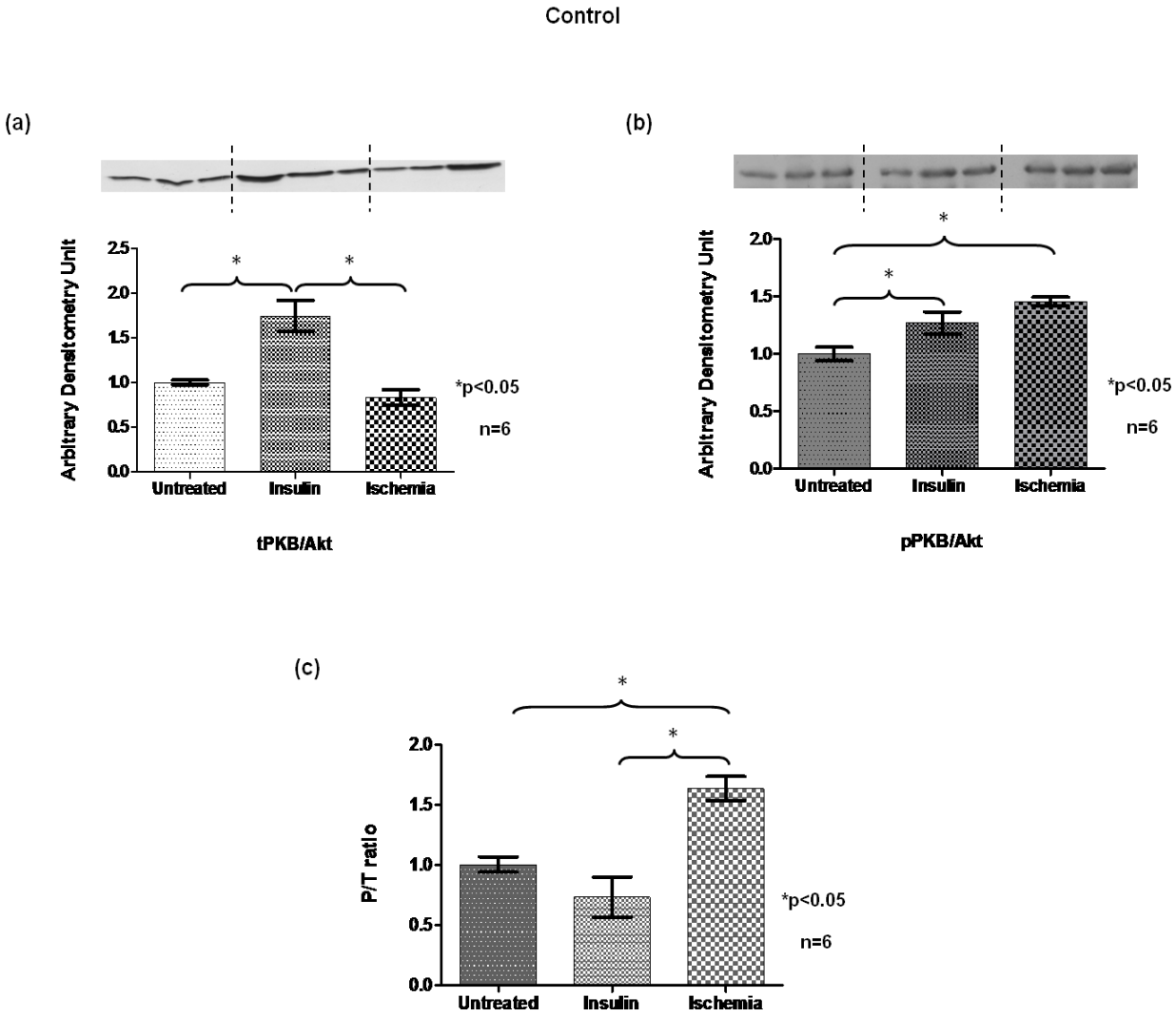

Figure 4.22: The mitochondrial tPKB/Akt (a) and pPKB/Akt (b) levels as well as the P/T ratio (c) in untreated versus insulin versus ischemia control animals (n=6 per group), following 20 weeks of their respective diets.

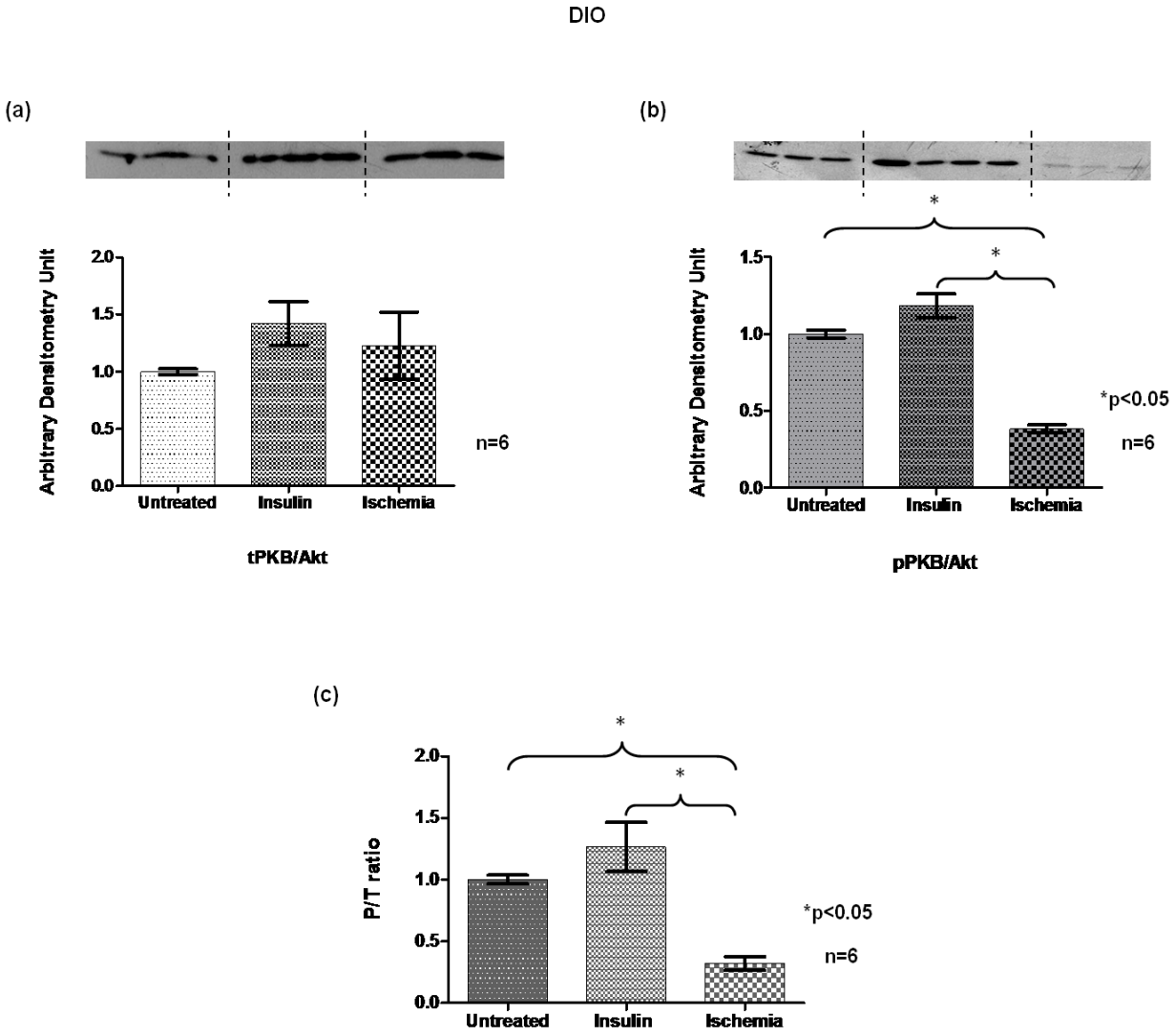

Figure 4.23: The mitochondrial tPKB/Akt (a) and pPKB/Akt (b) levels as well as the P/T ratio (c) in untreated versus insulin versus ischemia DIO animals (n=6 per group), following 20 weeks of their respective diets.

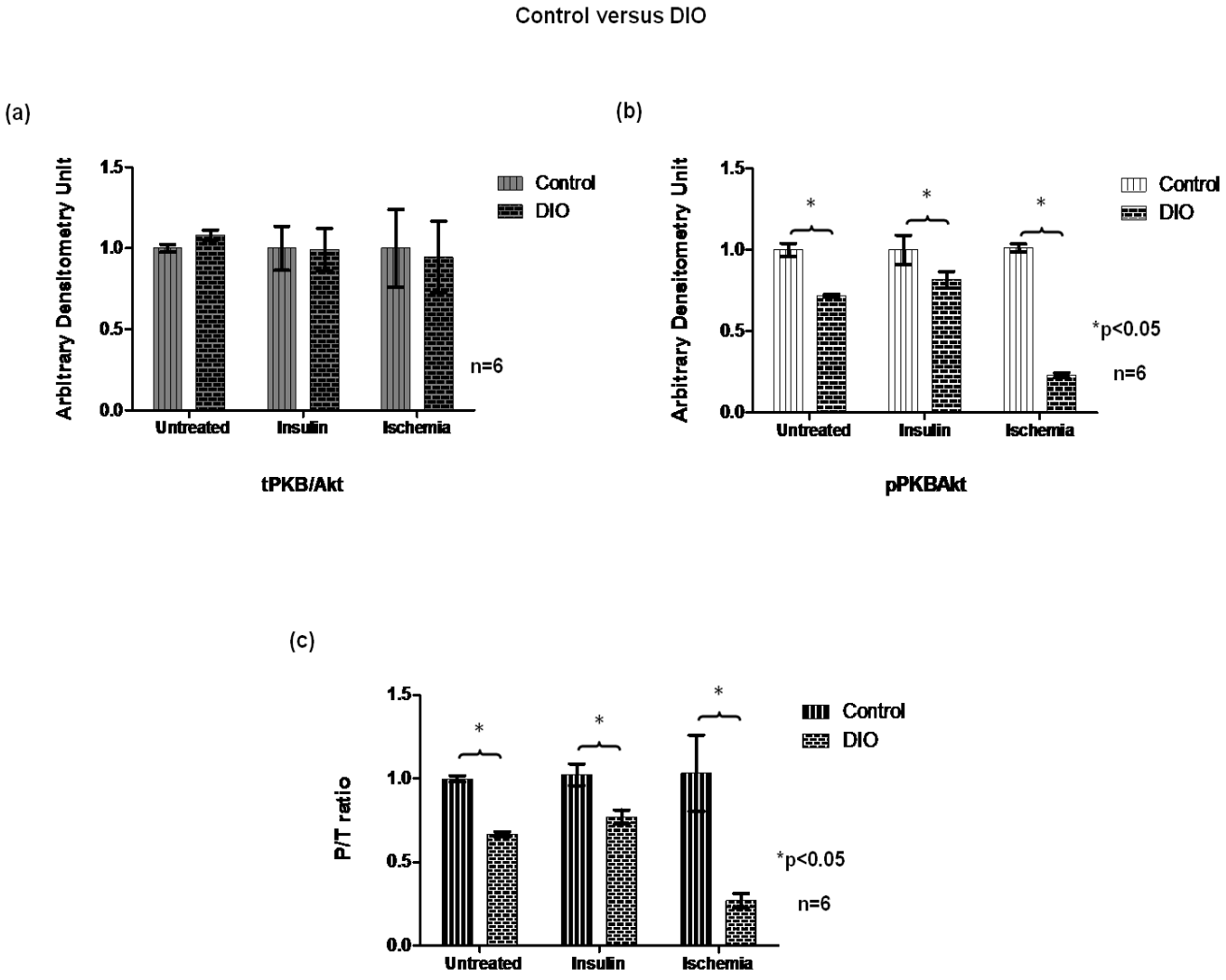

Figure 4.24: The mitochondrial tPKB/Akt (a) and pPKB/Akt (b) levels as well as the P/T ratio (c) in untreated, insulin and ischemia control versus DIO animals (n=6 per group), following 20 weeks of their respective diets.

4.8.1.3 Glycogen synthase kinase-3 α/β (GSK-3 α/β)

Control: The tGSK-3 α/β subunit level was found to be significantly lower in the insulin and ischemia groups when compared to the untreated group. No significant difference was found between the insulin and ischemia groups. Refer to figure 4.25 (a).

The ischemia group had a significantly higher level of pGSK-3 α/β and P/T ratio in comparison to the untreated group (figure 4.25 (b) and (c), respectively). No significant differences were found between the insulin and untreated groups, as well as the insulin and ischemia groups, in terms of the protein level of pGSK-3 α/β (figure 4.25 (b)). The P/T ratio was found to be significantly elevated in the insulin and ischemia groups in comparison to the untreated group, while no significant difference was found between the insulin and ischemia group (figure 4.25 (c)).

DIO: The tGSK-3 α/β protein level was significantly lower in both the insulin and ischemia groups in comparison to the untreated group. No significant difference was found between the insulin and ischemia groups in terms of tGSK-3 α/β protein level. Refer to figure 4.26 (a).

The level of pGSK-3 α/β and the P/T ratio was significantly elevated in both the insulin and ischemia groups when compared to the untreated group. Additionally, the ischemia group had a significantly higher level of pGSK-3 α/β, as well as a significantly elevated P/T ratio, in comparison to the insulin group. Refer to figures 4.26 (b) and (c), respectively.

Control versus DIO: No significant differences were found between any of the groups in terms of the myocardial tGSK-3 α/β protein level at the mitochondria (figure 4.27 (a)). The pGSK-3 α/β protein level as well as the P/T ratio was found to be significantly elevated in

the untreated, insulin and ischemia DIO groups when compared to their controls. Refer to figures 4.27 (b) and (c), respectively.

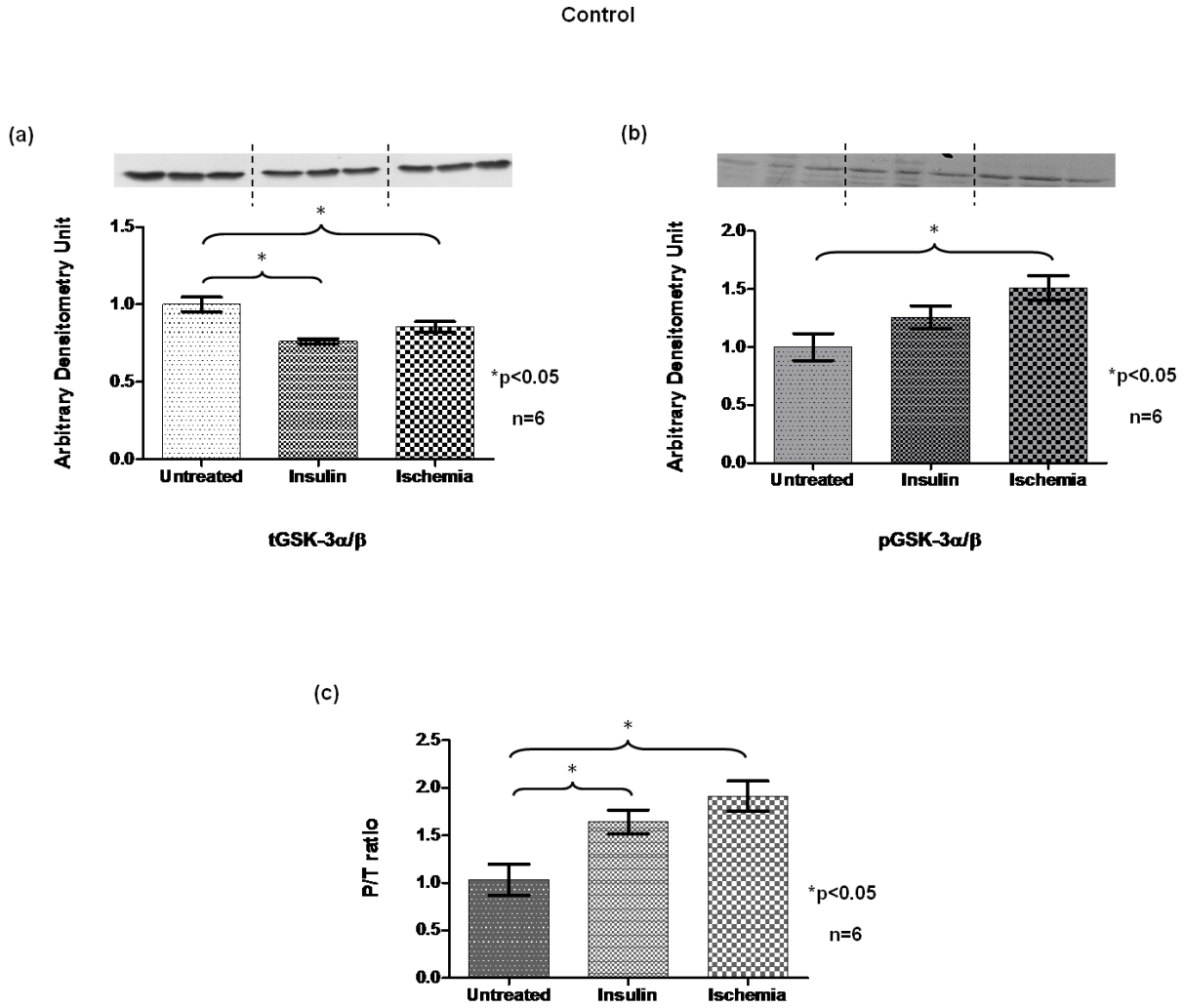

Figure 4.25: The mitochondrial tGSK-3 α/β (a) and pGSK-3 α/β (b) levels as well as the P/T ratio (c) in untreated versus insulin versus ischemia control animals (n=6 per group), following 20 weeks of their respective diets.

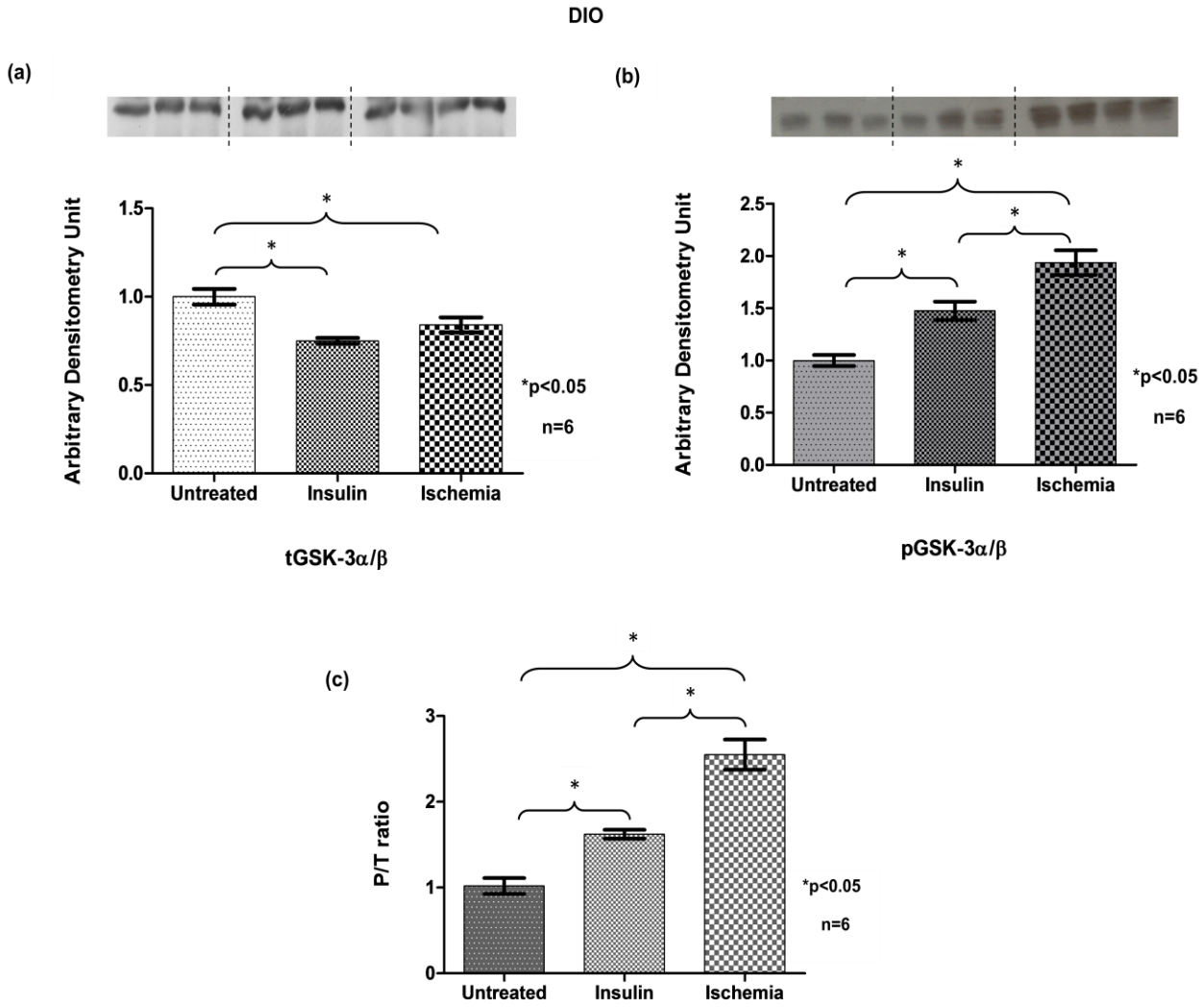

Figure 4.26: The mitochondrial tGSK-3 α/β (a) and pGSK-3 α/β (b) levels as well as the P/T ratio (c) in untreated versus insulin versus ischemia DIO animals (n=6 per group), following 20 weeks of their respective diets.

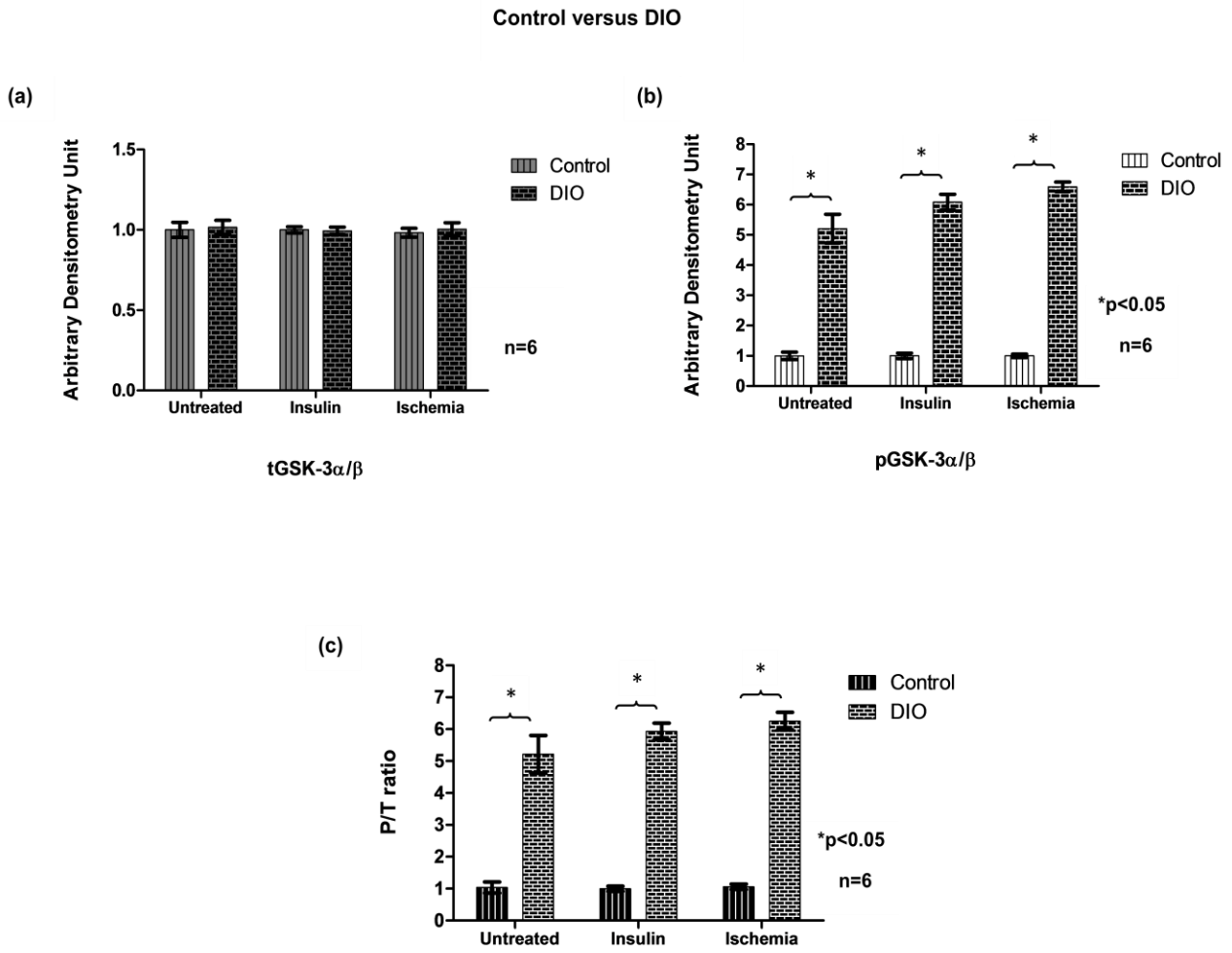

Figure 4.27: The mitochondrial tGSK-3 α/β (a) and pGSK-3 α/β (b) levels as well as the P/T ratio (c) in untreated, insulin and ischemia control versus DIO animals (n=6 per group), following 20 weeks of their respective diets.

4.8.1.4. Bcl-2-associated death promoter (Bad) protein

Control: No significant differences were found amongst any of the groups in terms of myocardial tBad and pBad protein levels, as well as P/T ratio, present at the mitochondria. Refer to figures 4.28 (a), (b) and (c), respectively.

DIO: The tBad and pBad levels were significantly higher in the ischemia group in comparison to the untreated group. In terms of the tBad and pBad levels, no significant differences were found between the untreated and ischemia groups as well as between the insulin and ischemia groups. Refer to figures 4.29 (a) and (b).

No significant differences were found amongst any of the groups when the P/T ratio was assessed (figure 4.29 (c)).

Control versus DIO: The tBad protein level was significantly higher in the untreated, insulin and ischemia DIO groups in comparison to their controls (figure 4.30 (a)).

When matched with their controls, the pBad protein level was significantly elevated in the ischemia DIO group; while no significant differences were found between the insulin and untreated DIO groups, and their controls (figure 4.30 (b)).

The P/T ratio was significantly lower in the untreated, insulin and ischemia DIO groups in comparison to their controls (figure 4.30 (c)).

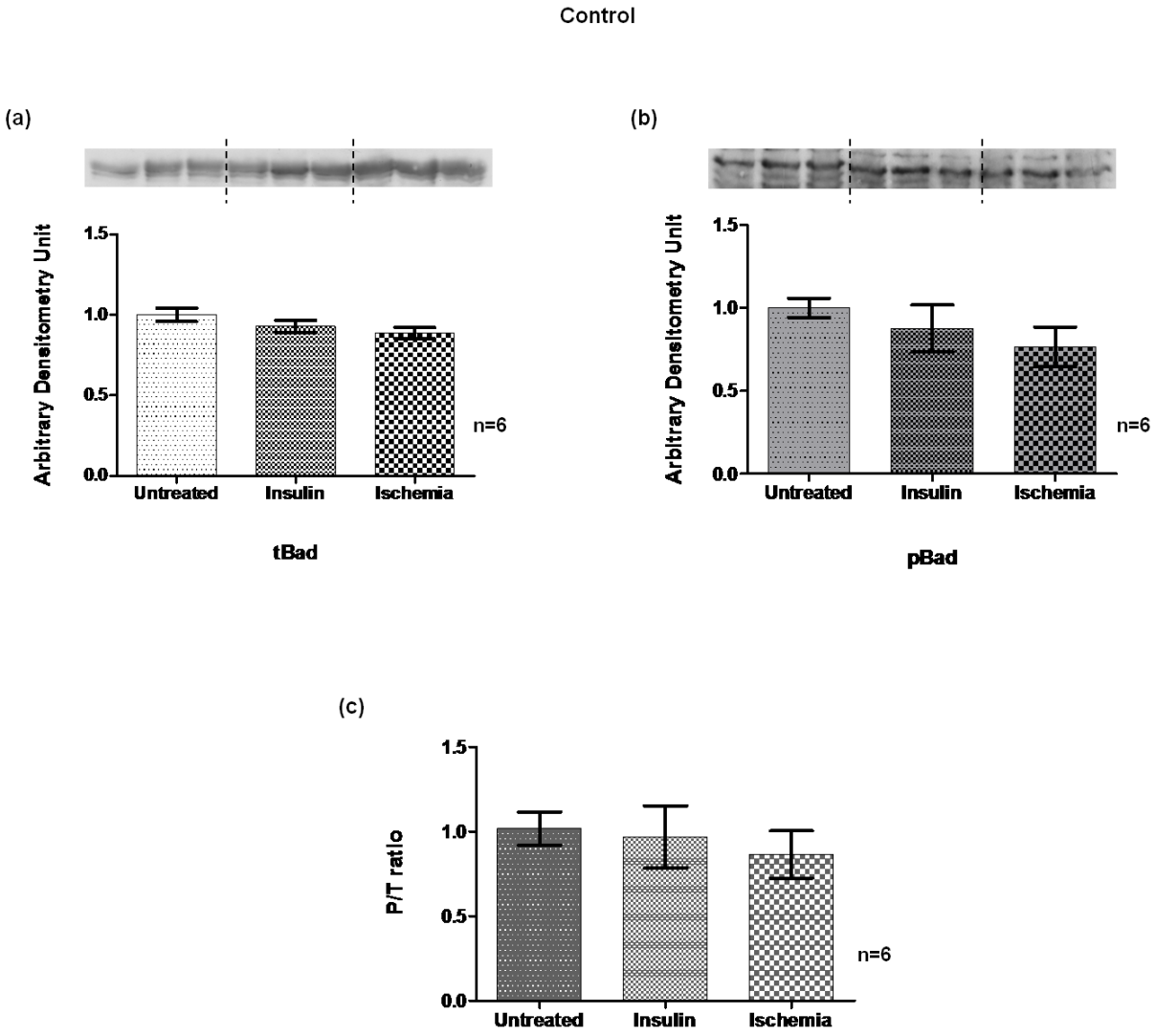

Figure 4.28: The mitochondrial tBad (a) and pBad (b) levels and the P/T ratio (c) in untreated versus insulin versus ischemia control animals (n=6 per group), following 20 weeks of their respective diets.

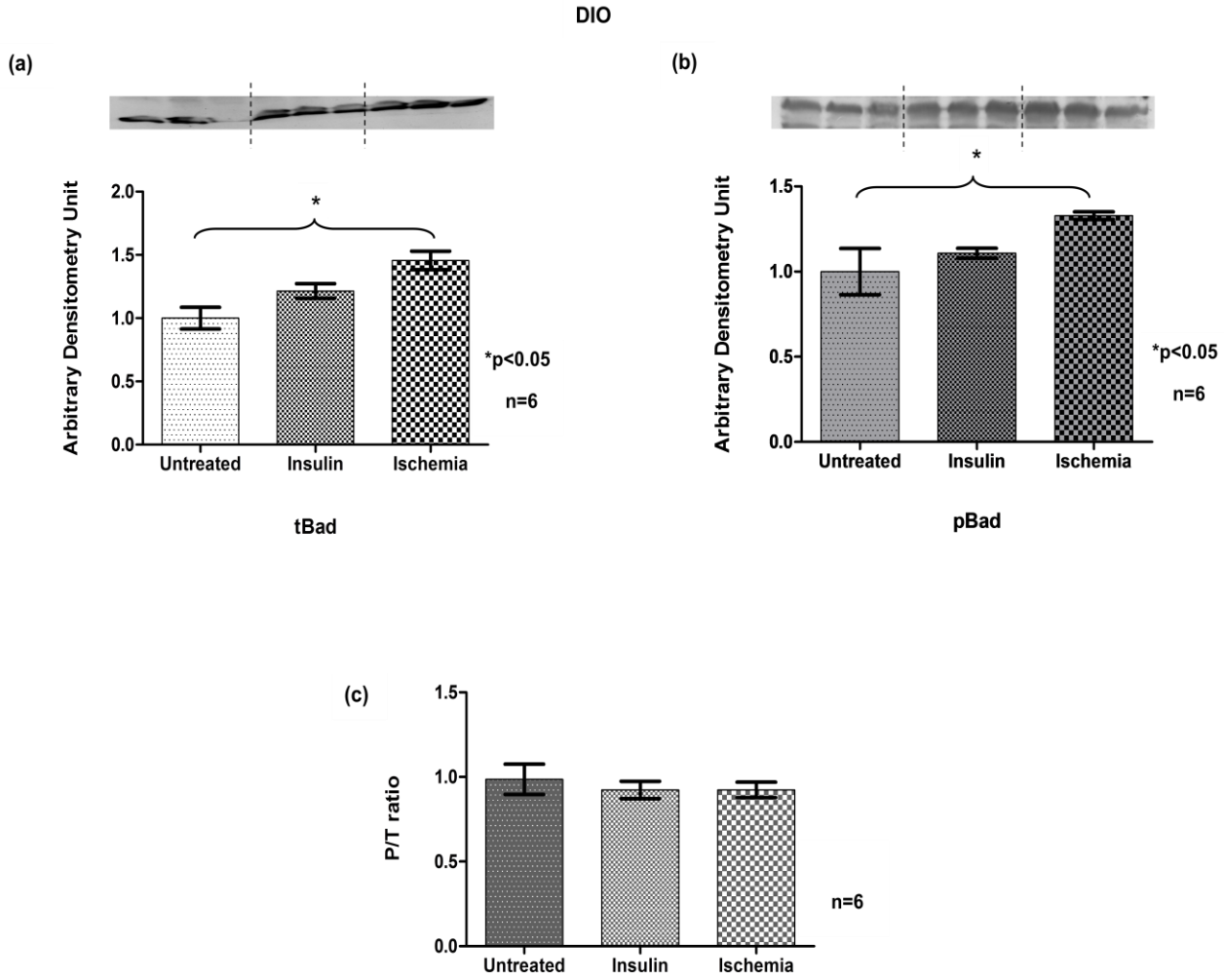

Figure 4.29: The mitochondrial tBad (a) and pBad (b) levels and the P/T ratio (c) in untreated versus insulin versus ischemia DIO animals (n=6 per group), following 20 weeks of their respective diets.

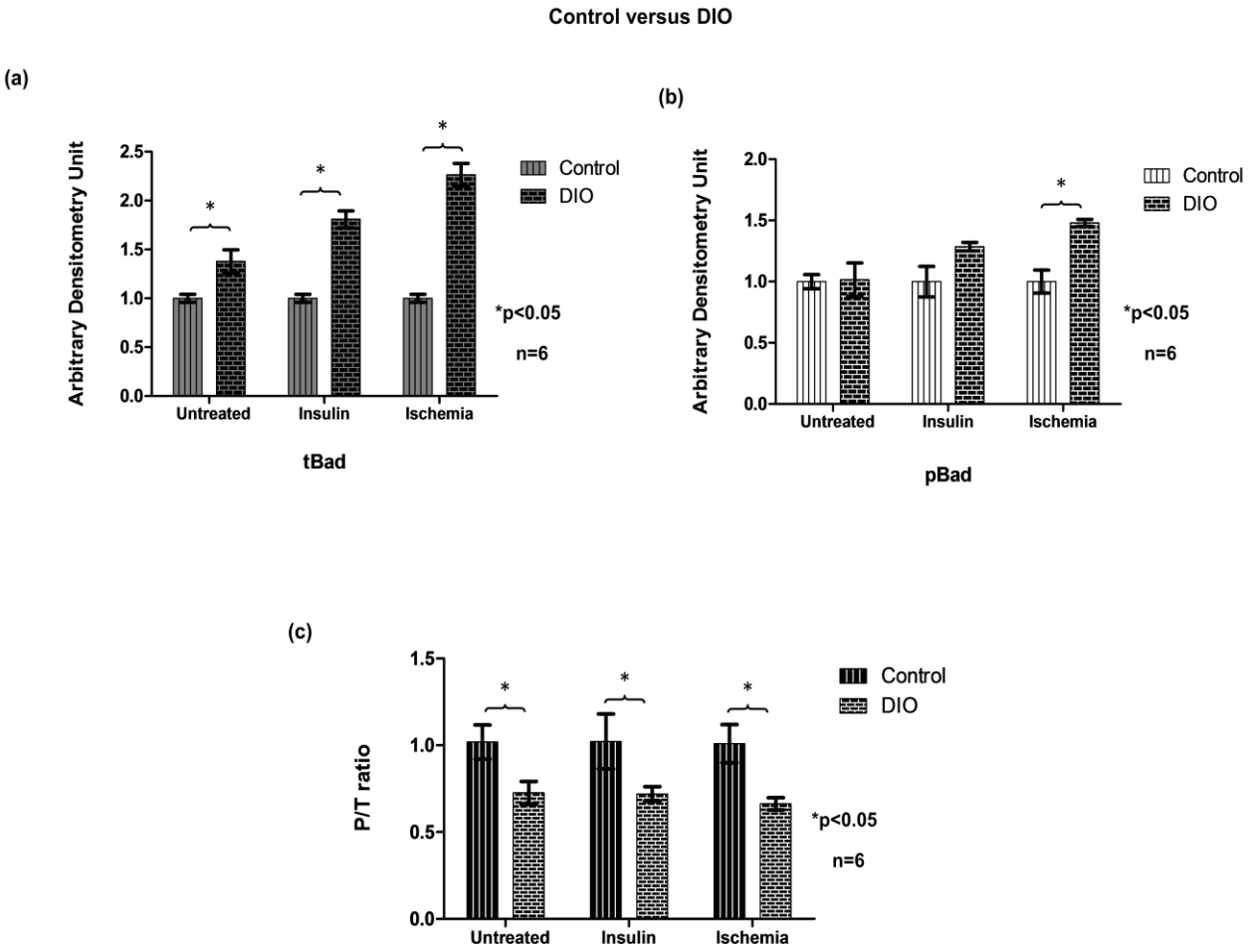

Figure 4.30: The mitochondrial tBad (a) and pBad (b) levels as well as the P/T ratio (c) in untreated, insulin and ischemia control versus DIO animals (n=6 per group), following 20 weeks of their respective diets.

4.8.1.5. Bcl-2 associated X (Bax) protein

Control: No significant differences were found amongst any of the groups when the Bax protein level at the myocardial mitochondria was determined (figure 4.31 (a)).

DIO: The insulin and the ischemia groups were significantly higher than the untreated group in terms of the Bax protein level. Additionally, the ischemia group displayed significantly elevated levels of Bax in comparison to the insulin group. Refer to figure 4.31 (b).

Control versus DIO: The untreated, insulin and ischemia DIO groups all had significantly higher levels of Bax protein than their controls (figure 4.31 (c)).

4.8.1.6. B-cell lymphoma/leukemia2 (Bcl-2) protein

Control: In terms of the cardiac Bcl-2 protein level at the mitochondria, no significant differences were found amongst any of the groups (figure 4.32 (a)).

DIO: The Bcl-2 protein level was significantly lower in the insulin and ischemia groups in comparison to the untreated group, while no significance was found between the insulin and ischemia groups (figure 4.32 (b)).

Control versus DIO: The untreated, insulin and ischemia DIO groups all had significantly higher levels of Bcl-2 protein than their controls (figure 4.32 (c)).

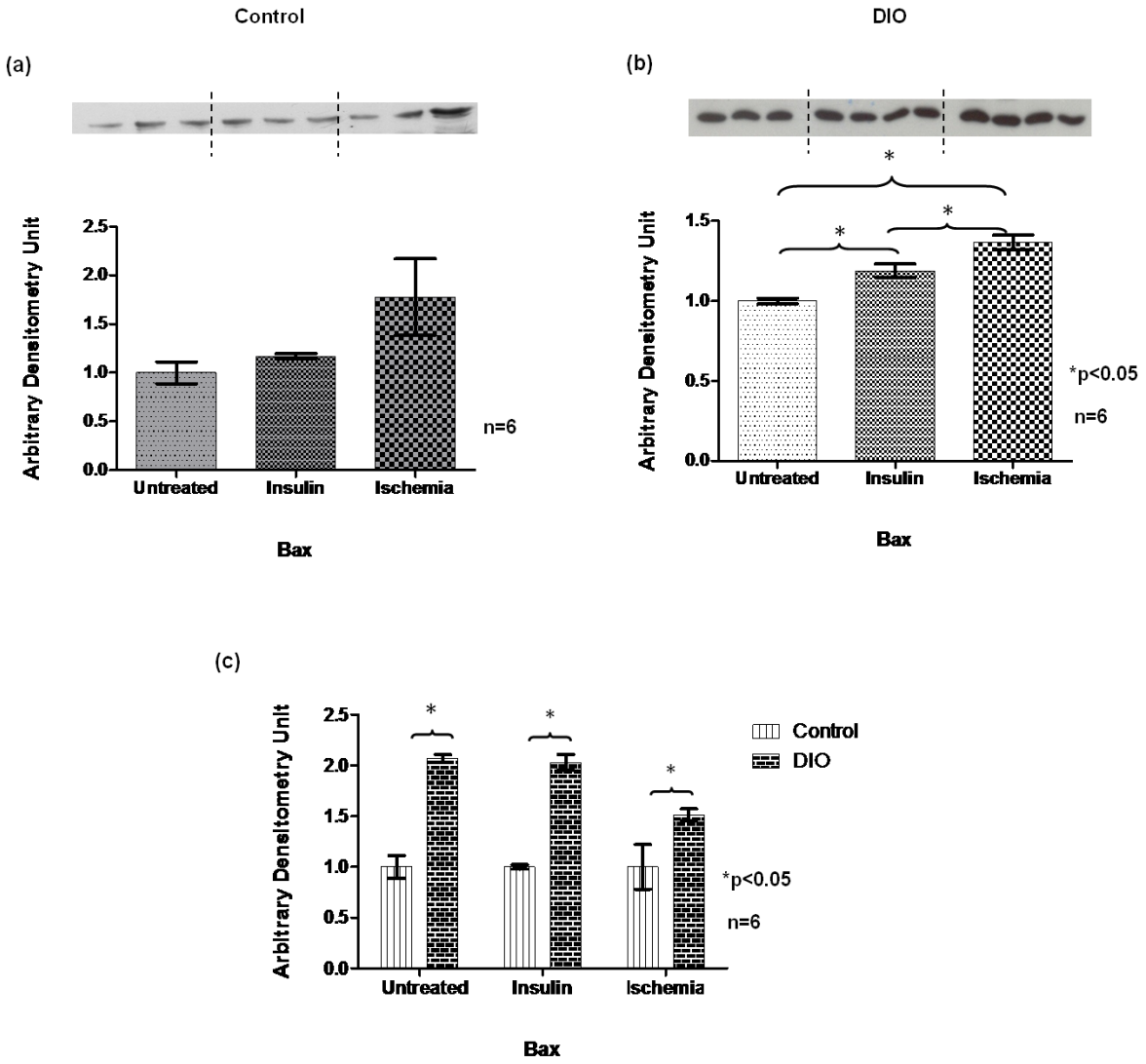

Figure 4.31: The mitochondrial Bax protein level in untreated, insulin and ischemia control hearts (a) as well as DIO hearts (b). The P/T ratio in untreated, insulin and ischemia control versus DIO hearts (c), following 20 weeks of their respective diets. n=6 per group.

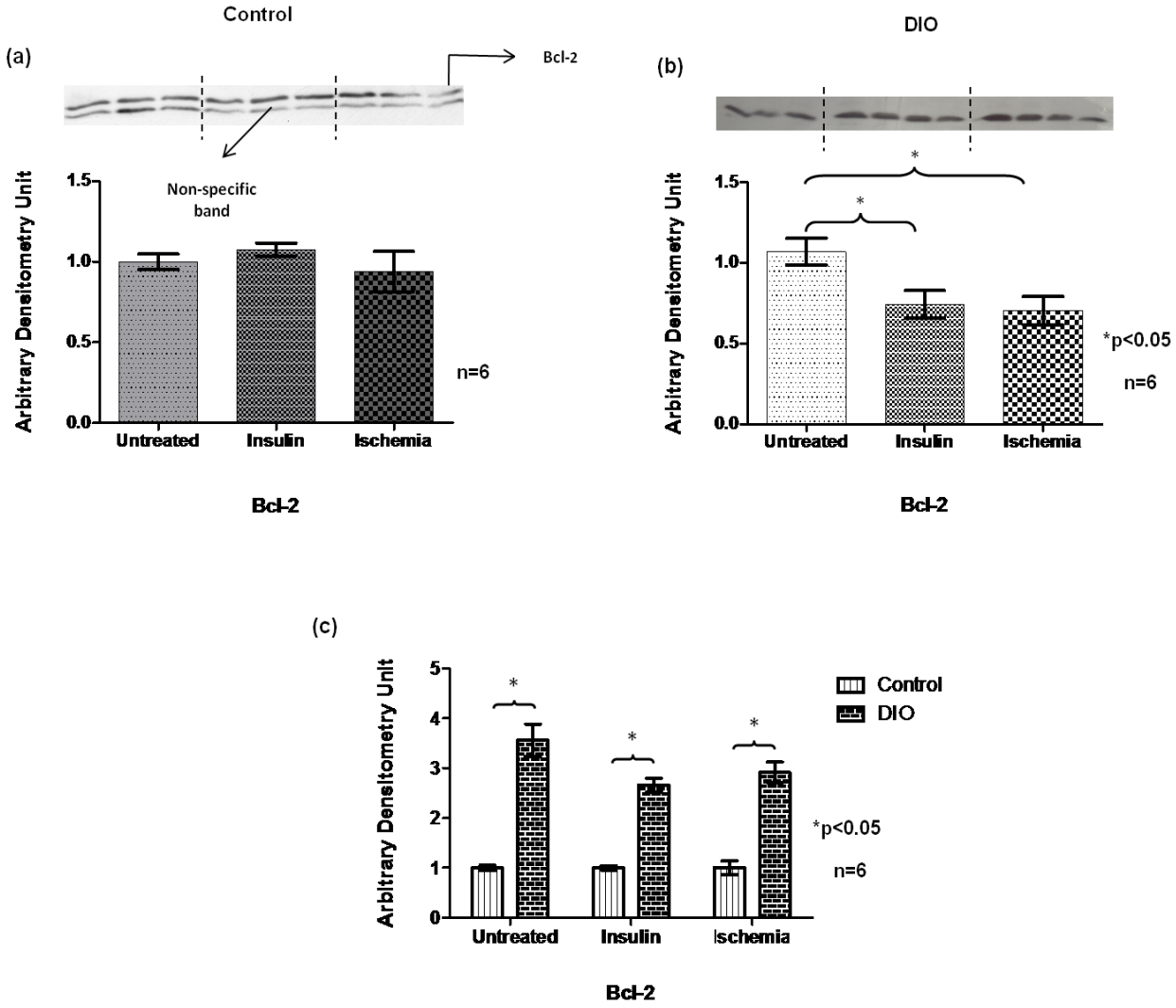

Figure 4.32: The mitochondrial Bcl-2 protein level in untreated, insulin and ischemia control hearts (a) as well as DIO hearts (b). The P/T ratio in untreated, insulin and ischemia control versus DIO hearts (c), following 20 weeks of their respective diets. n=6 per group.

Chapter 5: Discussion

5.1 Overview of the study

The correlation between obesity, insulin resistance and myocardial disease is well known today, however this association is a convoluted one and not straightforward as one would think [Bergman et al. 2007, Reaven 2008]. What adds to the complexity of this relationship between these diseases is that it has not been completely elucidated on a molecular level.

A study conducted by Park et al., published in 2005, reported the development of myocardial insulin resistance in C57BL/6 mice after just one and a half weeks of high-fat feeding. Associated with the insulin resistance was a decline in PKB/Akt activity, GLUT 4 protein levels and glucose uptake [Park et al. 2005], indicating that a high caloric diet, as often followed by obese individuals, can negatively affect myocardial insulin-mediated PI3K/PKB/Akt signalling.

Lu et al. (2007) observed in their study that genetically obese rats had decreased myocardial anti-apoptotic Bcl-2 levels while the pro-apoptotic BNIP3 and Bad protein levels were elevated, in comparison to their lean counterparts. Furthermore, other studies involving a variety of animal models of obesity have showed that a number of cardiovascular diseases or aberrations involve the highly controlled process of apoptosis [Yue et al. 2005, Shibata et al. 2005].

It is now common knowledge that insulin regulates the process of apoptosis via the PI3K/PKB/Akt pathway, as reviewed elsewhere [Duronio 2008, Iliadis et al. 2011]. However, what has received less attention thus far is the role of insulin in the context of apoptosis, specifically in the myocardium during obesity.

The focus of the present study was thus to elucidate if the insulin-mediated PI3K/PKB/Akt pathway played a role in the regulation of the mitochondrial-dependent pathway of apoptosis in the myocardium during obesity. This was achieved by utilizing a rat model of diet induced obesity and determining if any changes occurred in the proteins associated with PI3K/PKB/Akt pathway signalling in the cytosol, specifically PI3K, PKB/Akt and GSK-3α/β, of these animals. In addition, their hearts were probed for any changes in the apoptotic markers Bad, Bax and Bcl-2. These proteins were characterized 8 as well as 20 weeks after the completion of the obesity-inducing diet.

After 20 weeks, the presence of these apoptotic markers and PI3K/PKB/Akt pathway proteins were also probed for specifically in the mitochondria to further elucidate the interplay between the two pathways during obesity.

The study further aimed to establish if obesity resulted in cardiac mitochondrial dysfunction by analyzing mitochondrial respiration function during both anoxia/reperfusion and ETC complex inhibition after 20 weeks. Moreover, the protein profile of the various ETC complexes was analyzed for any changes after 8 as well as 20 weeks of diet to determine if structural changes had occurred in the mitochondria.

The aim of the various experiments conducted after the 8 week time point was to assess the early effects of obesity on the myocardium, while the 20 week time point was used to evaluate the advanced effects.

5.2 Physiological and biometric data

The obesity-inducing high caloric diet used in this study was causal in elevating total body weight gain when followed for a period of 20 weeks. Then again, when followed for a period of 8 weeks this diet did not cause a significant increase in total body weight gain (table 4.1). Nevertheless, regardless of the time period the DIO animals were on their diet, both of the experimental groups showed an elevation in intra-peritoneal fat accumulation (table 4.1). This augmented intra-peritoneal adipose deposition was associated with increased fasting blood glucose levels and serum insulin levels in both groups of obese animals. This indicates that an increase in intra-peritoneal fat accumulation has a positive correlation, more so than an increase in total body weight, with elevated blood glucose and serum insulin levels during obesity. Our data coincides with a number of other studies in which visceral obesity exhibited a greater correlation with various metabolic aberrations than overall or peripheral obesity [Fujioka et al. 1987, Poirier et al. 2005, Bergman et al. 2007].

Impaired glucose handling is often a consequence of obesity [Attallah et al. 2006, Fall et al. 2008], reviewed in Chapter 2, and would thus explain the presence of high serum insulin levels in both groups of DIO animals. Furthermore, this would be an indication that our obese animals were whole-body insulin resistant and that the excess insulin secretion is a compensatory mechanism, required by these animals to maintain their blood glucose levels. Although the DIO animals had significantly higher fasting blood glucose levels, after 8 as well as 20 weeks high caloric diet, they were not characterized by T2DM. The fasting blood glucose levels of both groups were below 6.1mmol /L, which are considered within the normal range [Kahn et al. 1997].

In addition to these metabolic parameters, our 8 as well as 20 weeks DIO animals also had a lower glucose tolerance during their 2 hour IPGTT (figure 4.1; figure 4.2), in

comparison to their non-obese controls, as illustrated by their greater IPGTT AUC. This substantiates that both obese groups had systemic insulin resistance and corresponds with previous data found in our laboratory, where the obese animals were whole body insulin resistant and had higher fasting blood glucose and insulin levels after 8 weeks of following a high caloric diet [Huisamen et al. 2012]. Additionally, Liao et al. (2011) found that both high fat diet sedentary and high fat diet exercise groups (consisting of male Sprague-Dawley rats) had larger IPGTT areas under the curve after 6 weeks of protocol, once again illustrating that a high fat diet correlates with impaired glucose tolerance.

5.3 Signalling proteins associated with the cytosol after 8 weeks

5.3.1 Western blot analysis after 8 weeks

Analysis of these hearts revealed that the obesity-inducing diet, had up-regulated the cytosolic PI3K/PKB/Akt and blunted the apoptotic signalling in these animals after 8 weeks, when compared with their control counterparts. This was revealed by the increased levels of total (a) and phosphorylated (b) p85 subunit of the pro-survival [Duronio 2008] kinase PI3K, as well as an elevated p85 subunit P/T ratio (c) in the DIO animals (figure 4.4).

Furthermore, the phosphorylated PKB/Akt (figures 4.5 (b)) and GSK-3α/β levels (figure 4.6 (b)), as well as their P/T ratios (figures 4.5 (c) and 4.6 (c), respectively), were elevated in these hearts. The total PKB/Akt and GSK-3α/β levels remained unchanged as seen in figures 4.5 (a) and 4.6 (a), respectively.

The DIO animals concurrently displayed heightened pBad (b) and an increased Bad P/T ratio (c), while the tBad protein level in these animals did not differ from the controls (a)

(figure 4.7). It has been established that phosphorylation of pro-apoptotic Bad by various kinases, including PKB/Akt, allows the scavenging of this protein by the 14-3-3 scaffold proteins, conferring a pro-survival status [Danial 2009, Sussman et al. 2011].

Our results also revealed that the obese animals had increased myocardial levels of the anti-apoptotic protein Bcl-2 after 8 weeks of diet (figure 4.8 (b)), while concurrently having increased pro-apoptotic Bax levels as seen in figure 4.8 (a). Since these data contradicted each other, we calculated at the Bax/Bcl-2 ratio which can be used as an indicator of a cell`s apoptotic status (death versus survival) [Anarkooli et al. 2008]. It was found that the ratio did not differ between the obese and control animals. However, activation of PKB/Akt, as well as GSK-3α/β, and the increased pBad level and Bad P/T ratio in the DIO animals indicate that the pro-apoptotic signalling was decreased and that cell survival was favoured.

Insulin has been shown to be cardioprotective in patients undergoing cardiac surgery [Carvalho et al. 2011, Ng et al. 2012] and of course, in the popular studies involving ischemic post-conditioning in rodent models [Jonassen et al. 2001, Zhu et al. 2006, Yin et al. 2009]. These reviews and studies have also indicated that insulin signalling and insulin–mediated cardiac protection are complex and occur via a number of different pathways. However, the 2009 experimental findings by Yin et al. and the 2012 review published by Ng et al., suggest that insulin is able to mediate these cardioprotective effects mainly via the PI3K/PKB/Akt pathway.

In fact, the 2006 study conducted by Zhu et al. found that myocardial ischemic post-conditioning elevated the protein levels, as well as its activity of PKB/Akt and GSK-3β in both healthy and “remodelled” hearts. This was in comparison to healthy and remodelled hearts which had undergone ischemia without post-conditioning. Moreover, the post-

conditioning was associated with smaller infarct sizes and increased functional recovery in the “remodelled” hearts.

Interestingly, when the enzyme activity of extracellular signal-regulated kinases 1 and 2 (ERK1/2) was analyzed, it did not differ significantly between the healthy and “remodelled” hearts during post-conditioning. This suggests that the PI3K/PKB/Akt pathway is better associated with the cardioprotection of ischemic post-conditioning than the ERK1/2/MAPK pathway. [Zhu et al. 2006]

In the present study, we therefore propose that the hyperinsulinemia during the initial stages of obesity-related insulin resistance is an adaptive mechanism not only to reduce plasma glucose levels but to elicit cardioprotection, after 8 weeks of a high caloric diet. A previous study conducted in our laboratory could substantiate this proposition as it found that DIO animals developed smaller myocardial infarct sizes in comparison to controls. This was after both groups followed an 8 weeks high caloric diet, and their hearts exposed to 25 minutes regional ischemia and subsequent reperfusion [Huisamen et al. 2012].

We propose that insulin mediates this protection via the PI3K/PKB/Akt signalling pathway, in a manner similar to the above mentioned studies. This would substantiate why we found increased PI3K/PKB/Akt and downregulated apoptotic signalling in the hearts of our obese animals.

5.3.2 Mitochondrial ETC complex western blot analysis after 8 weeks

NADH ASHII, SDH, α- and core protein-2 subunits are key protein components of the ETC complexes I, II, III and IV respectively, in that they are essential to the assembly and thus function of these complexes. With regard to these subunit levels, we found no significant

differences between the DIO and control animals (figure 4.9 (a)-(d)) indicating that an 8 week obesity-inducing diet had no effect on ETC complex assembly.
It would seem that the cardioprotective effects on the cytosolic level, provided by the elevated PI3K/PKB/Akt signalling (discussed in 5.3.1), were also exerted on the mitochondrial level after an 8 weeks high-caloric diet. That is, the augmented insulin-mediated PI3K/PKB/Akt signalling prevented obesity-induced alterations in complex subunit assembly, allowing the mitochondria to maintain its ETC integrity.

On the whole, it would thus seem that after 8 weeks the high caloric diet improved the hearts response to systemic insulin resistance and could be cardioprotective. Evidence of this would be that the mitochondrial integrity appears unchanged after 8 weeks of the diet.

5.4 Signalling proteins associated with the cytosol after 20 weeks

5.4.1 Western blot analysis after 20 weeks

Whole heart tissue analysis from our obese animals revealed that the high energy diet, when followed for 20 weeks, was associated with reduced cytosolic PI3K/PKB/Akt and enhanced apoptotic signalling in these animals.

Our results showed decreased levels of myocardial phosphorylated p85 PI3K subunit (figure 4.10 (b)), PKB/Akt (figure 4.11 (b)) and GSK-3α/β (figure 4.12 (b)) in the obese animals after 20 weeks of diet. Furthermore, the tPKB/Akt protein level (figure 4.11 (a)) as well as the p85 PI3K subunit and GSK-3α/β P/T ratios (figures 4.10 (c) and 4.12 (c) respectively) and were reduced in these animals.

Similar tendencies were observed in other animal models of high caloric diet. Lee et al. (2010) researched whether whole-body and myocardial insulin resistance developed

together, by comparing the insulin signalling in skeletal and cardiac muscle in micropigs after 7 months of either a control (low fat) or high caloric diet. The results showed that the obese pigs had decreased phosphorylation and activation of PI3K and PKB/Akt in both myocardial and skeletal muscle tissue [Lee et al. 2010].

When transgenic mice, for the cardiac myocyte overexpression of IGF-1, were subjected to a high-fat diet for 5 months, the diet was associated with cardiac damage and dysfunction. The diet also correlated with decreased cardiac IRS (tyrosine), PKB/Akt and GSK-3β phosphorylation, and this is thought to most likely underlie the myocardial aberrations [Zhang et al. 2012].

The present study corroborates the findings in these two studies in that it indicates that obesity, induced after 20 weeks of a high caloric diet, is associated with attenuated myocardial PI3K/PKB/Akt signalling.

Concurrent to the PI3K/PKB/Akt pathway protein aberrations, the apoptotic pathway was up-regulated in the obese animals after 20 weeks as revealed by the elevated tBad protein level and decreased Bad P/T ratio (figure 4.13 (a) and (c)). The Bax as well as the Bcl-2 protein levels in the DIO rats did not differ significantly, in comparison to the controls (figure 4.14 (a) and (b)). This prompted us to once again look at the Bax/Bcl-2 ratio to obtain a clearer indication of what was happening in the cell in terms of cell death versus survival. The ratio was not significantly different between the control and DIO animals. Nevertheless, the increase in tBad and the reduction in its P/T ratio suggest that these hearts were more susceptible to apoptosis after following an obesity-inducing diet for 20 weeks.

In terms of the Bad protein levels in the 20 weeks DIO animals, our findings are similar to that of Lu et al. 2007 in that the obese Zucker rats had increased cardiac levels of pro-apoptotic Bad at 5 to 6 months of age.

In addition to the impaired cardiac insulin signalling (discussed above), Zhang et al. (2012) also found that the cardiomyocytes of high fat fed transgenic mice had significantly attenuated levels of anti-apoptotic Bcl-2. However, this study also reported significantly elevated levels of phosphorylated Bax and Bad in these cardiomyocytes. Phosphorylation of these two molecules has been shown to promote cell survival as it inhibits their pro-apoptotic activities [Gardai et al. 2004, Wente et al. 2006]. It is most likely that the Bax/Bcl-2 ratio in these cardiomyocytes would have given a more appropriate indication of the apoptotic status of these cells.

Nevertheless, it has been shown that a small amount of apoptosis is detrimental to the heart [Masri et al. 2008]. This would, in conjunction with the above studies, support our hypothesis that the obese animal hearts will be more susceptible to apoptosis and damage as a result of their decreased PI3K/PKB/Akt and increased apoptotic signalling.

Experimental findings in previous studies conducted in our laboratory can substantiate the susceptibility of the 20 weeks DIO animals to myocardial damage in the current study. du Toit et al. (2008) and Nduhirabandi et al. (2011) both found that animals given a high caloric diet for 16 weeks developed hyperphagia-induced obesity. Furthermore, these obese animals in both studies had significantly larger myocardial infarct sizes after ex-vivo exposure to ischemia/reperfusion, indicating they were more susceptible to ischemia/reperfusion injury and had reduced cardioprotection.

5.4.2 Mitochondrial ETC complex western blot analysis after 20 weeks

In contrast to the findings obtained after 8 weeks of diet, analysis after 20 weeks revealed that the integrity of complexes I and II had been compromised in the DIO rats, indicated by the reduction of NADH ASHII and SDH subunit levels in these animals. In contrast, α- and core protein-2 subunit levels were increased, demonstrating that complex III and V assembly and integrity were enhanced in the obese animals.

The loss of complexes I and II integrity in these animals can be substantiated by the decreased PI3K/PKB/Akt signalling, and possible reduction in cardioprotection, as seen on the cytosolic level (discussed in 5.4.1). Contrasting levels of subunit expression are not foreign findings, as similar results were observed in other studies, for example, Liesa et al. 2008. In their study, PGC-1β knockout mice were fed a high fat diet for 6 months and their liver assessed for mitochondrial ETC complex protein subunit expression. These mice displayed elevated subunit expression for two of the ETC complexes, while no significant differences were found in the subunit levels for the other complexes. The mitochondrial ETC complexes changes seen in their study were associated with attenuated Mitofusin 2 expression, a protein essential for mitochondrial fusion [Chen et al. 2005].

The western blot ETC complex analysis data in the current study, suggests that mitochondria from the obese animals had disrupted integrity. In contrast, the integrity had remained intact in mitochondria from the obese animals, after following a high fat diet for 8 weeks.

5.5 Cardiac mitochondrial function after 20 weeks

In obesity, and diabetes, there is attenuated myocardial function which is associated with elevated fatty acid and reduced glucose metabolism, as well as increased cardiac oxygen consumption. Mitochondrial uncoupling proteins have been implicated in these cardiac aberrations, however little concrete evidence exists for this [Boudina et al. 2005].

Our study thus aimed to assess if different substrates could alter mitochondrial function in obese animals by evaluating oxidative phosphorylation capacity and performing anoxia/reperfusion analysis. Furthermore, we conducted mitochondrial ETC complex inhibition analysis to determine if complex inhibition or uncoupled respiration could mediate these cardiac dysfunctions.

5.5.1 Oxidative phosphorylation capacity and anoxia/reperfusion analysis after 20 weeks

When both glutamate (table 4.2) and palmitoyl-L-carnitine chloride (table 4.3) were used as substrates the ADP/O ratio was lower in the DIO animals, indicating that these animals consumed more natoms oxygen than the control animals for the same amount of nmoles ADP utilized.

Moreover, we found that the mitochondrial state 3 respiration rate was higher in the obese rats (table 4.2) with glutamate as substrate; an increase (not significant) was also observed when palmitoyl-L-carnitine was used as substrate, indicating that these animals were consuming significantly more oxygen during ATP production. With both substrates, the state 4 respiration rates showed that it was also higher (not significant) in the obese

animals causing a reduction in RCI, which is an indication of uncoupled mitochondrial respiration.

This implies that the obese rats had poor respiratory control and that the coupling between mitochondrial respiration and phosphorylation was weaker than that of their lean counterparts. Taken overall, the above parameters indicate that the mitochondrial function in the obese hearts have been negatively affected when either glucose or fatty acids were used as their main source of energy.

It would therefore appear that the elevated plasma free fatty acid level observed in the DIO animals had an in vivo effect on their mitochondrial oxidative phosphorylation capacity, which persisted in vitro when mitochondria were isolated and incubated under optimal conditions. This demonstrates the uncoupling effect of fatty acids on mitochondrial function [Stanley et al. 2005] and illustrates that the obesity-inducing diet indeed altered mitochondrial function.

Interestingly, when palmitoyl-L-carnitine was used as substrate, the percentage mitochondrial functional recovery (as indicated by state 3 respiration) after a period of anoxia was greater in the obese animals, despite having a reduced ADP/O ratio. The percentage recovery, with glutamate as a substrate, did not differ between the obese and control groups, suggesting that mitochondria isolated from obese animals fare better with respect to their mitochondrial function when incubated in the presence of a fatty acid substrate such as palmitoyl-L-carnitine.

Our findings indeed indicate that there is a shift in cardiac substrate utilization from glucose to fatty acids during obesity. Despite their improved recovery after exposure to anoxia, mitochondria isolated from hearts of obese animals have a significantly impaired oxidative phosphorylation. In the long-term this may have a profound effect on myocardial

contractile function as shown by du Toit et al. (2008). In their study, du Toit et al. found that the DIO animals had a significantly reduced aortic output at reperfusion (and prior to ischemia) in comparison to the controls. Additionally, these obese animals were marked by attenuated percentage recovery post-ischemia.

5.5.2 ETC complex inhibition analysis after 20 weeks

In order to assess if mitochondrial electron transport chain complexes plays a role in diet-induced obesity myocardial dysfunction we inhibited and uncoupled the complexes with various complex specific inhibitors and uncouplers. Thereafter, we determined the state 3 respiration rate as a measure of mitochondrial function in the control and obese animals.

Neither the addition of succinate nor the complex inhibition with rotenone or oligomycin, using either glutamate or palmitoyl-L-carnitine as substrate, yielded any differences between the DIO and control animals with respect to their state 3 respiration rates. However, OXPHOS uncoupling with CCCP [Benard et al. 2007] produced a higher respiration rate in the obese animals with glutamate as substrate but not when palmitoyl-L-carnitine was used. This further substantiates the uncoupled state of the mitochondria in the DIO animals, especially when glutamate served as substrate.

5.6 Mitochondrial integrity after 20 weeks

5.6.1 Citrate synthase assay

Citrate synthase is the primary enzyme that mediates the binding of acetyl coenzyme A acetyl CoA and oxaloacetate to form citrate in the TCA cycle. Furthermore, this enzyme is located in the mitochondrial matrix and is used as a well-established marker to determine the amount of undamaged mitochondria present in a sample, and is achieved by measuring the activity of the enzyme [Raffaella et al. 2012]. Our study revealed that the citrate synthase activity was lower in the obese rats (figure 4.16), indicating that these animals had a lower number of intact cardiac mitochondria per mg isolated protein. This suggests that either there were fewer intact mitochondria initially present in the tissue or that the mitochondria were easily damaged upon isolation.

These findings correlate to other studies in which the CS activity was lower and mitochondrial damage elevated, in animals fed high fat diets [Raffaella et al. 2012].

The decreased number of intact mitochondria, taken together with the reduced mitochondrial ETC complex integrity (section 5.4.2); indicate that the obese animals had attenuated mitochondrial integrity after 20 weeks of diet.

5.6.2 HPLC analysis after 20 weeks

As described on in Chapter 3, the total amount of ATP formed during state 3 respiration was determined by HPLC analysis. No significant differences were found amongst the control and DIO animals with respect to the ATP yield, when either (a) glutamate or (b) palmitoyl-L-carnitine were used as substrates (figure 4.17). However, when we calculated the ATP/O ratio, from the ATP values obtained and the amount of oxygen taken up during

state 3 respiration, we saw that this was significantly reduced in the obese animals (figure 4.18). This denotes that for both of these substrates, the obese animals produced less ATP than the controls but utilized more oxygen in order to do so, according to their lower ADP/O ratio. This confirms that the obese animals indeed had elevated cardiac oxygen consumption and were wasting it during ATP synthesis as discussed in 5.5.1.

Overall, our data from the anoxia/reperfusion (section 5.5.1), ETC complex inhibition (section 5.5.2) and HPLC analyses indicate that there was a reduction in mitochondrial function in the heart after 20 weeks of diet-induced obesity. This especially seemed to be the case when glutamate acted as substrate. When palmitoyl-L-carnitine was used, the obese animals had a better recovery during anoxia/reperfusion analysis. We suspect that this is as a result of a metabolic substrate switch and increased use of fatty acids in these animals.

Furthermore, the elevated complexes III and V integrity, could explain the increased percentage recovery after anoxia within the mitochondria from the DIO group, when utilizing palmitoyl-L-carnitine as a substrate.

5.7 Signalling proteins associated with the mitochondria after 20 weeks

Obesity associated cardiovascular diseases often stem from structural and functional aberrations as a result of irregularities in both cardiac cytosolic and mitochondrial signalling [Kim et al. 2008].

Thus, our study further compared PI3K/PKB/Akt and apoptotic signalling in cardiac mitochondria isolated from control and obese rats under basal conditions (i.e. untreated) as well as after insulin treatment or exposure to ischemia. Firstly, we did the comparison in

control animals, 20 weeks after their standard diet, and secondly in the obese high caloric diet group. The purpose of this was to establish how exogenous insulin and ischemia would affect signalling in these two pathways, as both insulin [Duronio 2008, Ilidias et al. 2011] and ischemia [Yong et al. 2008, Yin et al. 2009] have been shown to activate the PI3K/PKB/Akt pathway as a cardioprotective mechanism. Lastly, we compared myocardial markers of the PI3K/PKB/Akt and apoptotic signalling pathways, amongst control and DIO groups, at basal and when the hearts were treated with insulin and when exposed to ischemia.

5.7.1 Western blot analysis after 20 weeks

5.7.1.1 Mitochondrial signalling post insulin administration

(i) Control animals

Intra-peritoneal administration of insulin served to augment the PI3K/PKB/Akt signalling at the mitochondria in the control animals, while concurrently preventing an increase in apoptotic signalling.

This can be seen by the increased phosphorylation of the p85 PI3K subunit, despite a lack of increased tp85 PI3K subunit translocation. Furthermore, the P/T ratio was higher in the insulin treated controls in comparison to the untreated controls, indicating that a larger portion of the p85 subunit was phosphorylated than dephosphorylated (figure 4.19 (a), (b) and (c)).

In addition, not only was there an increase in tPKB/Akt translocation to the mitochondria in the insulin treated controls, there was also an increase in the phosphorylation of these PKB/Akt molecules (figure 4.22 (a) and (b)). Furthermore, we saw that the tGSK-3α/β

translocation level was lower (a) but that the phosphorylation of this molecule (b), as well as the P/T ratio (c), were elevated in these animals (figure 4.25).

In terms of apoptotic pathway signalling, the mitochondrial translocation of tBad (figure 4.87 (a)) and Bax (figure 4.31 (a)) in the insulin treated controls did not differ significantly from the untreated controls. The phosphorylation level of tBad in the insulin treated controls also did not differ significantly from that in the untreated controls, as seen in figure 4.28 (b). Furthermore, there were no increases in the anti-apoptotic Bcl-2 level at the mitochondria (figure 4.32 (a)).

The lack of increased apoptotic protein levels and translocation, to the mitochondria, and elevated PI3K/PKB/Akt pathway signalling indicates that the insulin treated control animals were afforded cardiac protection.

(ii) DIO animals

With regard to the insulin treated DIO animals, we found these animals displayed elevated mitochondrial insulin-mediated PI3K/PKB/Akt pathway protein translocation, and decreased apoptotic pathway protein translocation.

We found that the tp85 and pp85 translocation to the mitochondria increased upon insulin administration in the obese animals (figure 4.20 (a) and (b)). The translocation of tPKB/Akt however, and the phosphorylation of this protein, remained unchanged (figure 4.23 (a) and (b), respectively). At the same time, there was decreased translocation of downstream tGSK3α/β but the phosphorylation of this protein, as well as the P/T ratio, was elevated in the insulin treated DIO animals (figure 4.26 (a), (b) and (c)).

In terms of the apoptotic signalling, we saw no decreased levels of tBad translocation, and parallel to that the phosphorylation of tBad and its P/T ratio did not increase in the insulin treated DIO animals (figure 4.29 (a), (b) and (c)). Conversely, pro-apoptotic Bax translocation increased while anti-apoptotic Bcl-2 levels decreased, indicating an increase in apoptotic signalling at the mitochondria.

The above results would then indicate that at the mitochondrial level, the enhanced PI3K/PKB/Akt signalling was unable to provide protection against myocardial apoptosis in the obese insulin treated animals.

On the whole, these findings denotes that exogenous insulin administration is able to elicit elevated PI3K/PKB/Akt signalling, in the mitochondria in the hearts of control as well as diet-induced obese animals after 20 weeks. However, it would seem that this pathway was only able to prevent increased intrinsic apoptotic signalling in the control but not the DIO animals. Thus, cardioprotection was lost at the mitochondrial level in the obese animals making these hearts more susceptible to apoptosis, while the control animal hearts were protected.

Yang et al. (2009) conducted a study, in which they compared the insulin-mediated PI3K/PKB/Akt pathway in control and type-1 (T1DM), as well as type-2 (T2DM), diabetic rats. The T1DM mice were obtained by injecting normal rats with a once-off dose of streptozotocin, while the T2DM mice were obtained by feeding the animals a high fat diet for 6 weeks. After all the groups were fasted overnight and administered insulin acutely via the inferior vena cava, western blot analysis revealed that the translocation of tPKB/Akt and pPKB/Akt to the mitochondria was significantly higher in the T1DM animals, in comparison to the controls. Furthermore, the PKB/Akt P/T ratio in the mitochondria was higher in these mice. In contrast, the translocation of tPKB/Akt and pPKB/Akt to the

mitochondria, as well as the P/T ratio in the mitochondria, were attenuated upon acute insulin administration. Yang et al. concluded that the insulin-mediated PI3K/PKB/Akt signalling in the mitochondria was elevated in the T1DM model due to the insulin deficiency, which is characteristic of this type of diabetes. This deficiency has been shown, by other studies, to increase the number of insulin receptors as well as the receptor signalling to PI3K in the heart [Wang et al. 1999].

On the contrary, Yang et al. (2009) further concluded that the attenuated PI3K/PKB/Akt signalling observed in the mitochondria of the T2DM animals were due to them being insulin resistant as other studies had shown that insulin receptor signalling is decreased in these animals [Bonnard et al. 2008, Milne et al. 2007].

The above conclusions could authenticate why the obese animals experienced a reduction in mitochondrial integrity and function, despite elevated PI3K/PKB/Akt signalling in the mitochondria. It is possible that as a result of our obese animals being insulin resistant, there was only a minimal amount of insulin receptor signalling to PI3K in the mitochondria. The signalling could have been sufficient to elevate tp85 PI3K subunit translocation and to enhance p85 phosphorylation in these animals. However, the insulin resistance most likely affected PI3K activation and phosphorylation of downstream PKB/Akt as Bax levels increased and pBad levels were unchanged in the mitochondria. Active PKB/Akt is known to phosphorylate Bad and Bax and thus inhibit their pro-apoptotic abilities [Wente et al. 2006, Gardai et al. 2004].

5.7.1.2 Mitochondrial signalling during cardiac ischemia

(i) Control animals

Similar to the insulin treated controls, mitochondria isolated from control hearts exposed to ischemia showed increased PI3K/PKB/Akt signalling, while the apoptotic signalling neglected to increase.

In our study, the level of translocation of tp85 PI3K subunit and tPKB/Akt to the mitochondria in the ischemia controls was not significantly different from that of the untreated controls, as seen in figures 4.19 (a) and 4.22 (a). However, the phosphorylation of p85 (figure 4.19 (b)) and PKB/Akt (figure 4.22 (b)), as well as both of their P/T ratios (figures 4.19 (c) and 4.22 (c)), were greater in the ischemia groups. We found that although the level of tGSK3α/β translocation decreased in the ischemia controls, the phosphorylation of the mitochondrial protein was amplified (figure 4.25 (a) and (b)). Additionally, the P/T ratio increased in these animals as seen in figure 4.25 (c).

In parallel, we found there were no significant changes in the translocation of apoptotic pathway proteins to the mitochondria in the ischemia controls, in comparison to the untreated controls: pro-apoptotic tBad did not translocate, nor did the phosphorylation thereof increase (figure 4.28 (a) and (b). Additionally, the Bad P/T ratio did not significantly increase in the ischemia controls as seen in figure 4.28 (c). We also failed to see an elevation in pro-apoptotic Bax levels nor an increased level of anti-apoptotic Bcl-2 mitochondrial translocation in the ischemia controls.

The elevated translocation of the insulin-mediated PI3K/PKB/Akt pathway proteins to the mitochondria during ischemia, as well as the lack of translocation of pro-apoptotic or anti-apoptotic protein, indicate that these control hearts were protected.

(ii) DIO animals

The DIO hearts in our study, which were subjected to ischemia, displayed both increased mitochondrial PI3K/PKB/Akt and decreased apoptotic signalling which indicates that these hearts were protected against ischemia.

We found that the translocation of tp85 PI3K subunit to the mitochondria, as well as the phosphorylation thereof, was higher in the ischemia treated DIO hearts (figure 4.20 (a) and (b)). Additionally, the P/T ratio was elevated in these animals as seen in figure 4.20 (c). tPKB/Akt translocation in the ischemia DIO group did not alter significantly from that in the untreated DIO group (figure 4.23 (a)) whilst the phosphorylation of PKB/Akt and the P/T ratio was lower (figure 4.23 (b) and (c)).

This finding produces a contrast as the changes regarding upstream PI3K p85 subunit indicate an increase in insulin-mediated PI3K/PKB/Akt signalling in the mitochondria, whilst those changes concerning downstream PKB/Akt signify a reduction in the signalling. To obtain a better understanding of the mitochondrial insulin signalling in the ischemia DIO animals, we analyzed the modifications regarding GSK3α/β. We found that less tGSK3α/β mitochondrial translocation occurred in these animals during ischemia (figure 4.26 (a)) however, the phosphorylation of this protein, as well as its P/T ratio, increased significantly (figure 4.26 (b) and (c)). On the whole, this indicates that the PI3K/PKB/Akt signalling pathway was upregulated in these animals.

When we analyzed the apoptotic signalling protein profile in the ischemia DIO group, our results yielded that the tBad translocation was higher in this group than the untreated DIO animals (figure 4.29 (a)) and, the phosphorylation of this protein had increased simultaneously (figure 4.29 (b). This explained why we saw no significant difference between the untreated and ischemia DIO animals in terms of their Bad P/T ratio, as seen

in figure 4.29 (c). Nonetheless, we found that the Bax translocation had increased (figure 4.31 (b)) while the Bcl-2 translocation had decreased collectively (figure 4.32 (b)), indicating that apoptotic signalling was elevated in these animals.

The overall mitochondrial protein profile, during ischemia of the DIO animals, reveals increased myocardial apoptosis and loss of cardiac protection despite augmented PI3K/PKB/Akt signalling.

It would thus seem that ischemia was able to instigate elevated PI3K/PKB/Akt signalling at the mitochondria in control as well as obese animals, after 20 weeks of their respective diets. However, this pathway was only able to prevent elevated apoptotic signalling in the control animals while it was unable to do so in mitochondria isolated from DIO ischemic hearts.

Increased mitochondrial PI3K/PKB/Akt signalling in ischemia was also observed by others. Ahmad et al. (2006) found that when the mitochondrial K_{ATP} (mitoK_{ATP}) channels were activated in a mouse model of I/R injury, the level of cardiomyocyte apoptosis decreased as a result of elevated PKB/Akt phosphorylation in the mitochondria. It was concluded that the PI3K/PKB/Akt pathway is essential for cardioprotection against this type of injury when mediated through activated mitoK_{ATP} channels. Interestingly, they found that if phosphorylation of PKB/Akt only took place in the cytosol, it would not suffice in protecting the heart from ischemia. The results of this study indicated that pPKB/Akt needed to translocate from the cytosol to the mitochondria, to put forth its protective effects. [Ahmad et al. 2006]

In the current study, the increased PI3K/PKB/Akt signalling is only associated with myocardial protection in the control animals whereas the obese animals showed elevated levels of cardiac apoptotic signalling. The fact that pPKB/Akt needed to translocate from

the cytosol to the mitochondria to protect the heart from ischemia, in the above study, indicates that PI3K/PKB/Akt signalling needs to be augmented in both the cytosol and mitochondria simultaneously for the cardioprotection to be exerted. The attenuated cytosolic PI3K/PKB/Akt signalling (section 5.4.1) could thus substantiate why our study found a reduction in cardiac mitochondrial function (sections 5.5.1, 5.5.2 and 5.6.2) and integrity (section 5.4.2. and 5.6.1) after 20 weeks. The augmented PI3K/PKB/Akt signalling in the mitochondria was thus not sufficient to protect the obese heart from mitochondrial damage and dysfunction.

5.7.1.3 Mitochondrial signalling in control versus obese animals

Comparisons amongst the untreated (basal), insulin and ischemia groups, in control versus DIO animals, indicated that PI3K/PKB/Akt as well as apoptotic signalling in the mitochondria was enhanced in the obese animals.

This is substantiated by the lack of a difference in the translocation level of tp85 PI3K subunit, tPKB and tGSK-3α/β subunit to the mitochondria in all three control groups. However, the DIO animals in all three groups had elevated pp85 and pGSK-3α/β levels, as well as increased p85 PI3K subunit and GSK-3α/β P/T ratios at the mitochondrial level. This was also reflected in the lack of elevated Bad P/T ratio. Despite this, the well-known cardioprotective GSK-3α/β presented at mitochondrial elevated phosphorylated levels. In contrast, the obese animals in all three groups had decreased levels of pPKB/Akt and PKB/Akt P/T ratios in the mitochondria.

In terms of apoptotic signalling, the tBad, Bax and Bcl-2 translocation to the mitochondria was augmented in all three of the obese groups. There was no difference in the pBad

levels in the mitochondria of the untreated and insulin DIO animals, in comparison to their controls. The DIO animals in the ischemia group on the other hand, displayed an increased level of pBad in the mitochondria when matched against its control. However, the Bad P/T ratios in all three groups of obese animals were blunted, indicating on the whole that Bad signalling was enhanced; while both Bax and Bcl-2 signalling was increased.

Therefore, it would seem that PI3K/PKB/Akt as well as the apoptotic pathway was enhanced in the mitochondria of the obese animals in the untreated, insulin and ischemia groups. This indicates that myocardial protection was blunted during diet-induced obesity, despite an upregulation in the cardioprotective PI3K/PKB/Akt signalling pathway.

The studies by Yang et al. (2009) and Ahmad et al. (2006), discussed in 5.7.1.1 and 5.7.1.2 respectively, can provide assistance in clarifying why there was a contrast in terms of increased PI3K/PKB/Akt signalling but loss of cardioprotection in the DIO animals. It might be that the insulin resistance in filtered down to the insulin receptor signaling in the mitochondria and blunted receptor signalling to PKB/Akt, thus explaining why we saw a reduction in phosphorylation of PKB/Akt in these animals. The receptor signalling was clearly sufficient to elevate p85 PI3K subunit phosphorylation to a certain extent although, we suspect that the signalling was not operating at optimal level as we failed to see increased recruitment of tp85 subunit to the mitochondria. [Yang et al. 2009] What is more, the obese animals only had increased PI3K/PKB/Akt signalling in the mitochondria, whereas in the cytosol this pathway`s signalling was downregulated. We have seen from the study conducted by Ahmad et al. (2006) that upregulation of PI3K/PKB/Akt signalling in both the cytosol and the mitochondrion is essential for myocardial protection, and that increased mitochondrial signalling alone will not be adequate.

In summation, comparison of p85, PKB/Akt and GSK-3α/β in the cytosol and mitochondria of control and obese hearts show a translocation of p85 and GSK-3α/β from the cytosol to the mitochondria, while PKB/Akt is reduced in both fractions. Loss of cardioprotection occurs despite a 5 fold increase in mitochondrial pGSK-3α/β.

GSK-3α/β can also be phosphorylated by other kinases but it seems as if the loss of PKB/Akt activation plays a significant role in the loss of mitochondrial function and cardioprotection, during obesity.

Chapter 6: Conclusions

6.1 Conclusions

We hypothesized initially that obesity would have different effects on the myocardium during the initial and advanced stages of the disease. We proposed cardiac protection would take place during the initial stages of obesity, whereas this protection would be lost during the advanced stages thus negatively affecting the heart. Furthermore, we consider these differences in myocardial protection to be mediated through the PI3K/PKB/Akt and intrinsic apoptotic pathways, at both the cytosolic and mitochondrial level of the cardiomyocyte.

Indeed we saw during the initial stages of obesity (8 weeks of diet-induced obesity), that the DIO animals had accumulated a significantly elevated amount of intra-peritoneal fat mass and were positive for systemic insulin resistance. These animals presented with augmented myocardial PI3K/PKB/Akt and blunted intrinsic apoptotic signalling at the cytosolic level, after 8 weeks. These changes correlated with a lack of change in mitochondrial ETC complex integrity during the initial stages of the disease, which could be associated with cardioprotection.

The 20 weeks diet-induced obese animals, representing the advanced stages of obesity, had increased intra-peritoneal fat mass and whole body insulin resistance, similar to the 8 weeks DIO animals. In contrast, the advanced stages were characterized by decreased PI3K/PKB/Akt and increased intrinsic apoptotic signalling at the cytosolic level. An unexpected finding was that these animals had elevated mitochondrial PI3K/PKB/Akt as well as apoptotic pathway signalling on the mitochondrial level. This was the case when the two pathways were compared in the control and obese animals, at basal level and

when insulin was administered as well as when the hearts were exposed to ischemia. We argue that this contrast seen, results from a resistance in the insulin receptor-mediated signalling to PKB/Akt, and because cardioprotection can only be mediated if PI3K/PKB/Akt signalling is upregulated in both the mitochondria and cytosol. Thus, these animals might be more susceptible to myocardial damage.

This is further substantiated by the reduction in citrate synthase activity and the downregulation in the expression of ETC complexes I and II, thus revealing aberrations in the mitochondrial integrity. Furthermore, on the whole mitochondrial oxidative phosphorylation function is also negatively affected during the advanced stages of obesity, regardless of the substrate used. We observed that the obese animals using glutamate as a substrate present with a reduced RCI ratio, a sign of uncoupled respiration.

In contrast, the mitochondrial function initially seems to be upregulated in the advanced obese animals as we see an increased percentage recovery after anoxia/reperfusion, when palmitoyl-L-carnitine serves as substrate. We do not see this elevated recovery when glutamate is used, indicating that the obese animals might have undergone a metabolic shift by increasing their fatty acid utilization.

In summation (figure 6.1), we find that the initial stage of obesity is associated with augmented myocardial protection due to increased PI3K/PKB/Akt and attenuated apoptotic signalling. Conversely, the advanced stage of the disease is marked by loss of cardioprotection and increased susceptibility to apoptosis, as a result of decreased cytosolic PI3K/PKB/Akt and enhanced apoptotic signalling.

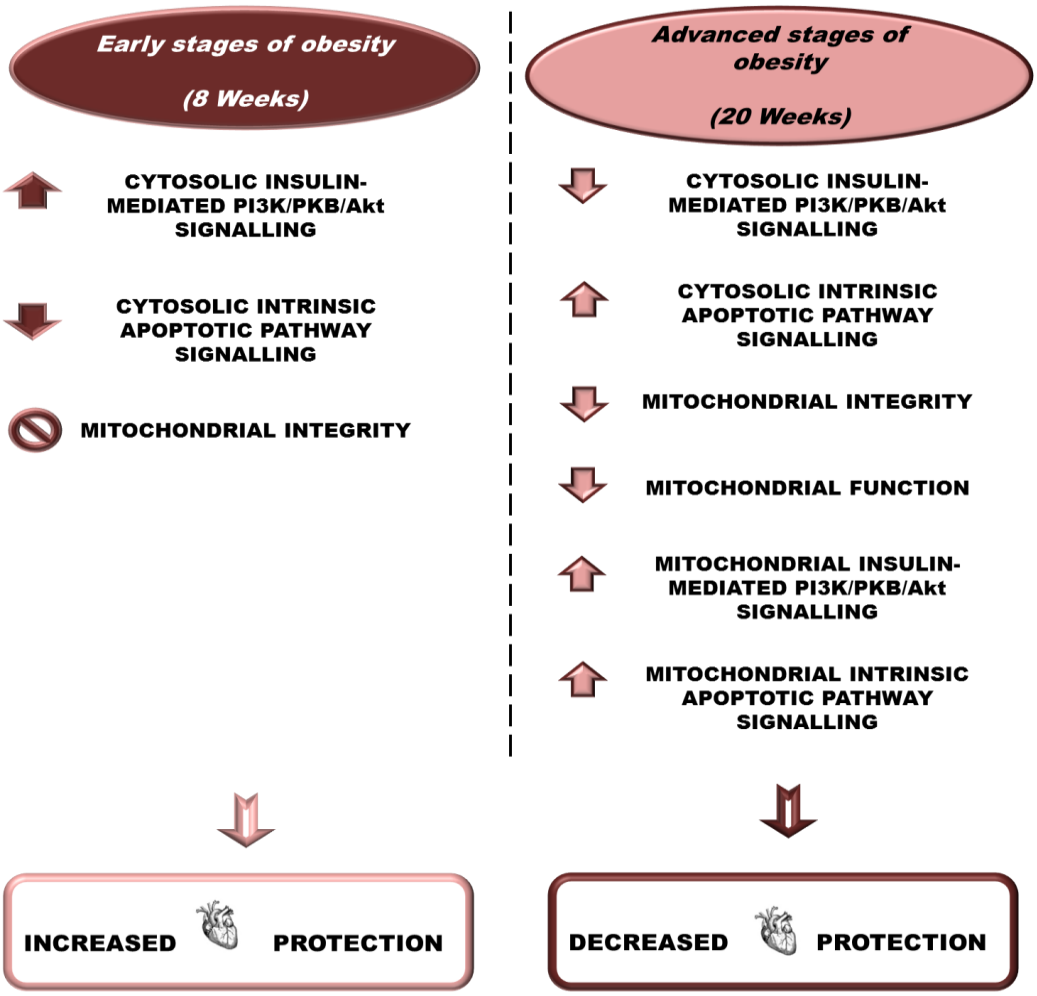

Figure 6.1: Summary of the present study`s experimental findings, regarding the myocardial changes at the cytosolic and mitochondrial level during the initial and advanced stages of diet-induced obesity.

6.2 Limitations of the study

The current study did not assess cardiac mitochondrial function as well as mitochondrial PI3K/PKB/Akt and apoptotic signalling in the heart after 8 weeks of diet-induced obesity.

Additionally, the study did not look at the effects of insulin administration and myocardial ischemia exposure on cytosolic PI3K/PKB/Akt and apoptotic signalling subsequent to 8 weeks of diet-induced obesity.

6.3 Future perspectives

In our study, we were able to demonstrate the role of the PI3K/PKB/Akt pathway in cardioprotection. It is likely that this pathway does not act alone and thus it would be of great therapeutic value to ascertain the roles of other pathways (ERK and SAFE pathways), and the influence these might have on PI3K/PKB/Akt signalling, in myocardial protection.

Furthermore, we showed that PI3K/PKB/Akt-mediated regulation of certain apoptotic markers, Bad, Bax and Bcl-2, was essential in determining the cells' apoptotic fate. In future studies, it would be beneficial to look at other markers of apoptosis such as, cleaved caspase-3 and-9, cleaved PARP as well as FOXO1 to establish an even bigger picture of the apoptotic signalling during the initial and advanced stages of obesity.

Bibliography

I: Journal articles

1. **Abbate A, Bussani R, Amin MS, Vetrovec GW and Baldi A.** Acute myocardial infarction and heart failure: role of apoptosis. *Int.J.Biochem.Cell Biol.* 38: 11: 1834-1840, 2006.
2. **Adrain C and Martin SJ.** The mitochondrial apoptosome: a killer unleashed by the cytochrome seas. *Trends Biochem.Sci.* 26: 6: 390-397, 2001.
3. **Aguilera C, Gil-Campos M and Canete R.** Alterations in plasma and tissue lipids associated with obesity and metabolic syndrome. *Clin.Sci.* 114: 183-193, 2008.
4. **Aharinejad S, Andrukhova O, Lucas T, Zuckermann A, Wieselthaler G, Wolner E and Grimm M.** Programmed cell death in idiopathic dilated cardiomyopathy is mediated by suppression of the apoptosis inhibitor Apollon. *Ann.Thorac.Surg.* 86: 1: 109-114, 2008.
5. **Ahmad N, Wang Y, Haider KH, Wang B, Pasha Z, Uzun Ö and Ashraf M.** Cardiac protection by mitoKATP channels is dependent on Akt translocation from cytosol to mitochondria during late preconditioning. *American Journal of Physiology - Heart and Circulatory Physiology* 290: 6: H2402-H2408, 2006.
6. **Anarkooli I, Sankian M, Ahmadpour S, Varasteh ARZ and Haghir H.** Evaluation of Bcl-2 family gene expression and caspase-3 activity in hippocampus STZ-induced diabetic rats. *Experimental Diabetes Research*, 6 pages: 1-6, 2008.
7. **Anversa P, Cheng W, Liu Y, Leri A, Redaelli G and Kajstura J.** Apoptosis and myocardial infarction. *Basic Res.Cardiol.* 93: 8-12, 1998.

8. **Arkan MC, Hevener AL, Greten FR, Maeda S, Li ZW, Long JM, Wynshaw-Boris A, Poli G, Olefsky J and Karin M.** IKK-β links inflammation to obesity-induced insulin resistance. *Nat.Med.* 11: 2: 191-198, 2005.
9. **Attallah H, Friedlander AL and Hoffman AR.** Visceral obesity, impaired glucose tolerance, metabolic syndrome, and growth hormone therapy. *Growth Hormone & IGF Research* 16: Suppl A: S62-S67, 2006.
10. **Baines CP and Molkentin JD.** STRESS signaling pathways that modulate cardiac myocyte apoptosis. *J.Mol.Cell.Cardiol.* 38: 1: 47-62, 2005.
11. **Barger PM and Kelly DP.** PPAR signaling in the control of cardiac energy metabolism. *Trends Cardiovasc.Med.* 10: 6: 238, 2000.
12. **Barkett M and Gilmore TD.** Control of apoptosis by Rel/NF-kappaB transcription factors. *Oncogene* 18: 49: 6910, 1999.
13. **Barouch LA, Gao D, Chen L, Miller KL, Xu W, Phan AC, Kittleson MM, Minhas KM, Berkowitz DE and Wei C.** Cardiac myocyte apoptosis is associated with increased DNA damage and decreased survival in murine models of obesity. *Circ.Res.* 98: 1: 119-124, 2006.
14. **Belfiore F, Iannello S and Volpicelli G.** Insulin sensitivity indices calculated from basal and OGTT-induced insulin, glucose, and FFA levels. *Mol.Genet.Metab.* 63: 2: 134-141, 1998.
15. **Beltrami CA, Finato N, Rocco M, Feruglio GA, Puricelli C, Cigola E, Sonnenblick EH, Olivetti G and Anversa P.** The cellular basis of dilated cardiomyopathy in humans. *J.Mol.Cell.Cardiol.* 27: 1: 291-305, 1995.
16. **Benard G, Bellance N, James D, Parrone P, Fernandez H, Letellier T and Rossignol R.** Mitochondrial bioenergetics and structural network organization. *Journal of Cell Science* 120: 5: 838-848, 2007.

17. **Bennett MR.** Apoptosis in the cardiovascular system. *Heart* 87: 5: 480-487, 2002.

18. **Bergman RN, Kim SP, Hsu IR, Catalano KJ, Chiu JD, Kabir M, Richey JM and Ader M.** Abdominal obesity: role in the pathophysiology of metabolic disease and cardiovascular risk. The *American Journal of Medicine* 120: 2: S3-S8, 2007.

19. **Bernardi P.** Mitochondrial transport of cations: channels, exchangers, and permeability transition. *Physiological Reviews* 79: 4: 1127-1155, 1999.

20. **Bernecker OY, Huq F, Heist EK, Podesser BK and Hajjar RJ.** Apoptosis in heart failure and the senescent heart. *Cardiovascular Research* 3: 3: 183-190, 2003.

21. **Bertrand L, Horman S, Beauloye C and Vanoverschelde JL.** Insulin signalling in the heart. *Cardiovascular.Research* 79: 2: 238-248, 2008.

22. **Bieler G, Hasmim M, Monnier Y, Imaizumi N, Ameyar M, Bamat J, Ponsonnet L, Chouaib S, Grell M and Goodman S.** Distinctive role of integrin-mediated adhesion in TNF-induced PKB/Akt and NF-κB activation and endothelial cell survival. *Oncogene* 26: 39: 5722-5732, 2007.

23. **Bishopric NH, Andreka P, Slepak T and Webster KA.** Molecular mechanisms of apoptosis in the cardiac myocyte. *Current Opinion in Pharmacology* 1: 2: 141-150, 2001.

24. **Bonen A, Luiken JJFP and Glatz JFC.** Regulation of fatty acid transport and membrane transporters in health and disease. *Molecular & Cellular Biochemistry* 239: 1: 181-192, 2002.

25. **Bonnard C, Durand A, Peyrol S, Chanseaume E, Chauvin MA, Morio B, Vidal H and Rieusset J.** Mitochondrial dysfunction results from oxidative stress in the skeletal muscle of diet-induced insulin-resistant mice. The *Journal of Clinical Investigation* 118: 2: 789, 2008.

26. **Boudina S, Sena S, O'Neill BT, Tathireddy P, Young ME and Abel ED.** Reduced mitochondrial oxidative capacity and increased mitochondrial uncoupling impair myocardial energetics in obesity. *Circulation* 112: 17: 2686-2695, 2005.

27. **Boura-Halfon S and Zick Y.** Phosphorylation of IRS proteins, insulin action, and insulin resistance. *American Journal of Physiology - Endocrinology and Metabolism* 296: 4: E581-E591, 2009.

28. **Bradford MM.** A rapid and sensitive method for the quantitation of microgram quantities of protein utilizing the principle of protein-dye binding. *Analytical Biochemistry* 72: 1-2: 248-254, 1976.

29. **Brocheriou V, Hagège AA, Oubenaïssa A, Lambert M, Mallet VO, Duriez M, Wassef M, Kahn A, Menasché P and Gilgenkrantz H.** Cardiac functional improvement by a human Bcl-2 transgene in a mouse model of ischemia/reperfusion injury. *The Journal of Gene Medicine* 2: 5: 326-333, 2000.

30. **Brunet A, Bonni A, Zigmond MJ, Lin MZ, Juo P, Hu LS, Anderson MJ, Arden KC, Blenis J and Greenberg ME.** Akt promotes cell survival by phosphorylating and inhibiting a Forkhead transcription factor. *Cell* 96: 857-868, 1999.

31. **Burgering BMT and Medema RH.** Decisions on life and death: FOXO Forkhead transcription factors are in command when PKB/Akt is off duty. *J.Leukoc.Biol.* 73: 6: 689-701, 2003.

32. **Burow ME, Weldon CB, Melnik LI, Duong BN, Collins-Burow BM, Beckman BS and McLachlan JA.** PI3-K/AKT regulation of NF-κB signaling events in suppression of TNF-induced apoptosis. *Biochemical and Biophysical Research Communications* 271: 2: 342-345, 2000.

33. **Cai D, Yuan M, Frantz DF, Melendez PA, Hansen L, Lee J and Shoelson SE.** Local and systemic insulin resistance resulting from hepatic activation of IKK-β and NF-κB. *Nature Medicine* 11: 2: 183-190, 2005.

34. **Candé C, Cohen I, Daugas E, Ravagnan L, Larochette N, Zamzami N and Kroemer G.** Apoptosis-inducing factor (AIF): a novel caspase-independent death effector released from mitochondria. *Biochimie* 84: 2-3: 215, 2002.

35. **Capano M and Crompton M.** Bax translocates to mitochondria of heart cells during simulated ischaemia: involvement of AMP-activated and p38 mitogen-activated protein kinases. *Biochem. J.* 395: Pt 1: 57-64, 2006.

36. **Carroll J, Fearnley IM, Shannon RJ, Hirst J and Walker JE.** Analysis of the subunit composition of complex I from bovine heart mitochondria. *Molecular & Cellular Proteomics* 2: 117-126, 2003.

37. **Cartron PF, Gallenne T, Bougras G, Gautier F, Manero F, Vusio P, Meflah K, Vallette FM and Juin P.** The first α helix of Bax plays a necessary role in its ligand-induced activation by the BH3-only proteins Bid and PUMA. *Molecular Cell* 16: 5: 807-818, 2004.

38. **Carvalho G, Pelletier P, Albacker T, Lachapelle K, Joanisse DR, Hatzakorzian R, Lattermann R, Sato H, Marette A and Schricker T.** Cardioprotective effects of glucose and insulin administration while maintaining normoglycemia (GIN therapy) in patients undergoing coronary artery bypass grafting. *J Clin Endocrinol Metab* 96: 5: 1469-1477, 2011.

39. **Casademont J and Miró Ò.** Electron transport chain defects in heart failure. *Heart Failure Reviews* 7: 2: 131-139, 2002.

40. **Chabowski A, Coort SLM, Calles-Escandon J, Tandon NN, Glatz JFC, Luiken JJFP and Bonen A.** The subcellular compartmentation of fatty acid transporters is regulated differently by insulin and by AICAR. *FEBS Letters* 579: 11: 2428-2432, 2005.

41. **Chen H and Chan DC.** Emerging functions of mammalian mitochondrial fusion and fission. *Human Molecular Genetics* 14: suppl 2: R283-R289, 2005.

42. **Chen L, Willis SN, Wei A, Smith BJ, Fletcher JI, Hinds MG, Colman PM, Day CL, Adams JM and Huang D.** Differential targeting of prosurvival Bcl-2 proteins by their BH3-only ligands allows complementary apoptotic function. *Molecular Cell* 17: 3: 393-403, 2005.

43. **Chen Q, Moghaddas S, Hoppel CL and Lesnefsky EJ.** Reversible blockade of electron transport during ischemia protects mitochondria and decreases myocardial injury following reperfusion. *The Journal of Pharmacology and Experimental Therapeutics* 319: 3: 1405-1412, 2006.

44. **Chen WS, Xu PZ, Gottlob K, Chen ML, Sokol K, Shiyanova T, Roninson I, Weng W, Suzuki R and Tobe K.** Growth retardation and increased apoptosis in mice with homozygous disruption of the Akt1 gene. *Genes & Development* 15: 17: 2203-2208, 2001.

45. **Chen Z, Chua CC, Ho YS, Hamdy RC and Chua BHL.** Overexpression of Bcl-2 attenuates apoptosis and protects against myocardial I/R injury in transgenic mice. *Molecular Cell* 280: 5: H2313-H2320, 2001.

46. **Ching C, Zhao B and Yang Z.** Enzyme activity and high-fat diet: citrate synthase activity in myostatin propeptide transgenic and wild-type mice. *Ethnicity & Disease* 18: S1: 18-19, 2008.

47. **Cho H, Mu J, Kim JK, Thorvaldsen JL, Chu Q, Crenshaw III EB, Kaestner KH, Bartolomei MS, Shulman GI and Birnbaum MJ.** Insulin resistance and a diabetes

mellitus-like syndrome in mice lacking the protein kinase Akt2 (PKBβ). *Science* 292: 5522: 1728, 2001.

48. **Ciaraldi TP, Oh DK, Christiansen L, Nikoulina SE, Kong APS, Baxi S, Mudaliar S and Henry RR.** Tissue-specific expression and regulation of GSK-3 in human skeletal muscle and adipose tissue. *American Journal of Physiology - Endocrinology and Metabolism* 291: 5: E891-E898, 2006.
49. **Clarke MCH, Littlewood TD, Figg N, Maguire JJ, Davenport AP, Goddard M and Bennett MR.** Chronic apoptosis of vascular smooth muscle cells accelerates atherosclerosis and promotes calcification and medial degeneration. *Circulation Research* 102: 12: 1529-1538, 2008.
50. **Clerk A, Cole SM, Cullingford TE, Harrison JG, Jormakka M and Valks DM.** Regulation of cardiac myocyte cell death. *Pharmacol.Ther.* 97: 3: 223-261, 2003.
51. **Clohessy JG, Zhuang J, de Boer J, Gil-Gómez G and Brady HJM.** Mcl-1 interacts with truncated Bid and inhibits its induction of cytochrome c release and its role in receptor-mediated apoptosis. *J.Biol.Chem.* 281: 9: 5750-5759, 2006.
52. **Coort SLM, Bonen A, van der Vusse GJ, Glatz JFC and Luiken JJFP.** Cardiac substrate uptake and metabolism in obesity and type-2 diabetes: role of sarcolemmal substrate transporters. *Mol.Cell.Biochem.* 299: 1: 5-18, 2007.
53. **Coort SLM, Hasselbaink DM, Koonen DPY, Willems J, Coumans WA, Chabowski A, van der Vusse GJ, Bonen A, Glatz JFC and Luiken JJFP.** Enhanced sarcolemmal FAT/CD36 content and triacylglycerol storage in cardiac myocytes from obese zucker rats. *Diabetes* 53: 7: 1655-1663, 2004.
54. **Cory S, Huang DCS and Adams JM.** The Bcl-2 family: roles in cell survival and oncogenesis. *Oncogene* 22: 53: 8590-8607, 2003.

55. **Côté J and Ruiz-Carrillo A.** Primers for mitochondrial DNA replication generated by endonuclease G. *Science* 261: 5122: 765, 1993.

56. **Crompton M, Barksby E, Johnson N and Capano M.** Mitochondrial intermembrane junctional complexes and their involvement in cell death. *Biochimie* 84: 2-3: 143, 2002.

57. **Crow MT, Mani K, Nam YJ and Kitsis RN.** The mitochondrial death pathway and cardiac myocyte apoptosis. *Circ.Res.* 95: 10: 957-970, 2004.

58. **Danial N.** BAD: undertaker by night, candyman by day. *Oncogene* 27: S53-S70, 2008.

59. **Das S, Wong R, Rajapakse N, Murphy E and Steenbergen C.** Glycogen synthase kinase 3 inhibition slows mitochondrial adenine nucleotide transport and regulates voltage-dependent anion channel phosphorylation. *Circ.Res.* 103: 9: 983-991, 2008.

60. **Datta SR, Brunet A and Greenberg ME.** Cellular survival: a play in three Akts. *Genes Dev.* 13: 22: 2905-2927, 1999.

61. **Davies M.** The cardiomyopathies: an overview. *Heart* 83: 4: 469-474, 2000.

62. **Delcommenne M, Tan C, Gray V, Rue L, Woodgett J and Dedhar S.** Phosphoinositide-3-OH kinase-dependent regulation of glycogen synthase kinase 3 and protein kinase B/AKT by the integrin-linked kinase. *Proc. Natl. Acad. Sci.* 95: 19: 11211-11216, 1998.

63. **Depre C and Vatner SF.** Mechanisms of cell survival in myocardial hibernation. *Trends Cardiovasc.Med.* 15: 3: 101-110, 2005.

64. **Di Lisa F and Bernardi P.** Mitochondria and ischemia–reperfusion injury of the heart: fixing a hole. *Cardiovasc.Res.* 70: 2: 191-199, 2006.

65. **Dijkers PF, Birkenkamp KU, Lam EWF, Thomas NSB, Lammers JWJ, Koenderman L and Coffer PJ.** FKHR-L1 can act as a critical effector of cell death induced by cytokine withdrawal protein kinase B–enhanced cell survival through maintenance of mitochondrial integrity. *J.Cell Biol.* 156: 3: 531-542, 2002.

66. **DiMauro S and Rustin P.** A critical approach to the therapy of mitochondrial respiratory chain and oxidative phosphorylation diseases. *Biochimica et Biophysica Acta* 1792: 12: 1159-1167, 2009.

67. **Dive C, Gregory CD, Phipps DJ, Evans DL, Milner AE and Wyllie AH.** Analysis and discrimination of necrosis and apoptosis (programmed cell death) by multiparameter flow cytometry. *Biochim.Biophys.Acta* 1133: 3: 275, 1992.

68. **Doble BW and Woodgett JR.** GSK-3: tricks of the trade for a multi-tasking kinase. *J.Cell.Sci.* 116: 7: 1175-1186, 2003.

69. **Dokken BB, Sloniger JA and Henriksen EJ.** Acute selective glycogen synthase kinase-3 inhibition enhances insulin signaling in prediabetic insulin-resistant rat skeletal muscle. *Am J Physiol Endocrinol Metab* 288: 6: E1188-E1194, 2005.

70. **Dong Y, Undyala VV, Gottlieb RA, Mentzer Jr RM and Przyklenk K.** Review: Autophagy: definition, molecular machinery, and potential role in myocardial ischemia-reperfusion injury. *J.Cardiovasc.Pharmacol.Ther.* 15: 3: 220-230, 2010.

71. **Doran E and Halestrap AP.** Cytochrome c release from isolated rat liver mitochondria can occur independently of outer-membrane rupture: possible role of contact sites. *Biochem.J.* 348: Pt 2: 343-350, 2000.

72. **Downey JM, Davis AM and Cohen MV.** Signaling pathways in ischemic preconditioning. *Heart Fail. Rev.* 12: 181–188, 2007.

73. **Downward J.** Cell biology: metabolism meets death. *Nature* 424: 6951: 896-897, 2003.

74. **Dragovich T, Rudin CM and Thompson CB.** Signal transduction pathways that regulate cell survival and cell death. *Oncogene* 17: 25: 3207-3213, 1998.

75. **Du Toit EF, Smith W, Muller C, Strijdom H, Stouthammer B, Woodiwiss AJ, Norton GR and Lochner A.** Myocardial susceptibility to ischemic-reperfusion injury in

a prediabetic model of dietary-induced obesity. *Am J Physiol Heart Circ Physiol* 294: 5: H2336-H2343, 2008.

76. **Du C, Fang M, Li Y, Li L and Wang X.** Smac, a mitochondrial protein that promotes cytochrome c-dependent caspase activation by eliminating IAP inhibition. *Cell* 102: 1: 33-42, 2000.
77. **Duronio V.** The life of a cell: apoptosis regulation by the PI3K/PKB pathway. *Biochem.J.* 415: 333-344, 2008.
78. **Edwards RJ, Saurin AT, Rakhit RD and Marber MS.** Therapeutic potential of ischaemic preconditioning. *Br.J.Clin.Pharmacol.* 50: 2: 87-97, 2000.
79. **Eichhorn EJ and Bristow MR.** Medical therapy can improve the biological properties of the chronically failing heart: a new era in the treatment of heart failure. *Circulation* 94: 9: 2285-2296, 1996.
80. **Eldar-Finkelman H and Krebs EG.** Phosphorylation of insulin receptor substrate 1 by glycogen synthase kinase 3 impairs insulin action. *Proc. Natl. Acad. Sci* 94: 18: 9660-9664, 1997.
81. **Eldar-Finkelman H, Schreyer SA, Shinohara MM, LeBoeuf RC and Krebs EG.** Increased glycogen synthase kinase-3 activity in diabetes-and obesity-prone C57BL/6J mice. *Diabetes* 48: 8: 1662-1666, 1999.
82. **Emily HYAC, Wei MC, Weiler S, Flavell RA, Mak TW, Lindsten T and Korsmeyer SJ.** BCL-2, BCL-XL sequester BH3 domain-only molecules preventing BAX-and BAK-mediated mitochondrial apoptosis. *Mol.Cell* 8: 705-711, 2001.
83. **Cheng EHYA, Wei MC, Weiler S, Flavell RA, Mak TW, Lindsten T and Korsmeyer SJ.** BCL-2, BCL-XL sequester BH3 domain-only molecules preventing BAX-and BAK-mediated mitochondrial apoptosis. *Mol.Cell* 8: 705-711, 2001.

84. **Enari M, Sakahira H, Yokoyama H, Okawa K, Iwamatsu A and Nagata S.** A caspase-activated DNase that degrades DNA during apoptosis, and its inhibitor ICAD. *Nature* 391: 6662: 43-50, 1998.

85. **Faergeman NJ and Knudsen J.** Acyl-CoA binding protein is an essential protein in mammalian cell lines. *Biochem.J.* 368: Pt 3: 679-682, 2002.

86. **Fall CHD, Sachdev HS, Osmond C, Lakshmy R, Biswas SD, Prabhakaran D, Tandon N, Ramji S, Reddy KS and Barker DJP.** Adult metabolic syndrome and impaired glucose tolerance are associated with different patterns of BMI gain during infancy data from the New Delhi birth cohort. *Diabetes Care* 31: 12: 2349-2356, 2008.

87. **Fantin VR, Wang Q, Lienhard GE and Keller SR.** Mice lacking insulin receptor substrate 4 exhibit mild defects in growth, reproduction, and glucose homeostasis. *Am J Physiol Endocrinol Metab* 278: 1: E127-E133, 2000.

88. **Ferrannini E.** Insulin resistance versus insulin deficiency in non-insulin-dependent diabetes mellitus: problems and prospects. *Endocr.Rev.* 19: 4: 477-490, 1998.

89. **Festjens N, Vanden Berghe T and Vandenabeele P.** Necrosis, a well-orchestrated form of cell demise: signalling cascades, important mediators and concomitant immune response. *Biochimica et Biophysica Acta* 1757: 9: 1371-1387, 2006.

90. **Fliss H and Gattinger D.** Apoptosis in ischemic and reperfused rat myocardium. *Circ.Res.* 79: 5: 949-956, 1996.

91. **Frame S and Cohen P.** GSK3 takes centre stage more than 20 years after its discovery. *Biochem.J.* 359: Pt 1: 1-16, 2001.

92. **Franke TF, Kaplan DR and Cantley LC.** PI3K: downstream AKTion blocks apoptosis. *Cell* 88: 4: 435, 1997.

93. **Fujioka S, Matsuzawa Y, Tokunaga K and Tarui S.** Contribution of intra-abdominal fat accumulation to the impairment of glucose and lipid metabolism in human obesity. *Metab.Clin.Exp.* 36: 1: 54-59, 1987.

94. **Gao HK, Yin Z, Zhou N, Feng XY, Gao F and Wang HC.** Glycogen synthase kinase 3 inhibition protects the heart from acute ischemia-reperfusion injury via inhibition of inflammation and apoptosis. *J.Cardiovasc.Pharmacol.* 52: 3: 286, 2008.

95. **Garcia-Dorado D, Rodriguez-Sinovas A, Ruiz-Meana M, Inserte J, Agulló L and Cabestrero A.** The end-effectors of preconditioning protection against myocardial cell death secondary to ischemia–reperfusion. *Cardiovasc.Res.* 70: 2: 274-285, 2006.

96. **Gardai SJ, Hildeman DA, Frankel SK, Whitlock BB, Frasch SC, Borregaard N, Marrack P, Bratton DL and Henson PM.** Phosphorylation of Bax Ser184 by Akt regulates its activity and apoptosis in neutrophils. *J.Biol.Chem.* 279: 20: 21085-21095, 2004.

97. **Gargiulo CE, Stuhlsatz-Krouper SM and Schaffer JE.** Localization of adipocyte long-chain fatty acyl-CoA synthetase at the plasma membrane. *J.Lipid Res.* 40: 5: 881-892, 1999.

98. **Gawryluk RMR, Chisholm KA, Pinto DM and Gray MW.** Composition of the mitochondrial electron transport chain in Acanthamoeba castellanii: Structural and evolutionary insights. *Biochimica et Biophysica Acta* 1817: 2027–2037, 2012.

99. **Gawryluk RMR and Gray MW.** A split and rearranged nuclear gene encoding the iron-sulfur subunit of mitochondrial succinate dehydrogenase in Euglenozoa. *BMC Research Notes* 2: 1: 16, 2009.

100. **Ghisla S.** β-Oxidation of fatty acids. *Eur. J. Biochem*. 271: 3: 459-461, 2004.

101. **Glatz JFC and Storch J.** Unravelling the significance of cellular fatty acid-binding proteins. *Curr.Opin.Lipidol.* 12: 3: 267-274, 2001.

102. **Gogvadze V, Orrenius S and Zhivotovsky B.** Multiple pathways of cytochrome *c* release from mitochondria in apoptosis. Biochimica et Biophysica Acta 1757: 5: 639-647, 2006.

103. **Gomez L, Paillard M, Thibault H, Derumeaux G and Ovize M.** Inhibition of GSK3β by postconditioning is required to prevent opening of the mitochondrial permeability transition pore during reperfusion. *Circulation* 117: 21: 2761-2768, 2008.

104. **Gomez-Bougie P, Bataille R and Amiot M.** The imbalance between Bim and Mcl-1 expression controls the survival of human myeloma cells. *Eur.J.Immunol.* 34: 11: 3156-3164, 2004.

105. **Goodpaster BH and Wolf D.** Skeletal muscle lipid accumulation in obesity, insulin resistance, and type 2 diabetes. *Pediatric Diabetes* 5: 4: 219-226, 2004.

106. **Gottlieb RA.** Mitochondria: ignition chamber for apoptosis. *Mol.Genet.Metab.* 68: 2: 227-231, 1999.

107. **Gottlob K, Majewski N, Kennedy S, Kandel E, Robey RB and Hay N.** Inhibition of early apoptotic events by Akt/PKB is dependent on the first committed step of glycolysis and mitochondrial hexokinase. *Genes Dev.* 15: 11: 1406, 2001.

108. **Gray S and Kim JK.** New insights into insulin resistance in the diabetic heart. *Trends in Endocrinology and Metabolism* 22: 10: 394-403, 2011.

109. **Gross A, McDonnell JM and Korsmeyer SJ.** BCL-2 family members and the mitochondria in apoptosis. *Genes Dev.* 13: 15: 1899-1911, 1999.

110. **Gupta S.** Molecular steps of death receptor and mitochondrial pathways of apoptosis. *Life Sci.* 69: 25: 2957-2964, 2001.

111. **Gustafsson ÅB and Gottlieb RA.** Bcl-2 family members and apoptosis, taken to heart. *Am J Physiol Cell Physiol* 292: 1: C45-C51, 2007.

112. **Hajduch E, Litherland GJ and Hundal HS.** Protein kinase B (PKB/Akt)–a key regulator of glucose transport? *FEBS Letters* 492: 3: 199-203, 2001.

113. **Hajri T and Abumrad NA.** Fatty acid transport across membranes: Relevance to nutrition and metabolic pathology 1. *Annu.Rev.Nutr.* 22: 1: 383-415, 2001.

114. **Halestrap A.** Calcium, mitochondria and reperfusion injury: a pore way to die. *Biochem.Soc.Trans.* 34: 232-237, 2006.

115. **Halestrap AP, Clarke SJ and Javadov SA.** Mitochondrial permeability transition pore opening during myocardial reperfusion—a target for cardioprotection. *Cardiovasc.Res.* 61: 3: 372-385, 2004.

116. **Halestrap AP, Clarke SJ and Khaliulin I.** The role of mitochondria in protection of the heart by preconditioning. *Biochimica et Biophysica Acta* 1767: 8: 1007-1031, 2007.

117. **Halestrap AP, Kerr PM, Javadov S and Woodfield K.** Elucidating the molecular mechanism of the permeability transition pore and its role in reperfusion injury of the heart. *Biochim.Biophys.Acta* 1366: 1-2: 79, 1998.

118. **Hall JE, Crook ED, Jones DW, Wofford MR and Dubbert PM.** Mechanisms of obesity-associated cardiovascular and renal disease. *Am.J.Med.Sci.* 324: 3: 127-137, 2002.

119. **Hamacher-Brady A, Brady NR, Logue S, Sayen M, Jinno M, Kirshenbaum L, Gottlieb R and Gustafsson ÅB.** Response to myocardial ischemia/reperfusion injury involves Bnip3 and autophagy. *Cell Death and Differentiation* 14: 1: 146-157, 2006.

120. **Han J, Goldstein LA, Gastman BR, Froelich CJ, Yin XM and Rabinowich H.** Degradation of Mcl-1 by granzyme B. *J.Biol.Chem.* 279: 21: 22020-22029, 2004.

121. **Harada H, Quearry B, Ruiz-Vela A and Korsmeyer SJ.** Survival factor-induced extracellular signal-regulated kinase phosphorylates BIM, inhibiting its association with BAX and proapoptotic activity. *Proc.Natl.Acad.Sci.U.S.A.* 101: 43: 15313-15317, 2004.

122. **Hausenloy DJ, Tsang A and Yellon DM.** The reperfusion injury salvage kinase pathway: a common target for both ischemic preconditioning and postconditioning. *Trends Cardiovasc.Med.* 15: 2: 69-75, 2005.

123. **Hausenloy DJ and Yellon DM.** Reperfusion injury salvage kinase signalling: taking a RISK for cardioprotection. *Heart Fail.Rev.* 12: 3: 217-234, 2007.

124. **Hausenloy DJ and Yellon DM.** Survival kinases in ischemic preconditioning and postconditioning. *Cardiovasc.Res.* 70: 2: 240-253, 2006.

125. **Hayden MS and Ghosh S.** Signaling to NF-κB. *Genes Dev.* 18: 18: 2195-2224, 2004.

126. **Hemmings BA.** Akt signaling-linking membrane events to life and death decisions. *Science* 275: 5300: 628-630, 1997.

127. **Henriksen EJ and Dokken BB.** Role of glycogen synthase kinase-3 in insulin resistance and type 2 diabetes. *Current Drug Targets* 7: 11: 1435-1442, 2006.

128. **Heusch G, Schulz R and Rahimtoola SH.** Myocardial hibernation: a delicate balance. *Am J Physiol Heart Circ Physiol* 288: 3: H984-H999, 2005.

129. **Hill MM and Hemmings BA.** Inhibition of protein kinase B/Akt: implications for cancer therapy. *Pharmacol.Ther.* 93: 2: 243-251, 2002.

130. **Hirotani S, Zhai P, Tomita H, Galeotti J, Marquez JP, Gao S, Hong C, Yatani A, Avila J and Sadoshima J.** Inhibition of glycogen synthase kinase 3β during heart failure is protective. *Circ.Res.* 101: 11: 1164-1174, 2007.

131. **Hochhauser E, Kivity S, Offen D, Maulik N, Otani H, Barhum Y, Pannet H, Shneyvays V, Shainberg A and Goldshtaub V.** Bax ablation protects against myocardial ischemia-reperfusion injury in transgenic mice. *Am J Physiol Heart Circ Physiol* 284: 6: H2351-H2359, 2003.

132. **Holloway G, Luiken J, Glatz J, Spriet L and Bonen A.** Contribution of FAT/CD36 to the regulation of skeletal muscle fatty acid oxidation: an overview. *Acta Physiol* 194: 4: 293-309, 2008.

133. **Huang XF and Chen JZ.** Obesity, the PI3K/Akt signal pathway and colon cancer. *Obesity Reviews* 10: 6: 610-616, 2009.

134. **Huisamen B, Dietrich D, Bezuidenhout N, Lopes J, Flepisi B, Blackhurst D and Lochner A.** Early cardiovascular changes occurring in diet-induced, obese insulin-resistant rats. *Mol.Cell.Biochem* 368: 37–45, 2012.

135. **Huss JM and Kelly DP.** Mitochondrial energy metabolism in heart failure: a question of balance. *J.Clin.Invest.* 115: 3: 547-555, 2005.

136. **Iliadis F, Kadoglou N and Didangelos T.** Insulin and the heart. *Diabetes Res.Clin.Pract.* 93: S86-S91, 2011.

137. **Imahashi K, Schneider MD, Steenbergen C and Murphy E.** Transgenic expression of Bcl-2 modulates energy metabolism, prevents cytosolic acidification during ischemia, and reduces ischemia/reperfusion injury. *Circ.Res.* 95: 7: 734-741, 2004.

138. **Iwakuma T and Lozano G.** MDM2, an introduction. *Mol Cancer Res* 1: 14: 993-1000, 2003.

139. **Iwata S, Lee JW, Okada K, Lee JK, Iwata M, Rasmussen B, Link TA, Ramaswamy S and Jap BK.** Complete structure of the 11-subunit bovine mitochondrial cytochrome bc1 complex. *Science* 281: 5373: 64-71, 1998.

140. **Jain SS, Snook LA, Glatz JFC, Luiken JJFP, Holloway GP, Thurmond DC and Bonen A.** Munc18c provides stimulus-selective regulation of GLUT4 but not fatty acid transporter trafficking in skeletal muscle. *FEBS Lett*ers 586, 2012.

141. **Jarreta D, Orús J, Barrientos A, Miró O, Roig E, Heras M, Moraes CT, Cardellach F and Casademont J.** Mitochondrial function in heart muscle from patients with idiopathic dilated cardiomyopathy. *Cardiovasc.Res.* 45: 4: 860-865, 2000.

142. **Jemmerson R and Wang X.** Induction of apoptotic program in cell-free extracts: requirement for dATP and cytochrome c. *Cell* 86: 147-157, 1996.

143. **Jiang X and Wang X.** Cytochrome c promotes caspase-9 activation by inducing nucleotide binding to Apaf-1. *J.Biol.Chem.* 275: 40: 31199-31203, 2000.

144. **Jonassen AK, Sack MN, Mjøs OD and Yellon DM.** Myocardial protection by insulin at reperfusion requires early administration and is mediated via Akt and p70s6 kinase cell-survival signaling. *Circ.Res.* 89: 12: 1191-1198, 2001.

145. **Jope RS and Johnson GVW.** The glamour and gloom of glycogen synthase kinase-3. *Trends Biochem.Sci.* 29: 2: 95-102, 2004.

146. **Juhaszova M, Wang S, Zorov DB, Bradley Nuss H, Gleichmann M, Mattson MP and Sollott SJ.** The identity and regulation of the mitochondrial permeability transition pore. *Ann.N.Y.Acad.Sci.* 1123: 1: 197-212, 2008.

147. **Juhaszova M, Zorov DB, Kim SH, Pepe S, Fu Q, Fishbein KW, Ziman BD, Wang S, Ytrehus K and Antos CL.** Glycogen synthase kinase-3 beta mediates convergence of protection signaling to inhibit the mitochondrial permeability transition pore. *J.Clin.Invest.* 113: 11: 1535-1549, 2004.

148. **Kahn R, Wareham N and Zinman B** (on behalf of the The Expert Committee). Report of the Expert Committee on the Diagnosis and Classification of Diabetes Mellitus. *Diabetes Care* 20: 7: 1183-1197, 1997.

149. **Kahn SE, Hull RL and Utzschneider KM.** Mechanisms linking obesity to insulin resistance and type 2 diabetes. *Nature* 444: 7121: 840-846, 2006.

150. **Kalra J, Sutherland B, Stratford A, Dragowska W, Gelmon K, Dedhar S, Dunn S and Bally M.** Suppression of Her2/neu expression through ILK inhibition is regulated by a pathway involving TWIST and YB-1. *Oncogene* 29: 48: 6343-6356, 2010.

151. **Kane LP, Shapiro VS, Stokoe D and Weiss A.** Induction of NF-κB by the Akt/PKB kinase. *Current Biology* 9: 11: 601-604, 1999.

152. **Kato K, Yin H, Agata J, Yoshida H, Chao L and Chao J.** Adrenomedullin gene delivery attenuates myocardial infarction and apoptosis after ischemia and reperfusion. *Am J Physiol Heart Circ Physiol* 285: 4: H1506-H1514, 2003.

153. **Katz AM.** The cardiomyopathy of overload: an unnatural growth response in the hypertrophied heart. *Ann.Intern.Med.* 121: 5: 363, 1994.

154. **Kemi OJ, Ceci M, Wisloff U, Grimaldi S, Gallo P, Smith GL, Condorelli G and Ellingsen O.** Activation or inactivation of cardiac Akt/mTOR signaling diverges physiological from pathological hypertrophy. *J.Cell.Physiol.* 214: 2: 316-321, 2008.

155. **Kennedy SG, Kandel ES, Cross TK and Hay N.** Akt/Protein kinase B inhibits cell death by preventing the release of cytochrome c from mitochondria. *Mol.Cell.Biol.* 19: 8: 5800-5810, 1999.

156. **Kevin LG, Camara AKS, Riess ML, Novalija E and Stowe DF.** Ischemic preconditioning alters real-time measure of O2 radicals in intact hearts with ischemia and reperfusion. *Am J Physiol Heart Circ Physiol* 284: 2: H566-H574, 2003.

157. **Kharas MG and Fruman DA.** ABL oncogenes and phosphoinositide 3-kinase: mechanism of activation and downstream effectors. *Cancer Res.* 65: 6: 2047-2053, 2005.

158. **Kim J, Wei Y and Sowers JR.** Role of mitochondrial dysfunction in insulin resistance. *Circ.Res.* 102: 4: 401-414, 2008.

159. **Kloner RA and Rezkalla SH.** Preconditioning, postconditioning and their application to clinical cardiology. *Cardiovasc.Res.* 70: 2: 297-307, 2006.

160. **Knudsen J, Neergaard TBF, Gaigg B, Jensen MV and Hansen JK.** Role of acyl-CoA binding protein in acyl-CoA metabolism and acyl-CoA–mediated cell signaling. *J.Nutr.* 130: 2: 294S-298S, 2000.

161. **Kobayashi T and Cohen P.** Activation of serum-and glucocorticoid-regulated protein kinase by agonists that activate phosphatidylinositide 3-kinase is mediated by 3-phosphoinositide-dependent protein kinase-1 (PDK1) and PDK2. *Biochem.J.* 339: Pt 2: 319-328, 1999.

162. **Koonen DPY, Glatz JFC, Bonen A and Luiken JJFP.** Long-chain fatty acid uptake and FAT/CD36 translocation in heart and skeletal muscle. *Biochimica et Biophysica Acta* 1736: 3: 163-180, 2005.

163. **Krysko DV, Vanden Berghe T, D'Herde K and Vandenabeele P.** Apoptosis and necrosis: detection, discrimination and phagocytosis. *Methods* 44: 3: 205-221, 2008.

164. **Kuwahara K, Saito Y, Kishimoto I, Miyamoto Y, Harada M, Ogawa E, Hamanaka I, Kajiyama N, Takahashi N and Izumi T.** Cardiotrophin-1 phosphorylates akt and BAD, and prolongs cell survival via a PI3K-dependent pathway in cardiac myocytes. *J.Mol.Cell.Cardiol.* 32: 8: 1385-1394, 2000.

165. **Kuwana T, Bouchier-Hayes L, Chipuk JE, Bonzon C, Sullivan BA, Green DR and Newmeyer DD.** BH3 domains of BH3-only proteins differentially regulate Bax-mediated mitochondrial membrane permeabilization both directly and indirectly. *Mol.Cell* 17: 4: 525-536, 2005.

166. **Kuwana T, Mackey MR, Perkins G, Ellisman MH, Latterich M, Schneiter R, Green DR and Newmeyer DD.** Bid, Bax, and lipids cooperate to form supramolecular openings in the outer mitochondrial membrane. *Cell* 111: 3: 331-342, 2002.

167. **Lanza IR and Nair KS.** Functional assessment of isolated mitochondria *in vitro*. *Meth.Enzymol.* 457: 349-372, 2009.

168. **Lawlor MA and Alessi DR.** PKB/Akt a key mediator of cell proliferation, survival and insulin responses? *J.Cell.Sci.* 114: 16: 2903-2910, 2001.

169. **Lazar M and Harold L.** Enhanced preservation of acutely ischemic myocardium and improved clinical outcomes using glucose-insulin-potassium (GIK) solutions. *Am.J.Cardiol.* 80: 3: 90A-93A, 1997.

170. **Lee J, Xu Y, Lu L, Bergman B, Leitner JW, Greyson C, Draznin B and Schwartz GG.** Multiple abnormalities of myocardial insulin signaling in a porcine model of diet-induced obesity. *Am J Physiol Heart Circ Physiol* 298: 2: H310-H319, 2010.

171. **Lee SD, Kuo WW, Bau DT, Ko FY, Wu FL, Kuo CH, Tsai FJ, Wang PS, Lu MC and Huang CY.** The coexistence of nocturnal sustained hypoxia and obesity additively increases cardiac apoptosis. *J.Appl.Physiol.* 104: 4: 1144-1153, 2008.

172. **Lee Y and Gustafsson ÅB.** Role of apoptosis in cardiovascular disease. *Apoptosis* 14: 4: 536-548, 2009.

173. **Leonard J and Schapira A.** Mitochondrial respiratory chain disorders I: mitochondrial DNA defects. *Lancet* 355: 9200: 299, 2000.

174. **Leung AWC and Halestrap AP.** Recent progress in elucidating the molecular mechanism of the mitochondrial permeability transition pore. *Biochimica et Biophysica Acta* 1777: 7: 946-952, 2008.

175. **Liao B and Xu Y.** Exercise improves skeletal muscle insulin resistance without reduced basal mTOR/S6K1 signaling in rats fed a high-fat diet. *Eur.J.Appl.Physiol.* 111: 11: 2743-2752, 2011.

176. **Liem DA, Honda HM, Zhang J, Woo D and Ping P.** Past and present course of cardioprotection against ischemia-reperfusion injury. *J.Appl.Physiol.* 103: 6: 2129-2136, 2007.

177. **Liesa M, Borda-d'Água B, Medina-Gómez G, Lelliott CJ, Paz JC, Rojo M, Palacín M, Vidal-Puig A and Zorzano A.** Mitochondrial fusion is increased by the nuclear coactivator PGC-1β. *PLoS ONE* 3: 10: e3613: 1-6, 2008.

178. **Liu X, Zou H, Slaughter C and Wang X.** DFF, a heterodimeric protein that functions downstream of caspase-3 to trigger DNA fragmentation during apoptosis. *Cell* 89: 2: 175-184, 1996.

179. **Lopaschuk GD, Folmes CDL and Stanley WC.** Cardiac energy metabolism in obesity. *Circ.Res.* 101: 4: 335-347, 2007.

180. **Lopaschuk GD, Ussher JR, Folmes CDL, Jaswal JS and Stanley WC.** Myocardial fatty acid metabolism in health and disease. *Physiol.Rev.* 90: 1: 207-258, 2010.

181. **Lowry OH, Rosebrough NJ, Farr AL and Randall RJ.** Protein measurement with the Folin phenol reagent. *J.Biol.Chem.* 193: 1: 265-275, 1951.

182. **Lu MC, Tzang BS, Kuo WW, Wu FL, Chen YS, Tsai CH, Huang CY and Lee SD.** More activated cardiac mitochondrial-dependent apoptotic pathway in obese Zucker rats. *OBESITY* 15: 11: 2634-2642, 2007.

183. **Lücker S, Wagner M, Maixner F, Pelletier E, Koch H, Vacherie B, Rattei T, Damsté JSS, Spieck E and Le Paslier D.** A Nitrospira metagenome illuminates the physiology and evolution of globally important nitrite-oxidizing bacteria. *PNAS* 107: 30: 13479-13484, 2010.

184. **Luiken JJFP, Coort SLM, Koonen DPY, Horst DJ, Bonen A, Zorzano A and Glatz JFC.** Regulation of cardiac long-chain fatty acid and glucose uptake by

translocation of substrate transporters. *Pflugers Arch - Eur J Physiol* 448: 1: 1-15, 2004.

185. **Luiken JJFP, Koonen DPY, Willems J, Zorzano A, Becker C, Fischer Y, Tandon NN, Van Der Vusse GJ, Bonen A and Glatz JFC.** Insulin stimulates long-chain fatty acid utilization by rat cardiac myocytes through cellular redistribution of FAT/CD36. *Diabetes* 51: 10: 3113-3119, 2002.

186. **MacAulay K, Doble BW, Patel S, Hansotia T, Sinclair EM, Drucker DJ, Nagy A and Woodgett JR.** Glycogen synthase kinase 3α-specific regulation of murine hepatic glycogen metabolism. *Cell Metabolism* 6: 4: 329-337, 2007.

187. **Majewski N, Nogueira V, Bhaskar P, Coy PE, Skeen JE, Gottlob K, Chandel NS, Thompson CB, Robey RB and Hay N.** Hexokinase-mitochondria interaction mediated by Akt is required to inhibit apoptosis in the presence or absence of Bax and Bak. *Mol.Cell* 16: 5: 819-830, 2004b.

188. **Majewski N, Nogueira V, Robey RB and Hay N.** Akt inhibits apoptosis downstream of BID cleavage via a glucose-dependent mechanism involving mitochondrial hexokinases. *Mol.Cell.Biol.* 24: 2: 730-740, 2004a.

189. **Manning BD and Cantley LC.** AKT/PKB signaling: navigating downstream. *Cell* 129: 7: 1261–1274, 2007.

190. **Masri C and Chandrashekhar Y.** Apoptosis: a potentially reversible, meta-stable state of the heart. *Heart Fail.Rev.* 13: 2: 175-179, 2008.

191. **Matsui T, Tao J, del Monte F, Lee KH, Li L, Picard M, Force TL, Franke TF, Hajjar RJ and Rosenzweig A.** Akt activation preserves cardiac function and prevents injury after transient cardiac ischemia in vivo. *Circulation* 104: 3: 330-335, 2001.

192. **Mattson MP and Kroemer G.** Mitochondria in cell death: novel targets for neuroprotection and cardioprotection. *Trends Mol.Med.* 9: 5: 196-205, 2003.

193. **Maurer U, Charvet C, Wagman AS, Dejardin E and Green DR.** Glycogen synthase kinase-3 regulates mitochondrial outer membrane permeabilization and apoptosis by destabilization of MCL-1. *Mol.Cell* 21: 6: 749-760, 2006.

194. **Mayo LD and Donner DB.** A phosphatidylinositol 3-kinase/Akt pathway promotes translocation of Mdm2 from the cytoplasm to the nucleus. *PNAS* 98: 20: 11598-11603, 2001.

195. **Millar AH, Eubel H, Jänsch L, Kruft V, Heazlewood JL and Braun HP.** Mitochondrial cytochrome c oxidase and succinate dehydrogenase complexes contain plant specific subunits. *Plant Mol.Biol.* 56: 1: 77-90, 2004.

196. **Milne JC, Lambert PD, Schenk S, Carney DP, Smith JJ, Gagne DJ, Jin L, Boss O, Perni RB and Vu CB.** Small molecule activators of SIRT1 as therapeutics for the treatment of type 2 diabetes. *Nature* 450: 7170: 712-716, 2007.

197. **Miramar MD, Costantini P, Ravagnan L, Saraiva LM, Haouzi D, Brothers G, Penninger JM, Peleato ML, Kroemer G and Susin SA.** NADH oxidase activity of mitochondrial apoptosis-inducing factor. *J.Biol.Chem.* 276: 19: 16391-16398, 2001.

198. **Mlinar B, Marc J, Janez A and Pfeifer M.** Molecular mechanisms of insulin resistance and associated diseases. *Clinica Chimica Acta* 375: 1-2: 20-35, 2007.

199. **Mora A, Komander D, van Aalten DMF and Alessi DR.** PDK1, the master regulator of AGC kinase signal transduction. *Seminars in Cell & Developmental Biology* 15: 161-170, 2004.

200. **Morales J, Mogi T, Mineki S, Takashima E, Mineki R, Hirawake H, Sakamoto K, Ōmura S and Kita K.** Novel mitochondrial complex II isolated from Trypanosoma cruzi is composed of 12 peptides including a heterodimeric Ip subunit. *J.Biol.Chem.* 284: 11: 7255-7263, 2009.

201. **Müller V and Grüber G.** ATP synthases: structure, function and evolution of unique energy converters. *Cell. Mol. Life Sci.* 60: 3: 474-494, 2003.

202. **Murphy E and Steenbergen C.** Inhibition of GSK-3beta as a target for cardioprotection: the importance of timing, location, duration and degree of inhibition. *Expert Opin.Ther.Targets* 9: 3: 447-456, 2005.

203. **Murray J, Zhang B, Taylor SW, Oglesbee D, Fahy E, Marusich MF, Ghosh SS and Capaldi RA.** The subunit composition of the human NADH dehydrogenase obtained by rapid one-step immunopurification. *J.Biol.Chem.* 278: 16: 13619-13622, 2003.

204. **Narula J, Haider N, Virmani R, DiSalvo TG, Kolodgie FD, Hajjar RJ, Schmidt U, Semigran MJ, Dec GW and Khaw BA.** Apoptosis in myocytes in end-stage heart failure. *N.Engl.J.Med.* 335: 16: 1182-1189, 1996.

205. **Narula J, Kolodgie FD and Virmani R.** Apoptosis and cardiomyopathy. *Curr.Opin.Cardiol.* 15: 3: 183-188, 2000.

206. **Narula J, Pandey P, Arbustini E, Haider N, Narula N, Kolodgie FD, Dal Bello B, Semigran MJ, Bielsa-Masdeu A and Dec GW.** Apoptosis in heart failure: release of cytochrome c from mitochondria and activation of caspase-3 in human cardiomyopathy. *Proc. Natl. Acad. Sci.* 96: 14: 8144-8149, 1999.

207. **Nduhirabandi F, Du Toit EF, Blackhurst D, Marais D, Lochner A.** Chronic melatonin consumption prevents obesity-related metabolic abnormalities and protects the heart against myocardial ischemia and reperfusion injury in a prediabetic model of diet-induced obesity. *J. Pineal Res.* 50: 171-182, 2011.

208. 206. **Nechushtan A, Smith CL, Hsu YT and Youle RJ.** Conformation of the Bax C-terminus regulates subcellular location and cell death. *EMBO J.* 18: 9: 2330-2341, 1999.

209. **Negoro S, Oh H, Tone E, Kunisada K, Fujio Y, Walsh K, Kishimoto T and Yamauchi-Takihara K.** Glycoprotein 130 regulates cardiac myocyte survival in doxorubicin-induced apoptosis through phosphatidylinositol 3-kinase/Akt phosphorylation and Bcl-xL/caspase-3 interaction. *Circulation* 103: 4: 555-561, 2001.

210. **Neuss M, Crow MT, Chesley A and Lakatta EG.** Apoptosis in cardiac disease—what is it—how does it occur. *Cardiovascular Drugs and Therapy* 15: 6: 507-523, 2001.

211. **Ng KW, Allen ML, Desai A, Macrae D and Pathan N.** Cardioprotective effects of insulin. *Circulation* 125: 5: 721-728, 2012.

212. **Nguyen DM and El-Serag HB.** The epidemiology of obesity. *Gastroenterol.Clin.North Am.* 39: 1: 1-7, 2010.

213. **Nikoulina SE, Ciaraldi TP, Mudaliar S, Mohideen P, Carter L and Henry RR.** Potential role of glycogen synthase kinase-3 in skeletal muscle insulin resistance of type 2 diabetes. *Diabetes* 49: 2: 263-271, 2000.

214. **Neill BT and Abel ED.** Akt1 in the cardiovascular system: friend or foe? *J.Clin.Invest.* 115: 8: 2059-2064, 2005.

215. **Olivetti G, Abbi R, Quaini F, Kajstura J, Cheng W, Nitahara JA, Quaini E, Di Loreto C, Beltrami CA and Krajewski S.** Apoptosis in the failing human heart. *N.Engl.J.Med.* 336: 16: 1131-1141, 1997.

216. **Ouwens D, Boer C, Fodor M, De Galan P, Heine R, Maassen J and Diamant M.** Cardiac dysfunction induced by high-fat diet is associated with altered myocardial insulin signalling in rats. *Diabetologia* 48: 6: 1229-1237, 2005.

217. **Ozes ON, Mayo LD, Gustin JA, Pfeffer SR, Pfeffer LM and Donner DB.** NF-κB activation by tumour necrosis factor requires the Akt serine–threonine kinase. *Nature* 401: 6748: 82-85, 1999.

218. **Parcellier A, Tintignac LA, Zhuravleva E and Hemmings BA.** PKB and the mitochondria: AKTing on apoptosis. *Cell.Signal.* 20: 1: 21-30, 2008.

219. **Park SY, Cho YR, Kim HJ, Higashimori T, Danton C, Lee MK, Dey A, Rothermel B, Kim YB and Kalinowski A.** Unraveling the temporal pattern of diet-induced insulin resistance in individual organs and cardiac dysfunction in C57BL/6 mice. *Diabetes* 54: 12: 3530-3540, 2005.

220. **Pastorino JG, Hoek JB and Shulga N.** Activation of glycogen synthase kinase 3β disrupts the binding of hexokinase II to mitochondria by phosphorylating voltage-dependent anion channel and potentiates chemotherapy-induced cytotoxicity. *Cancer Res.* 65: 22: 10545-10554, 2005.

221. **Pastukh V, Ricci C, Solodushko V, Mozaffari M and Schaffer SW.** Contribution of the PI 3-kinase/Akt survival pathway toward osmotic preconditioning. *Mol.Cell.Biochem.* 269: 1: 59-67, 2005.

222. **Patel S and Santani D.** Role of NF-kB in the pathogenesis of diabetes and its associated complications. *Pharmacological Reports* 61: 595: 595-603, 2009.

223. **Pearce NJ, Arch JRS, Clapham JC, Coghlan MP, Corcoran SL, Lister CA, Llano A, Moore GB, Murphy GJ and Smith SA.** Development of glucose intolerance in male transgenic mice overexpressing human glycogen synthase kinase-3β on a muscle-specific promoter. *Metab.Clin.Exp.* 53: 10: 1322-1330, 2004.

224. **Pedersen PL.** Mitochondrial events in the life and death of animal cells: a brief overview. *J.Bioenerg.Biomembr.* 31: 4: 291-304, 1999.

225. **Peter ME and Krammer P.** The CD95 (APO-1/Fas) DISC and beyond. *Cell Death and Differentiation* 10: 1: 26-35, 2003.

226. **Petersen KF and Shulman GI.** Pathogenesis of skeletal muscle insulin resistance in type 2 diabetes mellitus. *Am.J.Cardiol.* 90: 5A: 11G-18G, 2002.

227. **Poirier P, Lemieux I, Mauriège P, Dewailly E, Blanchet C, Bergeron J and Després JP.** Impact of waist circumference on the relationship between blood pressure and insulin: The Quebec health survey. *Hypertension* 45: 3: 363-367, 2005.

228. **Racz B, Gasz B, Gallyas Jr F, Kiss P, Tamas A, Szanto Z, Lubics A, Lengvari I, Toth G and Hegyi O.** PKA-Bad-14-3-3 and Akt-Bad-14-3-3 signaling pathways are involved in the protective effects of PACAP against ischemia/reperfusion-induced cardiomyocyte apoptosis. *Regul.Pept.* 145: 1: 105-115, 2008.

229. **Raffaella C, Francesca B, Italia F, Marina P, Giovanna L and Susanna I.** Alterations in hepatic mitochondrial compartment in a model of obesity and insulin resistance. *Obesity* 16: 5: 958-964, 2012.

230. **Rajabi M, Kassiotis C, Razeghi P and Taegtmeyer H.** Return to the fetal gene program protects the stressed heart: a strong hypothesis. *Heart Fail.Rev.* 12: 3: 331-343, 2007.

231. **Rajani T, Shubhangi P, Aruna J and Nirmalendu N.** An overview of caspase: Apoptotic protein for silicosis. 14: .

232. **Rao R, Hao CM, Redha R, Wasserman DH, McGuinness OP and Breyer M.** Glycogen synthase kinase 3 inhibition improves insulin-stimulated glucose metabolism but not hypertension in high-fat-fed C57BL/6J mice. *Diabetologia* 50: 2: 452-460, 2007.

233. **Rathmell JC, Fox CJ, Plas DR, Hammerman PS, Cinalli RM and Thompson CB.** Akt-directed glucose metabolism can prevent Bax conformation change and promote growth factor-independent survival. *Mol.Cell.Biol.* 23: 20: 7315-7328, 2003.

234. **Ravussin E and Smith SR.** Increased fat intake, impaired fat oxidation, and failure of fat cell proliferation result in ectopic fat storage, insulin resistance, and type 2 diabetes mellitus. *Ann.N.Y.Acad.Sci.* 967: 1: 363-378, 2002.

235. **Razeghi P, Young ME, Alcorn JL, Moravec CS, Frazier O and Taegtmeyer H.** Metabolic gene expression in fetal and failing human heart. *Circulation* 104: 24: 2923-2931, 2001.

236. **Reaven GM.** Insulin resistance: the link between obesity and cardiovascular disease. *Endocrinol.Metab.Clin.North Am.* 37: 3: 581-601, 2008.

237. **Reed JC and Paternostro G.** Postmitochondrial regulation of apoptosis during heart failure. *Proc. Natl. Acad. Sci.* 96: 14: 7614-7616, 1999.

238. **Regula KM, Ens K and Kirshenbaum LA.** Mitochondria-assisted cell suicide: a license to kill. *J.Mol.Cell.Cardiol.* 35: 6: 559-567, 2003.

239. **Ricquier D.** Respiration uncoupling and metabolism in the control of energy expenditure. *Proc.Nutr.Soc.* 64: 1: 47-52, 2005.

240. **Robertson JD, Orrenius S and Zhivotovsky B.** Review: nuclear events in apoptosis. *J.Struct.Biol.* 129: 2: 346-358, 2000.

241. **Robey RB and Hay N.** Mitochondrial hexokinases: guardians of the mitochondria. *Cell Cycle* 4: 5: 654-658, 2005.

242. **Robey R and Hay N.** Mitochondrial hexokinases, novel mediators of the antiapoptotic effects of growth factors and Akt. *Oncogene* 25: 34: 4683-4696, 2006.

243. **Rodriguez J and Lazebnik Y.** Caspase-9 and APAF-1 form an active holoenzyme. *Genes Dev.* 13: 24: 3179-3184, 1999.

244. **Rosano G, Fini M, Caminiti G and Barbaro G.** Cardiac metabolism in myocardial ischemia. *Curr.Pharm.Des.* 14: 25: 2551-2562, 2008.

245. **Ruan H, Hacohen N, Golub TR, Van Parijs L and Lodish HF.** Tumor necrosis factor-α suppresses adipocyte-specific genes and activates expression of preadipocyte genes in 3T3-L1 adipocytes nuclear factor-κB activation by TNF-α is obligatory. *Diabetes* 51: 5: 1319-1336, 2002.

246. **Rubio M, Avitabile D, Fischer K, Emmanuel G, Gude N, Miyamoto S, Mishra S, Schaefer EM, Brown JH and Sussman MA.** Cardioprotective stimuli mediate phosphoinositide 3-kinase and phosphoinositide dependent kinase 1 nuclear accumulation in cardiomyocytes. *J.Mol.Cell.Cardiol.* 47: 1: 96-103, 2009.

247. **Rustin P, Chretien D, Bourgeron T, Gerard B, Rötig A, Saudubray J and Munnich A.** Biochemical and molecular investigations in respiratory chain deficiencies. *Clin.Chim.Acta* 228: 1: 35-51, 1994.

248. **Sack MN, Disch DL, Rockman HA and Kelly DP.** A role for Sp and nuclear receptor transcription factors in a cardiac hypertrophic growth program. *Proc. Natl. Acad. Sci.* 94: 12: 6438-6443, 1997.

249. **Sale E and Sale G.** Protein kinase B: signalling roles and therapeutic targeting. *Cell. Mol. Life Sci.* 65: 1: 113-127, 2008.

250. **Schaap FG, Binas B, Danneberg H, van der Vusse GJ and Glatz JFC.** Impaired long-chain fatty acid utilization by cardiac myocytes isolated from mice lacking the heart-type fatty acid binding protein gene. *Circ.Res.* 85: 4: 329-337, 1999.

251. **Schägger H and Pfeiffer K.** The ratio of oxidative phosphorylation complexes I–V in bovine heart mitochondria and the composition of respiratory chain supercomplexes. *J.Biol.Chem.* 276: 41: 37861-37867, 2001.

252. **Scheubel RJ, Tostlebe M, Simm A, Rohrbach S, Prondzinsky R, Gellerich FN, Silber RE and Holtz J.** Dysfunction of mitochondrial respiratory chain complex I in human failing myocardium is not due to disturbed mitochondrial gene expression. *J.Am.Coll.Cardiol.* 40: 12: 2174-2181, 2002.

253. **Schulz H.** Regulation of fatty acid oxidation in heart. *J.Nutr.* 124: 2: 165, 1994.

254. **Schwenk RW, Holloway GP, Luiken JJFP, Bonen A and Glatz JFC.** Fatty acid transport across the cell membrane: regulation by fatty acid transporters. *Prostaglandins, Leukotrienes and Essential Fatty Acids* 82: 4: 149-154, 2010.

255. **Schwenk RW, Luiken JJFP, Bonen A and Glatz JFC.** Regulation of sarcolemmal glucose and fatty acid transporters in cardiac disease. *Cardiovasc.Res.* 79: 2: 249-258, 2008.

256. **Sciacchitano S and Taylor SI.** Cloning, tissue expression, and chromosomal localization of the mouse IRS-3 gene. *Endocrinology* 138: 11: 4931-4940, 1997.

257. .**Scorrano L, Petronilli V and Bernardi P.** On the voltage dependence of the mitochondrial permeability transition pore. *J.Biol.Chem.* 272: 19: 12295-12299, 1997.

258. .**Shanmuganathan S, Hausenloy DJ, Duchen MR and Yellon DM.** Mitochondrial permeability transition pore as a target for cardioprotection in the human heart. *Am J Physiol Heart Circ Physiol* 289: 1: H237-H242, 2005.

259. **Shibata R, Sato K, Pimentel DR, Takemura Y, Kihara S, Ohashi K, Funahashi T, Ouchi N and Walsh K.** Adiponectin protects against myocardial ischemia-reperfusion injury through AMPK-and COX-2–dependent mechanisms. *Nature Medicine* 11: 10: 1096-1103, 2005.

260. **Silverman HS and Stern MD.** Ionic basis of ischaemic cardiac injury: insights from cellular studies. *Cardiovasc.Res.* 28: 5: 581-597, 1994.

261. **Singal P, Li T, Kumar D, Danelisen I and Iliskovic N.** Adriamycin-induced heart failure: mechanisms and modulation. *Mol.Cell.Biochem.* 207: 1: 77-86, 2000.

262. **Sodha NR, Clements RT, Feng J, Liu Y, Bianchi C, Horvath EM, Szabo C and Sellke FW.** The effects of therapeutic sulfide on myocardial apoptosis in response to ischemia–reperfusion injury. *European Journal of Cardio-thoracic Surgery* 33: 5: 906-913, 2008.

263. **Solaini G and Harris DA.** Biochemical dysfunction in heart mitochondria exposed to ischaemia and reperfusion. *Biochem.J.* 390: Pt 2: 377-394, 2005.

264. **Spector A.** Plasma lipid transport. *Clin.Physiol.Biochem.* 2: 2-3: 123-134, 1984.

265. **Stanley WC, Recchia FA and Lopaschuk GD.** Myocardial substrate metabolism in the normal and failing heart. *Physiol.Rev.* 85: 3: 1093-1129, 2005.

266. **Strasser A, O'Connor L and Dixit VM.** Apoptosis signaling. *Annu.Rev.Biochem.* 69: 217-245, 2000.

267. **Suleiman M, Halestrap A and Griffiths E.** Mitochondria: a target for myocardial protection. *Pharmacol.Ther.* 89: 1: 29-46, 2001.

268. **Susin SA, Lorenzo HK, Zamzami N, Marzo I, Snow BE, Brothers GM, Mangion J, Jacotot E, Costantini P and Loeffler M.** Molecular characterization of mitochondrial apoptosis-inducing factor. *Nature* 397: 6718: 441-446, 1999.

269. **Sussman MA, Völkers M, Fischer K, Bailey B, Cottage CT, Din S, Gude N, Avitabile D, Alvarez R and Sundararaman B.** Myocardial AKT: the omnipresent nexus. *Physiol.Rev.* 91: 3: 1023-1070, 2011.

270. **Taha M and Lopaschuk GD.** Alterations in energy metabolism in cardiomyopathies. *Ann.Med.* 39: 8: 594-607, 2007.

271. **Taniyama Y, Ito M, Sato K, Kuester C, Veit K, Tremp G, Liao R, Colucci WS, Ivashchenko Y and Walsh K.** Akt3 overexpression in the heart results in progression from adaptive to maladaptive hypertrophy. *J.Mol.Cell.Cardiol.* 38: 2: 375-385, 2005.

272. **Thurmond DC, Kanzaki M, Khan AH and Pessin JE.** Munc18c function is required for insulin-stimulated plasma membrane fusion of GLUT4 and insulin-responsive amino peptidase storage vesicles. *Mol.Cell.Biol.* 20: 1: 379-388, 2000.

273. **Tirone TA and Brunicardi FC.** Overview of glucose regulation. *World J.Surg.* 25: 4: 461-467, 2001.

274. **Tong H, Imahashi K, Steenbergen C and Murphy E.** Phosphorylation of glycogen synthase kinase-3β during preconditioning through a phosphatidylinositol-3-kinase–dependent pathway is cardioprotective. *Circ.Res.* 90: 4: 377-379, 2002.

275. **Tong H, Rockman HA, Koch WJ, Steenbergen C and Murphy E.** G protein-coupled receptor internalization signaling is required for cardioprotection in ischemic preconditioning. *Circ.Res.* 94: 8: 1133-1141, 2004.

276. **Trivedi PS and Barouch LA.** Cardiomyocyte apoptosis in animal models of obesity. *Curr.Hypertens.Rep.* 10: 6: 454-460, 2008.

277. **Tumane RG, Pingle SK, Jawade AA and Nath NN.** An overview of caspase: Apoptotic protein for silicosis. *Indian J. Occup. Environ. Med.* 14: 2: 31-38, 2010.

278. **Tuteja G and Kaestner KH.** SnapShot: Forkhead transcription factors II. *Cell* 12: 192-193, 2007.

279. **Uchiyama T, Engelman RM, Maulik N and Das DK.** Role of Akt signaling in mitochondrial survival pathway triggered by hypoxic preconditioning. *Circulation* 109: 24: 3042-3049, 2004.

280. **Van Der Vusse GJ, Van Bilsen M and Glatz JFC.** Cardiac fatty acid uptake and transport in health and disease. *Cardiovasc.Res.* 45: 2: 279-293, 2000.

281. **Van Gaal LF, Mertens IL and Christophe E.** Mechanisms linking obesity with cardiovascular disease. *Nature* 444: 7121: 875-880, 2006.

282. **Vanden Berghe T, Declercq W and Vandenabeele P.** NADPH oxidases: new players in TNF-induced necrotic cell death. *Mol.Cell* 26: 6: 769-771, 2007.

283. **Verhagen AM, Ekert PG, Pakusch M, Silke J, Connolly LM, Reid GE, Moritz RL, Simpson RJ and Vaux DL.** Identification of DIABLO, a mammalian protein that promotes apoptosis by binding to and antagonizing IAP proteins. *Cell* 102: 1: 43-53, 2000.

284. **Villunger A, Michalak EM, Coultas L, Müllauer F, Böck G, Ausserlechner MJ, Adams JM and Strasser A.** p53-and Drug-Induced Apoptotic Responses Mediated by BH3-Only Proteins Puma and Noxa. *Proc.Natl.Acad.Sci.* 100: 1-7, 2003.

285. **Vo TD, Greenberg HJ and Palsson BO.** Reconstruction and Functional Characterization of the Human Mitochondrial Metabolic Network Based on Proteomic and Biochemical Data. *The Journal of Biological Chemistry* 279: 38: 39532–39540, 2004.

286. **Walker KS, Deak M, Paterson A, Hudson K, Cohen P and Alessi DR.** Activation of protein kinase B beta and gamma isoforms by insulin in vivo and by 3-phosphoinositide-dependent protein kinase-1 in vitro: comparison with protein kinase B alpha. *Biochem.J.* 331: Pt 1: 299-308, 1998.

287. **Walsh K.** Akt signaling and growth of the heart. *Circulation* 113: 17: 2032-2034, 2006.

288. **Wang K, Yin XM, Chao DT, Milliman CL and Korsmeyer SJ.** BID: a novel BH3 domain-only death agonist. *Genes Dev.* 10: 22: 2859-2869, 1996.

289. **Wang PH, Almahfouz A, Giorgino F, McCowen KC and Smith RJ.** In vivo insulin signaling in the myocardium of streptozotocin-diabetic rats: opposite effects of diabetes on insulin stimulation of glycogen synthase and c-Fos. *Endocrinology* 140: 3: 1141-1150, 1999.

290. **Wang S and El-Deiry WS.** TRAIL and apoptosis induction by TNF-family death receptors. *Oncogene* 22: 53: 8628-8633, 2003.

291. **Wang X.** The expanding role of mitochondria in apoptosis. *Genes Dev.* 15: 22: 2922-2933, 2001.

292. **Waselle L, Gerona RRL, Vitale N, Martin TFJ, Bader MF and Regazzi R.** Role of phosphoinositide signaling in the control of insulin exocytosis. 19: 12: 3097-3106, 2005.

293. **Wei MC, Zong WX, Cheng EHY, Lindsten T, Panoutsakopoulou V, Ross AJ, Roth KA, MacGregor GR, Thompson CB and Korsmeyer SJ.** Proapoptotic BAX and BAK: a requisite gateway to mitochondrial dysfunction and death. *Science* 292: 5517: 727-730, 2001.

294. **Weiss JN, Korge P, Honda HM and Ping P.** Role of the mitochondrial permeability transition in myocardial disease. *Circ.Res.* 93: 4: 292-301, 2003.

295. **Wencker D, Chandra M, Nguyen K, Miao W, Garantziotis S, Factor SM, Shirani J, Armstrong RC and Kitsis RN.** A mechanistic role for cardiac myocyte apoptosis in heart failure. *J.Clin.Invest.* 111: 10: 1497-1504, 2003.

296. **Wente W, Efanov AM, Brenner M, Kharitonenkov A, Köster A, Sandusky GE, Sewing S, Treinies I, Zitzer H and Gromada J.** Fibroblast growth factor-21 improves pancreatic β-cell function and survival by activation of extracellular signal–regulated kinase 1/2 and Akt signaling pathways. *Diabetes* 55: 9: 2470-2478, 2006.

297. **Willis SN, Chen L, Dewson G, Wei A, Naik E, Fletcher JI, Adams JM and Huang DCS.** Proapoptotic Bak is sequestered by Mcl-1 and Bcl-xL, but not Bcl-2, until displaced by BH3-only proteins. *Genes Dev.* 19: 11: 1294-1305, 2005.

298. **Wong C and Marwick TH.** Obesity cardiomyopathy: diagnosis and therapeutic implications. *Nature Clinical Practice Cardiovascular Medicine* 4: 9: 480-490, 2007.

299. **Xu C, Kim NG and Gumbiner BM.** Regulation of protein stability by GSK3 mediated phosphorylation. *Cardiovascular Research* 8: 24: 4032-4039, 2009.

300. **Yach D, Stuckler D and Brownell KD.** Epidemiologic and economic consequences of the global epidemics of obesity and diabetes. *Nat.Med.* 12: 1: 62-66, 2006.

301. **Yamaguchi H and Wang HG.** The protein kinase PKB/Akt regulates cell survival and apoptosis by inhibiting Bax conformational change. *Oncogene* 20: 53: 7779-7786, 2001.

302. **Yan J, Young ME, Cui L, Lopaschuk GD, Liao R and Tian R.** Increased glucose uptake and oxidation in mouse hearts prevent high fatty acid oxidation but cause cardiac dysfunction in diet-induced obesity. *Circulation* 119: 21: 2818-2828, 2009.

303. **Yang JY, Yeh HY, Lin K and Wang PH.** Insulin stimulates Akt translocation to mitochondria: implications on dysregulation of mitochondrial oxidative phosphorylation in diabetic myocardium. *J.Mol.Cell.Cardiol.* 46: 6: 919-926, 2009.

304. **Yang X, Chang HY and Baltimore D.** Autoproteolytic activation of pro-caspases by oligomerization. *Mol.Cell* 1: 2: 319-325, 1998.

305. **Yellon DM and Downey JM.** Preconditioning the myocardium: from cellular physiology to clinical cardiology. *Physiol.Rev.* 83: 4: 1113-1151, 2003.

306. .**Yin Z, Gao H, Wang H, Li L, Di C, Luan R and Tao L.** Ischaemic post-conditioning protects both adult and aged Sprague-Dawley rat heart from ischaemia–reperfusion injury through the phosphatidylinositol 3-kinase–akt and glycogen synthase kinase-3β pathways. *Clinical and Experimental Pharmacology and Physiology* 36: 8: 756-763, 2009.

307. **Yong QC, Lee SW, Foo CS, Neo KL, Chen X and Bian JS.** Endogenous hydrogen sulphide mediates the cardioprotection induced by ischemic postconditioning. *Am J Physiol Heart Circ Physiol* 295: 3: H1330-H1340, 2008.

308. **Yu SW, Wang H, Poitras MF, Coombs C, Bowers WJ, Federoff HJ, Poirier GG, Dawson TM and Dawson VL.** Mediation of poly (ADP-ribose) polymerase-1-dependent cell death by apoptosis-inducing factor. *Science* 297: 5579: 259-263, 2002.

309. **Yue TL, Bao W, Gu JL, Cui J, Tao L, Ma XL, Ohlstein EH and Jucker BM.** Rosiglitazone treatment in Zucker diabetic Fatty rats is associated with ameliorated cardiac insulin resistance and protection from ischemia/reperfusion-induced myocardial injury. *Diabetes* 54: 2: 554-562, 2005.

310. **Zamzami N and Kroemer G.** The mitochondrion in apoptosis: how Pandora's box opens. *Nature Reviews: Molecular Cell Biology* 2: 1: 67-71, 2001.

311. **Zhang Y, Yuan M, Bradley KM, Dong F, Anversa P and Ren J.** insulin-like growth factor 1 alleviates high-fat diet–induced myocardial contractile dysfunction role of insulin signaling and mitochondrial function. *Hypertension* 59: 3: 680-693, 2012.

312. **Zhu M, Feng J, Lucchinetti E, Fischer G, Xu L, Pedrazzini T, Schaub MC and Zaugg M.** Ischemic postconditioning protects remodeled myocardium via the PI3K–PKB/Akt reperfusion injury salvage kinase pathway. *Cardiovasc.Res.* 72: 1: 152-162, 2006.

313. **Zong WX, Lindsten T, Ross AJ, MacGregor GR and Thompson CB.** BH3-only proteins that bind pro-survival Bcl-2 family members fail to induce apoptosis in the absence of Bax and Bak. *Genes Dev.* 15: 12: 1481-1486, 2001.

314. **Zou H, Li Y, Liu X and Wang X.** An APAF-1· cytochrome c multimeric complex is a functional apoptosome that activates procaspase-9. *J.Biol.Chem.* 274: 17: 11549-11556, 1999.

II: Books

1. **Garrett R. and Grisham CM.** Biochemistry. *Fort Worth, Tex.: Saunders* 2nd Ed.: 679-692, c1999.
2. **Nicholls DG and Ferguson SJ.** Bioenergetics 3. *Amsterdam : Academic Press: 69-126,* 2001.

III: Websites

1. http://rosswiki2009.pbworks.com/w/page/11977900/Glycolysis
2. http://www.coenzyme-a.com/tca.htm
3. http://thealchemistkitten.files.wordpress.com/2009/11/blaze_tca_cycle.jpg